Characterisation of the imprinted genes in mouse: *Grb10* and *Dlk1*

Marta Małgorzata Madoń

A thesis submitted for the degree of Doctor of Philosophy

University of Bath

Department of Biology and Biochemistry

September 2011

Moim rodzicom

w podziękowaniu za miłość,

wsparcie i to, że zawsze we mnie wierzyli

To my parents

for their love, endless support

and for always believing in me

Nothing in life is to be feared, it is only to be understood. Now is the time to understand more, so that we may fear less.

- Maria Skłodowska-Curie -

Acknowledgements

First and foremost, I would like to thank my supervisor Dr Andrew Ward for guiding me through this journey. Without his support, advice and our long discussions I would not have been able to understand what it really means to be a scientist.

Heartfelt thanks go to Dr Mike Cowley, who was a perfect colleague, supporter and friend throughout my times in the lab. Thanks to our 'Grb10 brainstorming sessions' I was able to solve so many problems, his help and advice have been invaluable. I am indebted to Dr Al Garfield for his support and technical assistance during my first months as a PhD student, to Iryna Withington for her enormous help with solving all histological issues and Adrian Rogers for his help with using FACS machine. Thanks to Dr Kim Moorwood, Dr Joanne Stewart-Cox and my other colleagues from 'zebramouse lab' who provided me their technical support and made times spent in the lab really enjoyable. I would also like to mention my project students Sean Porazinski and Joseph Burgon who have contributed to this project, animal technicians whose help have been invaluable, and members of Tosh and Chalmers labs and other members of the department who frequently offered me their technical expertise. I am very grateful to our collaborators: Prof Anne Ferguson-Smith (University of Cambridge) and Dr Janet Smith (University of Birmingham) and members of their labs for stimulating discussions and their input into this project, to Dr Mark Perry (University of Bristol) for lending us DXA machine and his assistance with bone cryosectioning and to Dr Steven Bauer (Center for Biologics Evaluation and Research, Food and Drug Administration, Bethesda, US) for kindly providing us with *Dlk1*$^{+/p}$ knockout mice.

Special thanks go to my 'partners in crime': (Drs) Gaby Miron, Fred Rodrigues, Yolanda Sanchez and Laura Vibert, for making last few years an unforgettable experience, I am so happy I have met you all. Finally, I would like to thank my parents, grandpa and my boyfriend Michał, their love gave me strength to make this work.

My PhD was funded by the Department of Biology and Biochemistry at the University of Bath.

List of abbreviations

aa	amino acid
Ag	Androgenetic
AHO	Albright's hereditary osteodystrophy
ALL	Acute lymphoblastic leukaemia
ANOVA	Analysis of variance
AS	Angelman syndrome
BAT	Brown adipose tissue
β-geo	*β-galactosidase*
BMC	Bone mineral composition
BMD	Bone mineral density
bp	base pair
BPS	Between PH and SH2 domain
BSA	Bovine serum albumin
BWS	Beckwith-Wiedemann syndrome
cDNA	Complimentary Deoxyribonucleic acid
clpg	*callipyge*
cm	centimetre
CNS	Central nervous system
CML	Chronic myelogenous leukaemia
CpG	Cytosine and guanidine containing dinucleotide unit
CO_2	Carbon dioxide
DAPI	4',6-diamidino-2-phenylindole
DMEM	Dulbecco's modified Eagle's medium
DMSO	Dimethyl sulfoxide
DMR	Differentially methylated region
DNA	Deoxyribonucleic acid
DNAse	Deoxyribonuclease
DOS	Delta and OSM-11 motif
DSL	Delta:Serrate:Lag-2 domain
DXA	Dual X-ray absoptiometry
EDTA	Ethylenediaminetetraacetic acid

EG cells	Embryonic germ cells
EGF	Epidermal growth factor
ES cells	Embryonic stem cells
eX	Embryonic day X
FACS	Fluorescent activated cell sorting
FBS	Foetal bovine serum
FSC	Forward scatter
g	gram
g	gravity
GM	Grb10 and Mig
GTT	Glucose tolerance test
GYF domain	Glycine-tyrosine-phenylalanine domain
HCl	Hydrogen chloride
H&E	Haematoxylin and Eosin staining
ICR	Imprinting control region
IG-DMR	Intergenic germline-derived DMR
IGF	Insulin-like growth factor
IGFR	Insulin-like growth factor receptor type X
INS	Insulin
IR	Insulin receptor
iPSC	Induced pluripotent stem cells
JM	Juxtamembrane domain
Kb	Kilobase pairs
kDa	Kilo-Dalton
KO	Knockout
LOI	Loss of imprinting
M	Molar
MAP	Mitogen-activated protein
Mb	Mega base pairs
Mg	milligram
Min	minute
Ml	millilitre
mM	millimolar
µg	microgram

µl	microlitre
µm	micrometer (micron)
MQ	Water
mRNA	Messenger ribonucleic acid
mUPD	Maternal uniparental disomy
NaCl	Sodium chloride
NaOH	Sodium hydroxide
ncRNA	Non-coding ribonucleic acid
OTC	Optimal cutting temperature (compound)
pA or poly-(A)	Poly-adenylation
PAS	Periodic Acid - Schiff Staining
PAGE	Polyacrylamide gel electrophoresis
PBS	Phosphate buffered saline
PcG	Polycomb group
PCR	Polymerase chain reaction
P domain	Proline-rich domain
Pg	Parthenogenetic
PH domain	Pleckstrin homology domain
PFA	Paraformaldehyde
pMEF	Primary mouse embryonic fibroblast
pUPD	Paternal uniparental disomy
PWS	Prader-Willi syndrome
RA	Ras-association-like domain
RNA	Ribonucleic acid
RTK	Receptor tyrosine kinase
SA	Splice acceptor
SDS	Sodium dodecyl sulphate
SEM	Standard error of means
SH2	Src-homology 2 domain
SH3	Src-homology 3 domain
snoRNA	Small nucleolar ribonucleic acid
SRS	Silver-Russell syndrome
SSC	Side scatter
TM	Transmembrane domain

TNDM	Transient neonatal diabetes mellitus
UPD	Uniparental disomy
UV	Ultraviolet
V	Volt
v/v	Volume/volume
w/v	Weight/volume
X-gal	5-bromo-4-chloro-3-indolyl-β-D-galactopyranoside
WAT	White adipose tissue
WW	Tryptophan-rich domain

Genotype abbreviations

WT	Wild type
***Dlk1*$^{+/p}$**	Paternal transmission *Dlk1* heterozygote
***Grb10*$^{m/+}$**	Maternal transmission *Grb10* heterozygote
***Grb10*$^{m/+}$*/Dlk1*$^{+/p}$**	Double knockout with maternal transmission of *Grb10* ablation and paternal transmission of *Dlk1* ablation

Table of contents

List of figures

List of tables

Abstract

Genomic imprinting provides an exception to the Mendelian rule of inheritance, as imprinted genes are preferentially expressed in a parent-of-origin specific manner. They play important roles in the development of embryonic and extra-embryonic lineages and postnatally in the maintenance of correct metabolic homeostasis as well as regulation of adult behaviour. The parental conflict theory predicts that maternally expressed genes act as growth suppressors, limiting the usage of maternal resources, and that paternally expressed genes function in an opposite manner to promote growth at the expense of maternal resources. Growth factor bound protein 10 (*Grb10*) is an imprinted gene encoding an intracellular adaptor protein that can interact with several receptor tyrosine kinases and downstream signalling molecules. Recently, our lab has identified *Grb10* as a unique imprinted gene capable of influencing fetal growth, postnatal energy metabolism and adult behaviour depending on functions of each of the parental alleles in distinct tissues. *Grb10* predominantly expressed from the maternal allele during embryogenesis affects fetal and placental growth along with postnatal glucose homeostasis, whereas paternal *Grb10* expression within the CNS influences social behaviour. Delta-like homologue 1 is (*Dlk1*) a paternally expressed imprinted gene coding for a protein belonging to the Notch/Delta family that acts as a membrane-associated or a soluble protein known to regulate differentiation of various cell types, notably adipocytes. *In vivo Dlk1* has been associated with perinatal survival, regulation of normal growth and development and maintenance of the correct course of adipogenesis. Here a hypothesis is proposed that *Grb10*, as a predominantly maternally expressed growth inhibitor and *Dlk1*, a paternally expressed growth promoter, act antagonistically in a common genetic pathway. To test this hypothesis, we have generated $Grb10^{m/+}/Dlk1^{+/p}$ double knockout mice and performed a phenotypic characterisation in comparison with wild type as well as the respective single knockout animals. Results obtained from allometric and metabolic analyses, together with histological studies, reveal strong similarities between the phenotypes of $Grb10^{m/+}$and $Grb10^{m/+}/Dlk1^{+/p}$ knockout mice. We found that overgrowth of $Grb10^{m/+}/Dlk1^{+/p}$ embryos and placentae resemble the phenotype seen in $Grb10^{m/+}$ mutants and that tissue overgrowth most likely results from higher proliferation rates of $Grb10^{m/+}$and $Grb10^{m/+}/Dlk1^{+/p}$ cells. Furthermore, $Grb10^{m/+}$and $Grb10^{m/+}/Dlk1^{+/p}$ knockout mice each exhibit improved glucose clearance and share an unusual characteristic accumulation of lipid in neonatal liver. These results are consistent with the proposed hypothesis and indicate that the *Dlk1* and *Grb10* genes might be involved in the same genetic pathway. Moreover, the data suggest *Dlk1* is an inhibitor of *Grb10* which is in turn acting as a growth suppressor.

CHAPTER 1

1 Introduction

1.1 Genomic imprinting

1.1.1 Introduction

The vast majority of genes are inherited and expressed in agreement with Mendelian rule of inheritance, which assumes the equality of both of the parental genomes. In contrast to that, there is a small subset of so-called imprinted genes that do not follow this rule and exhibit expression predominantly from only one of the parental alleles, either maternal or paternal (**Figure** 1.1). Imprinted genes are usually thought to account for only a minor part of the total number of genes in the genome. However, a recent genome-wide screen suggests that more than 1,300 loci could show imprinted expression within the mouse brain (Gregg et al., 2010), which implies an important role of imprinting within the brain that was previously under-appreciated. These predictions, however, should be carefully tested and confirmed by detailed analysis of differential allelic expression along with investigation of functional roles of genes identified in the study by Gregg et al (2010). The presence of imprinted genes is limited to only a few taxa, including placental mammals, marsupials and seed plants. The comparison of imprinted genes between different species serves several purposes. First of all, it aims to identify genes that are prone to be imprinted. Secondly, it intends to recognise the DNA sequences responsible for monoallelic gene expression. Finally, this type of comparison should allow for identification of conserved functions of imprinted genes and help to understand the evolution of imprinting. So far 144 imprinted genes have been identified in mice (see http://www.har.mrc.ac.uk/research/genomic_imprinting/ or http://igc.otago.ac.nz/home.html) and approximately 100 in humans, and among them many were found to share the imprinting status between these two species.

The first experiments indicating the existence of imprinted genes showed that gynogenetic (possessing two maternal genome copies) and androgenetic (possessing two paternal genome copies) mouse embryos were not viable and exhibited a variety of growth abnormalities of both fetus and placenta (Barton et al., 1984; Mann and Lovell-Badge, 1984; McGrath and Solter, 1984; Surani et al., 1984; Barton et al., 1985). Furthermore, it was noted that the development of tissues that made up the fetuses was somewhat different: parthenogenotes consisted mainly of embryonic material, with poorly developed placentae and extra-embryonic membranes, while androgenotes showed more advanced development of extra-embryonic tissues with disrupted fetal development. At around the same time, specific chromosomal domains with imprinted genes were identified in mouse genetic

experiments that revealed opposite developmental phenotypes arising from uniparental disomic (UPD) inheritance of specific chromosome regions from either the mother or father, further confirming the functional non-equivalence of the genomes (Cattanach and Kirk, 1985). These experiments supported the idea that two genomes are unequal and that disruptions in development during parthenogenesis are the result of allele-specific expression of imprinted genes.

The term 'imprinting of the genome' that referred to the phenomenon of non-genetic difference distinguishing two parental genomes and leading to their functional non-equivalence was originally used by Surani and colleagues (1984), who were the first to suggest that in order for normal development to occur the contributions from both male and female pronuclei are crucial.

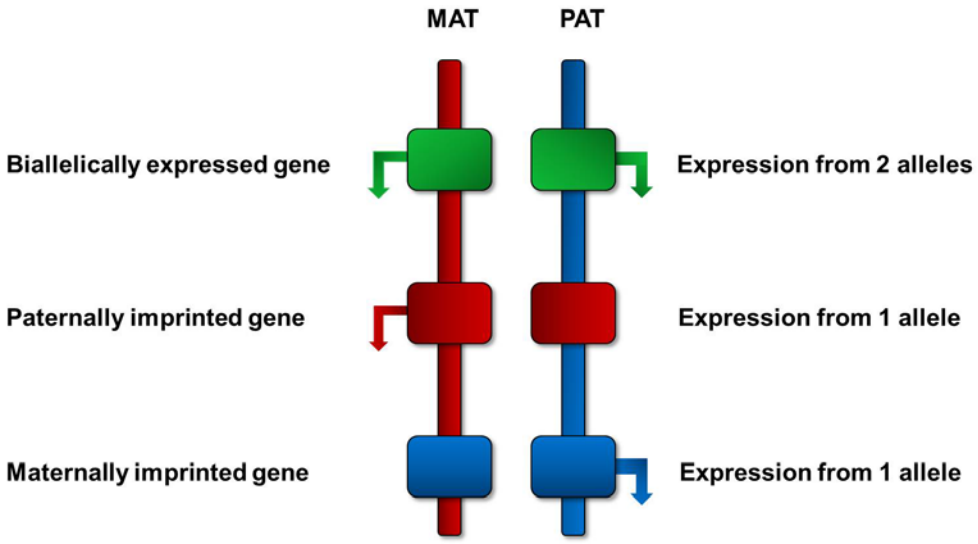

Figure 1.1 Mode of expression in biallelic and imprinted genes.
Three hypothetical genes are depicted on chromosomes inherited either maternally (Mat) or paternally (Pat), with transcriptional activity indicated by arrows. The majority of genes when transcriptionally active are expressed equally from both of the parental alleles (green). A small subset of genes is imprinted, meaning that they are expressed predominantly from only one of the parental alleles: either maternal (red) or paternal (blue) and silenced (imprinted) on the other allele. In the case of uniparental disomies (UPDs), double expression results from duplication of one of the parental alleles, while gene silencing occurs following duplication of the opposite parental allele.

In the past, the key to identification of imprinted genes was based on mapping candidates within chromosomal regions which displayed opposite phenotypes when inherited as

uniparental disomies or following uniparental transmission of a deletion. In this way, Insulin-like growth factor 2 receptor (*Igf2r*) leading to the maternal-effect mutation in *Tme* mice was discovered as one of the first imprinted genes (Barlow et al., 1991). The growth retarded *Igf2r* mutants were seen only upon transmission of the mutation through the paternal line. At about the same time, the Insulin-like growth factor 2 *(Igf2)* (DeChiara et al., 1991) and *H19* (Bartolomei et al., 1991) genes were identified as imprinted genes. Once this complex, unique mode of monoallelic expression was discovered, investigation of the underlying mechanisms regulating imprinted expression and functions of imprinted genes was initiated.

1.1.2 Evolution of genomic imprinting

The obvious advantage of diploids over haploids comes down to protection against detrimental results of genetic damage or mutation. Where expression of a gene from only one of the chromosomes is sufficient, the presence of two copies can offer a 'backup' in the event of malfunction or damage of the other. From an evolutionary point of view, having diploid chromosomes and potentially more genetic variety provides a better chance of survival in case one of the chromosomes is not well adapted to the environment. An organism can discard the advantage of diploidy by inactivation of a group of genes and becoming functionally haploid at these loci. This is the case for imprinted genes which are inherited in two copies, but only one of them is transcriptionally active. The obvious question then concerns the advantage of imprinting that is able to compensate for the loss of diploidy. Since the discovery of genomic imprinting in the mid-1980s (Surani et al., 1984), evolutionary biologists have been trying to establish the selective pressures and mechanisms that led to the evolution of imprinting (Moore and Haig, 1991; Spencer et al., 1999; Iwasa and Pomiankowski, 2001; Wolf and Hager, 2006). There is an overabundance of theories trying to explain the role of imprinting in mammalian evolution. The majority of proposed hypotheses aim to explain most of the typical characteristics of imprinted genes, which include localisation within clusters, tissue specificity, effects of encoded gene products on growth, presence of imprinting in the germline of both sexes and phylogenetic distribution of imprinting. Nonetheless, so far a single model explaining the variety of roles of imprinted genes has not been discovered (Hurst and McVean, 1997; Morison et al., 2001; Wilkins and Haig, 2003).

Haig and Westoby (1989) laid the foundation for the most widely discussed model explaining the evolution of imprinting called the parental conflict theory. They suggested that

genomic imprinting is a result of a conflict between males and females over the allocation of maternal resources. According to this theory, the father (and paternally expressed genes in the embryo or/and placenta) will favour the acquisition of maternal resources for his offspring at the expense of the mother and her potential future offspring. Males, whose energy investment in raising the litter is small in contrast to females, will try to promote the nutrient transfer to their offspring and, as any particular male might not father future offspring with the same female, he will try to give his offspring the best chance of survival regardless of damage to the fitness of the female. On the other hand, the mother will try to maximise her lifetime reproductive performance by limiting allocation of resources to particular offspring or litters and trying to allocate them equally between all of her offspring. Consequently, an equilibrium between differentially expressed maternal and paternal imprinted genes is achieved in order for normal growth and development to occur (Moore and Haig, 1991).

Interestingly, in addition to eutherians, imprinting has also been identified in angiosperms (flowering plants) and the phenotypic differences in seed size resulting from imprinting manipulation in them greatly resemble those observed in mouse phenotypes caused by imprinting manipulation (reviewed in Feil and Berger, 2007). There is no definite explanation for the imprinted genes existence within the angiosperm plants, but it has been indicated that angiosperm plants are similar to mammals in a way that biparental seeds are also grown by one of the parents and demands of the embryo need to be in balance with the fitness of the mother, so both interests are controlled by inactivation of certain growth-related genes in one of the parents, which is in agreement with parental conflict theory (Moore and Haig, 1991).

Surprisingly, the authors who first mentioned parental conflict hypothesis were able to correctly predict the sites and times of expression of imprinted genes. They suggested any genes associated with maternal resources acquisition could be affected, in particular those functioning in placental growth and efficiency, suckling and appetite, neonatal behaviour, postnatal growth and metabolism. With time and increasing number of identified imprinted genes it became clear that the majority of them are indeed expressed in relevant tissues and are involved in the processes described above. For example, both the *Grb10* and *Dlk1* genes were found to have major roles in regulation of embryonic and postnatal growth as well as metabolism (Moon et al., 2002; Charalambous et al., 2003; Lee et al., 2003; Smith et al., 2007).

Many of the initially discovered imprinted genes seemed to act consistently with the conflict hypothesis, including the reciprocally imprinted *Igf2* and *Igf2r* genes that exerted opposite effects on fetal growth (Barlow et al., 1991; DeChiara et al., 1991). As mammals tend

to require maternal resources not only during fetal development but also in early postnatal life, it has been suggested that imprinted genes acting in agreement with conflict hypothesis play roles in resource acquisition pre- and post-natally. For example, the reciprocal postnatal effects on metabolic rate and deposition of brown fat are the result of mutations in the *Gsa* and *Gnasxl* transcripts in the *Gnas* imprinted cluster (Plagge and Kelsey, 2006). Moreover, concordant with paternally expressed genes functioning to enhance acquisition of maternal resources, poor suckling and inability to thrive have been noted in mice with loss of functional copies of the paternally expressed *Gnasxl* gene (Plagge et al., 2004).

The phenotypic characteristics of a number of mouse knockout models lacking imprinted genes undoubtedly provided support for the conflict hypothesis as a driving force for evolution of genomic imprinting. But even though it provides a justification for the function of multiple imprinted genes, it still fails to explain some other aspects of imprinting, for example the fact that paternally expressed genes are outnumbered by maternally expressed genes in the placenta. Therefore, it seems increasingly likely that this hypothesis will not be able to clarify and explain forces that led to maintenance of all the imprinted genes (Hurst and McVean, 1997; Hurst and McVean, 1998), especially those not associated with any clusters (Smith et al., 2003; Davies et al., 2004; Choi et al., 2005).

Parthenogenesis is a process of asexual reproduction based on lack of male investment but giving each organism within a species that consists of only females the ability to independently produce offspring, which in theory enables each individual to unilaterally introduce this species into a new habitat. Parthenogenesis does not occur in mammals but has been found in over 80 species of other vertebrates, including reptiles, amphibians and fish (Alves et al., 2001; Lampert, 2008). It has therefore been suggested that the reason for the presence of imprinting only in mammals might be protection against parthenogenesis, especially in light of experiments that used manipulated imprinted gene dosage to infer that imprinting disruption prevents the successful parthenogenetic mouse development (Barton et al., 1991; Fundele et al., 1991). It is interesting to note that human parthenogenetic bimaternal ovarian teratomas and androgenetic bipaternal conceptuses (complete hydatidiform moles) show similar phenotypes to the ones observed in mice.

Another hypothesis that attempts to explain the mechanism behind the evolution of parent-of-origin-specific gene expression is the ovarian time bomb hypothesis. It predicts that imprinting is a way of protection against ovarian trophoblastic disease in females (Varmuza and Mann, 1994), which is a result of a spontaneous development of an unfertilised egg in the

ovaries. The ovarian time bomb theory tries to explain the reason for some early embryonic growth enhancing genes (*e.g.* mouse *Igf2*) being maternally rather than paternally imprinted and also why the reciprocal imprinting status can be observed at some growth-restricting loci (*e.g.* mouse *Igf2r*). However, this hypothesis suggests that only a limited number of genes with critical role in embryonic development would be imprinted and fails to explain functions of imprinted genes in postnatal life (Plagge et al., 2004; Plagge et al., 2005). Hence, the existence of a relatively high number of imprinted genes argues against the ovarian time bomb hypothesis as, clearly, silencing of a single maternal allele should be enough to protect against parthenogenesis (Haig, 1994). Moreover, this model does not provide any explanation for imprinting of paternal loci. Also, the frequency of mammalian ovarian teratomas is very low, and the fact that the evolution of imprinting would act to protect specifically against such a rare disease is rather unlikely (Solter, 1994). Finally, it has also been argued that even if rarely occurring teratomas are able to preserve imprinting, higher pressure would be required for imprinting to develop in the first place (Weisstein et al., 2002).

The recently suggested intralocus sexual conflict hypothesis implies that the driving force behind genomic imprinting is selection which at a particular locus favours different alleles in males versus females. This theory concentrates on the evolution of the locus that causes the imprinting instead of the locus that is imprinted (Day and Bonduriansky, 2004). It suggests that natural selection should act to silence expression from maternally inherited alleles in males and paternally inherited alleles in females. However, in disagreement with that, there are multiple maternal and offspring traits that both favour the increased fitness of the offspring, suggesting that they evolved as a result of mother and offspring traits positively complementing each other rather than as an outcome of conflict between two different interests. This adaptive connection between maternal and offspring traits has been proven by experiments in different species (Kolliker et al., 2000; Agrawal et al., 2001; Hager and Johnstone, 2003; Lock et al., 2004), and even in humans it has been found that offspring with intermediate birth weights are the fittest (Ulizzi et al., 1981), suggesting that increase in investment of maternal resources is not always preferable. This model might explain imprinting at loci under different selection in both sexes, but cannot justify the abundance of imprinted genes in the placenta. An explanation for this has been incorporated into the coadaptation theory (Wolf and Hager, 2006).

Wolf and Hager (2006) demonstrated that natural selection favours expression of maternal gene copies because it leads to higher offspring fitness by increasing genetic

integration of the traits coadapted between maternal and offspring genomes. This coadaptation hypothesis is based on the prediction that loci associated with mother-offspring interaction have a greater chance of being maternally expressed, which could account for the high number of maternally expressed genes during placental (Wagschal and Feil, 2006) and seed development (Baroux et al., 2002). Therefore, unlike the conflict and intralocus hypotheses, this model tries to explain the overabundance of maternally expressed imprinted genes in placenta. The suggestion that imprinting evolved due to a variety of different selective pressures is particularly visible when it comes to maternal-offspring interactions, which are driven in some cases by genes that might be playing a role in conflict over investment of maternal resources, while other genes might be influenced as a result of maternal-offspring coadaptation.

In order to thoroughly understand the function of imprinted genes in mammals, it is vital to further investigate the evolutionary basis and mechanisms driving this phenomenon, alongside with its influence on a range of developmental and physiological processes. Analyses of knockout mouse models together with genome-wide screens can provide important tools in this exciting investigation. It will be interesting to discover which of the hypotheses, if any, will be supported by the results obtained in the future. Moreover, it will be important to compare and study in detail differences between the imprinting status of genes in mice and humans, especially given that some crucial differences between both of the species have been discovered, especially in the placenta.

Taken together, it still remains impossible to point at a single hypothesis as the only one explaining all the aspects of genomic imprinting. Instead, it seems increasingly likely that imprinted genes emerged as a result of variety of selective pressures at different loci in different taxa and as a result the imprinted genes counterparts between species might show differential special and/or temporal expression.

1.1.3 Characteristics and mechanisms regulating imprinted genes

There is an ongoing debate not only over the causes of genomic imprinting but also over the mechanisms that regulate this unique phenomenon. Up until now it is not clear if there is one universal mechanism governing parental allele-specific expression or there are different modes of regulation depending on the gene (reviewed in Edwards and Ferguson-Smith, 2007; Ideraabdullah et al., 2008; Bartolomei and Ferguson-Smith, 2011). So far, the examination of the subset of imprinted genes has revealed only a few common characteristics between them,

including location of the majority of imprinted genes within clusters, close vicinity to regions of parental allele-specific methylation and/or chromatin modifications, association with particular types of repeat sequences and the presence of antisense or overlapping transcripts. It is also known that imprinting occurs in a spatial and temporal manner rather than within all tissues in the body and throughout all developmental stages. Of particular interest is the regulation and role of imprinting in the earliest stages of development and its influence on cell cycle and associated growth, as many of imprinted genes identified so far have been demonstrated to be expressed during embryonic development (Weaver et al., 2009). It has been shown that in various cases parent-specific, monoallelic expression is generally conserved between mice and humans, with several exceptions including *IGF2R* that exhibits a monoallelic mode of expression in mice but is associated with polymorphic expression in humans, with only a small subset of individuals repressing the paternal copy of the gene to an appreciable extent (Kalscheuer et al., 1993; Pearsall et al., 1996).

The vast majority of imprinted genes show differences in methylation between parental alleles. However, these so-called differentially methylated regions (DMRs) have different characteristics. In some DMRs the differential methylation is established in parental germ cells and persists throughout development in all tissues (Neumann et al., 1995; Olek and Walter, 1997; Shemer et al., 1997), whereas in other DMRs changes in methylation are introduced at various stages of development and in different tissues (Feil et al., 1994). Moreover, methylation of the inactive allele is a typical feature of some DMRs while others are methylated on the active allele.

During the course of the life cycle of an organism, genomic imprints are known to undergo some specific changes. Early on, imprints are established in germ cells, following fertilisation they are maintained during chromosome duplication and segregation, then finally in the germ cells of a new organism the imprints are erased, which leads to establishment of new imprints in germ cells and the cycle starts all over again. The maintenance and modifications of imprints in somatic cells occur during development and following that imprints are read, which results in allele-specific expression.

In order for mature gametes to reflect the sex of the germline, the imprints in gametes need to be reset, which is thought to happen in two stages: first erasure of imprints and then establishment of new ones. In mouse, the erasure step is achieved by embryonic days 12 (E12) to 13 (E13) (Brandeis et al., 1993) and is based on a dramatic genome-wide DNA demethylation in germ cells. The evidence suggests that all the imprints are erased during this

stage (Tada et al., 1998; Davis et al., 2000). Following erasure, at late embryonic development stages, *de novo* DNA methylation occurs in germlines and continues after birth. Methylation in spermatocytes takes place before meiosis, whilst in oocytes, which are in meiotic arrest, it takes place during their growth (Obata et al., 1998; Ueda et al., 2000).

1.1.3.1 Establishment of imprinted genes

Methylation in vertebrates occurs on the cytosine residue of CpG dinucleotides by DNA methyltransferases. There are several candidate enzymes that could potentially govern *de novo* methylation in germ cells: Dnmt1 (DNA methyltransferase 1) but also Dnmt3a and Dnmt3b (Mertineit et al., 1998; Okano et al., 1999). The mode of their action is not perfectly clear, as DMRs in imprinted genes might be subject to *de novo* methylation in one of the germlines or *de novo* methylation could occur in both germlines but DMRs in only one of the germlines might be protected from it. There is a possibility that regulation of methyltransferases can be cell cycle-specific, as changes in replication timing might affect the availability of DNA for methylation. As it is possible for demethylation or *de novo* methylation to occur just after fertilisation, it is plausible to suspect that this is the time when some imprints might be established in only one of the parental alleles.

It has been demonstrated that Dnmt3a and Dnmt3b have important roles in *de novo* methylation and are vital in the course of embryonic development (Okano et al., 1999). They play crucial roles in the establishment of germline imprints in both lineages. So far it still remains unclear if the imprints in Imprinting Control Regions (ICRs) arise due to active methylation or protection from active methylation. Maintenance of methylation marks and allele-specific expression in a number of imprinted genes is the primary role of Dnmt1, although in the absence of Dnmt1 some other mechanisms are also used, for example in a subset of genes imprinted in mouse placenta, such as *Cd81*, *Phlda2*, *Kcnq*, *Osbpl1* and also *Ascl2/Mash2* (Caspary et al., 1998; Lewis et al., 2004). In these genes, a placenta-specific mechanism based on chromatin modifications rather than DNA methylation has evolved in order to maintain imprinting status (Umlauf et al., 2004). It has been discovered that differential histone modifications are common features of many imprinted genes but the exact function of chromatin modifications either as a cause or a result of allele-specific expression remains to be elucidated.

The important question for maintenance of imprinting is how DMRs manage to resist demethylation. Both active and passive mechanisms are believed to take part in demethylation

(**Figure** 1.2), with the paternal genome usually being subject to this process first, just after fertilisation. The maternal genome is affected later, by an inability to maintain methylation during DNA replication (Rougier et al., 1998; Oswald et al., 2000). Due to the fact that demethylation might be caused by chromatin remodelling of the sperm genome, it is believed that the maternal genome requires a protection mechanism against active demethylation during fertilisation. As each of the parental genomes seems to employ different methods of protection from demethylation, this might provide an explanation for the majority of methylation imprints being present on maternal genes.

The imprints in both of the germlines need to be read, and that is converted into differential gene expression. Regulation of imprinting is very complex, and a variety of epigenetic mechanisms have been implicated to play a role in it, including modifications of promoter sequences, silencers, boundary elements and perhaps even of overlapping antisense transcripts (Ferguson-Smith, 2011). In this way, imprinted genes control transcription using typical mechanisms, but unlike most genes they are subject to further regulation by differential epigenetic modifications on parental chromosomes.

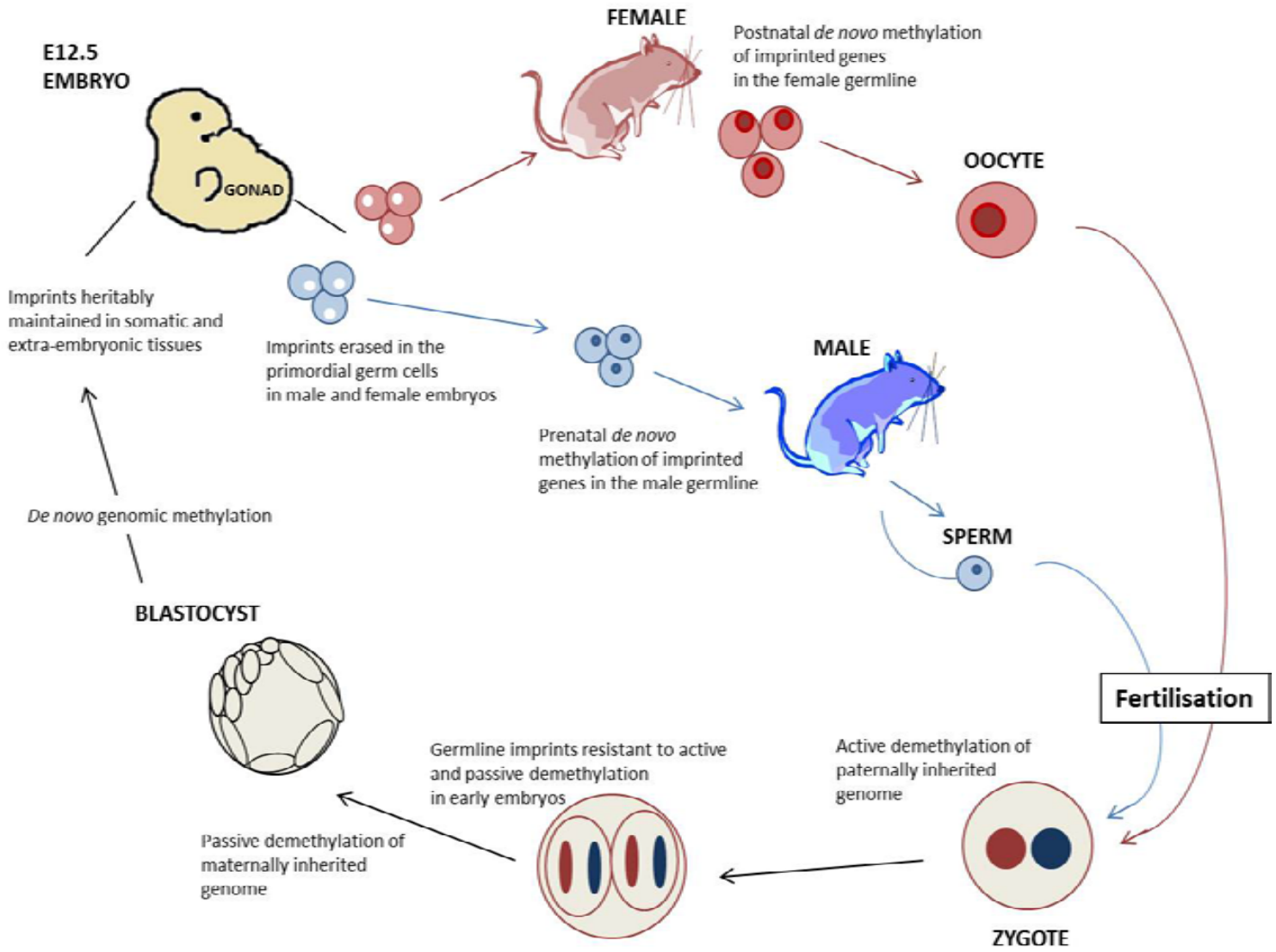
E12.5
EMBRYO
GONAD
FEMALE
Postnatal *de novo* methylation
of imprinted genes
in the female germline
OOCYTE
Imprints heritably
maintained in somatic and
extra-embryonic tissues
Imprints erased in the
primordial germ cells
in male and female embryos
MALE
Prenatal *de novo*
methylation of imprinted
genes in the male germline
SPERM
De novo genomic methylation
BLASTOCYST
Fertilisation
Germline imprints resistant to active
and passive demethylation
in early embryos
Active demethylation of
paternally inherited
genome
Passive demethylation of
maternally inherited
genome
ZYGOTE

Figure 1.2 Establishment, maintenance, and erasure of genomic imprints during mammalian development.

Imprinting in the germline is acquired in a sex-dependent manner, as maternal and paternal ICRs become hypermethylated in oocytes and sperm. Imprints persist after fertilisation despite reprogramming and changes in DNA methylation; active demethylation of the paternal genome in the zygote does not influence paternal imprints, nor does passive maternal demethylation in the preimplantation embryo change maternal imprints. At the end of the preimplantation stage of development *de novo* DNA methylation takes place and after that imprints persist in somatic cells throughout the entire lifetime. In preparation for transmission to the progeny, DNA methylation erasure occurs during migration of PGCs into the genital ridge and following that, imprinting status is re-established during gametogenesis. Figure adapted from (Bartolomei and Ferguson-Smith, 2011).

1.1.3.2 Clustering of imprinted genes

There are a few imprinted genes that do not appear to be closely linked to other imprinted gene, such as *Inpp5f*, *Nnat*, *Nap1l5* or *Peg13* (Kagitani et al., 1997; Smith et al., 2003; Choi et al., 2005), however, the majority tend to be localised within clusters which usually consist of a group of protein-coding genes and at least one non-coding RNA (ncRNA). The majority of imprinted clusters are controlled by a maternally inherited methylation mark, including *Igf2r/Air, IC2/Kcnq1, Gnas*, and *PWS/AS* regions, while only three paternally methylated germline-derived DMRs have been found up to date: *Igf2/H19* ICR, the *Dlk1-Dio3* imprinting control region, and the control region regulating the *Rasgrf1* locus. The so-called imprinting control region is a major *cis*-acting element that governs the cluster, however other elements might modify its function. These ICRs are able to control the genes within the given cluster as they are subject to differential methylation between the two copies in germ cells. In the case of imprinted genes that do not lie within clusters, typically their differentially methylated promoters act as their ICRs.

Two types of imprinted gene clusters have been identified: one with ICRs methylated during spermatogenesis following paternal inheritance and others with ICRs methylated during oogenesis after maternal inheritance. A number of common features, as well as some differences, can be drawn between the modes of regulation of parental allele-specific expression of imprinted genes situated within different clusters. The characteristic shared between all imprinted domains discovered so far is the ability of Dnmt3a to function in *cis*- in order to implement a germline-derived differentially methylated mark. Methylation on the maternal chromosome of the imprinted domain is usually located in a region responsible for repressing the protein-coding genes. Thus the expression of protein-coding genes is typically associated with a maternally methylated imprinting control element, with the exception of the *PWS/AS* domain, consisting of several paternally expressed protein coding genes. This region, however, has been demonstrated to have an intricate evolutionary origin and, in addition, two ancestral protein-coding genes situated within this region, *Ube3a* and *Atp10a,* exhibit maternal expression (Rapkins et al., 2006). Similarly, genes with a methylated paternally inherited control region show expression of the protein-coding genes from the paternally inherited chromosome that is controlled by a methylated paternally inherited imprinting control region. ncRNAs are expressed from the unmethylated chromosome and the ICR is usually a promoter for them. The reason for the epigenetic mechanisms of the two parental germlines that apply DNA methylation marks at different places at these particular loci is still unclear.

Allele-specific changes in DNA replication timing during S-phase are also common characteristics of imprinted genes, as asynchronous replication is established in the gametes and persists throughout development, which means that it may function as a primary epigenetic marker for distinguishing between the parental alleles (Simon et al., 1999). It has been shown that differential replication timing is linked to imprinted genes in a wide range of cell types, and occurs in the pre-implantation embryo following fertilisation. The erasure of this pattern takes place before meiosis in the germline, and afterwards parent-specific replication timing is reset in both sexes in late gametogenesis. The paternal copy of DNA in imprinted regions typically replicates earlier than the maternal one, however the underlying reason for this phenomenon is not understood. Furthermore, meiotic recombination occurring with different frequencies is commonly found in or next to imprinted clusters, along with increased recombination rate during male meiosis (Robinson and Lalande, 1995). The exact nature of association of these epigenetic changes with methylation and changes in chromatic structure remains to be elucidated. It is possible that all of the aforementioned epigenetic modifications could be linked to imprinting, however it is not known if chromatin modifications play roles in imprinting independent of DNA methylation, whereas the crucial role of methylation in maintenance of imprints has been established (Moore and Haig, 1991).

The regulation of genomic imprinting is clearly very complex, and the employed mechanisms seem to differ in mode of action depending on parental allele and specific gene clusters. Evidently very tight control over the regulation of these complicated mechanisms is needed in order to avoid detrimental consequences, as imprinted genes play vital roles in growth and metabolism, and as a consequence their disruption can result in quite severe human syndromes (discussed below).

1.1.4 Roles of imprinted genes in growth and metabolism

In order to determine the size of an organism, growth needs to be precisely regulated at different levels, from cellular to systemic, by a variety of molecular mechanisms. The mechanisms controlling rates of cell growth, differentiation, proliferation and apoptosis need to be carefully coordinated for normal growth and development to commence, and during the course of development the provision of nutrients, hormones, growth factors and energy is also of great importance. Mouse knockout experiments have provided useful information about functions of individual imprinted genes. By these means it has been discovered that many

genes showing allele-specific expression are able to govern correct development, as in many cases lack of imprinted genes led to perturbed growth that affected the ultimate embryo size.

Expression of the majority of imprinted genes has been identified in embryos at early stages of development and/or in placenta, an organ with a pivotal role in nutrient provision for developing embryos. This led to speculation that the effects of imprinted genes on growth might be consequence of either their perturbed expression in embryo or through discrepancies in correct nutrient supply due to abnormal expression in the placenta. In agreement with the conflict theory, conflict over nutrient acquisition would predict that embryo-expressed genes favour resource acquisition while genes expressed in the placenta try to limit resource supply. Further to that, regulation of metabolism is another known function of some imprinted genes. Various imprinted genes were found to be capable of influencing glucose tolerance, food intake, and adiposity. Interestingly, several imprinted genes have even been implicated in influencing postnatal behaviour (Plagge et al., 2005; Garfield et al., 2011). As many features identified in mice with altered imprinted gene expression can be compared with phenotypes seen in humans with perturbed function of the orthologous genes, some of them will be discussed here in more detail. A group of imprinted genes with their sites and modes of expression are shown in **Table** 1.1 whilst the most widely studied human disorders resulting from abnormal changes within imprinted genes are presented in **Table** 1.2.

One of the most widely studied growth factors, the insulin like growth factor (Igf) forms a part of a major growth signalling system in mouse embryo that includes two ligands, Igf1 and Igf2, two membrane associated receptors, Igf1r and Igf2r and several Igf-binding proteins (Igfbps). A 40% growth reduction has been reported in neonatal mice with disrupted paternally expressed *Igf2* or homozygous disruption of the non-imprinted *Igf1* (DeChiara et al., 1991; Liu et al., 1993), whilst ablation of maternally expressed *Igf2r* resulted in significant overgrowth, elevated serum and tissue levels of *IGF2* and frequent perinatal lethality (Lau et al., 1994; Leighton et al., 1995; Ludwig et al., 1996). The cause of the observed lethality has been associated with an excess of IGF2 overstimulating IGF1R, due to lack of IGF2R-mediated turnover, which has been proven by generation of fully viable *Igf2/Igf2r* double mutants (Lau et al., 1994; Ludwig et al., 1996). Additional information on the *in vivo* interactions between members of the *Igf* family was provided by characterisation of mice with targeted deletion of both *Igf1* and *Igf2* and also those lacking *Igf1* and *Igf1r* (Liu et al., 1993). The survival of nullizygous *Igf1* knockout mice exhibiting 40% growth reduction depends on the genetic

background but an even more dramatic phenotype (45% of normal growth and immediate death after birth due to respiratory failure) has been observed in *Igf1r* nullizygous animals.

	Maternally expressed	Paternally expressed
Embryo	*Cdkn1c, Gtl2, Grb10, Igf2r*	*Dlk1, Igf2, Peg1, Peg3, Zac1*
Placenta	*Ascl2, Cdkn1c, Grb10, H19, Igf2r, Phlda2*	*Igf2 P0, Peg1, Peg3, Peg10, Rtl1, Zac1*
Metabolism	*Atp10c, Gnasα , Grb10*	*Dlk1, Dio3, Gnasxl, Igf2, Zac1/Hyma1, Peg3, Rasgrf1*
Behaviour	*Ndn, Nesp55, Ube3a*	*Gnasxl, Grb10, Peg1, Peg3, Rasgrf1*

Table 1.1 Modes of expression and sites of action of several imprinted genes.
Maternally and paternally expressed mouse imprinted genes affecting embryonic and placental growth, metabolic homeostasis and behaviour (Barlow et al., 1991; Bartolomei et al., 1991; DeChiara et al., 1991; Da Costa et al., 1994; Kagitani et al., 1997; Lefebvre et al., 1998; Li et al., 1999; Grandjean et al., 2000; Constancia et al., 2002; Charalambous et al., 2003; Font de Mora et al., 2003; Ma et al., 2004; Plagge et al., 2004; Salas et al., 2004; Curley et al., 2005; Plagge et al., 2005; Takahashi et al., 2005; Ono et al., 2006; Yevtodiyenko and Schmidt, 2006; da Rocha et al., 2007; Lin et al., 2007; Lui et al., 2008; Sekita et al., 2008; Garfield et al., 2011).

Igf2/Igf1r and *Igf1/Igf2* double mutants exhibited identical phenotypes, suggesting that IGF1R is responsible for mediating growth effects of both IGF ligands (Liu et al., 1993). *Igf1/Igf1r* double mutants were indistinguishable from *Igf1r* knockout mice, unequivocally demonstrating that IGF1 interacts exclusively with IGF1R. A 70% reduction in normal body weight of *Igf2/Igf1r* double mutants, significantly more pronounced than in either of single knockout animals (Liu et al., 1993), implied interaction between these two genes and a role for an additional receptor with an effect on growth, identified later as insulin receptor (*IR)* (Louvi et al., 1997). The mitogenic effects of *Igf2* are in part regulated by insulin-like growth factor 2 receptor (*IGF2R*), also called the mannose-6-phosphate receptor (M-6-Pr), which has been identified as a negative regulator of *Igf2*. Following maternal transmission of the disrupted *Igf2r* locus significant embryonic overgrowth has been noted (Lau et al., 1994; Ludwig et al., 1996). Deletion of an element vital for repression of the paternal allele resulted in biallelic expression of *Igf2r* as did paternal inheritance of the non-imprinted allele, causing 20% fetal weight reduction maintained until adulthood (Wutz et al., 2001). The lethal phenotype of *Igf2r* maternal knockouts was overcome following loss of *Igf2*, as *Igf2/Igf2r* mutants were viable.

Human syndrome	Epigenetic causes	Clinical features
Beckwith–Wiedemann syndrome (BWS)	Epimutation of IGF2/H19 DMR1, epimutation of KCNQ1/CDKN1C DMR2 both on 11p15, hypomethylation of DMR2 (50%), hypermethylation DMR1 (2%–7%), PatUPD11, CDKN1C mutation	Pre/postnatal overgrowth, neonatal hypoglycemia, exompholos, macroglossia, hemihypertrophy, increased embryonal tumours
Prader–Willi syndrome (PWS)	De novo paternal deletion in 15q11-q13 (70%), MatUPD15 (29%), imprinting defects (1%)	Neonatal hypotonia, childhood obesity, cognitive impairment, behavioural characteristics, hypogonadism
Angelman syndrome (AS)	15q11.2-q13 deletion (70%) PatUPD15 (7%), UBE3A mutation (11%), methylation defects (3%), epimutation	Mental retardation, speech impairment, ataxia, seizure, microcephaly
Silver–Russell syndrome (SRS)	Paternal DMR1 hypomethylation at 11p15 (>50%), MatUPD7 (5%) Matdup11p15, unknown (30%)	Intrauterine/postnatal growth retardation, variable features (including 5th finger clinodactyl, learning disabilities)
Pseudohypo-parathyroidism type b (PHP1b)	Microdeletion upstream of GNAS at 20q, maternal hypomethylation, PatUPD20	Resistance to parathyroid hormone, hypocalcaemia, hyperphophatemia
Transient neonatal diabetes mellitus type (TNDM)	Paternal UPD6, paternal duplication 6q22-q23, maternal hypomethylation at ZAC1/PLAGL1 DMR	Growth retardation, hyperglycemia with low/undetectable insulin resolved by 6 months old, 40% Type-2 diabetes later in life
Maternal UPD14 (and UPD14 mat-like) syndrome	MatUPD14, paternal microdeletions at 14q32.2, hypomethylated DMRs at DLK1/GTL2	Low birth weight, short stature, characteristic faces, premature puberty, hypotonia
Paternal UPD14 (and UPD14 pat-like) syndrome	PatUPD 14, maternal microdeletions at 14q32.2, hypermethylation at DMRs at DLK1/GTL2	Bell-shaped thoracic cage, mental retardation, placentomegaly, polyhydramnios

Table 1.2 Several widely-studied human imprinting disorders with their epigenetic causes and observed clinical features. Table adapted from (Bartolomei and Ferguson-Smith, 2011).

Moreover, although individual *Igf1r* and *Igf2r* knockout mice were not viable, loss of both of these receptors did not result in lethality, which has been associated with *Igf2* functioning through *IR*, as *Igf2/Igf1r/Igf2r* triple mutants were nonviable (Ludwig et al., 1996).

Even though the knockout experiments helped to delineate *in vivo* roles for a number of imprinted genes, because many of them are expressed simultaneously in embryo and placenta it proved difficult to pinpoint their functions in each of these lineages. In particular, altered imprinted gene expression in the placenta might directly change growth or function of the placenta, with an indirect effect on overall growth of the embryo. Both embryo and placenta are affected in *Igf2* and *Igf2r* mutants, but deletion of *Igf2P0* transcripts provided a useful tool for identifying the role of *Igf2* specifically in the placenta. Even though only 10% of the placental *Igf2* transcripts arise from the tissue specific promoter *Igf2P0,* loss of *Igf2P0* transcripts leads to restriction of placental size during early- and mid-gestation comparable to that observed for complete *Igf2* knockout embryos (DeChiara et al., 1991; Constancia et al., 2002). Interestingly, growth retardation of the placenta in *Igf2P0* mice had a relatively small influence (embryos weighed 96% and 78% of wild type at E16 and E19, respectively) on overall embryonic growth retardation compared with *Igf2* knockout embryos (approximately 60%).

One of the best characterised human imprinted disorders is Beckwith-Wiedemann syndrome (BWS), localised to human chromosome 11p15.5 containing a cluster of 15 genes, 9 of which are imprinted (Walter and Paulsen, 2003). Up until now three imprinted genes within this cluster have been most commonly associated with BWS, that is *IGF2*, *H19* and *CDKN1C/p57^{KIP2}* (Maher and Reik, 2000). Individuals affected by BWS suffer from intrauterine overgrowth of both embryonic and extra-embryonic tissues, with overgrowth persisting into adulthood. Furthermore, they display macroglossia (hypertrophy of the tongue), exomphalos (anterior abdominal wall defects) and a predisposition to childhood cancers (Maher and Reik, 2000). Around 20% of sporadic BWS cases are associated with *IGF2* elevated expression (and decrease in *H19* expression) resulting from pUPD of the locus, with two paternally-derived copies of chromosome 11p15 and no maternal contribution for that region (Henry et al., 1991). In many cases an increase in *Igf2* expression seems to play a crucial role in causing overgrowth, including the vast majority of BWS patients who lack cytogenetic abnormalities (Weksberg et al., 1993). *IGF2* imprinting is typically disturbed by changes in the methylation status of ICRs that result in both parental alleles adopting the epigenotype of the expressed paternal allele (Maher and Reik, 2000). *H19*, a maternally expressed, untranslated gene located in the vicinity of *IGF2* on chromosome 11 can also be silenced as a result of alterations in methylation status of the parental alleles (Maher and Reik, 2000). Another imprinted gene,

the maternally-expressed *p57^{KIP2}* gene also lies within the BWS locus. Mutations in this gene have been reported in 5-10 % of sporadic and 40 % of familial BWS cases (Weksberg et al., 2005). Interestingly, the symptoms in these patients resemble ones noted for cases with disrupted *IGF2/H19*, although the expression or methylation of both of these genes is not altered (Maher and Reik, 2000), which might indicate that patients with *CDKN1C* mutations might lack protein involved in the IGF2 signalling pathway. Indeed, one of the suggested roles for *Igf2* has been negative regulation of *Cdkn1c* (Grandjean et al., 2000). Another mouse model with loss of *Igf2* imprinting as well as inactivation of *p57^{KIP2}* has been generated in order to understand the possible relationship of *p57^{KIP2}* and *Igf2* genes in the aetiology of BWS (Caspary et al., 1999). The mutant mice exhibited a number of BWS characteristics, such as placentomegaly, kidney dysplasia, macroglossia, cleft palate and polydactyly and some of the observed phenotypes were found to depend on *Igf2*. Additionally, it has been found that both of these genes are acting in an antagonistic manner in two of the affected tissues (Caspary et al., 1999), adding to the concept that BWS results from a mutation in either *p57^{KIP2}* or *Igf2* gene. BWS can also be a consequence of loss of methylation on the maternal allele at the ICR located within *KCNQ1*, which was originally identified in BWS cases with inversion breakpoints in this region. This has been linked to biallelic *IGF2* expression without disruption of imprinted *H19* expression and normal methylation patterns at the *IGF2*/*H19* locus, which could indicate *IGF2* expression being controlled independently of *H19* in a manner yet to be elucidated. A schematic representation of the BWS locus and mechanisms regulating imprinted genes within this region is presented in **Figure** 1.3.

Imprinted genes have also been implicated in other human disorders, such as Prader-Willi and Angelman syndromes (PWS/AS) which have been mapped to an imprinted locus on human chromosome 15 (Ohta et al., 1999). Patients suffering from AS exhibit ataxia and severe mental retardation, whilst those with PWS have obesity, mild mental retardation and short stature (Walter and Paulsen, 2003). Both of these disorders are believed to affect neurological development and are results of deletions and UPDs at the *PWS/AS* locus (Mann and Bartolomei, 1999). PWS is caused by a deficiency of paternal gene expression and AS is the switch between the maternal and paternal epigenotypes resulting from a deficiency of maternal gene expression. The AS/PWS imprinting control centre deletions have been found in some of AS patients. On the other hand, thorough analysis of both human patients and mouse models suggests the contribution of other genes to the AS phenotype (reviewed in Buiting, 2010).

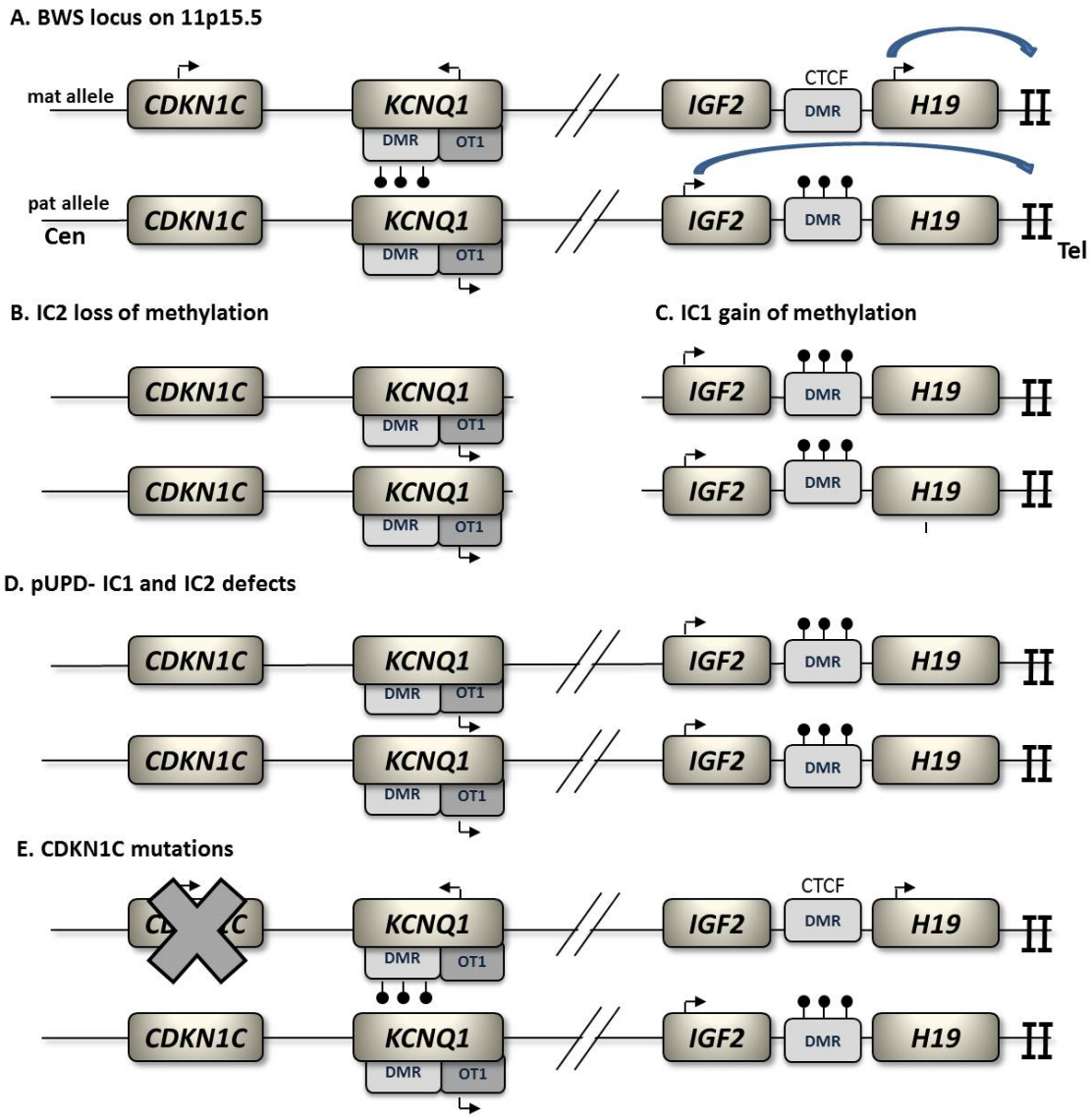

Figure 1.3 Schematic representation of the BWS locus on 11p15.5 (not drawn to scale).

H19 and *IGF2* imprinting is regulated by IC1 acting as an insulator or chromatin boundary element. IC1 on the maternal allele is unmethylated, which allows for binding of the CTCF insulator protein and prevents the access of the *IGF2* promoter to downstream enhancers so that *H19* maternal copy utilises these enhancers and is transcribed. Methylation of IC1 on the paternal chromosome blocks binding of CTCF to IC1, thus *IGF2* can access downstream enhancers and is expressed whereas *H19* is silenced. **A)** Normal parent-of-origin-specific imprinted allelic expression within BWS locus, **B)** and **C)** only show the region that is altered as a result of loss (IC2) and gain (IC1) of methylation, respectively, **D)** IC1 and IC2 defects during pUPD, **E)** CDKN1C mutations. IC: imprinting centre, Cen- centromere, Tel- telomere, mat- maternal, pat- paternal, DMR- differentially methylated region, OT1- KCNQ1 antisense transcript KCNQ1OT1, arrows- expression of a gene, filled lollipops- hypermethylation, bars at the telomeric region- enhancer. Figure adapted from (Choufani et al., 2010).

Another complex human disorder associated with an imprinted locus is Silver-Russell syndrome (SRS), characterised by both intrauterine and postnatal growth retardation as well as other distinct characteristics, including triangular facial features, hemihypertrophy of trunk and limbs, brachydactyly of the fifth finger and cranial sparing (Preece, 2002). Around 10% of SRS cases are associated with mUPD of chromosome 7 which consists of at least three imprinted genes: *MEST* and *COPG2* at 7q32 and *GRB10* at 7p12 (Hannula et al., 2001). *Mest* has been identified as a paternally expressed growth enhancer as its ablation in mice resulted in growth retardation of both embryos and placentae (Lefebvre et al., 1998). The case of one patient with SRS that has been identified with mUPD of the 7q32 region has been confirmed (Hannula et al., 2001), however, the majority of cases are associated with mUPD of 7p11.2-p12 at which *GRB10* is situated (Preece, 2002). Two other genes within this region, biallelically-expressed *IGFBP1* and *EGFR* seem to be less likely than *GRB10* to be a cause of SRS. Targeted deletion of *Grb10* in mice resulted in overgrowth (Charalambous et al., 2003) and its overexpression caused the reciprocal phenotype (Shiura et al., 2005; Shiura et al., 2009). This was similar to the opposite growth phenotypes associated with paternal and maternal duplication, respectively, of mouse proximal chromosome 11, the region that includes *Grb10* (Cattanach et al., 1996). Arnaud et al (2003) demonstrated that there was no change in methylation status of *GRB10* ICRs in 24 SRS patients, suggesting another control mechanism for the expression of *GRB10*, if indeed it is the cause of SRS. It is yet to be established if *GRB10*, *MEST* or both of these genes really play a role in causing SRS, and recently the *IGF2* gene, known for its crucial role in control of growth, has been implicated as the cause of some SRS cases. In 2005 the hypomethylation of the differentially methylated ICR of *IGF2-H19* at chromosome 11p15 was reported in a few SRS patients for the first time (Gicquel et al., 2005), and further studies have confirmed this finding in more SRS patients in whom reduction or loss of methylation at telomeric ICR1 on chromosome 11 was found to be a likely primary cause of SRS (Bliek et al., 2006; Eggermann et al., 2006; Netchine et al., 2007; Yamazawa et al., 2008). It has also been found that reciprocal methylation changes within the *IGF2-H19* locus were observed in a small group of patients (5%-10) suffering from BWS. Recent study of 201 patients with SRS or SRS-like phenotypes have provided more evidence for changes within *IGF2-H19* locus as a cause of SRS, as these kinds of epimutations were recognised in approximately 40% of SRS patients (Bartholdi et al., 2009). This study was also the first one to report familial cases of hypomethylation at the *IGF2-H19* locus (Bartholdi et al., 2009).

Reciprocal methylation changes at the ICR controlling *IGF2-H19* lead to opposite alterations within *IGF2-H19* expression and subsequently, can result in BWS and SRS as two

contrasting disorders. It has been shown that reciprocal *IGF2-H19* imprinting is controlled by DNA methylation of the ICR that blocks binding of the insulator protein CTCF. A recent study has demonstrated that altered histone modifications, changes within CTCF-cohesin binding and DNA methylation at the ICR of BWS and SRS can be associated with the higher chromatin structure at the *IGF2-H19* locus (Nativio et al., 2011). Specific changes within the ICR chromatin structure were shown to have contrasting effects on the parent-of-origin-specific looping conformation and also *IGF2- H19* expression potential, demonstrating an interesting and novel case of modified transcriptional genomic neighbourhood being able to participate in causing human disease.

In contrast to the abovementioned genes, the *Gnas* locus, located on mouse chromosome 2, is typically involved in the regulation of metabolism, rather than growth (for more details see Section 1.1.4 and Chapter 5). The *Gnas* locus consists of a maternally-expressed *Nesp* gene as well as paternally expressed genes, *Nespas*, *Gnasxl* and *Exon1a,* and also *Gnas* (Plagge and Kelsey, 2006), which is biallelically expressed in the majority of tissues but maternally expressed in the proximal renal tubules, anterior pituitary gland, thyroid gland, ovary (Hayward et al., 2001; Germain-Lee et al., 2002; Mantovani et al., 2002) and white and brown adipose tissue (Yu et al., 1998). Exon 2 is a transcript shared between all members of the *Gnas* family except for *Nespas* (which generates a non-coding RNA). Knockout experiments demonstrated that *Gnas* has different maternal and paternal gene products, and mice lacking *exon 2* on the maternal and paternal alleles exhibited reciprocal metabolic phenotypes (Yu et al., 1998; Yu et al., 2000; Yu et al., 2001). Disruption of *Gnas* through the maternal line resulted in a hypometabolic phenotype while disruption through the paternal line resulted in mice that were lean and hypermetabolic. The metabolic phenotype of mice lacking *Gnasxl* was similar to that observed for animals with paternal transmission of the *Gnas* exon 2 deletion (Plagge et al., 2004), whereas paternal deletion of *Gnas* exon 1 resulted in a phenotype that resembled that of maternal exon 2 ablation (Chen et al., 2005). As a result, *Gnas* and *Gnasxl* exhibit reciprocal effects on glucose and lipid metabolism and these opposing effects of maternally and paternally expressed products of the *Gnas* locus can be considered to support the parental-conflict hypothesis of imprinting.

The imprinting of *GNAS* locus in humans has clinical significance, as heterozygous inactivating mutations within *Gsα*-encoding *GNAS* exons have been identified in individuals with pseudohypoparathyroidism type 1a (PHP-Ia), who also exhibit physical features called Albright's hereditary osteodystrophy (AHO). AHO features include subcutaneous ectopic

ossifications, obesity, cognitive defects and brachydactyly. Patients with typical AHO features but not displaying hormone resistance, who are said to suffer from so-called pseudopseudohypoparathyroidism (PPHP), also carry heterozygous inactivating *Gsα* mutations. Maternal inheritance of this mutation results in PHP-Ia (AHO plus hormone resistance), while paternal inheritance leads to PPHP (AHO only) (Bastepe, 2008). Predominantly maternal expression of *Gsα* in specific tissues is thought to be a cause for this imprinted mode of inheritance of hormone resistance.

In addition, some individuals suffer from PHP-Ib caused by loss of imprinting at the exon A/B DMR that determines tissue-specific monoallelic expression of *GNAS*. It is believed that a marked reduction of *Gsα* levels in this epigenetic disorder is a result of *cis*- silencing of *Gsα* expression in maternally expressed tissues. PHP1b is, interestingly, a unique imprinted gene syndrome with *cis*-acting mutations altering methylation of germline-derived imprint marks (Kelsey, 2010). Despite some overlapping features of both PHP1a and PHP1b, and the fact that they both involve decreased *Gsα* expression in tissues with allele-specific *GNAS* expression, the underlying basis for both of these disorders and all the differences between them are yet to be elucidated.

Transient neonatal diabetes mellitus type (TNDM) is a rare type of diabetes which presents in the neonatal period, resolves in the first months after birth, but often recurs in later life (Temple and Shield, 2002). The symptoms usually include growth retardation and hypoglycaemia. TNDM is associated with imprinted region situated on human chromosome 6q24 that encompasses two imprinted, paternally expressed genes: *ZAC* (which encodes a proapoptotic zinc finger protein) and *HYMA1* located approximately 50kb upstream of *ZAC* (which encodes an untranslated mRNA) (Gardner et al., 2000; Arima et al., 2001). Rather than being a result of mutation in these genes, TNDM is a consequence of their overexpression due to pUPD6 in 40% of cases, duplication of 6q24 on the paternal allele in another 40% or hypomethylation at the DMR on the maternal allele in 20% of cases (Temple and Shield, 2010). Mice with overexpression of the human TNDM locus were shown to have hyperglycemia and impaired glucose tolerance. The expression of human *ZAC* and *HYMA1* in these animals recapitulated the distinct characteristics of TNDM and indicated a role of abnormal development of the endocrine pancreas and defective β-cell function in this disorder (Ma et al., 2004).

Analysis of TNDM patients provided interesting insights into the causes of imprinting disorders. Many patients with maternal hypomethylation at the TNDM locus also show

hypomethylation of other maternally methylated imprinted genes throughout the genome (*GRB10*, *MEST*, *PEG3* and *KvDMR*) (Mackay et al., 2006), which could point at the existence of a novel imprinting syndrome resulting from maternal hypomethylation at multiple loci, as has also been described in several publications (Rossignol et al., 2006; Boonen et al., 2008). Up until now, the exact causes of TNDM and hypomethylation syndrome have not been identified and future studies of these disorders are necessary to gain further insights not only into the biological mechanisms of imprinting, but also the role of epigenetics in diabetes.

Other imprinted genes have also been implicated in the regulation of both growth and metabolism. This includes the Delta like-homologue 1 gene (*Dlk1*), whose ablation in mice resulted in significant growth retardation and later on in life in increased adiposity associated with adipocyte hypertrophy and altered differentiation (Moon et al., 2002). Conversely, overexpression of this gene led to a reciprocal, overgrowth phenotype with reduced adiposity, hyperglycemia and insulin resistance (Lee et al., 2003). As a result, *Dlk1* is believed to play a role in controlling adipocyte differentiation and act as a paternally expressed growth enhancer, in agreement with the parental conflict hypothesis. Overexpression of *Dlk1* in skeletal muscle, along with *Peg11*, is thought to be a source of the *callipyge* phenotype in sheep (Cockett et al., 2005), however its disruption and definite implication in any human disorders are yet to be reported.

Overall, even though the group of imprinted genes within mammalian genomes is relatively small, their roles in development and postnatal metabolic homeostasis seem to be of great importance, as confirmed by severe phenotypes of knockout mice lacking some of these genes alongside many related human disorders. Knockout mice and UPD mouse models have been a powerful tool to study genomic imprinting and have helped with characterisation of recessive diseases and genomic imprinting disorders in humans. Recent progress in genomic technologies as well as conventional microsatellite marker methods that played a role in a functional and mechanistic investigation of UPD, have helped gather clinically valuable data providing further insight into diverse genetic processes and disease pathogenesis. Such investigations might benefit affected children and families as with more detailed knowledge clinicians will be able to define recurrence risk, predict phenotype, and suggest medical treatment.

1.2 Growth factor receptor bound protein 10

1.2.1 The Grb7/10/14 protein family

1.2.1.1 Protein structure

Growth factor receptor binding protein 10 (Grb10) is a member of an adapter protein family identified in both humans and mice that also includes Grb7 and Grb14. They share a distinct, highly conserved structure with almost 60% similarity between Grb7 protein family members that is also present in the *Caenorhabditis elegans* Mig-10 protein and thus referred to as the GM region, for Grb and Mig (Manser et al., 1997). This conserved region is represented by N-terminal proline rich sequences, a Ras-association-like domain (with homology to the *C.elegans* Mig-10 protein), a central pleckstrin homology (PH) domain, a C-terminal Src homology 2 (SH2) domain and a conserved, unique receptor binding domain situated between the PH and the SH2 domains named BPS. Mig-10 seems to have a function similar to Grb10 as it is responsible for transducing signals required for cell migration (Manser et al., 1997). A recent study of tandem RA-PH domains of Grb10 and Grb14 has provided valuable details of mechanism by which Grb10 and Grb14 proteins are involved in IR signalling downregulation (Depetris et al., 2009, see **Figure** 1.4 and below). The tandem RA-PH domains of Grb7/10/14 are conserved in MRL proteins (Holt and Daly, 2005), another family of adapter proteins that also includes the *C.elegans* protein MIG-10 (Manser et al., 1997), the mammalian proteins RIAM (Lafuente et al., 2004; Jenzora et al., 2006) and lamellipodin (Lpd) (Krause et al., 2004) and the *Drosophila melanogaster* protein pico (Lyulcheva et al., 2008).

A recent report has for the first time provided information on the *Drosophila pico* gene being required for growth at the tissue and organismal level. Lower levels of *pico* expression caused a decrease in cell division rates along with growth retardation, an increase in monomeric (G) : filamentous (F) actin ratios and lethality (Lyulcheva et al., 2008), whereas *pico* overexpression caused reciprocal effects and resulted in increased growth and cell proliferation. These effects were confirmed in the mammalian orthologue of *pico*, *Lpd*, as both pico and Lpd were found to exert changes in actin dynamics and serum response factor (SRF) activation, consequently linking extracellular signalling to tissue growth (Lyulcheva et al., 2008).

The most highly conserved region between members of the Grb10 protein family is the SH2 domain, which shares 72% nucleotide identity between Grb10 and Grb14 and 67% between Grb10 and Grb7. This region plays a pivotal role in binding to receptor tyrosine kinases and other intracellular signalling molecules, such as Nedd4 (Huang and Szebenyi, 2010). Most probably, the SH2 domain is responsible the ability of Grb10 to efficiently bind to both insulin receptor and insulin-like growth factor receptor, however it is also able to interact with specific cytosolic proteins in a manner independent of tyrosine phosphorylation (Nantel et al., 1998). In contrast to the majority of SH2 motifs that are usually monomeric, this domain of Grb10 crystallises into a dimer which favours binding to IR and IGFR (Stein et al., 2003). The phosphorylated activation loops of the IR and IGFR are thought to show affinity to the Grb10 SH2 domain, as it preferentially interacts with turn-containing phosphotyrosine sequences instead of an extended conformation, which is the case for other SH2 domains. The unique BPS domain, initially identified in Grb10 (He et al., 1998), shares 56% and 63% amino acid sequence identity with Grb7 and Grb14, respectively. It belongs to a subset of intrinsically unstructured proteins (IUPs) (Moncoq et al., 2003). The isolated BPS maintains its activity and ability to interact with the activated IR and IGFR (He et al., 1998) and can inhibit catalytic activity of IR (Stein et al., 2001). Both SH2 and BPS domains of Grb10 are thought to have comparable ability to bind to the phosphorylated IR. The PH domain of Grb7/10/14 family members shares 60% sequence identity among them. PH domains are very common in the human proteome, usually responsible for facilitating localisation of proteins to membranes by binding to phosphoinositides. This mode of action, however, is debatable in the case of the human Grb10β isoform as it is still able to translocate to the cell membrane even though it lacks the PH domain (Dong et al., 1997). A Ras-association-like (RA) domain, located within the centre of the GM (Grb-Mig) region of Grb7/10/14, has been suggested to have a potential role in mediating interactions with members of the Ras protein superfamily, as has been previously described in the case of RasGTP effectors (Ponting and Benjamin, 1996). Presence of the highly conserved domains, discussed above, within Grb7/10/14 family highlights their capacity to bind and modify the activity of variety of proteins and, subsequently, regulate intracellular signalling.

Depetris et al (2009), as mentioned above, proposed a model for a multicomponent assembly by which domains of Grb10 and Grb14 proteins are able to negatively control insulin signalling. According to this model, Grb10 or Grb14 complex interacting with IR consists of: PH domain-mediated binding to phosphoinositides (their role is to target Grb proteins to membrane surfaces), the RA domain directing Grb10 proteins to activated GTPases and SH2

and BPS domains that interact with IR kinase domain at two different sites (Depetris et al., 2009). Consistent with this model, Grb10/14 capacity to regulate insulin receptor signalling is dependent upon all four interactions within their PH, RA, SH2 and BPS domains which have an ability to block further kinase-mediated phosphorylation events and, also to physically interrupt binding of IRS proteins with the insulin receptor. It is suggested that this multicomponent assembly might be necessary to permit for a sufficient amount of insulin receptor kinase signalling before the Grb10- or Grb14-mediated inhibition is established (Ceccarelli and Sicheri, 2009). Recent study showed Grb10 interaction with mammalian target of rapamycin (mTOR) *in vitro* and in cells, which was mapped to the sites situated within or in proximity of BPS or proline-rich domains of Grb10 (Hsu et al., 2011), providing further details of Grb10 mode of action within the pathway involved in insulin signalling regulation.

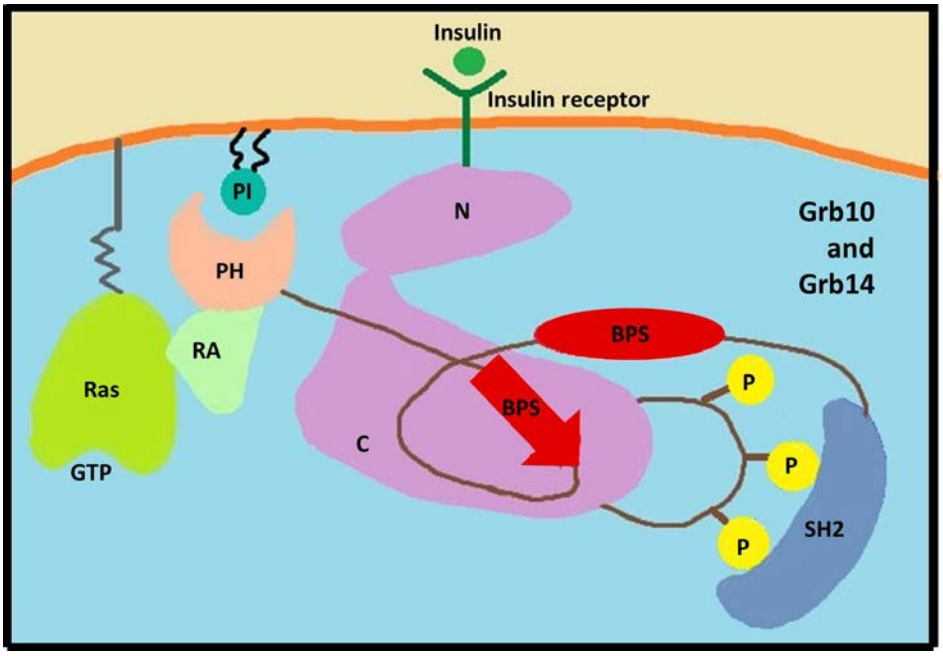

Figure 1.4 Schematic representation of Grb10 and Grb14-mediated negative regulation of IR signalling.

PH domain interactions with membrane-tethered Phosphoinositides (PI) target Grb proteins to membrane surfaces while the Grb RA domain interacts with activated GTPases accumulating upon insulin signalling. The SH2 and BPS domains bind the IR kinase domain at two phosphotyrosine sites (P) in the substrate binding cleft and the phosphorylated activation loop. No dimer or multimer arrangement of subunits is represented in this model. N, N lobe of insulin receptor kinase domain; C, C lobe of insulin receptor kinase domain. Figure adapted from (Ceccarelli and Sicheri, 2009).

Even though definitive roles for each of the Grb domains have not been fully elucidated yet, numerous studies have suggested that they are able to interact with a number of receptor and non-receptor signalling proteins (reviewed in Holt and Siddle, 2005). The conserved nature of the aforementioned protein family indicates important functions of its members, thus deciphering further details of potential functional redundancies between Grb proteins should provide invaluable insight into insulin signalling, diabetes and other disorders that result from abnormalities within Receptor Tyrosine Kinase (RTK) signalling.

1.2.2 *Grb10* gene and expression

Mouse *Grb10* is situated on the proximal region of chromosome 11, spans around 110 kb and consists of 18 exons (**Figure** 1.5). It is flanked telomerically by the dopa-decarboxylase (*Ddc*) and centromerically by cordon-bleu (*Cobl)* and *Egfr* genes. Its translational start sites are found in exon 3 and the termination site is located in exon 18. Most of the *Grb10* gene transcripts arise from the maternal chromosome, with *mGrb10α* and *mGrb10Δ* being two major species. Both transcripts are initiated in exon 1A, but *mGrb10Δ* lacks exon 5. It has proven difficult to pinpoint the differences in functions and tissue-specific expression between these two transcripts. Additionally, Sanz et al (2008) have identified an embryo-specific transcript initiating from exon 1A and splicing into exon 1C (Sanz et al., 2008). Paternal transcripts initiating from exons 1B1, 1B2 and 1C, splicing into exon 2, and with exons 5 and 6 either present or absent, have also been described (Arnaud et al., 2003).

The human *GRB10* gene, situated on chromosome 7 between the *DDC* and *COBL* genes, spans around 190kb and consists of 17 exons (22 if subdivided exons are considered). The hGrb10*γ* shares the most similarity with Grb7 and Grb14 and other Grb10 isoforms are formed by extensions at their N-terminal ends generated by alternative splicing with the use of different exons. The N-terminal region of Grb7/10/14 harbours the proline-rich region that contains a conserved P(S/A)IPNPFPEL sequence as well as other PXXP motifs (Holt and Siddle, 2005). Typically, sequences rich in proline interact with Src-homology 3 (SH3) and tryptophan-rich (WW) domains of other proteins. Two novel Grb10 interacting proteins, named GYGYF1 and GYGYF2, identified by yeast-two-hybrid screening, were found to bind to tandem proline-rich regions in the N-terminus of Grb10 via GYF motifs rather than SH3 domains (Giovannone et al., 2003). Both of the GYF proteins are thought to play a role in IGF1 signalling after experiments showed that stimulation of IGF1 receptor-expressing fibroblasts

with IGF1 increased binding of GIGYF1 to Grb10, and induced transient association of both of these proteins with the IGF1 receptors (Giovannone et al., 2003).

In 1998 *Grb10* imprinting status was first discovered in mouse (Miyoshi et al., 1998) and confirmed in humans two years later (Yoshihashi et al., 2000). This finding raised much interest because of a possible role for *Grb10* as a growth regulator, not least as a potential cause of Silver-Russell syndrome, due to the presence of *GRB10* on human chromosome 7 (see Section 1.1.5 for more details), and due to the location of *Grb10* on proximal chromosome 11 in mouse, a region previously linked to an imprinted growth phenotype (Cattanach et al., 1996).

The expression of mouse *Grb10* has been first reported in embryonic tissues of the heart, kidney, lung and liver as well as in the adult brain (Miyoshi et al., 1998), while paternal expression has been initially limited to adult tissues (Hikichi et al., 2003). Recent study by our lab has argued that within the brain *Grb10* is paternally expressed during fetal life into adulthood and that ablation of this expression causes changes within some aspects of social behaviour, especially social dominance (Garfield et al., 2011). In the same study maternal *Grb10* expression during fetal development has been noted in mesodermal and endodermal tissues but absent in the central nervous system (CNS) proper. The ventricular ependymal layers, the epithelium of the choroid plexus and the meninges were identified as sites of maternal *Grb10* expression in E14.5 brain. In consistence with the expression pattern during embryogenesis, predominantly paternal and almost completely absent maternal *Grb10* expression has also been observed in the adult brain (Garfield et al., 2011). Previous expression analysis in E14.5 embryos revealed *Grb10* maternal expression in the subependymal layers, the meninges and in the choroid plexus of the brain, in a variety of muscle tissue, liver, bronchioles, and cartilage of the atlas, ribs, and long bones (Charalambous et al., 2003). Additionally, maternal *Grb10* expression was clearly detectable in the developing tubules and the mesenchyme of the kidneys, the adrenal gland and the pancreatic bud. Adult expression of *Grb10* from the maternal allele was absent in the liver but highly pronounced in skeletal muscle, WAT, the intrinsic muscle of the tongue, and cells of pancreatic islets (Smith et al., 2007). Furthermore, in females maternal *Grb10* expression was present in the uterine horns and oviducts, whereas in male mice was noted in the Leydig cells of the testes.

The expression of human *GRB10* has also proven to be quite complex, with expression from the paternal allele in the human fetal brain, from the maternal allele in skeletal muscle and biallelic expression in peripheral tissues (Blagitko et al., 2000). The interesting pattern of paternal expression in the brain has been found to be conserved in humans and mice (Blagitko

et al., 2000; Arnaud et al., 2003; Hikichi et al., 2003) and more thorough investigation of *Grb10* allelic methylation patterns between these two species uncovered some similarities, such as maternal hypermethylation of a second CpG identified as a DMR (Arnaud et al., 2003). The authors have therefore suggested that any discrepancies in expression between humans and mice are due to differences in reading genetic marks rather than an acquisition of an imprint mark. Hikichi et al (2003) have also examined the mechanisms responsible for the regulation of mouse *Grb10* and human *GRB10* and found novel, brain-specific promoters that lead to paternal expression in the brain, in contrast to expression elsewhere that is either exclusively or predominantly maternal. As mentioned above, Garfield et al (2011) recently reported predominantly paternal *Grb10* expression in the adult brain which was studied by analysing *LacZ* expression in mice with a disrupted *Grb10* allele (Garfield et al., 2011). Paternal *Grb10* expression has been confirmed in thalamic, hypothalamic, midbrain and hindbrain nuclei, in septal nuclei and the cholinergic inter-neurons of the caudate putamen within the forebrain along with absence of cortical expression (Garfield et al., 2011). Median preoptic nucleus, medial habenular, medial amygdaloid nuclei and ventromedial hypothalamus were recognised as sites of biallelic *Grb10* expression in the brain.

In order to further explore the biological relevance of *Grb10* tissue-specific reciprocal pattern of imprinting, another study aimed to examine its conservation in humans (Monk et al., 2009). *GRB10* paternal expression was confirmed in human brain whereas maternal allele-specific expression was present in the placental villous trophoblasts (placental site necessary for nutrient transfer). The remaining fetal tissues showed biallelic *Grb10* expression. These findings highlight the potential evolutionally important role of *GRB10* placental expression in fetal growth control. Similarly to the situation in mouse, the maternal transcripts arise from a promoter region with no allelic chromatin differences located upstream of the ICR of the domain. Some features of the paternal brain-specific expression from the ICR are also reminiscent of situation in the mouse, as it is DNA-methylated on the maternal allele and is marked on the paternal allele by developmentally regulated bivalent chromatin, with the presence of both H3 lysine-4 and H3 lysine-27 methylation (Monk et al., 2009). This comparative analysis between mice and humans revealed significant similarities in *GRB10* imprinting mechanisms between these two species and suggested that conserved reciprocal allelic expression between placenta and brain indicated that imprinting of *GRB10* evolved to regulate different roles in mammalian growth and behaviour.

The mechanisms that govern the complex imprinting of mouse *Grb10* have been studied in detail (Arnaud et al., 2003; Hikichi et al., 2003; Sanz et al., 2008). Three CpG islands have

been localised in the promoter region of this gene. The first of the CpG islands (CpGl1) was hypomethylated on both alleles in all tissues and stages investigated, so it is does not form a DMR. On the other hand, a germline DMR (CpGI2) located 3' to exon 1A was hypermethylated on the maternal chromosome (Arnaud et al., 2003; Hikichi et al., 2003). The fact that methylation of CpGI2 permits for *Grb10* expression has been established by analysis of *Grb10* expression in primordial germ cell-derived mouse cloned embryos which showed imprint erasure and biallelic *Grb10* silencing (Lee et al., 2002). In addition, another study showed that ablation of *Grb10* maternal methylation in embryos lacking Dnmt3l results in silencing of *Grb10* gene (Arnaud et al., 2006).

A somatic, tissue-specific DMR that lies within CpGl3 appears to control the brain-specific transcripts that initiate from exons 1B1, 1B2 and 1C. CpGl3 is hypomethylated on the paternal allele but biallelically hypermethylated in peripheral tissues (Arnaud et al., 2003). The use of different promoters is linked to histone tail modifications. Histone tail modifications, in particular methylation of lysine 27 on histone H3 (H3K27me3) is usually present in the case of transcriptionally inactive chromatin. This repressive mark has been found by Sanz et al (2008) to be a very likely mechanism causing the promoter switch in *Grb10* as it was enriched on the unmethylated paternal allele at the germline DMR (CpGI2), whereas this was not the case in brain. Recent studies have found that the mouse *Grb10* DMR is vital for the imprinting within this locus (Shiura et al., 2009) and it is marked by mono-allelic bivalent chromatin, with enrichment of both H3K4me2 and H3K27me3 on the paternal allele (Sanz et al., 2008). Recent publication by Shiura et al (2009) demonstrated that the *Grb10* DMR controls in a tissue-specific manner a *Grb10* imprinting region that encompasses at least five imprinted transcripts of three genes: *Cobl*, *Grb10* Types I and II and *Ddc*-exon1 and –exon1a. Biased, maternally imprinted expression of *Ddc* in neonatal heart (consistent with previous finding by Menheniott et al., 2008), liver and yolk sac along with reciprocal imprinted expression of *Cobl* in yolk sac were reported. In addition, Shiura et al (2009) have established that genomic imprinting regulation is comparable between deletion of the *Grb10* DMR and fully methylated status of the maternal allele *Grb10* DMR.

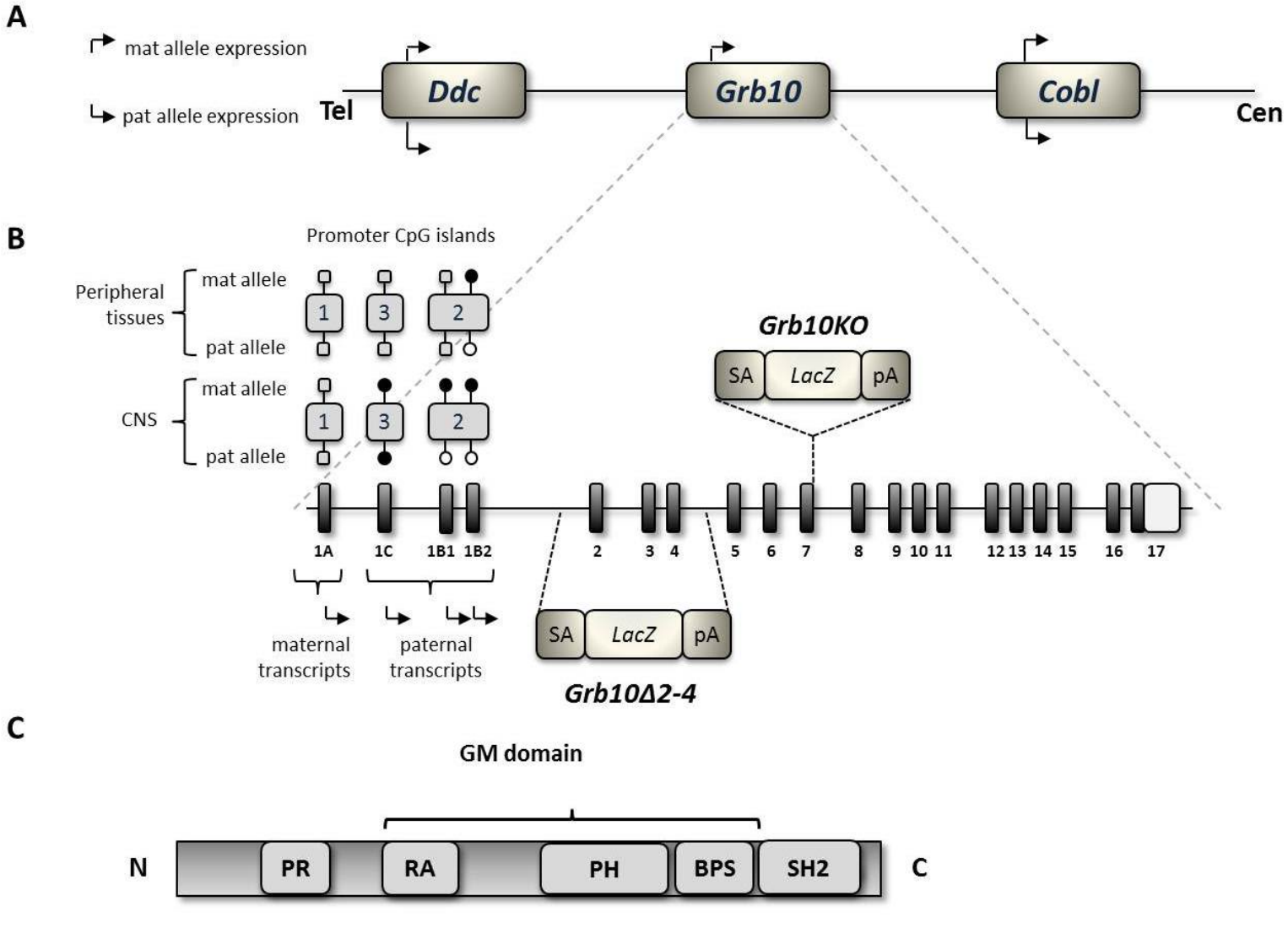
A
mat allele expression
pat allele expression
Tel
Ddc
Grb10
Cobl
Cen
B
Promoter CpG islands
Peripheral tissues
mat allele
pat allele
CNS
mat allele
pat allele
1
3
2
Grb10KO
SA
LacZ
pA
1A
1C
1B1
1B2
2
3
4
5
6
7
8
9
10
11
12
13
14
15
16
17
maternal transcripts
paternal transcripts
SA
LacZ
pA
Grb10Δ2-4
C
GM domain
N
PR
RA
PH
BPS
SH2
C

Figure 1.5 Schematic representation of *Grb10* gene localisation on mouse chromosome 11, *Grb10* gene organisation and Grb10 protein structure (not drawn to scale).

A) The localisation of *Grb10* gene, predominantly expressed from maternal allele but also showing brain-specific paternal expression, on proximal chromosome 11. *Grb10* is flanked by the biallelically expressed genes Dopa decarboxylase (*Ddc*) and Cordon blue (*Cobl*) which have been shown to exhibit biased expression in yolk sac, neonatal liver and heart (*Ddc*) and in yolk sac (*Cobl*), hence longer arrows representing slightly biased expression on the paternal and maternal alleles of these two genes, respectively. Tel, telomeric region; Cen, centromeric region. **B)** *Grb10* gene organisation (UCSC annotation). *LacZ* integration sites within *Grb10* are shown for the *Grb10KO* and *Grb10Δ2-4* mouse lines. Initiation of maternal transcripts starts from exon 1A within CpG island (CpGI) 1, hypomethylated on both parental alleles whereas paternal, brain-specific transcripts initiate from exons 1B1, 1B2 and 1C. Both 1B1 and 1B2 are situated within CpGI2, which is a germline differentially methylated region (gDMR), hypermethylated on the maternal allele and hypomethylated on the paternal allele in all tissues, with a crucial role of regulating imprinted expression of *Grb10* locus. CpGI3, displaying differential methylation on the parental alleles distinctly in brain, overlies exon 1C. White boxes, untranslated exonic sequence; black boxes, coding exons; empty and filled lollipops, hypo- and hyper-methylation, respectively. **C)** Different Grb10 splice variants share a similar structure with five distinct molecular interactions domains: P, a small proline-rich region (11 aa; aa- amino acids), the structural domain closest to the amino-terminus (N), is encoded by exon 4 and can interact with SH3 and WW domains; RA, Ras-associated-like domain (84 aa) is homologue to a region of the MIG-10 protein, it allows for interactions with Ras-like GTP-binding proteins; PH, pleckstrin homology domain (124 aa or 85 aa in isoform α of Grb10), encoded by exons 10-13, ensures association with phospholipid molecules and may play a part in targeting Grb10 to both the plasma and mitochondrial membranes; BPS, between PH and SH2 domain (48 aa), encoded by exons 13-16, necessary for binding to activated IR and, to a lesser extent, Igf1r; SH2, Src-homology 2 domain (104 aa) is encoded by exons 16-17 and is the structural domain closest to carboxyl- terminus (C). This domain allows for interactions with phosphotyrosine-containing domains of several proteins and is required for RTK binding. RA and PH domains form a region termed GM (Grb-Mig). Grb10 has an ability to dimerise/oligomerise due to interaction between the N-terminal domain of one molecule and the GM region of another.

The first *Grb10* knockout mice, termed *Grb10Δ2-4,* were generated by using a gene-trap construct that contained a *LacZ* reporter which was inserted within the *Grb10* locus such that it was controlled by endogenous *Grb10* promoters and enhancers. The *LacZ* reporter provided a method for detection of parental allele-specific expression, while mRNA *in situ* hybridisation and immunohistochemistry were used to assess tissue-specific expression of endogenous *Grb10*. Both experimental methods demonstrated primarily maternal *Grb10* expression in a range of tissues (described above). The adult hypothalamus showed *Grb10* paternal expression (Smith et al., 2007), which is consistent with previous predictions (Arnaud et al., 2003), while reporter expression failed to be demonstrated in fetal brain, with the exception of maternal expression within subependymal layers, the meninges and choroid plexus (Charalambous et al., 2003). On the other hand, anti-Grb10 antibody allowed for detection of additional expression in the brain (Charalambous et al., 2003). To overcome these potential discrepancies in detected expression, another transgenic mouse line (termed *Grb10KO*) with a *LacZ* reporter cassette inserted within exon 8 was created (Garfield et al., 2011). The maternal expression of *Grb10* detected in this mouse line resembled previously reported sites in *Grb10Δ2-4* animals, however, more pronounced *Grb10* paternal expression has been observed in the developing CNS of mice with paternally transmitted gene trap. Garfield et al (2011) have demonstrated paternal *Grb10* expression in fetal and adult brain as well as the consequences of lack of this expression resulting in abnormalities within social behaviour. The uniqueness of *Grb10* gene is pronounced by its ability to show tissue-specific, imprinted expression from each of the parental alleles which results in entirely distinct phenotypic outcomes, as ablation of maternally expressed *Grb10* leads to fetal and placental overgrowth and metabolic abnormalities (Charalambous et al., 2003; Smith et al., 2007). Hence, up until now, *Grb10* is the only example of an imprinted gene able to influence growth, metabolism and behaviour, depending on parent-of-origin-specific expression in different tissues. Generation of two *Grb10* knockout models, discussed above, allowed for detailed investigation of parent-of-origin -specific expression of *Grb10* and encouraged characterisation of the phenotypic effects resulting from disruption of this differential expression *in vivo*.

1.2.3 Grb10 signalling

Grb 7/10/14 protein family has been subject to number of biochemical studies which suggested potential binding partners for members of this family, however the outcomes of these studies do not always accurately reflect the real interactions *in vivo*. Mouse *Grb10* was initially identified during a yeast-two-hybrid experiment as one of the potential interacting

partners of EGFR (Ooi et al., 1995). However, the preference of Grb10 for interaction with a number of other receptor proteins and lack of evidence for EGFR interaction in *vivo* would suggest that binding to EGFR might not be physiologically relevant. Grb10, as an adaptor protein, is known to be able to bind to a wide spectrum of molecules, both RTKs and non-RTKs. Several experiments have demonstrated the ability of Grb10 to bind to various receptor tyrosine kinases, however a preference for binding with the IR has been acknowledged (Frantz et al., 1997; Laviola et al., 1997).

1.2.3.1 Grb10 and insulin signalling

Although the overall consensus from *in vivo* studies is that *Grb10* is a potent negative regulator of insulin signalling (Shiura et al., 2005; Smith et al., 2007; Yamamoto et al., 2008), the results from *in vitro* studies are not always consistent with this. Both negative and positive effects of Grb10 binding to IR have been reported in cell culture experiments. For example Deng et al (2003) showed that overexpression of *Grb10* in differentiated 3T3-L1 adipocyte cells, as well as mouse L6 cells, resulted in an increased metabolic response, including glycogen synthesis, glucose and amino acid transport and lipogenesis. In contrast, expression of a dominant-negative Grb10 SH2 domain in the same cells eliminated these responses. However, the majority of *in vitro* experiments have shown that, in parallel to its apparent role *in vivo*, Grb10 acts as an inhibitor of insulin signalling. Catalytic activity of the IR *in vitro* was shown to be inhibited by binding of Grb10 via its SH2 and BPS domains (Stein et al., 2001). It was also demonstrated that overexpression of *Grb10* in primary rat hepatocytes specifically inhibits insulin-stimulated glycogen synthase (GS) activity, and thereby glycogen synthesis, in a manner independent of IRS-1/2 and PI3-kinase (Mounier et al., 2001). Another group has revealed that inhibition of the IR by Grb10 could be due to blocking the binding between IRS proteins and IR (Wick et al., 2003). Overexpression of *Grb10* in Chinese hamster ovary cells expressing the insulin receptor or in 3T3-L1 adipocytes reduced insulin-stimulated phosphorylation of MAPK, and in rat primary adipocytes inhibited insulin-stimulated phosphorylation of the MAPK downstream substrate Elk1 (Langlais et al., 2004). From these findings the authors concluded that a direct block of insulin-stimulated Shc tyrosine phosphorylation is the most plausible explanation for the inhibitory effect of Grb10 on the MAPK pathway.

It is difficult to interpret the data suggesting that *Grb10* is able to act both positively and negatively on insulin signalling, as reciprocal effects of its overexpression have been reported in the same 3T3-L1 cell line which excludes the dependence on the cellular context as the

source of variation, at least in this instance. Other possible alternative explanations for observed discrepancies between experiments could include effects of different levels of expression or the use of different Grb10 isoforms, but the most important thing is to consider if these types of study provide information on the role of *Grb10* that is relevant in a physiological context. The majority of the overexpression studies have been conducted in cell lines that do not form typical insulin target tissues. Some of the more recent studies have overcome the problems associated with overexpression, potentially at super-physiological levels, by using techniques to investigate the effects of knocking down expression of endogenous *Grb10*. The importance of IGF1 in embryonic and postnatal growth is clearly established and the role of Grb10 in these processes is clearly evident, however there is conflicting information regarding the physiological interaction between the two factors. Several studies have demonstrated Grb10 interactions with the IGF1R and its role in IGF1 mediated mitogenesis (O'Neill et al., 1996; Morrione et al., 1997; Wang et al., 1999; Morrione, 2003) but they did not provide information on the role of endogenous levels of Grb10 in IGF1 signalling. A few studies used overexpressed full length Grb10 or Grb10 constructs to show that Grb10 has a positive role in insulin signalling, metabolic responses (Deng et al., 2003) and IGF1 induced mitogenesis (O'Neill et al., 1996; Wang et al., 1999). On the other hand, some other experiments demonstrated negative effects of the overexpression of Grb10 on insulin signalling (Liu and Roth, 1995; Wick et al., 2003; Langlais et al., 2004) and IGF1 mediated growth (Morrione et al., 1997; Morrione, 2003). The limitations of these studies are due to varied experimental approaches and the fact that *Grb10* overexpression levels might influence its interactions with receptors and downstream signalling molecules and therefore might not properly represent the real physiological interactions between them. As the IGF1 pathway is vital in early and postnatal development, it is of interest to identify the effects of endogenous Grb10 on IGF1 signalling in order to gain more insight into normal physiological functions of Grb10.

Langlais et al (2004) have used small interfering (si)mRNA knockdown of *Grb10* in HeLa cells overexpressing insulin receptors to determine Grb10 negative regulation of insulin signalling. In another study aiming to identify endogenous Grb10 function in the IGF signalling response, small interfering RNA has been used to show that *Grb10* knockdown leads to increased phosphorylation of IGF1-mediated IRS proteins, Akt/protein kinase B and ERK1/2, and to enhanced DNA synthesis (Dufresne and Smith, 2005). The authors suggested that Grb10 acts as an endogenous inhibitor of IGF1-stimulated cell signalling and DNA synthesis, which is in agreement with findings reported by Langlais et al (2004) concerning the effects of Grb10 on

insulin signalling. The mode of endogenous Grb10 action presented in this study depended on maintaining phosphorylation of IGF1 receptor tyrosine through inhibition of protein tyrosine phosphatases on activated receptors (Dufresne and Smith, 2005).

In summary, the majority of studies confirm Grb10 as a negative regulator of insulin signalling, however some evidence has proven otherwise, which might be due to context-specific function of Grb10. The overall conclusion from experiments performed so far is that Grb10 is involved in the regulation of insulin, and perhaps IGF signalling.

IGF1R tyrosine kinase signalling controls the normal course of growth and development through regulation of numerous physiological processes (reviewed in Annunziata et al., 2011). IGF1 or IGF2 activates IGF1R and leads to antiapoptotic and mitogenic responses. In some cases IGF1 also functions in differentiation, cell size regulation as well as transformation and motility. Changes within IGF1R signalling frequently result in growth abnormalities, such as acromegaly, gigantism or dwarfism (Abuzzahab et al., 2003; Manjila et al., 2010), depending on either an increase or decrease in IGF1R signalling. It is known that enhanced IGFR signalling plays a role in several cancers (Pollak et al., 2004; Pollak, 2008), including prostate and breast cancers. Receptor autophosphorylation on tyrosine residues and recruitment of signalling mediators, including IRS and Shc, to the activated receptor are stimulated by ligand binding to IGF1R. Phosphorylation of these compounds, mediated by the IGF1R, results in activation of MAPK and PI3-K signalling pathways, which leads to the downstream biological effects of IGF1 and IGF2. The activated IGF1R, following ligand binding, does interact with other molecules, among them Grb10 protein.

1.2.3.2 Grb10 and other interacting partners

As mentioned above, Grb10 has been shown to interact with insulin receptor and insulin-like growth factor 1 receptor, but also Raf1 kinase, MEK1 kinase and neural precursor cell expressed developmentally down-regulated protein 4 (Nedd4) (Giorgetti-Peraldi et al., 2001; Morrione, 2003; Murdaca et al., 2004; Dufresne and Smith, 2005; Ramos et al., 2006; Huang and Szebenyi, 2010). The SH2 domain of Grb10 has been identified as a target during yeast-two-hybrid screens using the Eph receptor family member ELK (Eph-related receptor tyrosine kinase) (Stein et al., 1996) as well as Ret tyrosine kinase receptor (Pandey et al., 1995). The Eph receptor belongs to a family of proteins with roles in a variety of physiological processes, such as cell migration, while ELK has a known function in endocrine organ development. Another yeast-two-hybrid experiment showed that Grb10 is able to interact with Tec, a non-receptor

tyrosine kinase and by overexpression inhibits downstream effector activation (Mano et al., 1998). MEK1 kinase was also used as bait in a yeast-two-hybrid screen and yielded the Grb10 SH2 domain as a region interacting with both Raf1 and MEK1 kinase in a phosphotyrosine-independent manner (Nantel et al., 1998). Grb10 also possesses the ability to interact with c-Abl (Frantz et al., 1997) which encodes the Bcr-Abl oncoprotein (Bai et al., 1998) that usually activates the PI 3-kinase, MAP kinase and STAT signalling cascades, and has been implicated in both chronic myelogenous leukaemia (CML) and acute lymphoblastic leukaemia (ALL). Moutoussamy *et al* (1998) implicated Grb10 in negative regulation of growth hormone (GH) signalling as they showed that interaction with GH receptor through the Grb10 SH2 domain is possible *in vitro* (Moutoussamy et al., 1998). Evidence has also been provided for Grb10 being a part of the c-kit signalling pathway and the fact that the expression level of *Grb10* has a great influence on Akt activity (Jahn et al., 2002).

The mammalian target of rapamycin (mTOR) protein kinase is a master growth promoter that nucleates two complexes, mTORC1 and mTORC2 and controls cell growth and metabolism in normal physiological and pathogenic states (Dobashi et al., 2011). Its substrates, however, are still under investigation. Recently two different studies have identified Grb10 as an mTORC1 substrate (Hsu et al., 2011; Yu et al., 2011). It was argued that *Nedd4* knockout mice, which have increased Grb10 protein levels and are insulin and IGF resistant (Cao et al., 2008) show a signalling phenotype reminiscent of cells with ablation of TSC1 or TSC2 (the tuberous sclerosis complex 1 or 2) described in this report (Hsu et al., 2011). Both studies showed Grb10 being directly phosphorylated by mTORC1 which resulted in increased Grb10 stability (Hsu et al., 2011; Yu et al., 2011). Moreover, in agreement with genetic experiments in mice, *Grb10* ablation from cells caused enhanced insulin sensitivity whilst its overexpression had an inhibitory effect on insulin signalling (Hsu et al., 2011; Yu et al., 2011). These publications have suggested that Grb10 forms part of a negative feedback loop in which, when activated downstream of insulin or IGFs, mTORC1 phosphorylates Grb10 and through that it raises the capacity of Grb10 to inhibit signals from insulin and IGF receptors (Hsu et al., 2011; Yu et al., 2011). This complements the already established feedback pathway with S6K1 phosphorylating IRS and targeting it for degradation. It has also been pointed out that downregulation of *Grb10* expression often accompanies various cancers and that *Grb10* ablation and loss of the well-established tumour suppressor phosphatase PTEN are mutually exclusive events, which indicated *Grb10* function might as a potential tumour suppressor controlled by mTORC1 (Yu et al., 2011), raising the possibility of *Grb10* role as a target in cancer therapy.

A recent study using a pro-apoptotic member of the Bcl-2 family, Bim L, as bait in yeast-two-hybrid experiment has identified Gr10 as an interacting partner of Bim L (Hu et al., 2010) and suggested that the anti-apoptotic activity of Grb10 depends on the phosphorylation of dynein binding domain (DBD) of Bim protein.

It has also been shown that even though Grb10 does not possess ubiquitin ligase activity, it can still bind the C2 domain of the of the E3 ubiquitin ligase Nedd4 through its SH2 domain, and through the formation of Grb10-Nedd4 complex it induces IGF1-stimulated multiubiquitination, internalization and IGF1R degradation (Morrione et al., 1999; Vecchione et al., 2003; Monami et al., 2008). It was unclear in what manner Grb10 SH2 domain was able to bind the C2 domain of Nedd4 and the kinase domain of IGF1R simultaneously until a recent report identified the Nedd4 C2/Grb10 SH2 complex structure. It was demonstrated that in the Nedd4/Grb10/IGF1R complex Grb10 acts as a connector, forming a bridge between Nedd4 and IGF1R, and Grb10 SH2 co-localises an ubiquitin ligase (Nedd4) and its substrate (IGF1R) (Huang and Szebenyi, 2010).

As discussed above, Grb10, as an adaptor protein, has an ability to bind to numerous receptors and ligands, however its mode of action is sometimes debatable. The explanations for the discrepancies in the true nature of its mechanism of action might be dependent on the variety of Grb10 isoforms and differences in the manner that various experiments have been performed. Relevant experimental variables include forced overexpression to different levels, the variety of tested cell types and the different endpoints used. Thus, *in vitro* binding experiments, yeast-two-hybrid screens and co-immunoprecipitation experiments used in the discussed studies might not always represent the true role of *Grb10 in vivo*.

1.2.4 Role of *Grb10* in development and metabolism

The *Grb10* imprinted expression pattern, specifically its predominant expression from the maternal allele, is in agreement with its role as a growth suppressor as predicted by the conflict hypothesis. Use of knockout mice provided a valuable tool to investigate the influence of *Grb10* on both fetal and postnatal development as well as adult metabolic status. As mentioned previously, Charalambous et al (2003) were the first to describe the phenotype of mice lacking functional *Grb10* gene. The *Grb10Δ2-4* animals were generated by insertion into the *Grb10* locus of a gene trap construct containing a splice acceptor, *β-geo* cassette and a polyadenylation sequence which caused the deletion of 36 kb between exons 2 to 4 that includes the translation initiation codon in exon 3. *In situ* analysis has shown that expression

from the *LacZ* reporter gene closely follows the endogenous pattern of *Grb10* expression. The characterisation of mice without functional *Grb10* following maternal transmission of the mutant allele (*Grb10Δ2-4*$^{m/+}$ animals) revealed significant overgrowth of the placenta (from E14.5) and embryos (from E12.5 onwards). This overgrowth phenotype resulted in a mean birth weight of *Grb10Δ2-4*$^{m/+}$ animals that was approximately 30% greater than their wild type littermates. In addition, neonatal *Grb10Δ2-4*$^{m/+}$ animals exhibited relative brain sparing and disproportionate overgrowth of the liver (Charalambous et al., 2003), an unusual effect as very few genes are known to have an effect on overall body size during embryogenesis and also cause the disproportional growth of different organs.

Smith et al (2007) followed up the phenotypic analysis of *Grb10Δ2-4*$^{m/+}$ mice by characterising their postnatal growth and metabolism. A 13% increase in body weight was noted in mutant animals, even at the age of 6 months. DXA analysis of these mice revealed significantly reduced fat tissue and enhanced lean tissue content but with no obvious alterations in fat and muscle cell histology. The food intake in *Grb10Δ2-4*$^{m/+}$ mice was not altered. Furthermore, glucose tolerance tests revealed that lack of functional *Grb10* led to improved whole-body glucose tolerance and insulin sensitivity in adult mice. It has been suggested that the increased muscle mass is the reason for increased glucose tolerance, caused by enhanced glucose clearance into the muscle. The *Grb10* knockout mice exhibited tissue-specific changes in insulin-induced IR and IRS-1 tyrosine phosphorylation as well as in level of IGF1R and IRS-1 tyrosine phosphorylation in response to IGF1R (Smith et al., 2007). Thus, enhanced signalling through IR and/or Igf1r could also directly contribute to the observed improvement in glucose handling. The increase in skeletal muscle tissue mass alone might not be enough to lead to significant abnormalities in the regulation of blood glucose as, in the case of *Mstn* knockout mice, lean tissue content was dramatically elevated without changes in glucose or insulin levels, or in the ability to clear a glucose load (McPherron and Lee, 2002). As expected, the phenotype of transgenic mice ectopically overexpressing *Grb10* was to some extent opposite to that of *Grb10Δ2-4*$^{m/+}$ mice (Shiura et al., 2005). The first described transgenic mice with ectopic expression of *Grb10* did not show any alterations in body size during embryonic development or at birth but at the age of 4 months they were 10 to 15% lighter than their wild type counterparts. The limitations of this model came down to the possibility that transgenic *Grb10* animals did not precisely mimic *Grb10* expression profile during development, as the transgene lacked the original promoter and was coupled with an external enhancer and it was likely that the contribution of the transgene expression increasing with time in some organs caused the postnatal growth retardation (Shiura et al.,

2005). Because *Grb10* expression is high during the late embryonic stages but diminishes after birth, it is possible that postnatal growth effects in *Grb10* transgenic animals were resulting from ectopic overexpression of the transgene. Metabolic characterisation of *Grb10* transgenic mice revealed insulin resistance which in some cases led to development of diabetes as a result of hyper-negative regulation of the insulin and IGF1 receptors (Shiura et al., 2005). Additionally, increased adipocyte content in the pancreas of has also been observed, though the overall fat tissue content was not reported. The altered body size and tissue composition in the *Grb10* transgenic mice mirrors that seen in *Grb10Δ2-4*$^{m/+}$ mice and might be the reason for disrupted glucose metabolism or at least contribute to it. A recent study of the same model suggested that *Grb10* transgenic mice resemble some characteristics of human type-2 diabetes (Yamamoto et al., 2008), as they showed decreased ability to clear glucose, significantly reduced levels of blood urea nitrogen and abnormally high levels of plasma triglyceride, insulin, adiponectin and resistin. These abnormal phenotypic changes have been accompanied by significantly decreased body, visceral fat and liver weights in *Grb10* transgenic mice and 60% higher incidence of type-2 diabetes in these mice when fed on a high fat diet (Yamamoto et al., 2008). A careful interpretation of these results is necessary as the ectopic transgene expression might have resulted in false phenotypic effects.

Recently another mouse model has been generated to overcome these limitations, as Shiura et al (2009) by deletion of the imprinting control region *Grb10*-DMR have created transgenic *Grb10* mice with double *Grb10* Type I transcript expression in organs and tissues that normally express Grb10. Type I transcripts from upstream promoters are maternally or biallelically expressed in the majority of tissues in mice and humans, respectively, whilst Type II transcripts from downstream promoters are paternally expressed in the brain of both species (Arnaud et al., 2003; Hikichi et al., 2003; Yamasaki-Ishizaki et al., 2007). Transgenic mice exhibited similar phenotype to the one observed for animals with maternal disomy Chromosome 11 (MatDi(11)) and maternally duplicated proximal Chromosome 11 (MatDp(prox11)), and an increased *Grb10* expression was suggested as a cause for the observed growth retarded phenotype in embryos and neonatal mice (Shiura et al., 2009).

A plausible explanation for the *Grb10* overexpression and knockout mice growth phenotypes was that Grb10 forms an inhibitory interaction with Igf1r, as Grb10 has a demonstrated capacity for binding directly with both IR and Igf1r. Furthermore, the overgrowth observed in *Grb10Δ2-4*$^{m/+}$ mice is comparable in magnitude to the growth retardation seen in mice lacking genes in the IGF signalling pathway (Efstratiadis, 1998). Additionally, the expression pattern of *Grb10* and its time of action appeared similar to that of

IGF2. *IGF2* is a known embryonic and placental growth factor with almost exclusive expression from the paternal allele which acts primarily through the IGF1 receptor in the embryonic growth and through insulin receptor in the placenta. By creating a cross between *Grb10Δ2-4*$^{m/+}$ female and *Igf2*$^{+/p}$ male mice (which gave rise to mice of four different genotype: wild type, *Grb10Δ2-4*$^{m/+}$, *Igf2*$^{+/p}$ and *Grb10Δ2-4*$^{m/+}$/*Igf2*$^{+/p}$) it was possible to analyse if *Grb10* was exerting its growth effects through any of these receptors (Charalambous et al., 2003). Grb10 interaction with Igf2 receptor would be associated with double mutants exhibiting similar phenotype to *Igf2*$^{+/p}$ animals. However, analyses of total body weights and organ weights from double mutants showed an additive effect of both parental genotypes and significantly differed from *Igf2*$^{+/p}$ neonates. In addition, E16.5 embryos and placentae of double mutants displayed an additive effect of the two gene deletions. These results suggested that Grb10 exerts its growth effects through a pathway that is possibly independent of IGF1 receptor and IR. However, it could still be argued that ablation of Igf1r (a component shared between Igf2 and Igf1 pathways) would provide more compelling evidence for Grb10 role in Igf-growth effects. As a result, genetic crosses between female *Grb10Δ2-4*$^{m/+}$and male *Igf1r*$^{-/-}$ animals were generated (Garfield, 2007), and similarly to the *Grb10Δ2-4*$^{m/+}$/*Igf2*$^{+/p}$ data, double knockout neonates displayed additive body weights between the two single mutants. Organ weight analysis showed the intermediate phenotypes in hearts, lungs and kidneys, but not brains and livers, suggesting that maternal *Grb10* does not have significant role in brain development whilst *Igf1r* does not exert its effects in the liver. This provides evidence independent of the *Grb10Δ2-4*$^{m/+}$/*Igf2*$^{+/p}$ cross indicating that the Igf-pathway is not that primarily responsible for the overgrowth phenotype in *Grb10* mutants. Overall, genetic experiments described above indicate that *Grb10* is controlling growth in an as yet unidentified way by interacting with signalling molecules that are to be elucidated. Further investigation of *Grb10* possible interactions with other genes, particularly imprinted ones with reciprocal expression pattern and phenotypic effects, seems to be a plausible way of looking more closely into Grb10 signalling pathways.

1.3 Delta-like homologue 1

1.3.1 The Dlk1 protein and signalling

The gene encoding Delta-like homologue 1 (*Dlk1*) is also known as Preadipocyte factor 1 (*Pref-1*) and Fetal antigen 1 (FA1). *Dlk1* is situated on mouse distal chromosome 12 (Gubina et al., 2000) and human chromosome 14q32 (Gubina et al., 1999). Together with *Dio3* and *Rtl1* it forms a part of an imprinted gene cluster, *Dlk1-Dio3* (**Figure** 1.6). Dlk1 encodes a transmembrane epidermal growth factor (EGF)-like protein which possesses six EGF-like repeats in the extracellular domain, a juxtamembrane region, a transmembrane domain and a short, intracellular tail (Smas et al., 1994). A soluble form of Dlk1 called fetal antigen 1 (FA1) acting as a growth factor during development can be generated from cleavage at the extracellular domain of Dlk1 (Jensen et al., 1994) . In addition, a constitutively membrane-bound Dlk1-C2 is yet another splice variant of Dlk1 lacking the proteolytic cleavage site (Floridon et al., 2000). EGF-like motifs present in Dlk1 are similar to those observed in members of the Delta/Notch/Serrate protein family (Laborda et al., 1993; Laborda, 2000). However, when compared with these signalling molecules, it has been noted that Dlk1 lacks a Delta:Serrate:Lag-2 (DSL) domain, which is generally thought to be crucial for activation of Notch signalling (Smas and Sul, 1993). Thus it was surprising that Dlk1 dimers, lacking the DSL motif, were able to increase thymocyte cellularity in an HES-1 dependent manner (Kaneta et al., 2000). Instead of DSL, Dlk1 N-terminal EGF-like repeats encompass a DOS (Delta and OSM-11) motif, which has been found in typical Notch ligands and other proteins able to act in the Notch pathway in the presence of DSL containing Notch ligands (Komatsu et al., 2008; Kopan and Ilagan, 2009)

Despite lack of the DSL domain, experiments both *in vivo* (Bray et al., 2008) and *in vitro* (Baladron et al., 2005; Nueda et al., 2007) have shown that Dlk1 is still able to bind to Notch receptor, without activating it, and that it can act as Notch antagonist (Baladron et al., 2005; Kopan and Ilagan, 2009). Dlk1 acts as Notch antagonist by interacting with Notch receptors through its EGF repeats as it has been demonstrated to bind to Notch in *Drosophila* and Notch1 in mammalian cell cultures (Baladron et al., 2005; Nueda et al., 2007; Bray et al., 2008). However a role for Dlk1 in enhancing Notch signalling has also been suggested in a study that implied the DSL and DOS motifs function together in order to activate Notch signalling (Komatsu et al., 2008).

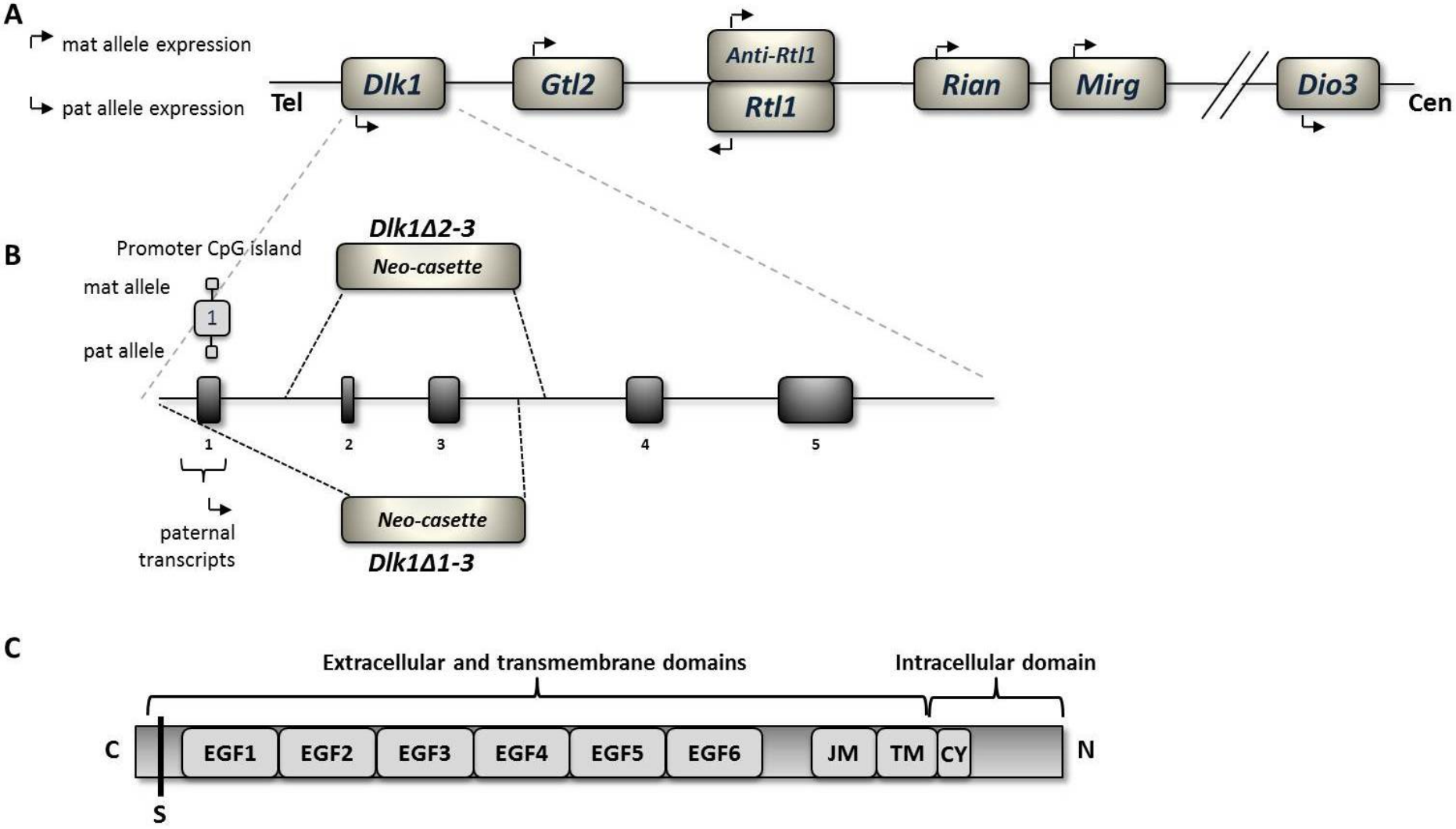
A
mat allele expression
pat allele expression
Tel
Dlk1
Gtl2
Anti-Rtl1
Rtl1
Rian
Mirg
Dio3
Cen
B
Promoter CpG island
mat allele
1
pat allele
Dlk1Δ2-3
Neo-casette
1
2
3
4
5
paternal
transcripts
Neo-casette
Dlk1Δ1-3
C
Extracellular and transmembrane domains
Intracellular domain
C
EGF1
EGF2
EGF3
EGF4
EGF5
EGF6
JM
TM
CY
N
S

Figure 1.6 Schematic representation of *Dlk1* gene localisation on chromosome 14, *Dlk1* organisation and Dlk1 protein structure (not drawn to scale).

A) Localisation of the maternally imprinted *Dlk1* gene on the distal part of chromosome 12. *Dlk1* is situated within the *Dlk1-Dio3* cluster, which also comprises two other imprinted, protein coding genes, paternally expressed retrotransposon-like 1 (*Rtl1*) and type III iodothyronine deiodinase (*Dio3),* as well as maternally expressed non coding RNA genes, gene trap locus 2 (*Gtl2)*, RNA imprinted and accumulated in nucleus (*Rian*) and miRNA containing gene *(Mirg)* and antisense *Rtl1 (Anti-Rtl1)*. Tel, telomeric region; Cen, centromeric region. **B)** *Dlk1* gene organisation. *Neo*-cassette integration sites within the *Dlk1* gene are shown for the knockout mouse lines generated in two different studies, *Dlk1Δ1-3* (Raghunandan et al., 2008) and *Dlk1Δ2-3* (Moon et al., 2002). Initiation of transcripts starts from exon 1 within a CpG island hypomethylated on both parental alleles. black boxes, coding exons; empty and filled lollipops, hypo- and hyper-methylation, respectively. **C)** Structure of Dlk1 protein which contains six EGF-like repeat domains and juxtamembrane domain (JM) in the extracellular region as well as a transmembrane (TM) domain and cytoplasmic (CY) region. Dlk1 protein, comprising 385 aa (amino acids) contains a signal sequence at the amino acid terminus (N) and a single transmembrane domain (amino acids 300-322). EGF-like repeats in Dlk1 protein are similar to those observed in proteins of the Notch/Delta/Serrate protein family, however Dlk1 lacks the DSL (Delta/Serrate/Lag-2) domain conserved in all classic Notch ligands in order to provide Notch-receptor : ligand interaction. In its place, the N-terminal EGF tandem repeats of Dlk1 comprise DOS (Delta and OSM-11), a motif found to act in the Notch pathway in the presence of DSL-containing Notch ligands. There are four major alternative splicing products of Dlk1, the largest full-length form as well as three shorter ones containing deletions in the JM region or part of the sixth EGF-like repeat domain. Proteolytic cleavage of Dlk1 at two sites of the extracellular domain leads to generation of soluble forms of Dlk1.

Komatsu et al (2008) also demonstrated that Dlk1 could substitute for OSM-11 in *C.elegans* development, which suggested conservation of DOS motif function across species. A recent study has shown that DLK1 can interact with another EGF-like protein, DLK2, and that through interacting with themselves and with each other they can modulate NOTCH signalling by acting as inhibitory non-canonical protein ligands for the NOTCH receptor (Sanchez-Solana et al., 2011). The suggestion was that DLK1-DLK2 interaction results in reciprocal inhibition of activities of each of the proteins which leads to induction of NOTCH signalling.

The membrane-bound form of Dlk1, but not the soluble form which lacks the transmembrane domain, has an ability to antagonise Notch in *Drosophila* wing development (Bray et al., 2008), while in contrast an experiment in *C.elegans* showed that Dlk1 activated Notch by binding to Notch ligand (Kopan and Ilagan, 2009). Up until now, the interaction of full length Notch with Dlk1 has not been reported and contradictory data on the influence of Notch on adipocyte differentiation has been published. On one hand, Notch has been suggested to be necessary for adipocyte differentiation (Garces et al., 1997) and also inhibition of adipocyte differentiation has been reported in the presence of the Notch ligand, Jagged1. On the other hand, it has been demonstrated that knockdown of Hes-1, the protein downstream of Notch, caused inhibition of adipocyte differentiation (Ross et al., 2004). Moreover, another group established that the role of Notch in adipocyte differentiation is not essential, as Notch1 knockout cells were able to undergo differentiation into adipocytes (Nichols et al., 2004). Other studies also suggested that Notch is not required for adipocyte differentiation and that it inhibits this process rather than activates it (Wang et al., 2010). These findings are yet to be confirmed by analyses of Dlk1 molecular and biochemical interactions so that a concrete insight into the basis and mechanisms of interactions between Dlk1 and Notch can be established. In order to inhibit adipocyte differentiation one of the Dlk1 mechanisms of action is to antagonise insulin/IGF1 signalling which leads to reduced activation of Erk1/2 and Akt pathways (Zhang et al., 2003). Dlk1 was also found to modulate ERK/MAPK signalling triggered by Insulin/IGF1 in response to specific differentiation factors (Ruiz-Hidalgo et al., 2002). In addition, Dlk1 binding to IGFBP1/IGF1 complexes appears to lead to release of IGF1R and increases the adipogenic potential of 3T3-L1 cells (Nueda et al., 2008), suggesting the role of membrane-bound Dlk1 variants in initiating adipogenesis in response to IGF1. Recent study has shown Dlk1 expression can be supressed directly by BMP7, which allows for adipogenesis to commence (Zhang et al., 2010).

Dlk1 can also interact with itself through its EGF-like repeat domains and can undergo (TACE)-mediated cleavage by ADAM17/tumour necrosis factor alpha converting enzyme to produce a soluble form of Dlk1 (Wang et al., 2006). Expression of *Dlk1* has been the most widely studied in preadipocytes, where it is highly expressed until the differentiation into adipocytes. The details of *Dlk1* mechanism of action in the inhibition of adipogenesis have been investigated recently (Kim et al., 2007; Wang and Sul, 2009; Wang et al., 2010). Using a yeast-two hybrid system Wang et al (2010) found that the Dlk1 juxtamembrane region binds to the C-terminal region of fibronectin. Following that, Dlk1 activates integrin downstream signalling to activate the MEK/ERK pathway, which in turn upregulates Sox9. Sox9 is a transcription factor important for chondrogenesis and osteogenesis. Wang et al (2009) also discovered that *Sox9* subsequently suppresses transcription of *C/EBPβ* and *C/EBPδ* by binding to their promoters and that it leads to the inhibition of adipocyte differentiation (**Figure** 1.7).

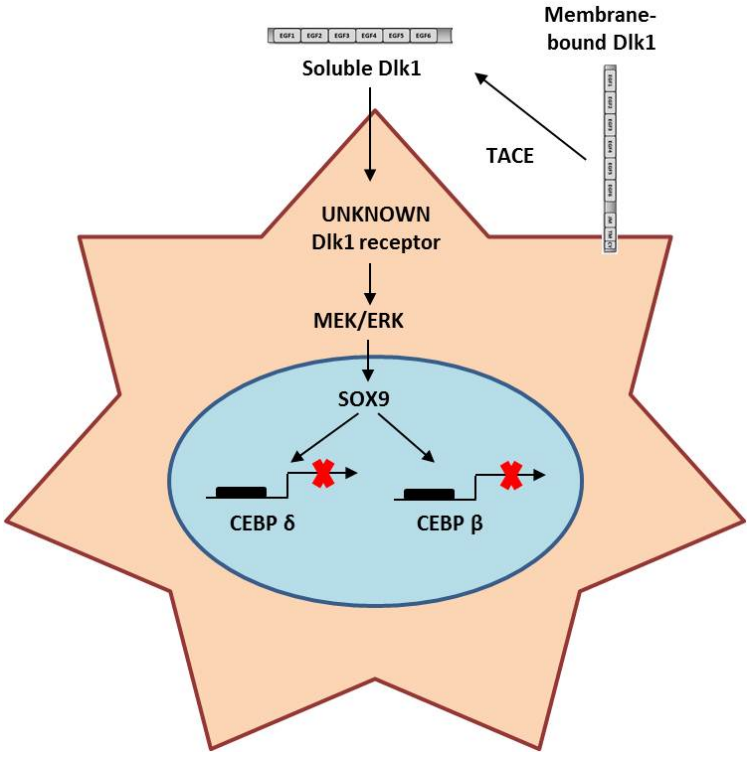

Figure 1.7 Schematic diagram of Dlk1 inhibition of adipogenesis.

Membrane-bound splice variants of Dlk1 undergo TACE-mediated cleavage at the juxtamembrane region in order to generate a soluble form of Dlk1. Soluble Dlk1 is then able to interact with a putative Dlk1 receptor at the preadipocytes membrane which activates MEK/ERK. MEK/ERK increases expression of Sox9 which in turn binds to C/EBPδ and C/EBPβ promoter regions to supress their transcription which leads to inhibition of adipocyte differentiation. Figure adapted from (Sul, 2009).

1.3.2 *Dlk1* gene and *Dlk1-Dio3* imprinted cluster regulation

Phenotypic analyses of mice with uniparental duplications of distal region of chromosome 12 (mUPD12 and pUPD12: maternal and paternal disomy for chromosome 12, respectively) (Georgiades et al., 2000; Tevendale et al., 2006) and observations of patients suffering from uniparental duplications of the orthologous region on human chromosome 14q (Georgiades et al., 1998; Kotzot, 2004; Kagami et al., 2005) suggested the presence of imprinted genes in this region. *Dlk1, Dio3* and *Rtl1* are protein coding, imprinted genes situated within 1Mb cluster on distal region of mouse chromosome 12 (**Figure** 1.6). These three genes are repressed on the maternally inherited chromosome, whereas in the same region exclusive maternal allele expression occurs from multiple non-coding RNA (ncRNA) genes, namely *Gtl2*, *AntiRtl1*, *Rian* and *Mirg*. The *Dlk1-Dio3* imprinting cluster contains the intergenic germline-derived DMR (IG-DMR) and *Gtl2*-DMR with methylation marks established in the germline or upon fertilisation, respectively (Takada et al., 2000; Takada et al., 2002). *Gtl2*, which lies at the proximal end of the cluster together with *Dlk1*, is a paternally imprinted gene whose ablation resulted in abnormal embryo size when paternally transmitted (Schuster-Gossler et al., 1996; Takahashi et al., 2009).

The intergenic germline derived differentially methylated region (IG-DMR) that is placed between *Dlk1* and *Gtl2* is thought to be responsible for the imprinting regulation of the 1Mb domain (Lin et al., 2003; Lin et al., 2007). Targeted disruption of the mouse IG-DMR has demonstrated that unmethylated maternally inherited IG-DMR is crucial in the maintenance of the unmethylated status of the *Gtl2*-DMR, expression of the ncRNAs and the repression of the protein-coding genes in the maternal allele in the embryo (Lin et al., 2003). It has been found that the phenotype of mice with pUPD12 (Lin et al., 2007) is similar to that of mice with a deletion of the IG-DMR on the maternal chromosome (Takada et al., 2002), a phenomenon referred to as an epigenetic switch. Da Rocha et al (2007) investigated the co-localisation of the expression of *Dlk1* and *Gtl2* genes throughout development and concluded that the mechanism of imprinting regulation of this 1Mb domain is different to insulator or co-ordinate non-coding RNA mechanisms previously noted for other domains, such as the *Igf2/H19* region, and that *Dlk1* and *Gtl2* are functioning in distinct tissues in an independent manner (da Rocha et al., 2007).

The *Gtl2*-DMR has an interesting characteristic as it has been shown to act as crucial long-range imprinting regulator. A maternally-inherited heterozygous microdeletion encompassing

the *MEG3*-DMR (the human orthologue of the mouse *Gtl2*-DMR) but not the IG-DMR, has been found in a neonatal patient with a paternal uniparental disomy 14-like phenotype in the body but not in the placenta (Kagami et al., 2010). This patient also had *DLK1* reactivation on the maternal allele.

Several recent studies using mouse knockout models with targeted deletions of the *Gtl2* locus spanning the *Gtl2*-DMR have pointed out the possibility that *Gtl2* and/or the *Gtl2*-DMR might be able to control maternally expressed gene expression (Takahashi et al., 2009; Zhou et al., 2010). These findings point at the methylation of the *Gtl2*-DMR as a vital part of *Dlk1-Dio3* imprinted domain. Moreover, a recent study showed that mouse induced pluripotent stem cells (iPSC) with repressed expression of maternally expressed ncRNAs within the *Dlk1-Dio3* domain contributed poorly to chimeras and were unable to generate all-iPSC mice (Stadtfeld et al., 2010). The repressed expression in ncRNAs has been linked to hypermethylation of both IG-DMR and *Gtl2*-DMR which is thought to be a result of iPSC reprogramming (Stadtfeld et al., 2010). This study has implicated a role for the *Dlk1-Dio3* cluster in cell proliferation and/or differentiation at early gestational stages, while another exciting study revealed that the conserved imprinted *Dlk1-Dio3* region was activated in fully pluripotent mouse stem cells but repressed in partially pluripotent stem cells and that the activation level of *Dlk1-Dio3* positively correlated with pluripotency levels (Liu et al., 2010). This implies that activity of *Dlk1-Dio3* could potentially act as a biomarker to identify fully pluripotent iPS cells, adding to the notion that Dlk1 might be an important regulator of not only proliferation and differentiation of embryonic and adult stem cells (Li et al., 2005; Abdallah et al., 2007; Wang and Sul, 2009), but also function to maintain the pluripotency of embryonic stem cells.

Taking into account the essential functions of *Gtl2* and *Gtl2*-DMR in imprinting control of this region, another recent study aimed to elucidate their mechanisms of action, revealing that methylation of *Gtl2*-DMR is not required for *Gtl2* imprinted expression and that *Gtl2* is possibly playing a role in regulation of cell proliferation and differentiation at early gestation stages (Sato et al., 2011). This study also reported that one of the regions of IG-DMR shows variations in allelic methylation patterns that are tissue-dependent, providing more insight into mechanisms by which allele-specific IG-DMR methylation results in *Dlk1-Dio3* imprinted expression.

Dlk1 does not only have an established role in affecting adipogenesis (Smas and Sul, 1993), but it is also involved in the differentiation of other cell types, including chondrocytes (Chen et

al., 2011), osteoblasts (Sul, 2009; Wang and Sul, 2009), thymocytes (Kaneta et al., 2000) and adrenal gland cells (Okamoto et al., 1997). Recent study has also shown that expression of membrane– bound and secreted DLK1 distinguishes neural stem cells (NSCs) and niche astrocytes and that differential processing of *DLK1* gene acting simultaneously in both cell types results in their distinct functional characteristics (Ferron et al., 2011). The same study also demonstrated that biallelic *Dlk1* expression is important for normal neurogenesis, as it showed specific and selective lack of *Dlk1* imprinting in the NSC and niche astrocyte populations starting at postnatal stages and continuing into adulthood. Several *in vitro* and transgenic mouse studies have indicated a role for *Dlk1* role in inhibition of bone development (Abdallah et al., 2004; Abdallah et al., 2007; Abdallah et al., 2011b). Increased *Dlk1* expression has been linked to many types of tumours including myeloid leukemia (Laborda et al., 1993; Astuti et al., 2005; Kawakami et al., 2006; Espina et al., 2009; Khoury et al., 2010; Yanai et al., 2010). Furthermore, various reports have indicated on *Dlk1* as a regulator of proliferation, differentiation but also pluripotency of embryonic stem cells (Smas and Sul, 1993; Li et al., 2005; Abdallah et al., 2007; White et al., 2008; Wang and Sul, 2009; Liu et al., 2010; Stadtfeld et al., 2010). *Dlk1* is widely expressed in the range of embryonic tissues and in placenta during development (Yevtodiyenko and Schmidt, 2006; da Rocha et al., 2007). Schmidt et al (2000) have shown that *Dlk1* expression starts as early as E11 in mouse embryo and its levels increase until late gestation. A dramatically elevated *Dlk1* expression has been noted during myogenesis, from E13 to E16 (da Rocha et al., 2007). *Dlk1* expression in adult tissues is limited primarily to preadipocytes and some endocrine tissues, including the somatotroph cells of the pituitary gland (Larsen et al., 1996), insulin-producing β-cells of the pancreas (Tornehave et al., 1993), Leydig cells of the testes and cells in the ovaries (Jensen et al., 1999).

1.3.3 Role of *Dlk1* in development and metabolism

Dlk1, encoding a constitutively membrane-bound or a cleaved circulating protein form, like many other imprinted genes plays an important role in normal growth and in development of several tissues in mammals. In agreement with the conflict hypothesis, the imprinted status of *Dlk1*, which is predominantly expressed from the paternal allele, predicts that *Dlk1* functions as an enhancer of growth. Similar to other imprinted genes, the role of *Dlk1 in vivo* has been established using a knockout mouse model lacking a functional *Dlk1* gene. Moon et al (2002) generated mice lacking paternal, maternal or both parental copies of the *Dlk1* gene and performed a phenotypic characterisation. The *Dlk1* disruption was achieved by targeted insertion of a neomycin-resistance cassette that replaced exons 2 and 3 of *Dlk1* (*Dlk1Δ2-3* in

Figure 1.4). A survival rate of about 50% beyond 2 days after birth indicated a role for *Dlk1* in perinatal growth and lethality (Moon et al., 2002). Absence of *Dlk1* expression in paternal heterozygotes and significant pre- and post-natal growth retardation in these mice comparable to that of *Dlk1* null mice confirmed that *Dlk1* is an imprinted gene, predominantly expressed from the paternal allele.

Besides an abnormal growth, other phenotypic malformations were also reported in *Dlk1* knockout mice. These included skeletal abnormalities, such as rib fusions and asymmetrical junction of ribs to sternum, and also eyelid malformations similar to blepharophimosis as reported in patients with mUPD14 or with a deletion of the 14q32 region that contains the *Dlk1* locus. Moon et al (2002) suggested that these skeletal and pulmonary defects, together with an impaired suckling ability arising from these defects, might have contributed to the high perinatal death rate in *Dlk1* knockout mice. At 15 weeks of age *Dlk1* null mice exhibited a slightly elevated fat mass, therefore, the authors decided to investigate whether a high fat diet would have a more pronounced effect on adiposity in *Dlk1* knockout animals. Indeed, the accelerated weight gain in *Dlk1* knockout mice was found to be due to excessive adiposity, manifested by significantly greater fat pad mass, which has been associated with adipocyte cell hypertrophy. Substantially enlarged, fatty livers with increased fatty acid synthetase (FAS) and stearoyl-Coenzyme A desaturase 1 (SCD-1) (markers of adipocyte differentiation) expression were also found in *Dlk1* knockout mice. Moreover, levels of lipid metabolites, including triglycerides, cholesterol and free fatty acids in serum of *Dlk1* knockout animals were considerably elevated, which further indicated that disrupted lipid metabolism is a major consequence of the lack of a functional *Dlk1* gene. Thus, Moon et al (2002) were the first to report that *Dlk1* is a gene involved in normal embryonic development, postnatal growth and adiposity.

Another *Dlk1* mouse knockout model has been generated more recently by deletion of exons 1-3 of *Dlk1* (*Dlk1Δ1-3*; **Figure** 1.6; Raghunandan et al., 2008). The study aimed to determine the role of *Dlk1* in B cell development *in vivo* and reported increased numbers of the earliest B-lineage cells and reduced numbers of re-circulated B-lineage cells in the bone marrow, along with alterations within B cells in peripheral lymphoid organs. In addition, they have found that *Dlk1* knockout mice showed aberrant levels of pre-immune serum immunoglobulin and reported an exaggerated antigen-specific humoral immune response. Taken together, these results suggested *Dlk1* as a potent regulator of a B cell development (Raghunandan et al., 2008).

Lee et al (2003) generated transgenic mice expressing the full ectodomain corresponding to the large soluble form of *Dlk1* fused to human immunoglobulin-γ constant (hFc) region. The specific expression of this fusion protein in adipose tissue resulted in abnormalities in adipogenesis that included a decrease in fat pad weight, adipocyte cell hypotrophy and reduced expression of adipocyte marker genes (Lee et al., 2003). Moreover, expression of the soluble Dlk1 fusion protein in the liver also resulted in lower adipose tissue weight. Transgenic *Dlk1* animals also exhibited several other impairments, including hypertriglyceridemia, slower glucose clearance and decreased insulin sensitivity. The authors concluded that the large soluble form of Dlk1 is able to inhibit adipocyte differentiation, similar to an effect previously reported in the differentiation of 3T3-L1 cells *in vitro* (Mei et al., 2002).

Dlk1 and the neighbouring *Gtl2* gene are expressed in the majority of tissues after E12.5 and the peak of their expression is reached after E15.5 in some tissues (Takada et al., 2000). The crucial role of IG-DMR and *Gtl2*-DMR in regulation of genes comprising the *Dlk1-Dio3* cluster has been provided by studies of mice with maternally transmitted deletions of these DMR regions (Lin et al., 2003; Takahashi et al., 2009; Kagami et al., 2010; Zhou et al., 2010). Prenatal and perinatal lethality along with abnormalities within tissues such as liver, lung, bone and skeletal muscle have been found in these animals (Takahashi et al., 2009; Kagami et al., 2010; Zhou et al., 2010). Several recent studies have pointed at *Dlk1* function in development of skeletal muscle. The levels of Dlk1 protein and transcripts were found to be the highest in developing fetal muscle and to decrease after birth (Floridon et al., 2000; Andersen et al., 2009). One study has reported that in some myopathies (for example in Becker and Duchenne muscular dystrophy, associated with muscle degeneration and regeneration) there were increased numbers of $Dlk1^{+}$ mononuclear cells (Andersen et al., 2009). In addition, the ability of *Dlk1* to increase neonatal skeletal muscle mass has been described in transgenic mice with *Dlk1* overexpression (Davis et al., 2004; da Rocha et al., 2009) and in sheep with *callipyge* (*clpg*) mutations, causing a rise in the levels of *Dlk1* expression (Davis et al., 2004; Perkins et al., 2006; Vuocolo et al., 2007). *Callipyge* sheep that overexpress *Dlk1* and at least one other imprinted gene, *Peg11* (also called *Rtl1* in mice), have a lean phenotype with muscle hypertrophy that is most pronounced in the pelvic limb (Koohmaraie et al., 1995; Jackson et al., 1997; Freking et al., 1998). This phenotype is characterised by an unusual mode of inheritance, called 'polar overdominance', meaning that the phenotype is expressed only in heterozygous animals paternally inheriting the *clpg* mutation (Cockett et al., 1996). Interestingly, a recent study of *Dlk1* allelic transmission pattern in obese children has provided evidence for the first time that polar dominance exists in humans (Wermter et al., 2008). The

clpg mutation is a single nucleotide substitution (A to G) that lies within the *Dlk1-Gtl2* domain (Freking et al., 2002). It has been demonstrated that the *callipyge* phenotype correlates with ectopic expression of *Dlk1* in hypertrophic muscle of *clpg* sheep and mice (Davis et al., 2004; Murphy et al., 2005; Perkins et al., 2006; Vuocolo et al., 2007). The definitive interpretation of the *callipyge* sheep phenotype is difficult as the *clpg* mutation also changes the expression of other imprinted genes in the proximity of the *Dlk1* allele (Bidwell et al., 2001; Charlier et al., 2001; Murphy et al., 2005; Perkins et al., 2006; Takeda et al., 2006; Fleming-Waddell et al., 2007; Vuocolo et al., 2007). However, given the antiadipogenic role of *Dlk1*, overexpression of this gene in callipyge sheep is likely to be the cause of the observed phenotype. Others have also indicated that *Dlk1* functions in the commitment and/or proliferation of fetal myoblasts as well as in the maintenance of hypertrophy in fully differentiated myofibers (White et al., 2008).

The exact mode of function and signalling mechanisms of the predominantly membrane-bound form of Dlk1 in skeletal muscle is not clear. To add to our understanding of it, another study of *Dlk1* role in mouse muscle development has been provided by generation of conditional knockout using a *Dlk1*-floxed allele with a Myf5-Cre driver (*Myf5* is a crucial muscle regulatory factor in early development), so that the function of local non-circulating Dlk1 in skeletal muscle development and regeneration could be examined (Waddell et al., 2010). Muscle-specific ablation of *Dlk1* in mice led to reduction in body weight (more prominent in older than younger mice) and skeletal muscle mass, associated with reduced numbers of myofibers as well as decreased myosin heavy chain IIB gene expression. Moreover, postnatal growth retardation and delayed muscle regeneration were also described as a result of altered myogenic inhibitory signalling in these animals (Waddell et al., 2010). Impaired regeneration of *Dlk1* conditional knockout fibers in adult mice was associated with lower expression levels of myogenin and the activated form of phosphorylated Akt. This might be a result of disturbed Akt/mTOR signalling pathway, which stimulates protein synthesis and myotube hypertrophy (Rommel et al., 2001), a result consistent with recent finding of improved Akt signalling in *DLK1* overexpressing *callipyge* sheep (Fleming-Waddell et al., 2009). Fleming-Waddell et al (2010) have also shown that *Dlk1*, at a progenitor cell level, non-cell autonomously promotes myogenic differentiation but inhibits myoblast proliferation. This provides evidence of a role for *Dlk1* in controlling proliferation and differentiation of satellite cells and suggests a way in which elevated *Dlk1* expression is able to cause muscle hypertrophy in *callipyge* sheep and transgenic mice (Charlier et al., 2001; Davis et al., 2004; da Rocha et al., 2009). Paternal and maternal uniparental disomies for chromosome 14 (pUPD14 and mUPD14) result in very distinct phenotypes.

Human pUPD14 is a cause of facial abnormality, small bell-shaped thorax, abdominal wall defects and polyhydramnios whereas mUPD14 leads to numerous abnormal features including pre- and postnatal growth failure, hypotonia, mild facial abnormalities, small hands and early onset of puberty. The phenotypes resulting from mUPD14 vary in severity and can range from a near normal phenotype to a very severe one, similar to that observed in Prader-Willi syndrome. Moreover, in pUPD14 placentomegaly has been reported, whereas the size of the placenta has not been studied in mUPD14.

Expression of the imprinted genes on the distal part of mouse chromosome 12 is monoallelic in both normal embryo and placenta. As a result, pUPD12 results in a variety of abnormal phenotypic features including prenatal lethality, cartilage defects, abdominal swelling and placentomegaly, whereas mUPD12 causes perinatal lethality, growth retardation (of around 60%), and placental hypoplasia. Despite more pronounced lethality in mice and more obvious rib anomalies in human pUPD14 disomies, the phenotypes of disomic (UPD12) mice show enough analogy to the features observed in individuals with human UPD14 to indicate similar regulatory mechanisms might operate within the conserved region of the two species.

The importance of the *Dlk1* gene in adipogenesis and differentiation of several other cell types, supported by numerous *in vitro* studies, has been confirmed *in vivo* by mouse knockout experiments and through them we have learned about its crucial role in normal growth and development. Some of the features found in mice with ablation of *Dlk1* share similarities between symptoms found in patients with UPD14, which could implicate a role for *Dlk1* in these human disorders. However, many aspects of *Dlk1* function, together with its interacting partners and pathways it is part of, remain to be established.

1.4 Concluding remarks and aims

The crucial role of imprinted genes in the course of normal development and in the maintenance of metabolic homeostasis postnatally should not be underestimated. Our knowledge, however, is not yet sufficient to understand all the underlying mechanisms, modes of regulation and the forces that have led to evolution of genomic imprinting, even though the parental conflict hypothesis is widely accepted to explain the evolution of imprinting. The ability to generate knockout mice with ablation of specific imprinted genes provides a powerful means of investigating their roles *in vivo*. Generation of double or triple knockouts has been used effectively to study the potential interaction of those genes with opposite phenotypic effects, such as the reciprocally expressed *Igf2/Igf2r* of *Grb10/Igf2* gene pairs.

Altered imprinting status of various genes leads to similar phenotypic features usually involving pre- and postnatal growth changes which indicated the possibility of imprinted genes acting in common genetic pathways. For example mice with a disrupted *Zac1* imprinted gene simultaneously show an abnormal transcription of many other imprinted genes. It has been suggested that *Zac1* might be involved in control of an imprinted gene network (including genes such as *Igf2*, *H19*, *Cdkn1c* and *Dlk1*) that is crucial in regulation of prenatal growth control (Varrault et al., 2006), however more detailed investigation is needed to establish if this prediction is true.

Grb10 and *Dlk1* are imprinted genes that seem to act in agreement with the parental conflict hypothesis. *Grb10* is a maternally expressed growth inhibitor and *Dlk1* is a paternally expressed growth enhancer. Both of these genes are expressed in the placenta (Yevtodiyenko and Schmidt, 2006; Charalambous et al., 2010) and there is evidence for co-expression of both of these genes in embryonic tissues, such as developing muscle and cartilage tissues, pancreatic bud, liver, lung bronchioles and developing kidneys and adult tissues, for example monoaminergic neurons in the CNS, cells within ovaries and testes as well as β- cells of pancreatic islets (Charalambous et al., 2003; Yevtodiyenko and Schmidt, 2006; da Rocha et al., 2007; Lui et al., 2008). Their overlapping expression sites during pre- and post-natal periods are summarised in **Table** 1.3. Germline ablation of *Grb10* results in adult mice with a lean phenotype (reduced adiposity) and an enhanced ability to clear a glucose load, whereas the lack of *Dlk1* leads to increased adiposity (mild obesity when fed on high fat diet) in adulthood (**Table** 1.4). As a result of the opposite imprinting status and phenotypic features seen in knockout mice, our hypothesis predicts that the reciprocally imprinted *Grb10* and *Dlk1* genes

are acting through a common genetic pathway. **Figure** 1.8 illustrates two possible pathways: one predicts that the paternally expressed *Dlk1* acts as inhibitor upstream of *Grb10*, while *Grb10* functions to inhibit growth and the other predicts *Grb10* inhibiting *Dlk1* which is in turn acting to promote growth.

	Grb10		*Dlk1*
	Maternal	**Paternal**	
Prenatal:	Adrenal gland, liver, kidney (developing tubules and the mesenchyme), pancreatic bud, muscle tissue (of the face and trunk, the intercostal muscles, diaphragm, cardiac muscle, tongue and limb), bronchioles, brain (the meninges, choroids plexus, subependymal layers), cartilage of the atlas, ribs, and long bones, absent from CNS	Cartilage (of the axis, ribs, head, and long bones), heart, lungs, gut, umbilicus, tongue, developing CNS (the meninges of the fourth ventricle, ventral midbrain, diencephalon, the medulla oblongata and ventral spinal cord)	Pituitary gland, adrenal gland, preadipocytes within brown adipose tissue, skeletal muscle (tongue, diaphragm, intercostal), diencephalon in the thalamus and more strongly in the hypothalamus and optic recess, endothelium of blood vessels, submandibular gland, β-cells of the pancreas, epithelium of terminal bronchioles and surrounding mesenchyme in the lung, hepatoblasts, and immature hepatocytes in the liver, primordial cartilage and distal regions of the developing bones
Postnatal	A- and β- cells of pancreatic islets, skeletal muscle and the intrinsic muscle of the tongue, white adipose tissue, heart, spleen, uterine horns and oviducts in females and Leydig cells of the testes in males	CNS: midbrain, thalamic, hypothalamic and hindbrain nuclei, septal nuclei and the cholinergic inter-neurons of the caudate putamen within the forebrain, most of monoaminergic cells within midbrain and hindbrain	The somatotroph cells of the pituitary gland, adrenal gland, preadipocytes, β-cells of islets of Langerhans, bone marrow, Leydig cells of the testes and cells in the ovaries, monoaminergic neurons in the CNS, brain (nucleus accumbens and several areas within the hypothalamus: suprachiasmatic nucleus, the arcuate nucleus, the supraoptic nucleus and the paraventricular hypothalamic nucleus)
	Biallelic expression (predominantly paternal) in CNS: median preoptic nucleus, medial habenular, medial amygdaloid nuclei and ventromedial hypothalamus		Biallelic expression in neural stem cells and niche astrocytes

Table 1.3 Sites of mouse *Grb10* and *Dlk1* expression pre- and postnatally (Tornehave et al., 1993; Jensen et al., 2001; Charalambous et al., 2003; Yevtodiyenko and Schmidt, 2006; da Rocha et al., 2007; Smith et al., 2007; Wang et al., 2007; Ferron et al., 2011; Garfield et al., 2011).

The aim of this project was to test the abovementioned hypothesis and gain further insight into the possible mechanisms of action of *Grb10* and *Dlk1* and their potential for interaction. This was to be achieved through characterisation of $Grb10^{m/+}/Dlk1^{+/p}$ double knockout mice and their comparison with wild type, $Grb10^{m/+}$ and $Dlk1^{+/p}$ single knockout animals.

Grb10	***Dlk1***
• Maternally expressed • Growth suppressor • *Grb10* knockout mice: - Overgrowth - Increased lean mass - Decreased adiposity	• Paternally expressed • Growth enhancer • *Dlk1* knockout mice: - Growth retardation - Slight obesity - Increased adiposity

Table 1.4. Comparison of *Grb10* and *Dlk1* genes and the phenotypes resulting from their ablation in mice.

Reciprocal effects of oppositely expressed *Grb10* and *Dlk1* genes on growth and lean and adipose tissue content.

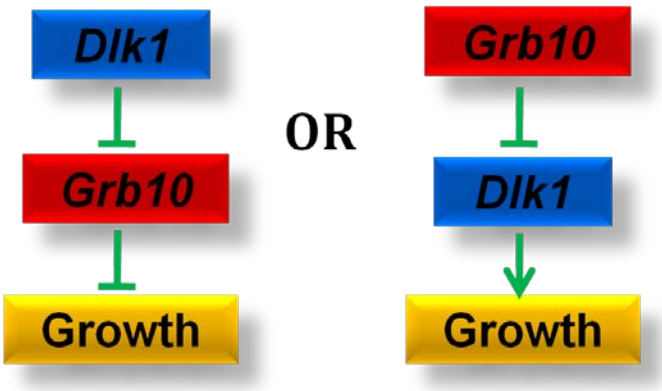

Figure 1.8 Possible modes of interactions between the *Grb10* and *Dlk1* genes in the same genetic pathway.

First of the proposed models predicts *Grb10* (acting as a growth suppressor) inhibition by *Dlk1*, whereas the alternative model proposes that *Grb10* is inhibiting *Dlk1* (potent growth enhancer). Note that the indicated genetic interactions do not necessarily imply direct physical interaction between Grb10 and Dlk1 proteins.

This study aimed to:

1. Analyse the roles of *Grb10* and *Dlk1* during embryonic development by studying cell growth, proliferation and prenatal growth differences in *Grb10*$^{m/+}$*/Dlk1*$^{+/p}$ double knockout mice.
2. Characterise the effects of *Grb10* and *Dlk1* ablation on postnatal growth and characterise the phenotype of *Grb10*$^{m/+}$*/Dlk1*$^{+/p}$ double knockout mice.
3. Investigate the influence of ablation of *Grb10* and *Dlk1* genes on energy homeostasis by characterising the glucose-regulated metabolic phenotype of *Grb10*$^{m/+}$*/Dlk1*$^{+/p}$ double knockout mice.

If the hypothesis is correct, *Grb10*$^{m/+}$*/Dlk1*$^{+/p}$ knockout mice should, in at least some respects, resemble phenotypically either *Grb10*$^{m/+}$ or *Dlk1*$^{+/p}$ single knockout animals.

CHAPTER 2

2 Materials and Methods

2.1 Animals

2.1.1 Animal husbandry

Mice were maintained in accordance with UK Home Office Regulations on an artificial light/dark cycle which provided 13 hours of light/11 hours of darkness (including 30 min of artificial dawn and dusk lighting). The temperature was maintained at 21°C ± 2°C with a relative humidity of 55 ± 10%. Animals were provided unrestricted access to food (CRM formula, Special Diets Services, UK) and water (unless otherwise stated). Mice were housed in individually ventilated cages at a density of one to six animals per cage.

2.1.2 Schedule 1 methods

Mice were culled by a Home Office Personal Licence holder according to recognised Schedule 1 methods. Embryos were culled by immersion in ice cold 0.1% (v/v) PBS (phosphate buffered saline, Oxoid, UK) for 10 min after removal from the uterus. Neonatal animals were sacrificed by decapitation and adult animals by cervical dislocation or by administration of a lethal dose of Euthatal (Merial Animal Health Ltd, UK).

2.1.3 Derivation of knockout mice

The *Grb10Δ2-4*$^{m/+}$ knockout mouse strain (from this point named *Grb10*$^{m/+}$) was created by Dr. William Bennett using the KST268 ES cell gene trap line (Baygenomics) in an ES cell co-culture method (Charalambous et al 2003) and maintained on a mixed C57BL/6/CBA genetic background. The mutant *Grb10*$^{m/+}$ allele includes the replacement of 3 exons, including the first 2 protein coding exons, with a *LacZ* reporter gene. *Dlk1Δ1-3*$^{+/p}$ knockout mice (from this point named *Dlk1*$^{+/p}$) were generated in the laboratory of Dr. Steven Bauer (Raghunandan et al., 2008). In the *Dlk1*$^{+/p}$ knockout mice a neomycin resistance cassette replaced 3.8 kbp of the endogenous allele, including the promoter and first three exons of *Dlk1. Dlk1Δ1-3*$^{+/p}$ animals were maintained on a C57BL/6 genetic background.

Both knockout strains described above (**Figure** 2.1) were interbred to derive *Grb10*$^{m/+}$*/Dlk1*$^{+/p}$ double knockout mice.

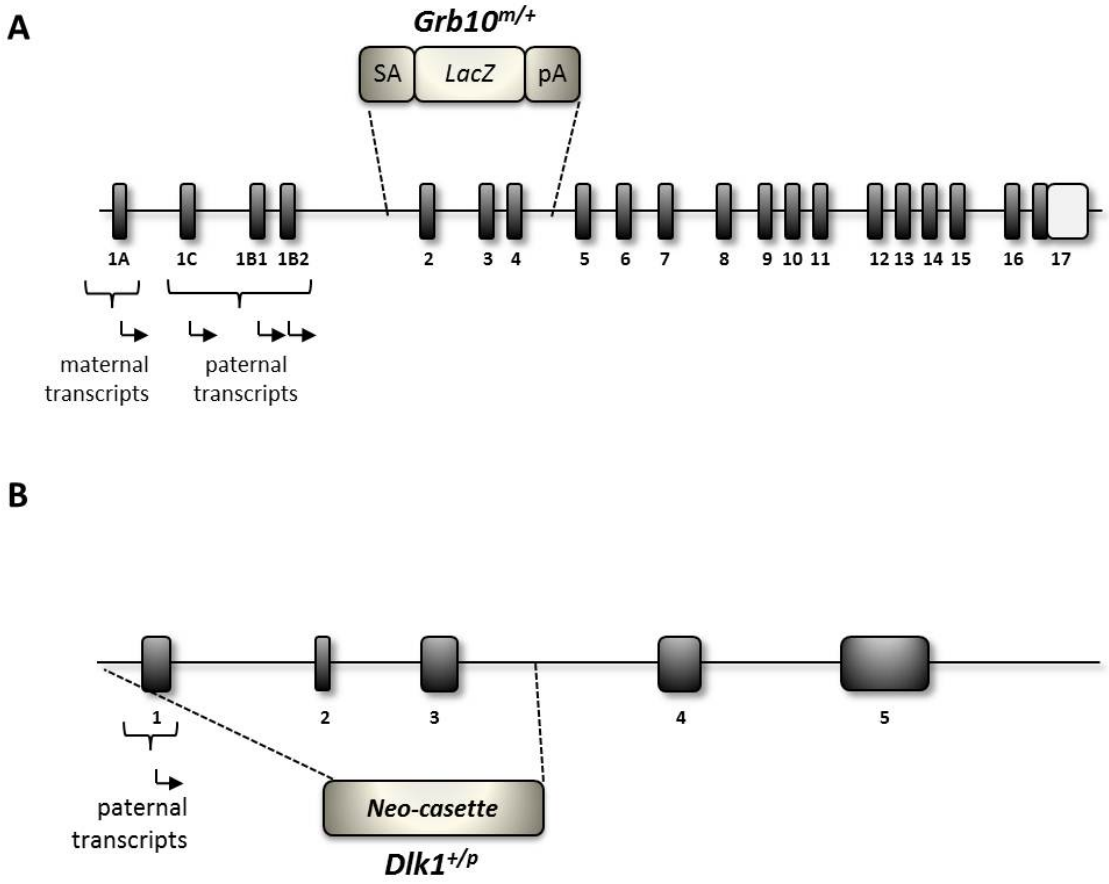

Figure 2.1 *Grb10* and *Dlk1* knockout alleles used to generate $Grb10^{m/+}$ and $Dlk1^{+/p}$ mice. A) *Grb10* allele with the insertion of a *LacZ* cassette replacing exons 2 - 4, which also included splice acceptor (SA) and poly-adenylation (pA) sites. **B)** *Dlk1* allele and *Neomycin* cassette replacing exons 1, 2 and 3.

$Grb10^{m/+}$ female mice (30% neonatal and 13% adult overgrowth, decreased fat tissue and increased lean tissue content, improved glucose tolerance) were generated by crossing of $Grb10^{m/+}$ female mice with wild type male mice. $Dlk1^{+/p}$ male mice were obtained by crossing $Dlk1^{+/p}$ male mice with wild type female mice. $Grb10^{m/+}$ and $Dlk1^{+/p}$ mice were crossed in order to generate wild type, $Grb10^{m/+}$, $Dlk1^{+/p}$ and $Grb10^{m/+}/Dlk1^{+/p}$ double knockout mice (**Figure** 2.2). Due to parent-of-origin-specific expression of both *Grb10* and *Dlk1*, generation of mice always involved crossing $Grb10^{m/+}$ female with $Dlk1^{+/p}$ male animals. Mice at of at least 6 weeks of age were bred in cages containing one male and either 1 or 2 females. Detection of a cervical plug (defined as day 0.5 *post coitum*) allowed for the recovery of embryos at the relevant gestational stage.

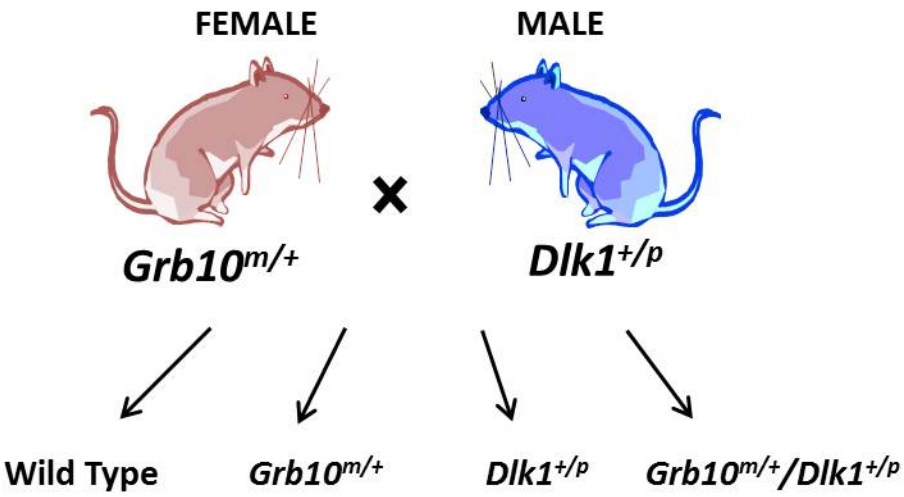

Figure 2.2 Cross of *Grb10*$^{m/+}$ and *Dlk1*$^{+/p}$ mice and resulting genotypes of animals used in this study.

In order to generate *Grb10*$^{m/+}$/*Dlk1*$^{+/p}$ double knockout mice, female mice with maternal transmission of *Grb10* deletion (*Grb10*$^{m/+}$) were crossed with male mice with paternal transmission of *Dlk1* ablation (*Dlk1*$^{+/p}$). The resulting genotypes of animals used in this study included wild type, *Grb10*$^{m/+}$, *Dlk1*$^{+/p}$ and *Grb10*$^{m/+}$/*Dlk1*$^{+/p}$.

2.2 Molecular methods

The majority of reagents used in the study were obtained from Sigma Aldrich, UK or Fisher Scientific, UK unless stated otherwise.

2.2.1 Genotyping of transgenic mice

Polymerase chain reaction (PCR) was used as a genotyping method for all transgenic mice. Crude DNA extracts were prepared from whole yolk sacs (from embryos), tail clips (approximately 2 mm of tail tip from neonates) or ear clips (1-3 ear-punch discs of approximately 2 mm diameter from adult mice). Tissues were boiled in 600 µl of 0.1 M sodium hydroxide for 10 min and subsequently vortexed for approximately 10 seconds. 50 µl of 1M Tris-HCL pH 8 solution was then added to each sample before vortexing again. 1 µl of DNA solution was used as the template in each PCR reaction. PCR reactions were then carried out in a total volume of 20 µl of GoTaq Green Master Mix (Promega, UK) with appropriate primers used at final concentration of 0.25 µM (Invitrogen, UK; **Table** 2.1). PCR was carried out using a G-Storm Mark 1 thermal cycler (Gene Technologies Ltd., UK). The primers used for *Grb10* and *Dlk1* genotyping are listed in **Table** 2.1 and reaction conditions given in **Table** 2.2. Upon amplification, 15 µl of each sample was loaded on a 1% (w/v) (*Grb10* genotyping) or 1.5% (w/v) (*Dlk1* genotyping) agarose (Invitrogen, UK) gel with an addition of 0.5 µg/ml ethidium bromide in 1x TAE buffer (2 M Tris 50 mM EDTA, 5.7% (v/v) acetic acid). A 1kb DNA ladder (Promega, UK) was run alongside the reactions for band size estimation. DNA samples were visualised under ultraviolet light (Alphaimager 3400) and data was recorded digitally.

Genotyping primers	Primer	Sequence	Band size
Grb10	**β-geo-F**	ttc aac atc agc cgc tac ag	571 bp
	β-geo-R	ctc gtc ctg cag ttc att ca	
Dlk1	**Dlk1 F**	cat ctg cac gag act agt g	423 bp + 339 bp
	Dlk1 R	ctg tat gaa gag gac caa gg	
	neo F	cca aat gtc tat agt ctc ctc	

Table 2.1. *Grb10* and *Dlk1* primers used for PCR genotyping.

Experimental parameters	*Grb10* genotyping	*Dlk1* genotyping
Initial denaturation	3 min at 94°C	3 min at 94°C
Annealing	36 cycles of: 1 min at 94 °C 1 min at 60 °C 1 min at 72°C	18 cycles of: 30 sec at 94 °C 30 sec at 64 °C 30 sec at 55.5 °C 30 sec at 72 °C 25 cycles of: 30 sec at 94 °C 30 sec at 55 °C 30 sec at 72 °C
Elongation	5 min at 72 °C	10 min at 72°C

Table 2.2. Experimental parameters for PCR used to genotype *Grb10*$^{m/+}$, *Dlk1*$^{+/p}$ and *Grb10*$^{m/+}$/*Dlk1*$^{+/p}$ transgenic mice.

2.2.2 Urine protein analysis using SDS- PAGE gels

Urine samples were collected from 3 months old male mice and placed on dry ice before transferring to -20°C. When needed, 15 µl of MQ water was added to 1.5 ml tubes before adding 5 µl of 5x reducing buffer (3.1 ml 2M Tris – HCl pH 6.8, 2.4 ml 20% SDS, 2.5 ml glycerol, 2.5 ml β– mercaptoethanol, 500µl 1% bromophenolblue). Urine samples were thawed on ice and then 5 µl of urine was added to reducing buffer mixed with water in the corresponding tube. Samples were boiled for 10 minutes and chilled on ice. After centrifuging for 20 seconds samples were run at 150 V for about 1 hour on a Criterion ® Precast Gel (10% Tris– HCl, 1.0 mm, 18 combs, 30 µl, BIO–RAD) containing 1x Running Buffer (made from 5x Running Buffer: 9 g Tris, 43.2 g of glycine, 3 SDS, made up to 600 ml with MQ water). The gel was then placed in Coomasie Blue Solution (40% methanol, 10% acetic acid in MQ water, 2.5 g Coomassie Brilliant Bluer – 50% dye content; filtered with filter paper, Whatman, UK) on a plastic tray on a rocking platform. After 1 hour the gel was washed in Coomasie Destain (40% methanol, 10% acetic acid), this step was repeated another 2 times for 20 minutes each, then for 1 hour. Protein was visualized with white light using an Alphaimager® 3400 machine. Results were compared to a dual colour Precision Plus Protein® Standards ladder (BIO-RAD).

2.3 Allometric analyses

2.3.1 Tissue dissection

Total body weights were recorded immediately following sacrificing of mice according to Schedule 1 methods. Organs collected from 1 day old mice included: livers, hearts, brains, kidneys and lungs. From adult mice gonads, pancreata, livers, kidneys, gonadal and renal fat pads, masseter and gastrocnemius muscles, tongues and brains were dissected. All tissues were dabbed on aluminium foil to get rid of excess liquid and weights were subsequently recorded. Organs were immediately frozen in liquid nitrogen and kept at -80°C until needed or processed further if necessary.

2.4 Histological analyses

Histological methods were based on Bancroft and Gamble (2002).

2.4.1 Tissue fixation and processing for wax embedding and sectioning

Whole organs destined for wax embedding were fixed in 4% (w/v) paraformaldehyde (PFA) in 0.1% PBS at 4^{o}C overnight. The following day organs were washed in 0.1% PBS, transferred into 70% ethanol solution and stored at 4^{o}C until needed. Organs were processed using a Leica TP 1020 machine. Firstly, they were washed for 3 hours in 70 % ethanol, then for 2 hours each in: 90% ethanol, twice in 100% ethanol, twice in histoclear and twice in wax.

After processing, organs were embedded in wax blocks using a Leica EG 1160 work station. Embedded tissues were then cut into 6 µm sections using a microtome (Leica RM 2155). Tissue sections were then transferred onto Polysine microscope slides (VWR International, UK) and left to dry overnight.

2.4.2 Tissue fixation and processing for cryosectioning

Organs destined for cryosectioning were fixed for 30 min in 2% PFA, 0.2% glutaraldehyde in 0.1% PBS and then were transferred into ice cold 30% (w/v) sucrose and incubated at 4°C overnight. Tissues were dried by dragging them across aluminium foil, embedded by placing in a cassette filled with Optimal Cutting Temperature (OCT) compound (VWR International, UK) and allowed to freeze on dry ice. Cryo-blocks were stored at -80°C before being sectioned at 10 µm using a cryostat (CM1850; Leica). Sections were transferred onto SuperFrost Plus microscope slides (VWR International, UK), air dried and stored at -80°C.

2.4.3 Haematoxylin and Eosin (H&E) staining

The wax embedded tissue sections were dewaxed in histoclear twice for 2 min and then hydrated through an alcohol series: 100%, 100%, 95%, 90%, 70% and 50% ethanol for 1 min in each. Sections were placed in MQ water for 1 min and then transferred to filtered haematoxylin for 15 min. Afterwards, sections were washed gently in running tap water for 3 min and then transferred into 1% concentrated HCl in 70% ethanol for 30 sec, 1% NH_3 in 70% ethanol for 1 min and then washed in 70% ethanol for 30 sec. Slides were transferred to filtered eosin for 5 min and then washed in 70% ethanol for 3 sec, 90% ethanol for 3 sec and then washed twice in 100% ethanol for 5 sec which was followed by two washes in histoclear

for 2 minutes. Samples were mounted under coverslips in DPX mounting medium (VWR International, UK).

2.4.4 Periodic Acid - Schiff (PAS) Staining

Sections were dewaxed in histoclear twice for 2 min, hydrated through an ethanol series (as for H&E staining) and washed in MQ water for 1 min. Slides were then placed in freshly prepared 1% periodic acid in MQ water for 6 min and washed under running tap water for 3 minutes. After incubation in MQ water for 1 min sections were placed for 15 min in Schiff reagent. Slides were washed under running tap water for 5 min, counterstained with haematoxylin for 2 min, dehydrated and mounted as described in section 2.4.3.

2.4.5 Oil Red O staining

0.5 g of Oil Red O (Lamb, UK) was dissolved in 100 ml of 100% isopropanol. MQ water was added to stock Oil Red O to make a working solution of Oil Red O in 60% isopropanol. The solution was heated and stirred at 100°C for 5 min and then filtered using 25 µm filter paper (Whatman, UK), first when hot and then again when cool. This solution was kept and filtered before every use. Cryosections were air-dried and rinsed with 60% isopropanol prior to incubating in Oil Red O solution for 15 min. Sections were then rinsed with 60% isopropanol and gently washed under running tap water until clear. Slides were counterstained with Meyer's haematoxylin or Light Green for 30 sec, washed under running tap water for approximately 3 min and mounted in gel mounting medium (VectaShield, Vector Laboratories, UK).

2.4.6 *LacZ* staining

Cryosections were fixed for 30 min in 4% PFA and then incubated in 1mg/ml 5-bromo-4-chloro-3-indolyl-beta-D-galactopyranoside (X-gal) in stain base (30 mM $K_4Fe(CN)_6$, 30 mM $K_3Fe(CN)_6.3H_2O$, 2 mM $MgCl_2$, 0.01 % (w/v) sodium deoxycholate, 0.02 % (v/v) Igepal CA-630 in 0.1% PBS) overnight at 37°C. Following incubation, sections were rinsed in 0.1% PBS and stained with Nuclear Fast Red (Vector Laboratories, UK) for 2 min, dehydrated through ascending ethanol series, placed in histoclear for 5 min and mounted in DPX.

2.4.7 Microscopy

Stained sections were viewed under a Nikon Eclipse E800 compound microscope under the magnification stated in each figure legend. Pictures were taken using a colour Nikon digital Sight DS-U1 camera operated with NIS Elements D 2.30 software.

2.4.8 Morphometric analysis

Pictures of tissue sections (including lungs, kidneys and adipocyte tissue) were taken under 200x magnification and were visualised on the computer screen. Using an 8 x 4 grid, the whole section was divided into 32 areas and five areas were randomly chosen from each slide. These same areas were used in each slide section for cell counting.

2.4.9 Alcian Blue/ Alizarin Red staining

Upon sacrifice, skin and dense organs were removed from mice. Skeletons were fixed in 100% ethanol for 3 days and then in acetone for 1 day. Skeletons were washed in MQ water for several minutes before staining in colour solution (1 part 0.3% Alcian Blue in 70% ethanol: 1 part 0.1% Alizarin Red in 95% ethanol: 1 part Glacial Acetic Acid: 17 parts 70% ethanol) for 3 days at room temperature. Skeletons were then washed in MQ water for several minutes and soft tissues cleared in 1% KOH until the skeleton was visible. They were then transferred into 50% glycerine, and on the following day into 80% glycerine. Afterwards skeletons were kept in 100% glycerine.

2.5 Metabolic analyses

2.5.1 Dual energy X-ray absorptiometry

Adult mouse carcasses were analysed by Dual energy X-ray absorptiometry (DXA) using a PIXImis scanner (Lunar, Madison, WI) with small-animal software. Bone mineral density and content, total area, lean and fat tissue weight were recorded. Lean and fat tissue weights were expressed as percentages of total body weight before performing statistical analysis.

2.5.2 Monitoring of food consumption

Mice were separated into single cages and left to acclimatize for 10 days. A recorded amount of food was then placed in each cage and the weight of both mice and food was recorded every other day for a period of two weeks at the same time of the day in order to calculate the amount of food consumed per gram of body weight per day which was calculated using a metabolic scaling exponent of $M^{2/3}$. The relationship between mammalian basal metabolic rate (BMR, ml of O_2 per h) and body mass (*M*, g) has been the subject of thorough investigation. Data encompassing five orders of magnitude variation in *M* and featuring 619 species from 19 mammalian orders in a study of the allometry of mammalian BMR that accounts for variation associated with body temperature, digestive state, and phylogeny supported use of a metabolic scaling exponent of $M^{2/3}$ (White and Seymour, 2003).

2.5.3 Measurement of serum triglyceride levels

Triglyceride assay was used to assess the blood serum levels of triglycerides. Mice were fasted for 16 hours prior to the start of the experiment. Between 50 µl and 100 µl of blood was obtained from the tail tip and the tail was sealed with tissue adhesive (Abbott Laboratories, UK). Triglyceride levels were measured using a Triglyceride Assay Kit (Cayman Chemical Company, UK) according to manufacturer's instructions.

2.5.4 Glucose tolerance tests

Glucose tolerance tests (GTT) were performed to assess whole body glucose clearance. Mice were fasted for 16 hours prior to the start of the experiment. Between 50 and 100 µl of blood was taken from the tail tip at time point '0' and the tail was sealed with tissue adhesive (Abbott Laboratories, UK). 30% D-glucose at 1 g per kg of body weight was administered by

intraperitoneal injection and timing began from the point of injection. Measurements of glucose level were performed on blood drawn from the tail tip at 15 min, 30 min, 60 min and 120 min post injection using a glucometer (One-Touch ULTRA, LifeScan, UK).

2.5.5 Measurements of glucose levels in fed and fasted mice

Mice with *ad libitum* access to food (fed) and mice fasted for 16 hours (fasted) prior to the start of the experiment were subject to measurements of glucose levels. Between 50 and 100 µl of blood was taken from the tail tip at time point '0' and the tail was sealed with tissue adhesive (Abbott Laboratories, UK). Measurements of glucose level were performed on blood drawn from the tail tip using a glucometer (One-Touch ULTRA, LifeScan, UK).

2.6 Cell culture-based techniques

2.6.1 Derivation of primary mouse embryonic fibroblast (pMEF) cell cultures

Derivation of primary embryonic fibroblast cells was carried out according to methods described in Mouse Cell Culture: Methods and Protocols (Ward and Tosh, 2008). 14.5 day old embryos were dissected out of the uterus and placed in ice cold 0.1% PBS. Weight of both embryos and placentae were recorded, placentae were frozen in liquid nitrogen and yolk sacs were stored in -20°C for genotyping. Embryos were then decapitated and heads were placed in X-Gal in stain base solution for β-galactosidase expression analysis. Decapitated embryos were transferred into 2 ml of complete pre-warmed Dulbecco's Modified Eagle's medium (DMEM) (Gibco, Invitrogen, UK) (DMEM media, 10% Fetal bovine serum *(*FBS), 1% penicillin/ streptomycin) and livers were removed and frozen in liquid nitrogen. Embryos were then dissociated in 1 ml of pre-warmed media without serum by pushing them through a 1 ml syringe and then P1000 pipette and transferred into 15 ml Falcon tube. 250 µl of 0.5**%** Trypsin-EDTA solution (Gibco, Invitrogen, UK) was added and the tubes were incubated at 37°C for 30 min, gently inverted every 5 min. The cell suspension was then transferred into a 25 cm^2 culture flask (Gibco, Invitrogen, UK) with 8ml of warm DMEM complete media. Flasks were incubated at 37°C in 5% CO_2 environment.

2.6.2 Maintenance of pMEFs cultures

DMEM media was changed every 1-2 days: old media was removed and cells washed twice with pre-warmed 0.1% PBS, 8 ml of fresh media was then added to the flask. Flasks with confluent cells were subject to passaging or freezing down. When passaged, media was removed and cells washed with 0.1% PBS. 1 ml of 0.5 **%** Trypsin-EDTA (Gibco, Invitrogen, UK) solution per 25 cm^2 was then added and flasks incubated for 5 min at 37°C. 3 ml of warm DMEM complete media per 25 cm^2 was added, the cell suspension was transferred into a 15 ml Falcon tube which was then centrifuged for 4 min at 180*g*. To freeze the cells the pellet was resuspended in 90% FBS and 10% Dimethyl sulfoxide (DMSO), frozen at -20°C overnight and then at -80°C before being stored in liquid nitrogen. To passage the cells, the pellet was resuspended in 1 ml of DMEM complete media and equal aliquots of the suspension were used to seed fresh flasks.

2.6.3 pMEFs growth curve analysis

Following the protocol for passaging cells (see Section 2.6.2), the pellet was resuspended in 1 ml of media and an aliquot of 15 µl was transferred to each side of a haemocytometer. Cells were counted in order to determine the number of cells present in 1 ml, using the following equation:

Average cell number from 5 squares within a haemocytometer grid x Dilution factor x 10^4

$1x10^4$ cells were then seeded into each well of a 24 well plate and incubated at 37°C. An initial count of the attached cell number was taken 24 hours later, after which point cells were counted every 48 hours over a 12 day period. Every second day cells from four wells were removed after 5 min incubation in 250 µl of 0.5 % Trypsin-EDTA (Gibco, Invitrogen, UK) solution and centrifuged for 4 min at 180*g* after adding 200 µl of media. Cells were resuspended in an appropriate volume of DMEM complete media/0.1% PBS and the number of cells per ml of medium in each well was determined twice per well by use of a haemocytometer filled with diluted cell suspension. Cells in the remaining wells were washed in 0.1% PBS and provided with fresh medium, as described before. Counting was carried out over 12 days for pMEFs derived from embryos of all 4 genotypes in 3 separate experiments and the results used to calculate mean values. Cell growth was calculated as a percentage of the initial seeding density.

2.6.4 Propidium iodide staining of embryos and pMEF cell cultures for fluorescence activated cell sorting (FACS) analysis

E11.5 embryos were dissected from the uterus and washed several times in 0.5 ml of filtered, ice cold 0.1% PBS. Embryos were disaggregated using a pestle inside the 1.5 ml tube, gently resuspended through a P1000 pipette tip and centrifuged for 10 min at 500*g*. Cell resuspension in ice cold 0.1% PBS and centrifugation were repeated twice. Cells were then gently dissociated by filtering through a 40 µm nylon cell strainer (BD Falcon, BD Biosciences, USA). In the case of pMEFs, in approximately 70% confluent 75 cm^2 flasks media was removed and cells were washed with 0.1% PBS. 1 ml of 0.5 % Trypsin-EDTA (Gibco, Invitrogen, UK) solution per 25 cm^2 was then added and flasks incubated for 5 min at 37°C. Cells were then washed twice in ice cold 0.1% PBS. Embryonic and pMEFs cell suspensions were inspected by

spreading droplets of suspensions onto glass slides and air dried at room temperature. Spreads were stained with DAPI (1 µg/ml) and viewed under a fluorescent microscope (Leica DMIRB).

Embryonic cell suspensions and pMEFs cultures were then stained for 30 min at 37°C in propidium iodide buffer (50 µg/ml propidium iodide, 100 µg RNAse A, 0.1% Igepal CA-630 and 50 µg/ml trisodium citrate in 0.1% PBS). Stained cells were then washed in 0.1% PBS and 100000 events were collected by FACS Canto (BD Biosciences, USA) at the excitation wavelength of 488 nm and an emission wavelength of 600 nm. Cells were analysed for cell size (forward scatter FSC vs side scatter SSC) (**Figure** 2.3) and cell cycle position (propidium iodide concentration) (**Figure** 2.4). Data was analysed using FlowJo software (v7.6, FlowJo Software. USA).

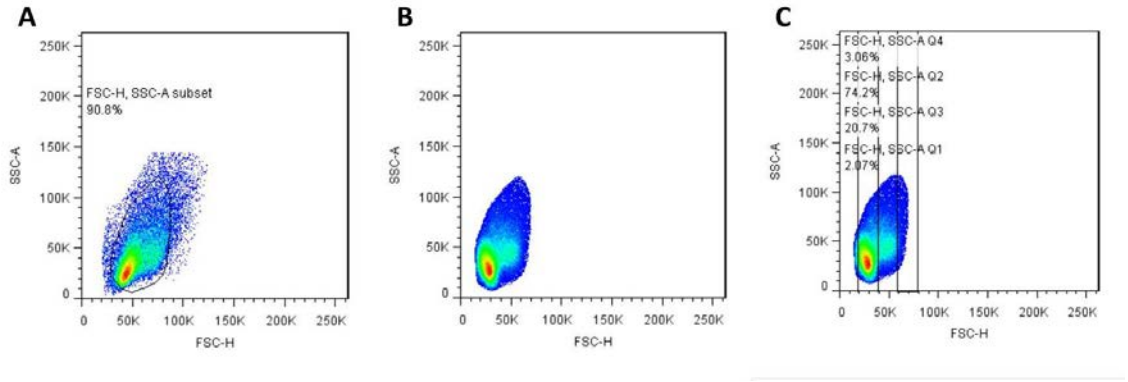

Figure 2.3 Scatter plot with 100,000 analysed cells and gates used for FACS analysis.
Side scatter (SSC) determines the granularity of the cell and forward scatter (FSC) the size. **A)** 100 000 analysed cells, displayed using side and forward scatter, were gated to get rid of any debris and dead cells **B)** Only gated cells were subject to further analysis C**)** Four equally-sized gates were created along the FSC-axis (0-25k, 25k-50k, 50k to 75k and 75k-100k) and the percentages of cells in each one of them were calculated.

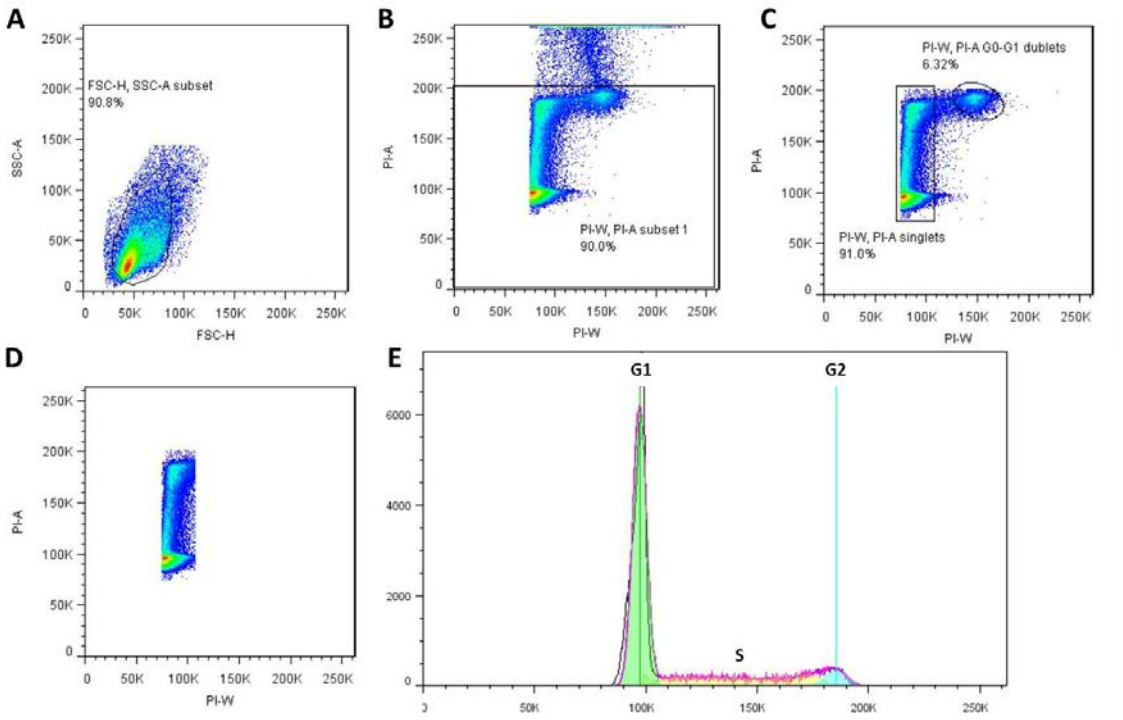

Figure 2.4 Scatter plots and representing 100,000 analysed cells and histogram with G1, S and G2 cell cycles phases indicated.

A) 100 000 analysed cells, displayed using side and forward scatter, were gated to get rid of any debris and dead cells **B)** Gated cells were then displayed using PI-A and PI-W and showed a characteristic shape and cells above 200K were excluded from further analysis **C)** Cells in the left hand side of obtained shape represented single cells whereas cells on right hand side represented doublet cells. **D)** Only single cells were subject to cell cycle analysis **E)** Analysed single cells presented on histogram with indicated G1, S and G2 phases of cell cycle.

2.7 Statistical analysis

GraphPad Prism (v5, GraphPad Software, CA, USA) was used for statistical analysis. Results were statistically analysed by tests stated in the corresponding figure legends. The majority of data was subject to one-way analysis of variance (One-way ANOVA), which is a way to test the equality of three or more means at one time by using variances. The assumptions for One-way ANOVA are: the populations from which the samples were obtained must be normally or approximately normally distributed, the samples must be independent and the variances of the populations must be equal. The null hypothesis will be that all population means are equal, the alternative hypothesis is that at least one mean is different. This test was used as a way to compare means for four different genotypes.

A post-hoc Tukey test was applied in order to find which means are significantly different from one another. It is a single-step multiple comparison procedure and statistical test generally used in conjunction with an ANOVA to find which means are significantly different from one another. It compares all possible pairs of means, and is based on a studentized range distribution. It is based on assumptions that the observations being tested are independent and that there is equal variation across observations. Graphs represent arithmetic means ± standard error mean (SEM). For the purpose of clarity, no stars representing significant differences are depicted in any of the graphs but all possible statistical comparisons and any significant differences are shown in tables that accompany each graph.

CHAPTER 3

3 Prenatal characterisation of *Grb10*$^{m/+}$*/Dlk1*$^{+/p}$ double knockout mice

3.1 Introduction

Cell growth (the increase in cell size and protein mass) and cell proliferation are highly coordinated processes that underlie correct growth of an organism. The preservation of precise control over the cell cycle is an essential condition for an organism to undergo normal development. Highly specific and accurately timed mitotic events are based upon progression through a range of molecular phases in a highly regulated order (Cooper, 2000). As a result, any disruptions of this well-organised process may lead to suppression of the process of proliferation and can result in tumourigenesis (reviewed in Malumbres and Barbacid, 2009). Similarly, misregulated signalling by factors that control cell cycle progression might have detrimental consequences on normal growth and development, which can be observed in a range of human growth disorders and corresponding mouse phenotypes resulting from an aberrant regulation of growth controlling genes.

A complex set of interactions that function on systemic, cellular and molecular levels is necessary for the control of growth, and all of them must operate correctly to achieve cell, tissue, organ and organism size within the normal range for a given species (Malumbres and Barbacid, 2001). Site- and time-specific coordination between cell growth (mass), as well as cell proliferation and cell death (number), are crucial requirements for normal growth and development of the organism (Weinkove et al., 1999; Crickmore and Mann, 2008). In mammals, cell number in the whole organism is largely determined by hormones, nutrient supply and growth factors (Burns and Hassan, 2001).

Identification of the IGF (Insulin Growth Factor) pathway as crucial during development was based on observations of *in utero* growth retardation following ablation of genes encoding proteins that were part of IGF-pathway (DeChiara et al., 1990; Liu et al., 1993), suggesting that this pathway functions to control the rate of normal cell proliferation. This was further supported by a study showing that embryonic growth retardation is a result of slower progression through the cell cycle which leads to the generation of lower numbers of cells during embryonic development (Baker et al., 1993), and was confirmed by analysis of *Ifg1r* deficient embryos-derived primary mouse embryonic fibroblasts (pMEFs) that displayed highly extended cell cycle phases and hypoproliferation (Sell et al., 1994).

Imprinted genes are regarded as key players in the regulation of the normal course of development (see Chapter 1). The essential contribution of both of the parental genomes

during embryogenesis was proven by mid-gestational lethality of uniparental embryos (Barton et al., 1984; Surani et al., 1984). A valuable model for studying the role of parental alleles in the cell cycle and tumourigenesis has been provided by generation of primary embryonic fibroblasts from uniparental embryos (Hernandez et al., 2003). Consistent with previously described parthenogenetic and androgenetic phenotypes in mice, the role of each genome in *in vitro* proliferation and survival was different: androgenesis (lack of maternal genome) caused faster cell cycle progression and, as a consequence, induced hyperproliferation, whilst parthenogenesis (loss of paternal genome) led to premature cell death and slight growth reduction (Hernandez et al., 2003). Both of these phenotypes were in consistence with parental conflict theory, which predicts that in the absence of the growth retarding influence of the maternal genome, cell growth is enhanced whereas absence of growth enhancing paternal genome leads to cell growth arrest (Moore and Haig, 1991). The rescue of hypoproliferative parthenogenetic pMEFs was possible by specific deletion of either the *Cdkn1C* or *Igf2r* genes, both maternally expressed imprinted genes acting to suppress proliferation through inhibition of transition from S- to G1-phase and enhancing the elimination of growth factors (Hernandez et al., 2003).

Several studies have suggested that *Grb10* interacts with a number of different growth-related pathways. Evidence for a *Grb10* growth inhibitory role has been directly demonstrated by the generation and characterisation of *Grb10*$^{m/+}$ knockout mice (Charalambous et al., 2003; Smith et al., 2007; Garfield et al., 2011) with a *LacZ* reporter gene incorporated within the *Grb10* gene, which allowed for ready visualisation of the sites of *Grb10* expression from early development and into adulthood (Charalambous et al., 2003). Maternal expression of *Grb10* in E14.5 conceptuses is widespread, including skeletal and cardiac muscle, liver and bronchioles, as well as pancreatic buds and developing tubules in the kidney (see Table 1.3 in Section 1.4; Charalambous et al., 2003). Expression of *Grb10* from the paternal allele proved to be much more limited, and has been found in some cells of the heart, gut, umbilicus, lungs, tongue and cartilage. Some of these tissues are therefore thought to be sites of biallelic *Grb10* expression, although with slight predominance from the maternal allele. One of the most interesting sites of *Grb10* expression is CNS, with limited contribution of the maternal allele, as confirmed by cranial sparing in *Grb10*$^{m/+}$ mice (Charalambous et al., 2003), but some evidence has been provided for paternal *Grb10* expression in the neonatal brain (Arnaud et al., 2003). Consistent with that, our group has recently detected similar pattern of predominantly paternal *Grb10* expression in the adult brain (Garfield et al., 2011). Detailed histological study of *LacZ* expression in mice with a knockout of the paternal *Grb10* allele revealed a specific pattern of

Grb10 expression present within thalamic, hypothalamic, midbrain and hindbrain nuclei and lack of cortical expression identified at any point in the brain. In addition, the septal nuclei as well as the cholinergic inter-neurons of the caudate putamen were the sites of expression within the forebrain (Garfield et al., 2011). Previously detected *Grb10* maternal expression in ependymal and choroid plexus in the embryo (Charalambous et al., 2003) did not persist until adulthood, however a few regions, such as the median preoptic nucleus, medial habenular, medial amygdaloid nuclei and ventromedial hypothalamus were recognised as sites of biallelic *Grb10* expression in the brain (Garfield et al., 2011). This unique, reciprocally imprinted pattern of *Grb10* expression seems to be of great importance in the regulation of distinct processes: early developmental growth and postnatal metabolism (maternal expression) and adult behaviour (paternal expression).

Transmission of a non-functional *Grb10* allele through the maternal line results in fetal and placental growth effects that are in agreement with the parental conflict hypothesis. Overgrowth of $Grb10^{m/+}$ placentae has been reported from E14.5 onwards, whereas embryos displayed overgrowth from E12.5 (Charalambous et al., 2003). In addition, an increase in placental efficiency has been noted in E17.5 $Grb10^{m/+}$ placentae and embryo/placenta weight ratio was around 10% higher in $Grb10^{m/+}$ embryos when compared to wild type controls (Charalambous et al., 2010). These results indicated a function for *Grb10* in limiting placental efficiency, and the increased volume of labyrinth in $Grb10^{m/+}$ placentae suggested an increased surface area for nutrient exchange as a possible explanation for the observed phenomenon.

The $Grb10^{m/+}$ placenta is a unique example of an overgrown placenta that also displays increased placental efficiency. There are examples of other maternally expressed, imprinted genes causing placental hyperplasia but not resulting in higher placental efficiency. For example, *Ipl* gene ablation results in placental overgrowth without associated embryonic weight increase (Frank et al., 2002), which is suggestive of a role for *Ipl* as a suppressor of nutrient supply but not demand. In the case of the *Grb10* gene, increased growth of both $Grb10^{m/+}$ embryos and placentae implies its functions as a suppressor of both supply and demand. It may seem that inhibition of embryonic demand for nutrients is not advantageous for the fetus, however, studies in humans have shown that the most optimal birth weight is not substantially higher than the mean, and severe overgrowth is in fact associated with increased lethality. The optimal birth weight was instead found to be slightly above the mean birth weight for the population (Sansing and Chinnici, 1976), suggesting that it is not in the interest of the embryo to reach a specific 'threshold' of nutrient demand. Presumably in

normal situations placental maternally-expressed genes, acting in the interest of the mother, suppress nutrient transfer, and as a result, the threshold of nutrient demand is not reached. Conversely, in the case of overabundance of nutrients due to a highly efficient placenta, activation of demand suppressors prevents potentially dangerous embryonic overgrowth.

Dlk1 is another gene expressed in a parent-of-origin-specific manner in the embryo and placenta, and its paternal expression was first identified at E11 in the mouse, with levels increasing until late gestation (Schmidt et al., 2000). The precise analysis of *Dlk1* expression revealed that in E12.5 mouse embryos high levels of *Dlk1* expression were present in the developing pituitary, pancreas, lung, adrenal and other mesodermally derived tissues and by E16.5 its expression diminished in most tissues, with exceptions of the pituitary, adrenal gland and skeletal muscle (Yevtodiyenko and Schmidt, 2006; da Rocha et al., 2007). Interestingly, *Dlk1* expression was also found in the growing branches of organs developing through the process of branching morphogenesis, including lungs, pancreas and submandibular gland (Yevtodiyenko and Schmidt, 2006). In addition, analysis of *Dlk1* expression in extra-embryonic tissues allowed for its detection in endothelial cells lining the fetal blood vessels of the labyrinth, and in the junctional zone on the membrane of some glycogen cells (Yevtodiyenko and Schmidt, 2006; da Rocha et al., 2007), which implied a potential role for *Dlk1* in regulation of the interactions between mother and fetus.

Growth and neurodevelopmental defects observed in human imprinting disorders are consistent with the placental and brain expression of numerous imprinted genes (Wilkinson et al., 2007; Fowden et al., 2011). Majority of the known imprinted genes show prominent expression in the placenta (Bressan et al., 2009) and an abnormal physiology and development of placenta is particularly characteristic of disrupted imprinting status, exemplified by lack of the *Igf2* placental specific isoform that results in an aberrant transport of nutrients between maternal and fetal tissues (Sibley et al., 2004). It has also been demonstrated that for example maternally expressed *Ascl2* (achaete-scute homolog complex 2) is necessary for the correct spongiotrophoblast cells differentiation during early development of murine placenta (Guillemot et al., 1995) and also paternally expressed 10 (*Peg10*) and retrotransposon-like 1 (*Rtl1)* are imprinted genes vital for normal function of the placenta (Ono et al., 2006; Sekita et al., 2008). In addition to placental imprinting being crucial in regulation of nutrient transfer between mother and fetus, disrupted imprinting within the embryo is also able to influence its growth in a manner not dependent on the imprinting status of the placenta.

Recently, da Rocha et al (2009) generated a unique model that allowed for studying the consequences in the growing embryo of single, double, and triple dosage of *Dlk1*. The authors were able to assess the developmental and physiological functions of *Dlk1*, and found that triple dosage of *Dlk1* leads to substantial organ malformations and, subsequently, to lethality. Conceptuses with a double dose of *Dlk1* displayed overgrowth, but they failed to thrive, showing that the advantage of higher fetal weight is overcome by increased postnatal mortality. In most cases, except for the brain, levels of *Dlk1* overexpression were in correlation with tissue specific overgrowth, indicating a role for *Dlk1* in organ growth (da Rocha et al., 2009). The authors suggested that imprinted levels of *Dlk1* are providing exactly the correct dose of this gene for maintaining balance between growth and lethality. One of the hypotheses they proposed was based on the prediction that *Dlk1* influences the differentiation versus proliferation equilibrium and the result is a trade-off between prenatal size and developmental maturity. Consistent with that, malformations found in a range of organs, including lung and liver, might be consequences of developmental immaturity at these sites. More detailed analysis of this interesting phenomenon of embryonic overgrowth and subsequent growth suppression is necessary. Another important outcome from study carried out by da Rocha et al (2009) was that, unlike many other studies that cannot discern between real embryonic growth changes and embryonic growth effects as secondary consequences of altered imprinting in the placenta, this model provided information on the influence of *Dlk1* on embryonic phenotype in the presence of a normal placenta with unaltered *Dlk1* expression. Obtained results demonstrated that *Dlk1* is able to influence embryonic growth in a placenta-independent manner.

Moon et al (2002), who generated the first *Dlk1* knockout mice, reported that lack of a functional *Dlk1* gene resulted in prenatal retardation, which is in agreement with predictions of the parental conflict hypothesis. Examination of E18.5 embryos revealed approximately 20% growth reduction in comparison with wild type controls, along with a range of abnormalities accumulated during gestation (including skeletal and pulmonary defects) that led to approximately 50% lethality within two days after birth (Moon et al., 2002). These results highlighted a crucial role for *Dlk1* in normal perinatal growth, development and survival.

The importance of the dosage of imprinted genes situated on mouse chromosome 12, including *Dlk1* and *Dio3*, has been highlighted by the dramatic phenotype of embryos with maternal and paternal uniparental disomy for chromosome 12 (Georgiades et al., 2000; Tevendale et al., 2006). Detailed analysis of phenotypes of these embryos and placentae

provided evidence of an essential role for the *Dlk1-Dio3* imprinted domain in fetal viability, prenatal growth control, and the normal development of extraembryonic tissues as well as some mesodermal and neural crest-derived lineages.

Several studies have indicated that different imprinting regulation mechanisms are employed in embryo and placenta (Chapman et al., 1984; Wagschal and Feil, 2006; Lin et al., 2007). Other studies showed a group of genes exhibiting imprinted expression only in the placenta (Coan et al., 2005). Together, these findings highlight the difference in the epigenetic profiles of embryonic versus extraembryonic tissues and suggest that regulation of the imprinting in these tissues is complex and requires further investigation.

It is striking that *Grb10* and *Dlk1* are two oppositely imprinted genes with many sites of co-expression and that they result in reciprocal growth and adiposity phenotypes in mice. Consistent with the parental conflict hypothesis, lack of the maternally expressed growth suppressor *Grb10* leads to significant fetal and placental overgrowth which is persistent after birth until the difference in weight starts to diminish due to decreased adiposity in these mice. In contrast, loss of the *Dlk1* gene in mice leads to pre- and post-natal growth retardation and predisposition to diet-induced obesity in adulthood. Assessment of the relationship between *Grb10* and *Dlk1* and their importance during fetal growth and development will be discussed in this chapter and hopefully will shed light on the early developmental consequences of knockouts of both of these genes. This will help to test the hypothesis that these two genes are acting in a common genetic pathway.

In order to investigate the mechanisms of Grb10/Dlk1 growth control *in vivo*, we improved on previous studies that employed weight and morphometry alone as measures of growth. Therefore, in this chapter, in addition to allometric analysis of embryos and placentae from three different gestational stages we generated cell suspensions from whole E11.5 embryos. This allowed us to employ fluorescence activated cell sorting (FACS) analysis to delineate any potential changes within cell cycle progression, analyse the cell size distribution and compare cells of the mutant genotypes to wild type controls. Moreover, we also examined the effects of *Dlk1* and *Grb10* ablation on *in vitro* growth by using primary fibroblasts from E14.5 embryos. Proliferation rates, cell cycle progression and cell size distribution were studied in fibroblasts from knockout embryos and compared to wild type controls. As a result, work in this chapter aims to assess the effects of ablation of $Dlk1^{+/p}$ and $Grb10^{m/+}$ genes on embryonic growth *in vivo* and, by using an *in vitro* approach, attempts to identify cellular mechanisms affected by the lack of these genes.

3.2 Results

3.2.1 Analysis of embryonic and placental growth and placental efficiency in *Dlk1*$^{+/p}$, *Grb10*$^{m/+}$ and *Grb10*$^{m/+}$/*Dlk1*$^{+/p}$ E12.5, E14.5 and E17.5 embryos.

Numerous maternally and paternally expressed imprinted genes have been implicated in causing serious growth malfunctions during fetal development (DeChiara et al., 1991; Liu et al., 1993; Ludwig et al., 1996; Curley et al., 2005). In accordance with that, our lab has previously demonstrated significant overgrowth of *Grb10*$^{m/+}$ embryos starting from E12.5 and of placentae starting from E14.5 (Charalambous et al., 2003), while another group has reported significant growth reduction as a consequence of *Dlk1* ablation in mice (Moon et al., 2002). To permit for an investigation of the growth phenotype resulting from lack of both *Grb10* and *Dlk1* genes, embryonic and placental wet weights together with placental efficiencies have been analysed at different gestational stages.

3.2.1.1 E12.5

First, placentae and fetuses were isolated 12 days after the observation of a cervical plug (E12.5). As previously demonstrated by our lab (Charalambous et al., 2003), in the present study we found that E12.5 *Grb10*$^{m/+}$ embryos were significantly larger than wild type controls and also *Dlk1*$^{+/p}$ littermates (**Figure** 3.1 A). The assessment of embryonic wet weight changes in E12.5 *Grb10*$^{m/+}$/*Dlk1*$^{+/p}$ also revealed similar significant increase in embryonic weights, while no changes were found in *Dlk1*$^{+/p}$ embryonic weights. Consistent with previous studies, no statistically significant alterations in placental mass of E12.5 *Grb10*$^{m/+}$ were noted, and also placental weights of other mutant genotypes did not show any significant deviations from wild type controls (**Figure** 3.1 B). Analysis of placental efficiency also failed to show a difference for any of the analysed genotypes in consistence with previous studies on *Grb10*$^{m/+}$ placentae (**Figure** 3.1 C), in which increased efficiency was not reported until later on in gestation (Charalambous et al., 2010).

3.2.1.2 E14.5

In agreement with previous findings from our group (Charalambous et al., 2003), *Grb10*$^{m/+}$ embryos and placentae were significantly enlarged at the stage of E14.5 (**Figure** 3.2 A and B).

Following on from the results obtained for E12.5 embryos, statistically significant overgrowth of both *Grb10*$^{m/+}$*/Dlk1*$^{+/p}$ embryos and placentae confirmed that *Grb10*$^{m/+}$*/Dlk1*$^{+/p}$ embryos shared the growth phenotype with *Grb10*$^{m/+}$ at the E14.5 stage. Similar to E12.5, all genotypes failed to show significant changes in placental efficiency at E14.5 (**Figure** 3.2 C). This is again consistent with a previous study showing that a statistically significant improvement in *Grb10*$^{m/+}$ placental efficiency was not detected until E17.5 (Charalambous et al., 2010). No statistically significant differences in placental or embryonic wet weights were found in *Dlk1*$^{+/p}$ embryos, although the trend of slightly decreased embryonic mass of *Dlk1*$^{+/p}$ embryos was noted.

3.2.1.3 E17.5

Comparative analysis of *Dlk1*$^{+/p}$, *Grb10*$^{m/+}$ and *Grb10*$^{m/+}$*/Dlk1*$^{+/p}$ E17.5 embryonic and placental wet weights showed persistent embryonic and placental overgrowth in *Grb10*$^{m/+}$ and *Grb10*$^{m/+}$*/Dlk1*$^{+/p}$ animals, but in the case of placental overgrowth only in comparison to *Dlk1*$^{+/p}$ (**Figure** 3.3 A and B). Although slightly lighter, the weights of *Dlk1*$^{+/p}$ embryos and placentae were not significantly smaller. An earlier report (Charalambous et al., 2010) indicated embryonic stage E17.5 as the time when placental efficiency in *Grb10*$^{m/+}$ became significantly increased, and the present study has confirmed this result (**Figure** 3.3 C), as improved *Grb10*$^{m/+}$ placental efficiency was again apparent. *Grb10*$^{m/+}$*/Dlk1*$^{+/p}$ placentae also showed significantly increased efficiency. Consistent with findings for earlier gestation stages, E17.5 *Dlk1*$^{+/p}$ placentae did not exhibit any changes in efficiency. We also identified significant overgrowth in wet weights and relative weights of *Grb10*$^{m/+}$ and *Grb10*$^{m/+}$*/Dlk1*$^{+/p}$ E17.5 livers (**Figure** 3.3 D and E). This results, however, should be further confirmed by analyses of larger animal cohort as analysed number do not provide enough evidence to draw firm conclusions.

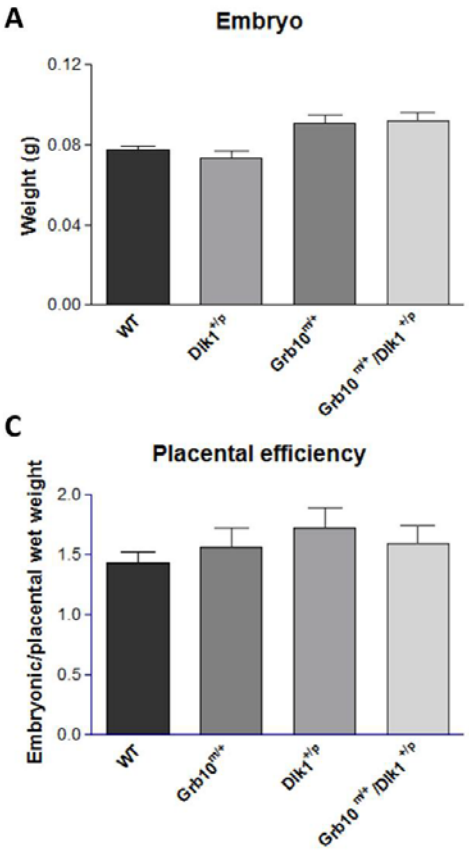

	Embryo	Placenta	Placental efficiency
WT vs Grb10$^{m/+}$	*	ns	ns
WT vs Dlk1$^{+/p}$	ns	ns	ns
WT vs Grb10$^{m/+}$/Dlk1$^{+/p}$	**	ns	ns
Grb10$^{m/+}$ vs Dlk1$^{+/p}$	*	ns	ns
Grb10$^{m/+}$ vs Grb10$^{m/+}$/Dlk1$^{+/p}$	ns	ns	ns
Dlk1$^{+/p}$ vs Grb10$^{m/+}$/Dlk1$^{+/p}$	**	ns	ns

Figure 3.1. Analysis of wet weights of wild type, *Dlk1$^{+/p}$*, *Grb10$^{m/+}$* and *Grb10$^{m/+}$/Dlk1$^{+/p}$* E12.5 embryos and placentae, together with placental efficiency.

A) Comparative analysis of wet weights of E12.5 embryos revealed that at this stage of development both *Grb10$^{m/+}$* (*p<0.05) and *Grb10$^{m/+}$/Dlk1$^{+/p}$* (**p<0.01) embryos were significantly heavier than their wild type and *Dlk1$^{+/p}$* littermates. **B)** Trends for increased placental mass in *Grb10$^{m/+}$* and *Grb10$^{m/+}$/Dlk1$^{+/p}$* have also been observed, however no significant changes have been noted. **C)** No changes have been detected in placental efficiency between the analysed genotypes. **D)** Table summarising results of statistical analysis. All values represent means ± SEM, one way ANOVA with Tukey's post-hoc analysis. WT n=23, *Dlk1$^{+/p}$* n=13, *Grb10$^{m/+}$* n=13, *Grb10 $^{m/+}$ /Dlk1 $^{+/p}$* n=16.

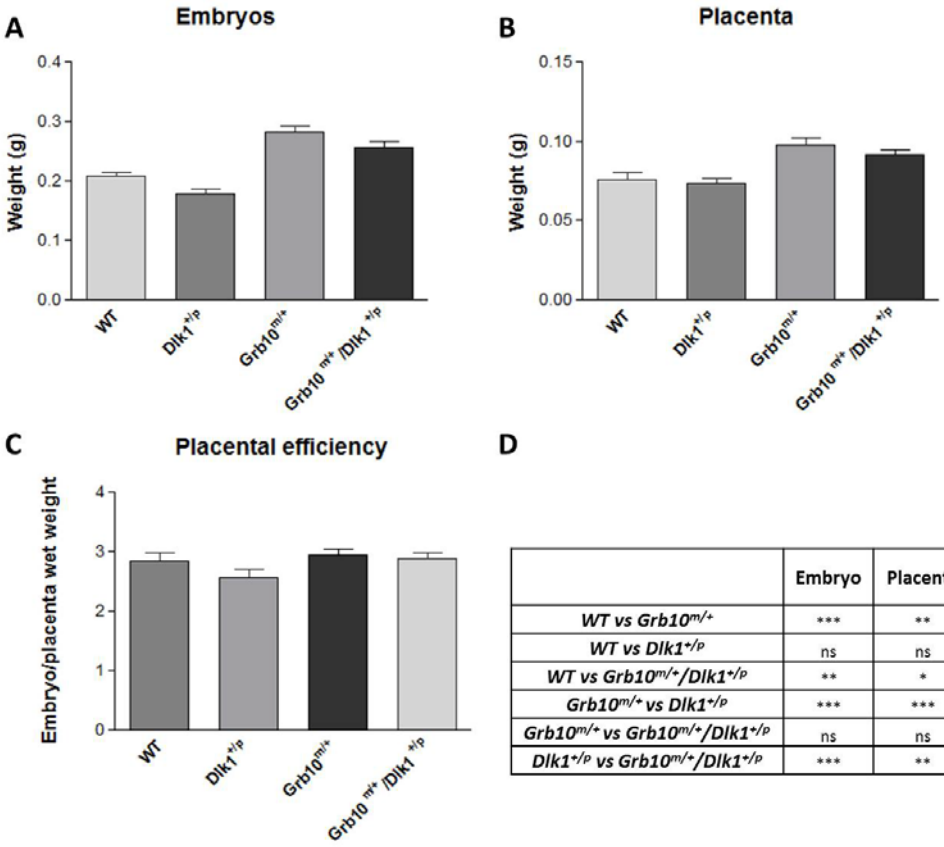

	Embryo	Placenta	Placental efficiency
WT vs Grb10$^{m/+}$	***	**	ns
WT vs Dlk1$^{+/p}$	ns	ns	ns
WT vs Grb10$^{m/+}$/Dlk1$^{+/p}$	**	*	ns
Grb10$^{m/+}$ vs Dlk1$^{+/p}$	***	***	ns
Grb10$^{m/+}$ vs Grb10$^{m/+}$/Dlk1$^{+/p}$	ns	ns	ns
Dlk1$^{+/p}$ vs Grb10$^{m/+}$/Dlk1$^{+/p}$	***	**	ns

Figure 3.2 Analysis of wet weights of wild type, *Dlk1$^{+/p}$*, *Grb10$^{m/+}$* and *Grb10$^{m/+}$/Dlk1$^{+/p}$* E14.5 embryos and placentae, together with placental efficiency.

A) E14.5 *Grb10$^{m/+}$* embryos were significantly overgrown when compared to wild type (****p*<0.001) and *Dlk1$^{+/p}$* (****p*<0.001) embryos and it was a similar case for *Grb10$^{m/+}$/Dlk1$^{+/p}$* embryos compared to wild type (**p<0.01) and *Dlk1$^{+/p}$* (****p*<0.001). **B**) Similarly, a higher placental wet weight mass was noted in *Grb10$^{m/+}$* when compared to wild type (**p<0.01) and *Dlk1$^{+/p}$* (****p*<0.001) and in *Grb10$^{m/+}$/Dlk1$^{+/p}$* placentae compared to wild type (*p<0.05) and *Dlk1$^{+/p}$* (***p*<0.01) for this stage in gestation. **C)** No statistically significant deviations in placental efficiency were found. **D)** Table summarising results of statistical analysis. All values represent means ± SEM, one way ANOVA with Tukey's post-hoc analysis. WT n=19, *Dlk1$^{+/p}$* n=22, *Grb10$^{m/+}$* n=22, *Grb10 $^{m/+}$ /Dlk1 $^{+/p}$* n=25.

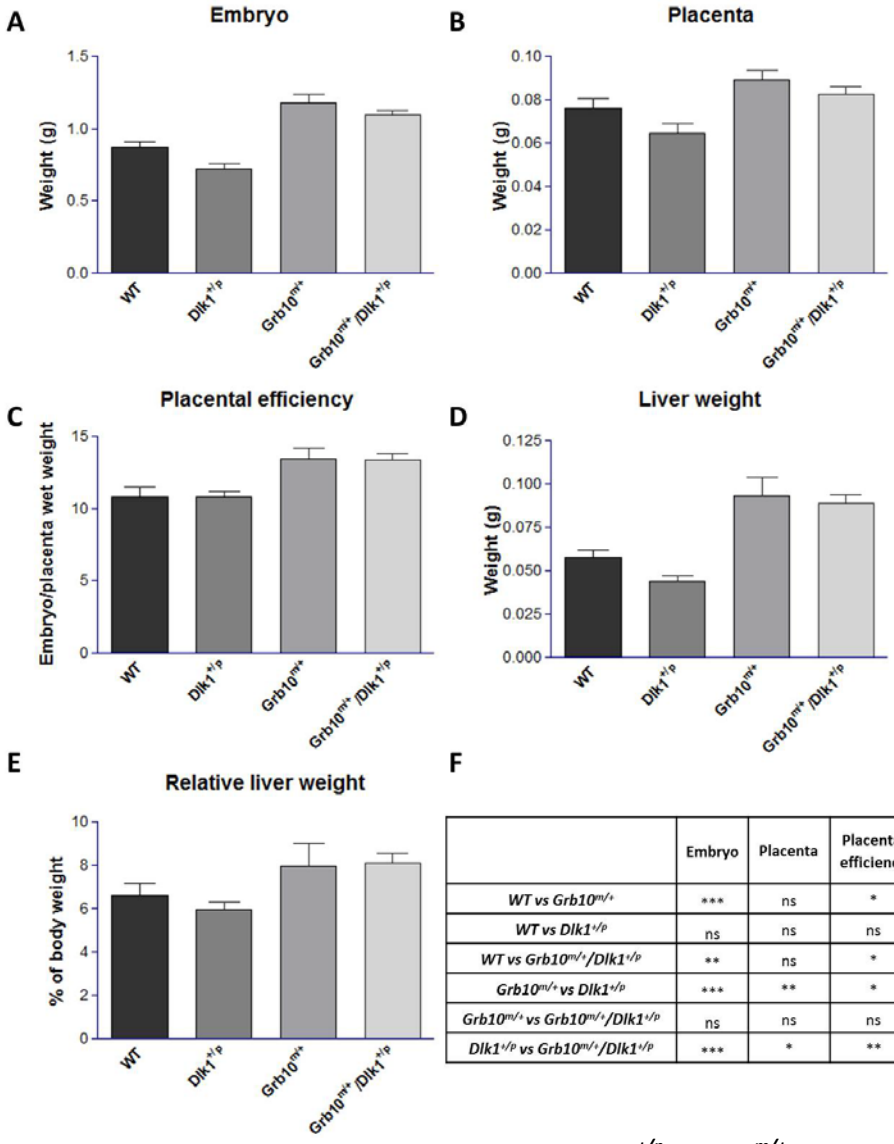

	Embryo	Placenta	Placental efficiency	Liver weight	Relative liver weight
WT vs Grb10$^{m/+}$	***	ns	*	*	ns
WT vs Dlk1$^{+/p}$	ns	ns	ns	ns	ns
WT vs Grb10$^{m/+}$/Dlk1$^{+/p}$	**	ns	*	*	ns
Grb10$^{m/+}$ vs Dlk1$^{+/p}$	***	**	*	***	*
Grb10$^{m/+}$ vs Grb10$^{m/+}$/Dlk1$^{+/p}$	ns	ns	ns	ns	ns
Dlk1$^{+/p}$ vs Grb10$^{m/+}$/Dlk1$^{+/p}$	***	*	**	***	*

Figure 3.3 Analysis of wet weights of wild type, *Dlk1$^{+/p}$*, *Grb10$^{m/+}$* and *Grb10$^{m/+}$/Dlk1$^{+/p}$* E17.5 embryos, livers and placentae, together with placental efficiency and relative liver weights.

A) Significant overgrowth was noted in E17.5 *Grb10$^{m/+}$* compared to wild type and *Dlk1$^{+/p}$* (***p<0.001) embryos and in *Grb10$^{m/+}$/Dlk1$^{+/p}$* compared to wild type (**p<0.01) and *Dlk1$^{+/p}$* (***p<0.001) embryos. **B)** *Grb10$^{m/+}$* (**p<0.01) and *Grb10$^{m/+}$/Dlk1$^{+/p}$* (*p<0.05) placentae were overgrown compared to *Dlk1$^{+/p}$*. **C**) Significantly higher placental efficiency was noted in *Grb10$^{m/+}$* (*p<0.05) compared to wild type and *Dlk1$^{+/p}$* and *Grb10$^{m/+}$/Dlk1$^{+/p}$* compared to wild type (*p<0.05) and *Dlk1$^{+/p}$* (**p<0.01) animals. **D)** *Grb10$^{m/+}$* and *Grb10$^{m/+}$/Dlk1$^{+/p}$* livers were overgrown compared to wild type (*p<0.05) and *Dlk1$^{+/p}$* (***p<0.001). **E)** Relative liver weights were increased in *Grb10$^{m/+}$* and *Grb10$^{m/+}$/Dlk1$^{+/p}$* compared to *Dlk1$^{+/p}$* (*p<0.05) liver weights. **F)** Table summarising results of statistical analysis. All values represent means ± SEM, one way ANOVA with Tukey's post-hoc analysis. WT n=4, *Dlk1$^{+/p}$* n=8, *Grb10$^{m/+}$* n=6, *Grb10 $^{m/+}$ /Dlk1 $^{+/p}$* n=8.

3.2.2 Analysis of cell proliferation in *Dlk1*$^{+/p}$, *Grb10*$^{m/+}$ and *Grb10*$^{m/+}$/*Dlk1*$^{+/p}$ E14.5 pMEFs

Specific and highly regulated rates of cell proliferation, cell death and cell size during embryogenesis are the basis of controlled growth during the normal course of development. Ablation of the *Grb10* gene has been previously reported to lead to overgrowth (Charalambous et al., 2003), whereas lack of the *Dlk1* gene resulted in growth retardation in mice (Moon et al., 2002). Moreover, Grb10 has already been shown as an interacting partner of several proteins involved in regulation of cell proliferation and apoptosis, such as Igf1r, growth hormone receptor or Raf1 and Akt (Moutoussamy et al., 1998; Nantel et al., 1998; Dufresne and Smith, 2005; Urschel et al., 2005), implying its possible role in controlling the kinetics of this processes. Also, a recent *in vitro* study in neuroblastoma cells demonstrated that overexpression of *DLK1* leads to protection from apoptosis by nutrient depletion (Kim, 2010) which was consistent with previous finding that exogenous *DLK1* prevented an increase of apoptosis caused by AS2O3 in K562 leukaemia cells (Qi et al., 2008).

Primary embryonic fibroblasts derived from E14.5 embryos with the absence of functional *Grb10* have previously been subject to analysis of the rate of cell proliferation and susceptibility to apoptosis (Garfield, 2007). Hyperproliferation was observed in *Grb10*$^{m/+}$ cells, while lack of a functional *Grb10* gene did not appear to alter susceptibility to at least some pro-apoptotic signals.

The differences in the growth phenotypes at the analysed embryonic developmental stages, in particular the overgrowth that was prominent in *Grb10*$^{m/+}$ and *Grb10*$^{m/+}$/*Dlk1*$^{+/p}$ embryos from E12.5 and then throughout the remaining gestation period, might be associated with either an increase in cell size or in cell number. To analyse the latter, an investigation of proliferation rates of primary embryonic fibroblasts derived from E14.5 embryos was carried out in a manner described in detail in Section 2.6.3. Cells were seeded at an initial density of $1x10^4$ per well and counted every 48 hours over a two week period. The results revealed that *Grb10*$^{m/+}$ and *Grb10*$^{m/+}$/*Dlk1*$^{+/p}$ cells exhibited hyperproliferation *in vitro* (**Figure** 3.4). Starting from 72 hours post-seeding, *Grb10*$^{m/+}$/*Dlk1*$^{+/p}$ cells displayed an increase in density, which was not apparent until 120 hours post-seeding for wild type, *Dlk1*$^{+/p}$ and *Grb10*$^{m/+}$ cells. From 168 hours post-seeding onwards a substantial increase in proliferation was noted for *Grb10*$^{m/+}$ cells, alongside an even more prominent increase (reaching up to three times those observed for wild type cells) for *Grb10*$^{m/+}$/*Dlk1*$^{+/p}$ cells and these trends continued until the end of the

investigation at the time of 264 hours post-seeding. Statistical analysis of areas under the growth curves revealed that over the course of the study both *Grb10*$^{m/+}$ and *Grb10*$^{m/+}$/*Dlk1*$^{+/p}$ cells showed a significant increase in total growth (**Figure** 3.4). No significant deviation from wild type growth was shown by *Dlk1*$^{+/p}$ cells, although they did exhibit a consistent trend to proliferate at a slightly lower rate than wild type cells.

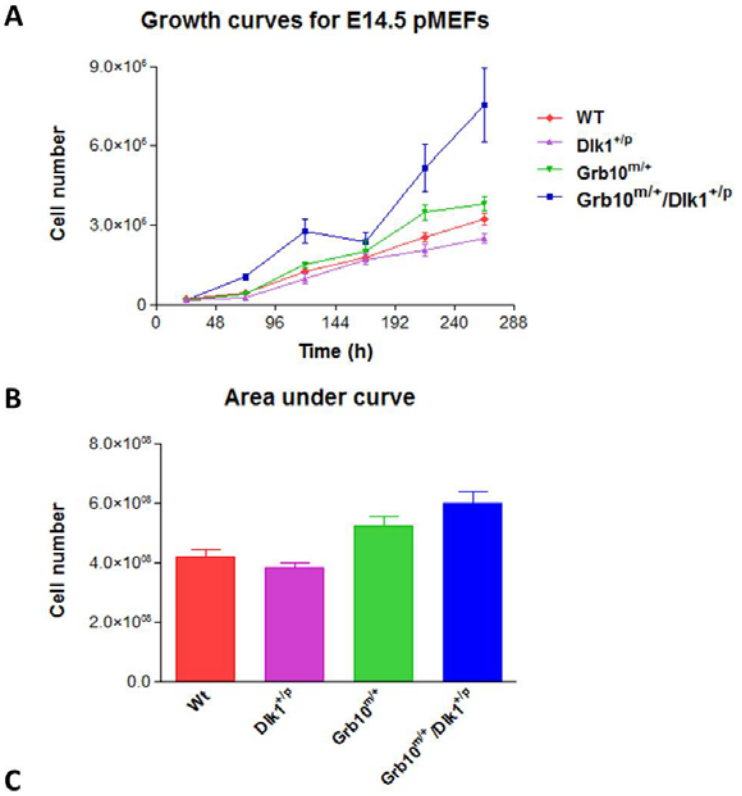

C

	Areas under curve
WT vs Grb10$^{m/+}$	*
WT vs Dlk1$^{+/p}$	ns
WT vs Grb10$^{m/+}$/Dlk1$^{+/p}$	***
Grb10$^{m/+}$ vs Dlk1$^{+/p}$	**
Grb10$^{m/+}$ vs Grb10$^{m/+}$/Dlk1$^{+/p}$	ns
Dlk1$^{+/p}$ vs Grb10$^{m/+}$/Dlk1$^{+/p}$	***

Figure 3.4 Analysis of growth rates in wild type, *Dlk1$^{+/p}$*, *Grb10$^{m/+}$* and *Grb10$^{m/+}$/Dlk1$^{+/p}$*E14.5 pMEFs.

Proliferation of wild type, *Dlk1$^{+/p}$*, *Grb10$^{m/+}$* and *Grb10$^{m/+}$/Dlk1$^{+/p}$*E14.5 pMEFs has been studied under standard growth conditions, starting from an initial seeding density of 1x10^4 cells. Changes in cell numbers for each genotype have been calculated every 48 hours. Growth curves (**A**) and areas under curves (**B**) are presented for wild type, *Dlk1$^{+/p}$*, *Grb10$^{m/+}$* and *Grb10$^{m/+}$/Dlk1$^{+/p}$* E14.5 pMEFs over the time of 264 hours post-seeding. Statistical analysis of total areas under growth curves showed significantly faster growth for *Grb10$^{m/+}$* pMEFs compared to wild type (*p<0.05) and *Dlk1$^{+/p}$* (**p<0.01) cells as well as for *Grb10$^{m/+}$/Dlk1$^{+/p}$* compared to wild type (***p<0.001) and *Dlk1$^{+/p}$* (***p<0.001) E14.5 pMEFs. Each data point represents the mean of 5 independent experiments, 4 replicates for each time point, counted twice. **C)** Table summarising results of statistical analysis. All values represent means ± SEM, tested using one way ANOVA with Tukey's post-hoc analysis. WT n=5, *Dlk1$^{+/p}$* n=5, *Grb10$^{m/+}$* n=5, *Grb10$^{m/+}$/Dlk1$^{+/p}$* n=5.

3.2.3 FACS analysis of *Dlk1*$^{+/p}$, *Grb10*$^{m/+}$ and *Grb10*$^{m/+}$/*Dlk1*$^{+/p}$ E11.5 embryos and E14.5 pMEFs

Fluorescently activated cell sorting (FACS) was employed to examine the basis for the hyperproliferative phenotype of *Grb10*$^{m/+}$ and *Grb10*$^{m/+}$/*Dlk1*$^{+/p}$ E14.5 pMEFs and to investigate the possibility of cellular hypertrophy. E14.5 pMEFs from all four genotypes, cultured under standard conditions and allowed to grow to approximately 80% confluence, were stained with propidium iodide and 100,000 individual cells were then used for an assessment of cell size and cell cycle progression.

To allow for more direct investigation of potential cell size modifications in transgenic embryos, we have used the same type of FACS analysis directly on cells freshly isolated from E11.5 embryos. Following isolation, embryos were disaggregated and rendered into single-cell-suspensions, which were then stained with propidium iodide. Similarly to pMEFs analysis, 100,000 individual cells were used for investigations of cell size and cytokinetic profile.

The reasons for choosing E11.5 whole embryos for FACS analysis were based upon the practical issues associated with disaggregation of embryos older than E11.5. Cells tend to aggregate significantly after the E11.5 stage of development and use of collagenase or proteases would be required for obtaining single cell suspension. This additional step might have resulted in loss of cells and interfering with real results. In addition, significant overgrowth has been identified in *Grb10*$^{m/+}$ E12.5 embryos by our group, so it is hypothesised that at E11.5 *Grb10*$^{m/+}$ cells will exhibit changes to the normal course of the cell cycle that lead to the alteration in embryonic growth evident at E12.5, and that similar changes might be occurring in *Grb10*$^{m/+}$/*Dlk1*$^{+/p}$ embryos. For these reasons we decided that the gestational stage of E11.5 would be suitable for the FACS analysis we wanted to perform.

3.2.3.1 Analysis of cell size in wild type, *Dlk1*$^{+/p}$, *Grb10*$^{m/+}$ and *Grb10*$^{m/+}$/*Dlk1*$^{+/p}$ E11.5 embryos and E14.5 pMEFs

Cell size and granulation can be analysed using diffraction and scattering of laser beams upon contact with individual cells. Side scatter (SSC) defines the granularity of the cell and forward scatter (FSC) the size. No deviations from wild type were found in the ranges of cell sizes upon FACS analysis of *Dlk1*$^{+/p}$, *Grb10*$^{m/+}$ and *Grb10*$^{m/+}$/*Dlk1*$^{+/p}$ cells from either E11.5 embryos (**Figure** 3.5) or E14.5 pMEFs (**Figure** 3.6), suggesting that the observed overgrowth

phenotypes in *Grb10*$^{m/+}$ and *Grb10*$^{m/+}$*/Dlk1*$^{+/p}$ embryos are not due to altered growth of individual cells (cell hypertrophy). However, the used method of gating out any debris from the actual cells did not separate the singlet and dublet cells as it did for cell cycle progression analysis, therefore it should be taken into account that obtained results might not reflect true cell sizes and the results from this experiment should be re-analysed using gating method described in **Figure** 2.4.

3.2.3.2 Analysis of cell cycle progression in wild type *Dlk1*$^{+/p}$, *Grb10*$^{m/+}$ and *Grb10*$^{m/+}$*/Dlk1*$^{+/p}$ E11.5 embryos and E14.5 pMEFs

Analysis of specific cell cycle stages can be achieved by staining cells with propidium iodide, which allows for an assessment of DNA content that is related directly to cell cycle progression. By studying the histogram representing cell cycle progression, percentages of cells in each of the cell cycle phases can be determined.

Comparative FACS analysis of cell cycle stages in freshly derived single cell suspensions from *Dlk1*$^{+/p}$, *Grb10*$^{m/+}$ and *Grb10*$^{m/+}$*/Dlk1*$^{+/p}$ E11.5 embryos revealed several differences in the distribution of cells within cell cycle phases between genotypes (**Figure** 3.7). We found that significantly lower percentages of *Grb10*$^{m/+}$ and *Grb10*$^{m/+}$*/Dlk1*$^{+/p}$ cells were in the S-phase of the cell cycle at the time of analysis when compared to *Dlk1*$^{+/p}$ cells (**Figure** 3.7 B). Conversely, there was an increased number of *Grb10*$^{m/+}$ and *Grb10*$^{m/+}$*/Dlk1*$^{+/p}$ cells in G2-phase of the cell cycle, this time in comparison to wild type cells (**Figure** 3.7 C). Similar observations were made with E14.5 pMEFs (**Figure** 3.8), as FACS analysis revealed a statistically significant decrease in the proportion of *Grb10*$^{m/+}$ and *Grb10*$^{m/+}$*/Dlk1*$^{+/p}$ cells in S-phase compared to *Dlk1*$^{+/p}$ and wild type cells (**Figure** 3.8 B) along with an increased number of *Grb10*$^{m/+}$ and *Grb10*$^{m/+}$*/Dlk1*$^{+/p}$ cells in G2-phase compared to wild type (**Figure** 3.8 C). *Dlk1*$^{+/p}$ cells from E11.5 embryos and E14.5 pMEFs did not exhibit any significant differences in their distribution within cell cycle phases when compared to wild type controls.

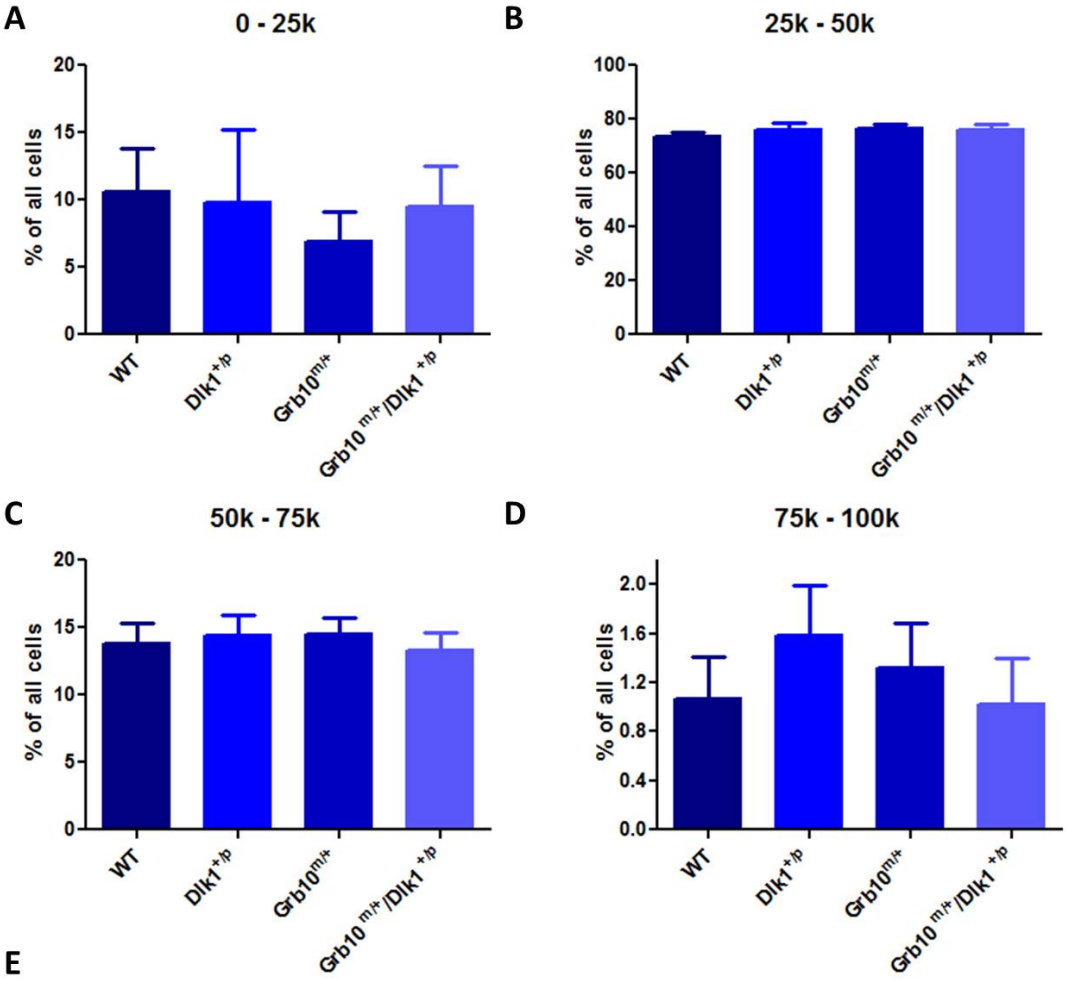

E

	0 – 25k	25k – 50k	50k – 75k	75k – 100k
WT vs Grb10$^{m/+}$	ns	ns	ns	ns
WT vs Dlk1$^{+/p}$	ns	ns	ns	ns
WT vs Grb10$^{m/+}$/Dlk1$^{+/p}$	ns	ns	ns	ns
Grb10$^{m/+}$ vs Dlk1$^{+/p}$	ns	ns	ns	ns
Grb10$^{m/+}$ vs Grb10$^{m/+}$/Dlk1$^{+/p}$	ns	ns	ns	ns
Dlk1$^{+/p}$ vs Grb10$^{m/+}$/Dlk1$^{+/p}$	ns	ns	ns	ns

Figure 3.5 FACS analysis of cell size in wild type, *Dlk1*$^{+/p}$, *Grb10*$^{m/+}$ and *Grb10*$^{m/+}$*/Dlk1*$^{+/p}$ E11.5 embryos.

Cells derived from wild type, *Dlk1*$^{+/p}$, *Grb10*$^{m/+}$ and *Grb10*$^{m/+}$*/Dlk1*$^{+/p}$ E11.5 embryos were stained with propidium iodide and analysed using FACS in order to reveal any potential changes in cell size. 100,000 cells were FACS analysed for each sample and calculations were carried out to identify cell size deviations between wild type, *Dlk1*$^{+/p}$, *Grb10*$^{m/+}$ and *Grb10*$^{m/+}$*/Dlk1*$^{+/p}$ E11.5 cells. Cell sizes were analysed and compared according to which one of four gates they fell into: **A)** 0-25k; **B)** 25k-50k; **C)** 50k-75k; **D)** 75k-100k. Statistical analysis did not reveal any differences in cell sizes between the studied genotypes. **E)** Table summarising results of statistical analysis. All values represent means ± SEM, one way ANOVA with Tukey's post-hoc analysis. WT n=10, *Dlk1*$^{+/p}$ n=8, *Grb10*$^{m/+}$ n=10, *Grb10* $^{m/+}$ */Dlk1* $^{+/p}$ n=8.

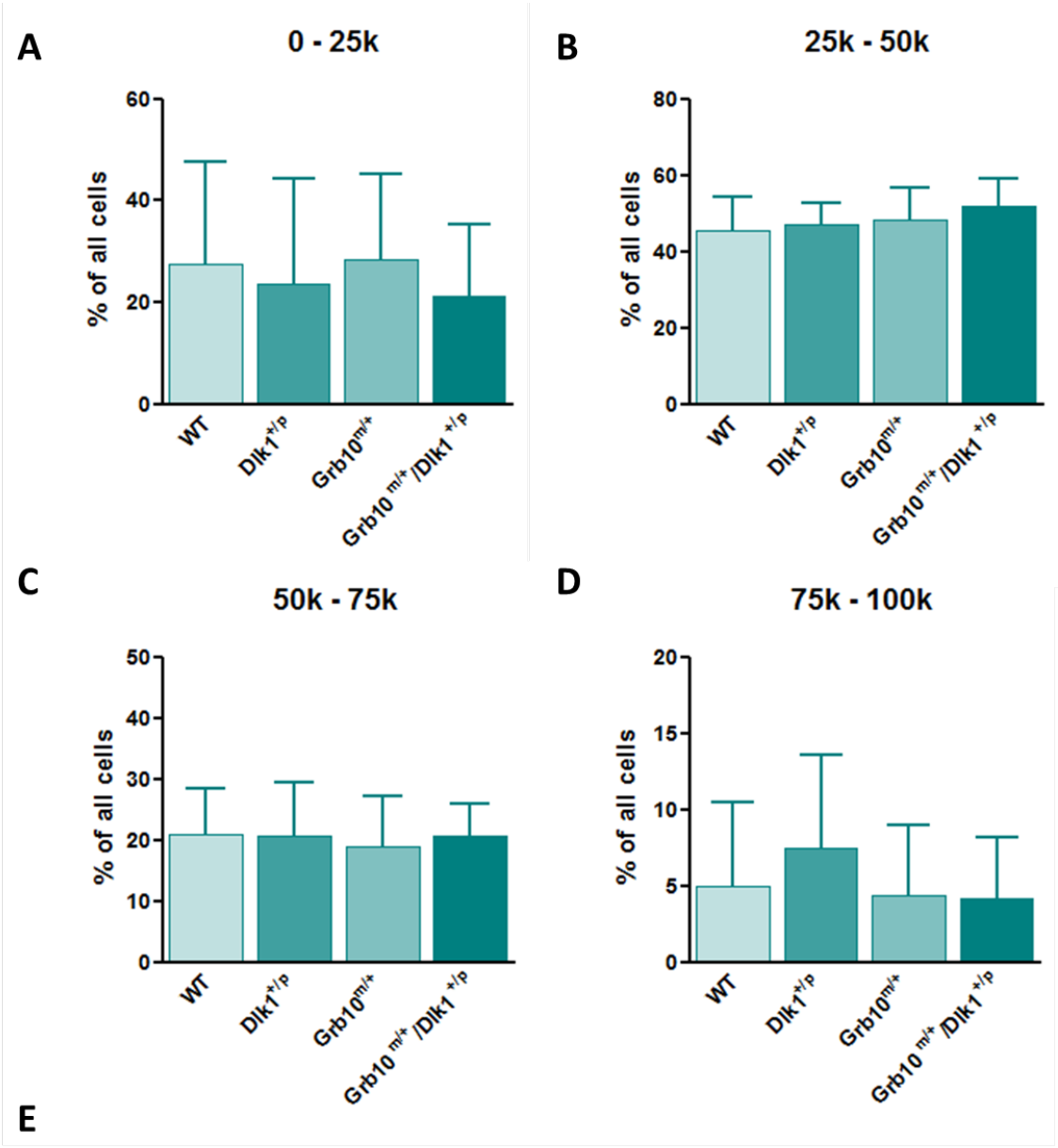

E

	0 – 25k	25k – 50k	50k – 75k	75k – 100k
WT vs Grb10$^{m/+}$	ns	ns	ns	ns
WT vs Dlk1$^{+/p}$	ns	ns	ns	ns
WT vs Grb10$^{m/+}$/Dlk1$^{+/p}$	ns	ns	ns	ns
Grb10$^{m/+}$ vs Dlk1$^{+/p}$	ns	ns	ns	ns
Grb10$^{m/+}$ vs Grb10$^{m/+}$/Dlk1$^{+/p}$	ns	ns	ns	ns
Dlk1$^{+/p}$ vs Grb10$^{m/+}$/Dlk1$^{+/p}$	ns	ns	ns	ns

Figure 3.6 FACS analysis of cell size in wild type, *Dlk1*$^{+/p}$, *Grb10*$^{m/+}$ and *Grb10*$^{m/+}$/*Dlk1*$^{+/p}$ E14.5 pMEFs.

Wild type, *Dlk1*$^{+/p}$, *Grb10*$^{m/+}$ and *Grb10*$^{m/+}$/*Dlk1*$^{+/p}$ E14.5 derived pMEFs, cultured under standard growth conditions, were stained with propidium iodide and analysed with FACS to determine any potential differences in cell size. 100,000 cells were FACS analysed for each sample and calculations were carried out to identify cell size deviations. Cell sizes were analysed and compared according to one of four gates they fell into: **A)** 0-25k; **B)** 25k-50k; **C)** 50k-75k; **D)** 75k-100k. Statistical analysis revealed no deviations in cell size ranges between examined genotypes. **E)** Table summarising results of statistical analysis. All values represent means ± SEM, one way ANOVA with Tukey's post-hoc analysis. WT n=9, *Dlk1*$^{+/p}$ n=7, *Grb10*$^{m/+}$ n=9, *Grb10* $^{m/+}$ */Dlk1*$^{+/p}$ n=7.

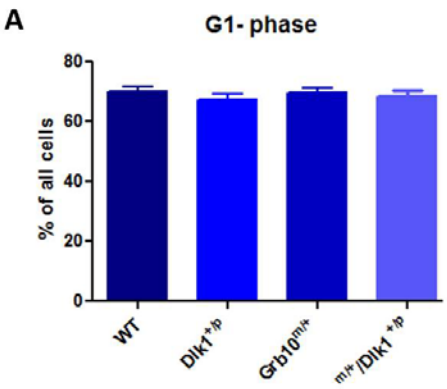

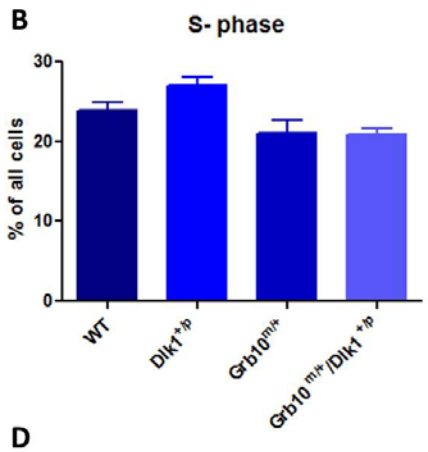

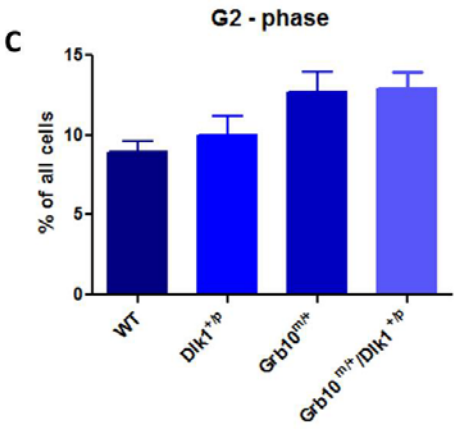

D

	G1-phase	S-phase	G2-phase
WT vs Grb10$^{m/+}$	ns	ns	*
WT vs Dlk1$^{+/p}$	ns	ns	ns
WT vs Grb10$^{m/+}$/Dlk1$^{+/p}$	ns	ns	*
Grb10$^{m/+}$ vs Dlk1$^{+/p}$	ns	*	ns
Grb10$^{m/+}$ vs Grb10$^{m/+}$/Dlk1$^{+/p}$	ns	ns	ns
Dlk1$^{+/p}$ vs Grb10$^{m/+}$/Dlk1$^{+/p}$	ns	*	ns

Figure 3.7 FACS analysis of cell cycle progression in wild type, *Dlk1$^{+/p}$*, *Grb10$^{m/+}$* and *Grb10$^{m/+}$/Dlk1$^{+/p}$* E11.5 embryos.

Cells derived from wild type, *Dlk1$^{+/p}$*, *Grb10$^{m/+}$* and *Grb10$^{m/+}$/Dlk1$^{+/p}$* E11.5 embryos were stained with propidium iodide and analysed with FACS in order to reveal any potential changes in cell cycle progression. 100,000 cells were FACS analysed for each sample and calculations were carried out to determine percentages of cells in each phase of cell cycle. **A)** No significant differences were found in cell distribution in the G1-phase of the cell cycle for any of the analysed genotypes. **B)** Statistical analysis revealed a significant decrease in percentages of cells in S-phase exhibited by *Grb10$^{m/+}$* (*p<0.05) and *Grb10$^{m/+}$/Dlk1$^{+/p}$* (*p<0.05) cells when compared to *Dlk1$^{+/p}$* cells. **C)** Significantly increased numbers of *Grb10$^{m/+}$* (*p<0.05) and *Grb10$^{m/+}$/Dlk1$^{+/p}$* (*p<0.05) cells were noted in G2-phase by when compared to wild type controls. **D)** Table summarising results of statistical analysis. All values represent means ± SEM, one way ANOVA with Tukey's post-hoc analysis. WT n=16, *Dlk1$^{+/p}$* n=16, *Grb10$^{m/+}$* n=9, *Grb10$^{m/+}$ /Dlk1 $^{+/p}$* n=10.

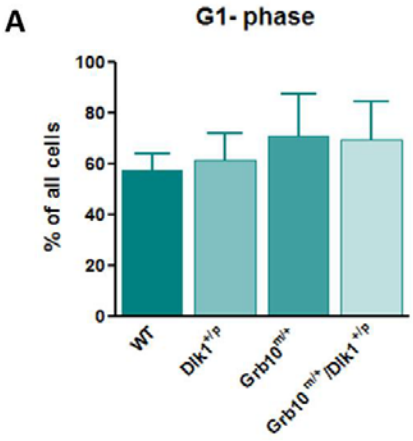

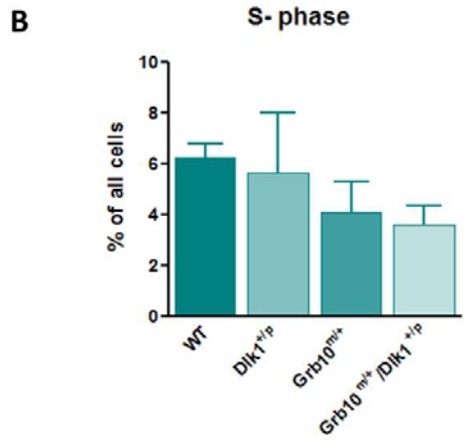

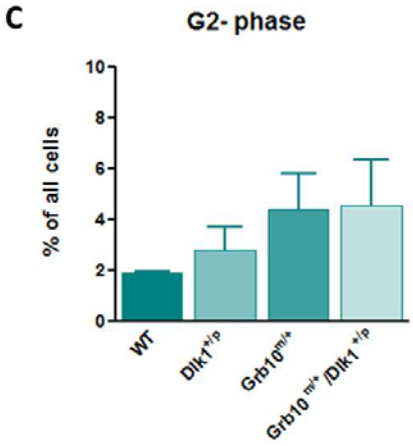

D

	G1-phase	S-phase	G2-phase
WT vs Grb10$^{m/+}$	ns	*	*
WT vs Dlk1$^{+/p}$	ns	ns	ns
WT vs Grb10$^{m/+}$/Dlk1$^{+/p}$	ns	*	*
Grb10$^{m/+}$ vs Dlk1$^{+/p}$	ns	*	ns
Grb10$^{m/+}$ vs Grb10$^{m/+}$/Dlk1$^{+/p}$	ns	ns	ns
Dlk1$^{+/p}$ vs Grb10$^{m/+}$/Dlk1$^{+/p}$	ns	*	ns

Figure 3.8 FACS analysis of cell cycle progression in wild type, *Dlk1$^{+/p}$*, *Grb10$^{m/+}$* and *Grb10$^{m/+}$/Dlk1$^{+/p}$* E14.5 pMEFs.

Wild type, *Dlk1$^{+/p}$*, *Grb10$^{m/+}$* and *Grb10$^{m/+}$/Dlk1$^{+/p}$* E14.5 derived pMEFs, cultured under standard growth conditions, were stained with propidium iodide and analysed with FACS to determine any differences in cell cycle progression. 100,000 cells were FACS analysed for each sample and calculations were carried out to determine percentages of cells in each phase of the cell cycle. **A)** No significant differences were found in cell distribution in the G1-phase of the cell cycle for any of the analysed genotypes. **B)** Statistical analysis revealed significantly lower percentages of *Grb10$^{m/+}$* (*p<0.05) and *Grb10$^{m/+}$/Dlk1$^{+/p}$* (*p<0.05) cells in S-phase of the cell cycle in comparison to wild type controls and to *Dlk1$^{+/p}$* cells. **C)** Significantly higher percentages of *Grb10$^{m/+}$* (*p<0.05) and *Grb10$^{m/+}$/Dlk1$^{+/p}$* (*p<0.05) cells were observed in G2-phase of the cell cycle when compared to wild type control cells. **D)** Table summarising results of statistical analysis. All values represent means ± SEM, one way ANOVA with Tukey's post-hoc analysis. WT n=5, *Dlk1$^{+/p}$* n=10, *Grb10$^{m/+}$* n=8, *Grb10 $^{m/+}$/Dlk1 $^{+/p}$* n=10.

3.3 Discussion

Genomic imprinting is a process based on epigenetic marking that results in parent-of-origin regulation of a subset of genes (see Chapter 1; Ferguson-Smith, 2011). This leads to functional non-equivalence of at least thirteen murine subchromosomal regions, for which both of the parental copies are required if development is to proceed normally (see MouseBook http://www.mousebook.org/imprinting/gen-map.html). Experiments that allowed for the generation of parthenogenetic and androgenetic embryos or chimaeras indicated crucial roles for imprinted genes in the development of the placenta as well as several mesodermal and ectodermal derivatives within the embryo (Barton et al., 1984; McGrath and Solter, 1984; Barton et al., 1991; Fundele et al., 1991). In agreement with these studies, the identification of imprinted genes, along with their roles and expression patterns, has highlighted the important function of imprinted genes in controlling the allocation of pre- and post-natal resources (Constancia et al., 2004) and influencing correct embryonic growth and development (Georgiades et al., 2000; Moon et al., 2002; Charalambous et al., 2003). Consistent with this, most of the imprinted genes identified up until now show expression in the extraembryonic tissues (reviewed in Coan et al., 2005; Fowden et al., 2011) and imprinted gene knockouts in mice have provided evidence that they contribute to many aspects of placental growth, organisation and morphology as well as nutrient transfer between mother and the developing embryo (Constancia et al., 2002; Reik et al., 2003; Sibley et al., 2004). Differential interest of parental genomes with regard to resource allocation is often considered as one of the selective pressures that led to evolution of imprinting. During pregnancy, maternally imprinted genes (e.g. *Igf2*) tend to increase the level of nutrient supply or demand necessary for the growth of the fetus, whilst maternally expressed imprinted genes (e.g. *Cdkn1c* or *Igf2r*) exert a reciprocal function.

Maintenance of proper control between proliferation, differentiation, apoptosis and correct cell size is a pivotal condition for a normal course of development to take place. Any disruptions within this set of cell characteristics may result in abnormal development that can lead to incorrect physiological and metabolic status later in life. The growth pathways and cellular basis through which *Grb10* and *Dlk1* mediate their effects need further investigation, therefore we decided to examine and describe the growth effects in $Grb10^{m/+}/Dlk1^{+/p}$ embryos and perform an *in vitro* investigation of proliferation, cell size and cell cycle kinetics in $Grb10^{m/+}/Dlk1^{+/p}$ primary embryonic fibroblast cultures.

Previously generated crosses between *Grb10*$^{m/+}$ and *Igf2*$^{+/p}$ mutant mice demonstrated an intermediate growth phenotype and pointed at a non-epistatic relationship between *Grb10* and the *Igf2* signalling pathway, suggesting that a non-IGF pathway regulates the overgrowth phenotype observed in *Grb10*$^{m/+}$ mice (Charalambous et al., 2003). Another examination of the possible interaction between *Igf* signalling and *Grb10* in growth regulation was performed by generating *Grb10*$^{m/+}$/*Igf1r*$^{-/-}$ double knockout mice (Gafield, 2007). This experiment once again showed an additive phenotype in double mutants, providing further evidence that the pathway predominantly involved in causing *Grb10* overgrowth phenotype is not the IGF pathway.

Investigation of fetal growth in *Grb10* and *Dlk1* knockout mice in the present study revealed that *Grb10*$^{m/+}$ embryos were significantly overgrown from gestational day 12 onwards (17% bigger than wild type), whereas *Dlk1*$^{+/p}$ embryos exhibited reciprocal fetal growth phenotype from E14.5, which, however, did not become statistically significant. These growth phenotypes are consistent with the ones observed in the original *Grb10* (Charalambous et al., 2003) and *Dlk1* (Moon et al., 2002) knockout lines, where *Grb10* embryos were found to be overgrown from E12.5 onwards (Charalambous et al., 2003), and *Dlk1* E18.5 embryos were significantly growth retarded (Moon et al., 2002). Both growth effects are in agreement with the parental conflict theory (Moore and Haig, 1991), and *Grb10* and *Dlk1* are therefore established as maternally expressed growth suppressor and paternally expressed growth enhancer, respectively.

Reciprocal phenotypes of *Grb10* and *Dlk1* knockout mice suggest that the *Grb10* and *Dlk1* imprinted genes might form part of a common genetic pathway, crucial for growth and development. In addition, there is some evidence for co-expression of both of these genes in embryonic tissues, such as developing muscle and cartilage tissues, pancreatic bud, liver, lung bronchioles and developing kidneys (Charalambous et al., 2003; Yevtodiyenko and Schmidt, 2006; da Rocha et al., 2007; Lui et al., 2008). Our main interest, therefore, was to investigate the growth phenotype of *Grb10*$^{m/+}$/*Dlk1*$^{+/p}$ double knockout embryos, in light of previous failure to identify a possible *Grb10* interacting pathway by generation of *Grb10*$^{m/+}$/*Igf2*$^{+/p}$ and *Grb10*$^{m/+}$/*Igf1r*$^{-/-}$ double knockout mutants (Charalambous et al., 2003, Garfield, 2007). In contrast, study of growth effects in *Grb10*$^{m/+}$/*Dlk1*$^{+/p}$ embryos revealed a growth phenotype similar to *Grb10*$^{m/+}$ embryos. Significant overgrowth of *Grb10*$^{m/+}$/*Dlk1*$^{+/p}$ conceptuses started from the day E12.5, when a 19% enlargement in comparison to wild types has been observed, and lasted throughout the rest of the gestational period (24% at E14.5 and 27% at E17.5).

Importantly, the overgrowth in *Grb10*$^{m/+}$*/Dlk1*$^{+/p}$ embryos was comparable to overgrowth of *Grb10*$^{m/+}$ fetuses (17% at E12.5, 35% E14.5 and 36% at E17.5). These results imply on similarity between *Grb10*$^{m/+}$*/Dlk1*$^{+/p}$ embryos and their *Grb10*$^{m/+}$ littermates, which raises the possibility of both genes interacting with each other in fetal growth control. More specifically, the data obtained through analysis of embryonic growth suggests that *Grb10*, a potent growth suppressor, might be epistatic, and antagonistic, to the paternally-expressed gene *Dlk1* during fetal development.

Birth size largely depends upon the nutrient supply, which is determined by the morphology, size and efficiency of the placenta (reviewed in Fowden et al., 2011). The observations made for growth of *Grb10*$^{m/+}$*/Dlk1*$^{+/p}$ embryos suggested an epistatic growth pathway involving both of these genes, therefore it was of interest to examine if it was the same case for extraembryonic tissues. *Dlk1* and *Grb10* are co-expressed in the fetal endothelium of the placenta (Yevtodiyenko and Schmidt, 2006; Charalambous et al., 2010) and *Grb10* is also present in the trophoblast of the placenta. Experiments presented in this chapter revealed no differences in the placental weights in E12.5 embryos. *Grb10*$^{m/+}$ and *Grb10*$^{m/+}$*/Dlk1*$^{+/p}$ placentae were overgrown from E14.5, so again *Grb10*$^{m/+}$*/Dlk1*$^{+/p}$ double mutant mice displayed a growth phenotype similar to *Grb10*$^{m/+}$ single mutants. The placental overgrowth at E17.5 was also significant, however, only when *Grb10*$^{m/+}$ and *Grb10*$^{m/+}$*/Dlk1*$^{+/p}$ placental weights were compared to *Dlk1*$^{+/p}$, whereas E17.5 *Grb10*$^{m/+}$ and *Grb10*$^{m/+}$*/Dlk1*$^{+/p}$ embryos were significantly overgrown when compared to *Dlk1*$^{+/p}$ and wild type. This could suggest that although changes within placental imprinting and subsequently in placental growth might influence embryonic growth, even without overgrown placentae *Grb10*$^{m/+}$ and *Grb10*$^{m/+}$*/Dlk1*$^{+/p}$ embryos maintained increased body weight, however it has to be taken into account that numbers of analysed E17.5 animals were small and need to be increased in order to draw any certain conclusions. The shortage of E17.5 embryos and lack of significant differences when comparing *Grb10*$^{m/+}$ and *Grb10*$^{m/+}$*/Dlk1*$^{+/p}$ placentae to those of wild type mice indicate that the obtained results need to be interpreted carefully and that more detailed investigation is needed in order to provide firm evidence for the role of placentae and their efficiency in observed *Grb10*$^{m/+}$ and *Grb10*$^{m/+}$*/Dlk1*$^{+/p}$ fetal overgrowth, as there exists a possibility that for example highly efficient *Grb10*$^{m/+}$*/Dlk1*$^{+/p}$ placenta could be the major contributor to the observed *Grb10*$^{m/+}$*/Dlk1*$^{+/p}$ embryonic overgrowth. The influence of placentomegaly on embryonic development seems to be less severe than that resulting from placental growth retardation, and despite placental overgrowth the associated embryos sometimes display normal growth (Fowden et al., 2011). It should, however, be noted that in

spite of a relatively frequent cases of overgrown placentae resulting from imprinted gene disruption, it seems that they are not associated with improved well-being of the fetus (Georgiades et al., 2001; Salas et al., 2004). The roles of *Grb10* and *Dlk1* in embryonic and placental growth regulation might be independent, as exemplified by different functions of *Igf2 P0* and embryonic transcripts (DeChiara et al., 1991; Constancia et al., 2002). It would therefore be interesting to analyse the outcomes of *Grb10* and *Grb10/Dlk1* overexpression and knockout solely within placentae and only in the embryo in order to uncover the real effects of *Grb10* and combination of *Grb10/Dlk1* imprinting in embryonic and extraembryonic tissues on normal growth and development of the embryo, as it has been done elsewhere for *Dlk1* (da Rocha et al., 2009).

Grb10 does not only possess an ability to affect embryonic and placental size, but also to control placental efficiency (Charalambous et al., 2010). *Grb10*$^{m/+}$ placentae were shown to have an increased volume of labyrinth and subsequently exhibited higher efficiency in enhancing the growth of the fetus, implying that the normal *Grb10* role is to reduce labyrinthine exchange of nutrients and thereby limit fetal growth. This type of mechanism might be employed to overcome the reciprocal forces of growth enhancement as well as to protect the mother from the disadvantageous consequences of fetal overgrowth (McLaren, 1965; Henriksen, 2008). As a result, *Grb10* seems to act as a regulator of the allocation of maternal resources, thereby mediating choice between different reproductive strategies (large pups within small litter versus small pups in a large litter), presumably in line with prevailing conditions (Charalambous et al., 2010).

Yevtodiyenko and Schmidt (2006) suggested the involvement of *Dlk1* in endothelial development and, at the same time, in control of branching morphogenesis in the placenta. They also pointed out that *Dlk1* expression patterns in the murine placental labyrinth is distinct from the pattern noted in human placenta, in which *DLK1* expression is detected in the stromal cells of the chorionic villi. Both of these structurally different tissues are situated in close proximity to maternal-fetal exchange sites, and *Dlk1* is expressed within cells separating fetal and maternal blood supplies, implying potential roles for *Dlk1/DLK1* in the regulation of maternal-fetal communication. A role for *Dlk1* in placenta has also been confirmed by observation of phenotypes resulting from uniparental disomies of chromosome 12 (Tevendale et al., 2006). Prenatal lethality was observed in both mUPD as well as pUPD animals, along with growth abnormalities and developmental defects in muscle, cartilage/bone and either a decrease or increase in placental growth, respectively (Georgiades et al., 2000; Georgiades et

al., 2001). Moreover, the observation of a disrupted fetal vasculature in pUPD12 placentae suggests the requirement for *Dlk1* in normal development of the labyrinth tissue, again supporting the idea that *Dlk1* functions within maternal and fetal exchange in placenta.

In the present study, significant growth retardation has been noted in $Dlk1^{+/p}$ placenta only at E12.5 and was not maintained until later stages of gestation although there was a trend for the $Dlk1^{+/p}$ placenta to remain smaller than wild type controls. Previously mentioned elegant study performed by da Rocha et al (2009) described a model in which embryonic *Dlk1* over-expression was engineered in the presence of a normal placenta with a normal *Dlk1* dose. The results showed that *Dlk1* is able to control embryonic growth independently of the placenta. That could explain the observation that despite significant growth retardation of $Dlk1^{+/p}$ fetuses, their placentae do not exhibit a dramatically altered growth phenotype.

So far there is a relatively poor understanding of the mechanisms of fetal growth control, and yet it is vital that at birth whole body and all the organs have reached correct sizes and proportions. A mammalian embryo during the onset of its growth and development relies on the accurate function of the placenta for most of the gestational period. Previously mentioned wide expression of imprinted genes in the placenta and identification of a number of genes with expression restricted only to this organ suggest a crucial role of imprinted genes in placental development and, subsequently, coordination of embryonic growth. As discussed above, *Grb10* and *Dlk1* exert effects on both embryonic and placental development, therefore it will be interesting to conduct more detailed analysis of $Grb10^{m/+}/Dlk1^{+/p}$ placentae, especially of their capacity for nutrient transfer *in vivo*, in order to uncover the influence of *Grb10* and *Dlk1* on placental morphology and physiology. Stereological analysis of specific tissues forming $Grb10^{m/+}/Dlk1^{+/p}$ placentae is under way, and hopefully it will shed more light on the outcomes of *Grb10* and *Dlk1* ablation on placental characteristics.

Various publications have demonstrated independent signalling pathways involved in regulation of cell growth and proliferation (Coelho and Leevers, 2000; Conlon et al., 2001; Echave et al., 2007). Generation and study of *Pdk1* knockout mice revealed a strong correlation between expression levels of *Pdk1* in various organs and both total animal size and organ volumes (Lawlor et al., 2002). Lawlor et al (2002) found that the size of primary MEFs derived from *Pdk1* knockout embryos was 35% reduced in comparison to wild type controls. In support of the fact that size and cell proliferation are processes usually regulated by different pathways, despite the reduction in $Pdk1^{-/-}$ MEFs cell size, no change was observed in their proliferation rate (Lawlor et al., 2002). On the other hand, in *Drosophila* the insulin

receptor/PI3- kinase pathway has been found to be equally important for controlling both cell size and cell number (Kozma and Thomas, 2002).

In study presented in this chapter we examined both cell size and cell proliferation, along with cell cycle progression, in order to determine the reason for the observed overgrowth phenotype in *Grb10*$^{m/+}$ and *Grb10*$^{m/+}$/*Dlk1*$^{+/p}$ animals. Fluorescent activated cell sorting (FACS) allowed us to determine any potential differences in cell sizes between mutant and wild type cells. We have decided not only to analyse primary MEFs from E14.5 embryos, as it has been done before for *Grb10*$^{m/+}$ cultures, but also to perform FACS analysis on freshly dissected E11.5 embryos. The method used for the generation of single cell suspensions was based on that described for analysis of cell proliferation and apoptosis in *Igf2* deficient mouse embryos between days 9 and 10 of gestation (Burns and Hassan, 2001). Burns and Hassan (2001) reported that genetic disruption of *Igf2* was associated with enhanced apoptosis and a decreased rate of cell proliferation in E9–E10 embryos, resulting in reduced cell numbers with no alterations in cell size. Their novel method has proven to be particularly useful for detecting the causes of a growth phenotype which would be otherwise difficult to identify using commonly used cell culture techniques. In the case of *Igf2* knockout mice, a size difference was first detectable from embryonic stage E11, with a growth reduction of 40% apparent at birth that was maintained throughout life, but despite this size difference these animals were fertile and exhibited normal proportions (DeChiara et al., 1990; DeChiara et al., 1991). A similar phenotype was seen in insulin receptor substrate 1 (*Irs1*) knockout mice, which were born 40-60% smaller than their wild type counterparts and their proportional size differences persisted throughout life, but despite that they underwent normal bone development and did not show any changes in fertility (Araki et al., 1994).

Increased cell proliferation, lower rate of apoptosis or enhanced cell size could be potential factors that influence the embryonic overgrowth phenotype in *Grb10*$^{m/+}$ animals. Previous analysis of *Grb10*$^{m/+}$proliferation rates revealed that the *Grb10*$^{m/+}$cells proliferated significantly faster in comparison to wild type controls (Garfield, 2007). On the other hand, study of the apoptotic basal rate and its potential contribution to the observed hyperproliferative phenotype showed that *Grb10*$^{m/+}$ fibroblasts did not exhibit a reduced frequency of apoptosis in response to at least some pro-apoptotic signals, excluding a primary role for disrupted apoptosis in the generation of increased cell numbers (Garfield, 2007).

This finding is in line with reports that the total loss of maternal genome in primary embryonic fibroblasts results in more rapid cell cycle and hyperproliferation along with

formation of tumours at low passage number, as androgenetic MEFs displayed anchorage-independent growth and produced fibrosarcomas when injected into adult nude mice (Hernandez et al., 2003). It is also in agreement with the parental conflict theory, as cell proliferation is enhanced due to loss of the maternal genome's growth suppressing function. Another study suggested that significant *Igf1r*-mediated growth inhibition was the consequence of an overexpression of functional *Grb10* gene that caused a delay in the S- and G2-phases of the cell cycle (Morrione et al., 1997), implying a *Grb10* negative function in cell proliferation, which has also been shown elsewhere (Liu and Roth, 1995). On the other hand, our group has previously demonstrated that $Grb10^{m/+}$ animals do not owe their overgrowth phenotype to altered Igf signalling (Charalambous et al., 2003; Garfield, 2007). Additionally, a variety of studies have shown that *Grb10* overexpression causes phosphorylation changes of several downstream signalling proteins, such as Akt and PI3K (Holt and Siddle, 2005), suggesting that Grb10 inhibits cell proliferation through yet unknown pathway. Furthermore, two recent studies identified Grb10 as a substrate of mTOR, a cellular enzyme called mechanistic (or mammalian) target of rapamycin responsible for regulation of cell growth and division, and implicated as an important drug target in cancer (Hsu et al., 2011; Yu et al., 2011). Both reports provided evidence for Grb10 as a participant in a negative feedback loop in which mTORC1, activated downstream of insulin or IGFs, phosphorylates Grb10 and enhances its ability to inhibit signals from IGF and insulin receptors (Hsu et al., 2011; Yu et al., 2011), a mechanism which complements an already established feedback pathway, with S6K1 phosphorylating IRS and targeting it for degradation.

In the present study we have used FACS to analyse cell size by looking at forward scatter, with cells separated into four different size gates. We found that the apparent overgrowth phenotype in $Grb10^{m/+}$ and $Grb10^{m/+}/Dlk1^{+/p}$ embryos could not be obviously associated with an increased cell size at the embryonic stage of E11.5, as the cells acquired from knockout embryos did not differ from wild type controls. The same negative result was obtained during FACS analysis of cell size in $Grb10^{m/+}$ and $Grb10^{m/+}/Dlk1^{+/p}$ E14.5 pMEFs, which is consistent with previous results provided for $Grb10^{m/+}$ cultures (Garfield, 2007). These results need to be interpreted with care and their analysis repeated using similar gating method as the one used for analyses of cell cycle phases, as gating of the cells for the cell size analysis allowed for excluding the debris from the experiment but did not distinguish between singlet and dublet cells, which could have had a great impact on the obtained results.

Our finding of significantly increased proliferation rates in E14.5 *Grb10*$^{m/+}$*/Dlk1*$^{+/p}$ pMEFs is also in line with earlier studies of *Grb10*$^{m/+}$. Moreover, as the *Grb10*$^{m/+}$*/Dlk1*$^{+/p}$ E14.5 pMEFs hyperproliferative phenotype is similar, or even more pronounced than the one previously observed for *Grb10*$^{m/+}$ fibroblasts, we can conclude that *Grb10* and *Dlk1* genes might be indeed acting in the same genetic pathway to regulate proliferation rates in embryonic cells, consistent with the hypothesis we have proposed. Certainly, *Grb10*$^{m/+}$*/Dlk1*$^{+/p}$ E14.5 pMEFs growth rates are not exhibiting an additive phenotype between *Grb10*$^{m/+}$ and *Dlk1*$^{+/p}$ knockout cells, which provides evidence against the possibility of these two genes acting independently in two distinct genetic pathways to control proliferation.

A hyperproliferative phenotype can be associated with alterations to the normal cell cycle, specifically with more rapid cell cycle progression. For that reason we have employed FACS to analyse cell cycle kinetics in *Grb10*$^{m/+}$*/Dlk1*$^{+/p}$ E14.5 pMEFs and compare them to single knockout cells and wild type controls. No alterations were detected in the G1-phase of the cell cycle for any of the analysed genotypes, indicating that the observed hyperproliferative phenotype in *Grb10*$^{m/+}$ and *Grb10*$^{m/+}$*/Dlk1*$^{+/p}$ cultures was not due to a role for *Grb10* in the transition from G1- to S-phase, a result also consistent with a previous study (Morrione et al., 1997). We found that the most likely reason for increased proliferation rates in *Grb10*$^{m/+}$ and *Grb10*$^{m/+}$*/Dlk1*$^{+/p}$ cells lies within changes in the S- and G2-phases of cell cycle. Significantly lower *Grb10*$^{m/+}$ and *Grb10*$^{m/+}$*/Dlk1*$^{+/p}$ cell numbers were observed in S-phase, with a concomitant significantly increased accumulation of cells in G2-phase.

The progression of cells through the division cycle is controlled by a variety of extracellular signals from the environment, such as growth factors, as well as by a number of internal signals that act to regulate the processes that take place within particular cell cycle phases (Malumbres and Barbacid, 2009). In addition, the complex cellular processes that take place within different phases of cell cycle, such as cell growth, DNA replication and mitosis, must be coordinated during cell cycle progression. This is accomplished by a series of control points that regulate progression through various phases of the cell cycle (Kastan and Bartek, 2004).

During S-phase of the cell cycle the precise replication of the entire DNA content of the nucleus must take place, usually within a period of several hours. The length of S-phase differs not only between species, but also between different developmental stages within a species, however within the same type of cell the duration of S-phase is usually consistent (Cooper, 2000). Following completion of DNA synthesis the G2-phase takes place, during which cell growth and protein synthesis continues before mitosis (Norbury and Nurse, 1992). FACS

analysis allowed us to distinguish cells within different stages of the cell cycle by analysing changes in their DNA content, however it did not specify if the elongated G2- phase indicates that more *Grb10*$^{m/+}$ and *Grb10*$^{m/+}$*/Dlk1*$^{+/p}$ cells are undergoing mitosis. In order to clarify this issue, for example MPM-2 or phospho-Histone H3 antibodies could be used as markers for mitosis during FACS analysis in the future.

Morrione et al (1997) conducted *in vitro* experiments to investigate the effects of *Grb10* overexpression on cell proliferation. They have found that excess *Grb10* resulted in a delay in the S- and G2-phases of the cell cycle upon *Igf1* stimulation. It would appear that, as found in the present study, decreased numbers of *Grb10*$^{m/+}$ and *Grb10*$^{m/+}$*/Dlk1*$^{+/p}$ cells within S-phase are indicative of more rapid progression through the S-phase of the cell cycle, and as a consequence of a reduced likelihood of detection of the cell in this phase of the cell cycle during FACS analysis. It seems that *Grb10* is able to affect only the S- and G2-phases, in contrast to *Igf1r* which has been found not to be specific to these phases of the cell cycle (Sell et al., 1994), which falls in line with previous findings of *Grb10* growth regulation being independent of IGF pathway (Charalambous et al., 2003; Garfield, 2007).

Usually shorter G1- and/or G2-phases of cell cycle or shorter cell cycle in general are thought to initiate an increase in cell proliferation, so it is rather difficult to explain the observed hyperproliferative phenotype without more detailed analysis of each of the cell cycle phases, together with total cell cycle length. The fact that the same effects on S-phase of cell cycle phase has been reported previously in *Grb10*$^{m/+}$ cells is, however reassuring that the hyperproliferation and shorter S-phase of cell cycle are real consequences of a lack of *Grb10* activity. Thus, it would be of interest to examine the basis of increased pMEFs growth by studying the length of each of the cell cycle phases together with overall cell cycle duration by using FACS analysis. Variations of cell labelling experiments could be used to determine the length of different stages of the cell cycle, for example cells in S-phase could be identified because they incorporate radioactive thymidine, which is used exclusively for DNA synthesis.

Our analysis of the embryonic phenotype of *Grb10*$^{m/+}$*/Dlk1*$^{+/p}$ animals and *in vitro* study of *Grb10*$^{m/+}$*/Dlk1*$^{+/p}$ pMEFs cultures provides evidence supporting the hypothesis of an epistatic and antagonistic relationship between the *Grb10* and *Dlk1* genes in regulation of embryonic growth. The resemblance of the growth phenotype between *Grb10*$^{m/+}$ and *Grb10*$^{m/+}$*/Dlk1*$^{+/p}$ animals during early development indicates that *Grb10* influences growth by acting as an inhibitor downstream of *Dlk1* at this developmental stage. These results, however, are complicated by 4 different genotypes obtained in each cross and the use of the *Grb10*$^{m/+}$

mothers in all the crosses, which are known to have altered body composition and glucose metabolism (more lean tissue mass and improved glucose tolerance), which could have an effect on the developing progeny during gestation and interfere with identifying the real effects of the *Dlk1* and *Grb10* ablation on embryos and their placentae. However, female mice with paternal transmission of *Grb10* deletion (exhibiting normal body composition and glucose homeostasis but different social behaviour) could not be used in generation of our crosses as we aimed for maternal *Grb10* and paternal *Dlk1* ablation in our double knockout mice. On the other hand, homozygous mothers could be used if we wanted to reduce the number of obtained offspring genotypes from 4 to 3 which could be beneficial during statistical analyses and because we were mostly interested in comparing our double knockout mice to $Dlk1^{+/p}$ and $Grb10^{m/+}$, and this type of cross generation should be considered during future investigation. It also needs to be taken into account that overgrowth of $Grb10^{m/+}/Dlk1^{+/p}$ embryos might be consequence of double mutant placentae being much more efficient in supplying nutrients and subsequently leading to overgrown double mutant embryos similar to $Grb10^{m/+}$. Therefore, there is a need to analyse the morphology and efficiency of the transport systems within the $Grb10^{m/+}/Dlk1^{+/p}$ placentae that will aid to clarify the nature of the observed $Grb10^{m/+}/Dlk1^{+/p}$ embryonic overgrowth.

Further experiments, including Western Blot analysis of whole embryos from various developmental stages and double *Grb10* and *Dlk1* antibody staining will be useful in identifying the details of possible *Grb10* and *Dlk1* interaction and will provide more information on their mode of action during embryonic growth and development. Western Blots would help to delineate specific changes in the expression of *Grb10* in $Dlk1^{+/p}$ animals and *Dlk1* in $Grb10^{m/+}$mice and clarify the relevance of our hypothesis of them interacting in the same genetic pathway, however so far attempts of Western Blot analysis on whole embryos and embryonic livers proved unsuccessful due to unspecific binding of the used antibodies, and this solving this issue in the future would be necessary in supporting the hypothesis of *Grb10* and *Dlk1* interaction. Also the antibody staining experiments (especially in whole embryos and in organs with known, well-pronounced expression of both *Grb10* and *Dlk1*, e.g. liver) could be informative of altered expression associated with forming a part of the same genetic pathway in specific tissues and stages of development. Results from this chapter imply that *Dlk1* might indeed be acting upstream of *Grb10* which in turns is inhibiting embryonic growth, as the data from the allometric study of the embryos and placentae of three developmental stages show that the growth phenotype of $Grb10^{m/+}/Dlk1^{+/p}$ mice is similar to that observed in $Grb10^{m/+}$. In addition, the increased growth rates of E14.5 pMEFs have been confirmed in $Grb10^{m/+}/Dlk1^{+/p}$

and *Grb10*$^{m/+}$ cells along with shortened S-phase and elongated G2-phase in E11.5 embryonic cells and E14.5 pMEFs from these two genotypes, findings that could also point at *Dlk1-Grb10* interactions in regulation of cell proliferation during embryonic development. Analysis of *Grb10*$^{m/+}$*/Dlk1*$^{+/p}$ placental morphology and any potential physiological changes within this crucial site of nutrient exchange between mother and offspring is under way. We hope it will give us an insight into, primarily, the effects of combined lack of *Grb10* and *Dlk1* genes on normal placental function and additionally will be informative of the role of *Dlk1* in the placenta on its own, as there is a shortage of studies on *Dlk1* knockout placentae until now. In addition, more precise experiments, particularly study of total cell number in embryos at E11.5 and earlier using the FACS analysis method described by Burns and Hassan (2001) will be employed in order to shed more light on the basis of the *Grb10*$^{m/+}$ and *Grb10*$^{m/+}$*/Dlk1*$^{+/p}$ overgrowth phenotype.

CHAPTER 4

4 Postnatal characterisation of *Grb10*$^{m/+}$*/Dlk1*$^{+/p}$ double knockout mice

4.1 Introduction

Adult diseases, for example metabolic complications such as diabetes or obesity, can be consequences of disproportionate growth of tissues during embryonic and postnatal development (Eriksson et al., 2003). A range of maternal characteristics, including type of diet, body composition, stress levels and fitness contribute to reaching appropriate body size and proportions (Victora et al., 2008; George et al., 2010), although mouse genetic studies have unequivocally implicated several genes that play crucial roles in controlling this process. There is rather poor understanding of the function of mother-offspring genetic interactions affecting correct growth and adult health status. The on-going arguments over the explanation for the existence of genomic imprinting do not undermine the vital role of this phenomenon in both pre- and post-natal development, as in mammals imprinted genes involved in nutrient acquisition through the placenta have been shown to play a part in fetal programming.

Opposing interests of parental genomes over allocation of maternal resources are frequently considered to be among selective pressures that resulted in evolution of imprinting. Throughout gestation, paternally expressed are genes usually thought to increase the level of nutrient supply or demand required for embryonic development, in contrast to maternally expressed imprinted genes with an opposite function. Consequently, reciprocal interests of parental genomes could also explain the ability of imprinted genes to disrupt the interaction between mother and pre-weaning offspring due to persisting dependence of mammalian offspring on maternal resources up to this stage of development. Postnatal regulation of resource acquisition by imprinted genes might be based on control of milk release in the mother or regulation of sucking behaviour in the offspring. After weaning, imprinted genes might also function to allocate the resources acquired by the offspring into growth, deposition of adipose tissue and other processes involved in the maintenance of homeostasis, like regulation of glucose metabolism and body temperature, as fetal and postnatal growth and metabolism are linked and frequently regulated by the same genetic pathways. It has been shown that a number of adult disorders result from impairment in normal embryonic development and epigenetic regulation of the metabolic gene network has been linked to *in utero* availability of nutrients (reviewed in Waterland and Jirtle, 2004).

Various mouse genetic studies suggested a role for imprinted genes in regulation of postnatal relationship between mother and offspring (Isles et al., 2002; Hager and Johnstone, 2003), but their physiological roles in maternal behaviour and offspring growth have been first

exemplified by knockout experiments of two paternally expressed genes: *Peg1* and *Peg3* (Lefebvre et al., 1998; Li et al., 1999). Both acting as potent growth enhancers, they were found to control maternal care, including placentophagia, nest-building, and pup gathering. Disruption of *Peg3* resulted in mice with reduced growth and difficulties with suckling and thermoregulation which led to delayed weaning and puberty (Curley et al., 2004), while mothers with *Peg3* paternal knockout were deficient in milk secretion caused by reduced numbers of oxytocin-producing neurons in hypothalamus (Li et al., 1999). Due to *Peg3* having previously been implicated in controlling maternal behaviour in adult females, it seems that proper maternal care and ability to extract resources by offspring are an example of coadaptation at this locus.

An imprinted *Gnas* cluster, able to produce various proteins by using alternative promoters and initial exons splicing onto a group of downstream exons (Holmes et al., 2003), generates the G-protein α subunit (Gsα) and paternally expressed, neuroendocrine-specific Gsα isoform XLα. They both have been found to exert reciprocal effects on metabolism, as *Gnasxlα* paternal knockout mice displayed an insulin-sensitive, lean phenotype (Plagge et al., 2004) and mice with paternal deletion of *Gsα* exon 1 showed insulin resistance and obesity (Chen et al., 2005). Mice with *Gnasxlα* paternal knockout were growth retarded upon birth, which led to an increased rate of lethality (Plagge et al., 2004). Moreover, these animals showed a disrupted suckling ability confirmed by identification of *Gnasxlα* in sites of the brain that are responsible for motor innervation of the orofacial, jaw and tongue muscles (Plagge et al., 2004).

Interestingly, our lab has recently discovered that *Grb10*, with already recognised roles in regulating mother-offspring interaction during gestation (Charalambous et al., 2010), might also be acting to promote mother-offspring coadaptation postnatally. Our investigation focused on *Grb10* imprinting in mammary gland, an organ crucial in postnatal nutrient acquisition and a site of conflict over maternal resources. We have found that imprinted *Grb10* in mammary gland throughout pregnancy and lactation is able to control nutrient supply and postnatally nutrient demand, regulating the size of the offspring (Cowley et al., submitted). Interestingly, maternal *Grb10* has been found to exert effects on adiposity whereas *Grb10* in the offspring controlled lean tissue content. These findings support a role for *Grb10* in influencing mother-offspring coadaptation to optimise fitness of the progeny, as achieving correct body proportions and fat/lean ratio requires functional *Grb10* in both mother and pup (Cowley et al, submitted). The capacity for *Grb10* to control postnatal nutrient supply and

demand and subsequently to influence body composition and proportions highlights its role in connecting early development and postnatal health status through fetal programming.

Generation of *Grb10*$^{m/+}$ knockout animals by our lab allowed for an investigation of the *in vivo* role of the *Grb10* gene in not only early stage development but also in postnatal life. Neonatal *Grb10*$^{m/+}$ animals were 36% heavier than their wild type counterparts and their organs (including hearts, lungs and kidneys) were also proportionally enlarged with the exception of the liver and brain in which disproportionate overgrowth and sparing have been noted, respectively (Charalambous et al., 2003). The total body overgrowth effect decreased during postnatal life and by 6 months of age, *Grb10*$^{m/+}$ knockout animals were only 13% heavier than wild types (Smith et al., 2007). Weights of a cohort of animals were monitored from birth for 80 days, which revealed that the weight difference between *Grb10*$^{m/+}$ knockout and wild type mice diminished mainly during the post-weaning period. It was also noted that that relative weights of abdominal and renal fat pads in *Grb10*$^{m/+}$ knockout mice of both sexes were significantly reduced in size when compared to wild type littermates (Smith et al., 2007). These results indicate a crucial role for *Grb10* in the regulation of postnatal growth and development. In support of that, a model studying the effects of overproduction of *Grb10* has been provided by Shiura et al (2005). Although the described study has not proven useful in delineating the effects of *Grb10* in embryonic growth control due to poor *Grb10* transgene expression during fetal development, mice overexpressing *Grb10* postnatally displayed growth retardation commencing from the age of 4 weeks, with a 10-15% decrease in weight when compared to wild type controls at the age of 4 months (Shiura et al., 2005). However, these results should be interpreted with care, as the ectopic postnatal overexpression of *Grb10* in several organs such as liver, skeletal muscle and adipose tissue might have contributed to the observed phenotypes, producing artifactual effects.

In addition to the mouse phenotypes resulting from modifications of the expression of the *Grb10* gene situated on chromosome 11, mutations encompassing human chromosome 7 (which includes *GRB10*) have been implicated in the aetiology of Silver-Russell Syndrome (SRS) and several other conditions associated with growth restriction phenotypes (Kotzot et al., 1995). A number of observations have highlighted the potential role for *GRB10* as a cause of this disorder, especially that a group of SRS patients has been found to exhibit maternal duplication of the region including the *GRB10* locus (Joyce et al., 1999; Yoshihashi et al., 2000) and, in support of that, a recent publication described a family carrying a maternally inherited duplication of chromosome 7 not including GRB10 and without SRS (Leach et al., 2007).

Nevertheless, several studies have argued against a role for *GRB10* in this syndrome and up until now various screening studies failed to provide evidence for either point mutations in the coding region or aberrant methylation of *GRB10* in Silver-Russell syndrome patients (Mergenthaler et al., 2001; Arnaud et al., 2003; Monk et al., 2003). Currently the most common epimutations and mutations found in SRS patients are associated with chromosomal region 11p15, with hypomethylation at the telomeric *H19* imprinting control region believed to result in *IGF2* downregulation, which has been found in 38-63% of SRS cases (reviewed in Eggermann et al., 2010). The underlying causes of hypomethylation are unknown in the majority of cases, however in some instances they have been found to be based on mosaic maternal uniparental disomy of chromosome 11 (Bullman et al., 2008), maternal duplication of 11p15 (Eggermann et al., 2011) and potentially gene mutations of *H19*-ICR (Demars et al., 2011).

Moon et al (2002) were the first to report that mice lacking the paternal allele of the *Dlk1* gene showed pre- and post-natal growth retardation. Growth restriction of around 20% was shown to persist until weaning in both male and female mice. The authors also fed knockout mice on a high fat diet in order to investigate the effect that a lack of *Dlk1* might have on overall weight and adipose tissue content. At 65 days in males and 95 days in females differences in total body weight between wild type and *Dlk1* knockout mice were no longer evident. The catch-up in body weights of *Dlk1* knockout mice has been linked to increased adipose tissue mass in these animals. At the age of 8 weeks, weights of white fat pads (including inguinal, retroperitoneal and gonadal fat pads) in *Dlk1* knockout mice were not different to wild types. However, at 16 weeks of age, and after feeding on a high fat diet for 13 weeks, a significant increase in relative fat pad weights have been noted for both male and female *Dlk1* knockout mice. Weights of other organs, including kidneys, pancreata, lungs and thymus stayed persistently smaller than wild type, whereas livers were reported to be significantly enlarged with increased total lipid content in both sexes (Moon et al., 2002).

The importance of *Dlk1* in perinatal survival has been highlighted by an increased incidence of lethality in *Dlk1* knockout mice (Moon et al., 2002), as approximately 50% of them died within 2 days from birth. Several skeletal malformations were also reported in *Dlk1* knockout mice, including asymmetrical junction of ribs to sternum and fusion of ribs in embryos and mice that died within 2 days from birth. The authors suggested that these problems, leading to defects including poor suckling ability, as well as pulmonary abnormalities, might be the reasons for the low survival rate in *Dlk1* knockout mice. They also

described numerous cases of eyelid abnormalities that resembled the malformations detected in individuals with blepharophimosis. Blepharophimosis has been reported in people with deletions of 14q32 that encompass the *DLK1* locus, as well as in patients with mUPD14 (Yamamoto et al., 1986; Sutton and Shaffer, 2000). Human mUPD14 results in clinical features that also include pre- and post-natal growth retardation, hypotonia, mild facial abnormalities and early onset of puberty. The phenotypic characteristics of patients with pUPD14 range from an almost normal phenotype to a rather severe condition that involves facial anomalies, a small, bell-shaped thorax with rib deformities and associated respiratory insufficiency, and mental retardation that varies in severity (Georgiades et al., 1998; Sutton and Shaffer, 2000; Kagami et al., 2005; Kagami et al., 2008). Interestingly, some of these feature including skeletal abnormalities and pulmonary defects, are similar to the phenotypic characteristics observed in *Dlk1* knockout mice (Moon et al., 2002).

Dlk1 shares a structural similarity with members of the Delta/Notch family of membrane-associated receptors and ligands involved in cell signalling and cell fate determination, however, it lacks the DSL domain conserved between most of the Notch ligands to allow for receptor-ligand interaction for Notch. So far there is no evidence of direct interaction between biologically active Dlk1 and Notch (Baladron et al., 2005; D'Souza et al., 2008). Moreover, there are also contradictory reports regarding Dlk1 effects on expression of Hes-1, a downstream target of Notch (Kaneta et al., 2000; Ross et al., 2004). The most likely prediction for Dlk1 action is that it functions by binding to one or more as yet unknown interacting proteins/receptors that probably contain EGF-repeats to facilitate protein-protein interactions (see Section 1.3.1). Identification of the Dlk1 interacting partner(s) and clear establishment of its biochemical and functional interaction with Dlk1 are necessary in elucidating Dlk1 action. Lack of any obvious correlation of Dlk1 with the IGF-pathway, distinct growth phenotype of *Dlk1* knockout mice and the onset of clinical features present in UPD14 patients all indicate a signalling role for Dlk1 in an IGF-independent mitogenic axis.

The expression sites of *Grb10* in adult mice encompass primarily insulin-responsive tissues, such as skeletal muscle, adipose tissue and endocrine cells of the pancreas, which is in agreement with a role for *Grb10* in mediating insulin signalling (discussed in more detail in Chapter 5). Other sites of *Grb10* expression include the Leydig cells of the testes, the oviduct and uterine horns of the female reproductive system, and some cell populations of the CNS (Smith et al., 2007; Garfield et al., 2011). Expression of *Dlk1* in adulthood is also restricted, being most prominent in preadipocytes, β-cells of islets of Langerhans, testes, pituitary and

adrenal glands as well as in monoaminergic neurons in the CNS (Tornehave et al., 1993; Jensen et al., 2001; Yevtodiyenko and Schmidt, 2006).

Given the substantial roles of both of the imprinted *Grb10* and *Dlk1* genes in fetal growth and development and their evident importance in adult metabolic homeostasis, together with the fact that they both appear to act in an IGF-independent manner, the idea of a potential interaction between these two genes seems plausible. To investigate this further and gain more knowledge about the postnatal effects that result from a lack of both the *Grb10* and *Dlk1* genes, we have analysed postnatal growth of $Grb10^{m/+}/Dlk1^{+/p}$ double knockout mice and compared them to wild type and single knockout littermates. Should an interaction between *Grb10* and *Dlk1* be a part of the same genetic pathway, it would be predicted that $Grb10^{m/+}/Dlk1^{+/p}$ double mutants would be phenotypically similar to one of the single knockouts.

In this chapter, analyses of various aspects of the postnatal phenotypes of $Grb10^{m/+}/Dlk1^{+/p}$ double knockout mice are presented and compared to wild type, $Grb10^{m/+}$ and $Dlk1^{+/p}$ animals. Following on from investigations of prenatal growth discussed in the previous chapter, allometric analyses of neonatal and adult mice have been performed. Several organs have also been investigated in detail, either histologically or morphometrically, these included kidneys, bones and lungs. Through these analyses we hoped to gain more knowledge about the role of *Grb10*, *Dlk1* and their potential to interact during postnatal life in mice.

4.2 Results

4.2.1 Characterisation of neonatal *Dlk1*$^{+/p}$, *Grb10*$^{m/+}$ and *Grb10*$^{m/+}$/*Dlk1*$^{+/p}$ mice.

It has been previously reported that loss of the *Grb10* gene resulted in significant overgrowth of neonatal mice (Charalambous et al., 2003), whereas lack of the *Dlk1* gene caused a reciprocal effect, as *Dlk1* knockout mice displayed significant growth retardation on the day of birth (Moon et al., 2002). By characterising the growth of neonatal *Grb10*$^{m/+}$/*Dlk1*$^{+/p}$ double knockout animals, along with histologically and morphometrically examining several tissues, we aimed to study the effects of loss of both of these genes and test the hypothesis that the two genes work in the same genetic pathway.

4.2.1.1 Body and organ weight analysis

Neonatal mice of all four genotypes were sacrificed by decapitation and their total body weights were recorded. Additionally, the wet weights of organs including livers, brains, kidneys, lungs and hearts were noted (**Figure** 4.1). The weights of all analysed organs were also expressed as percentages of total body weights (**Figure** 4.2).

As expected, *Dlk1*$^{+/p}$ knockout mice were significantly smaller than wild type mice whilst *Grb10*$^{m/+}$ knockout mice were significantly overgrown on the day of birth (**Figure** 4.1 A). *Grb10*$^{m/+}$/*Dlk1*$^{+/p}$ double knockout mice were similar in weight to *Grb10*$^{m/+}$ single knockouts, also displaying a significantly overgrown phenotype. Analysis of organ wet weights showed that livers, brains, lungs and hearts were also significantly enlarged in *Grb10*$^{m/+}$and *Grb10*$^{m/+}$/*Dlk1*$^{+/p}$ double knockout mice, with kidney weights remaining comparable between all the genotypes.

When all the organ weights were expressed as percentages of total body weights (**Figure** 4.2), sparing of the brain and of kidneys was seen in *Grb10*$^{m/+}$ and *Grb10*$^{m/+}$/*Dlk1*$^{+/p}$ double knockout neonates, whereas livers in mice of these genotypes were disproportionately overgrown. In contrast, the weights of hearts and lungs changed in proportion to total body weights in animals of all analysed genotypes, as no differences were noted in the relative weights of these organs.

4.2.1.2 Histological and morphometric analyses

Following the previous reports of neonatal death in some *Grb10*$^{m/+}$mice that was associated with blood filled lung alveoli (Charalambous et al., 2003) and pulmonary defects noted in *Dlk1* knockout mice (Moon et al., 2002), we performed histological analysis on H&E stained neonatal lungs (**Figure** 4.3). Histological examination indicated slightly increased thickness of lung epithelial walls in both *Grb10*$^{m/+}$and *Grb10*$^{m/+}$*/Dlk1*$^{+/p}$ knockout mice. To confirm this observation, morphometric analysis of neonatal lungs was carried out (as described in Section 2.4.8; **Figure** 4.4), revealing that indeed, *Grb10*$^{m/+}$ and *Grb10*$^{m/+}$*/Dlk1*$^{+/p}$ neonatal mice had significantly thicker epithelial walls than both *Dlk1*$^{+/p}$ and wild type mice.

Due to the clear weight differences between mice of all analysed genotypes, one obvious issue was to consider the growth effects on the skeletons of neonatal animals. Skeletal malformations were previously reported in *Dlk1* knockout mice (Moon et al., 2002) and its soluble form Fetal Antigen-1 (FA1) has been identified as a novel endocrine factor regulating bone and fat mass *in vivo* along with chondrocyte differentiation (Abdallah et al., 2007; Chen et al., 2011). A recent study of gene expression in growth plate in rats revealed that the expression of imprinted gene network, including *Grb10* and *Dlk1*, unsurprisingly changes from the date of birth and towards adulthood(Andrade et al., 2009), which might imply the contribution of a number of imprinted genes in postnatal growth deceleration. As the expression of *Grb10* in bone has not been investigated previously, we decided to employ *LacZ* staining in order to track the expression *Grb10* in neonatal bones of *Grb10* knockout mice that incorporate a β-galactosidase reporter gene within the endogenous *Grb10* locus (**Figure** 4.5). *Grb10* expression was detected in growth plates of developing neonatal *Grb10*$^{m/+}$and *Grb10*$^{m/+}$*/Dlk1*$^{+/p}$ bones, indicating a possible role for *Grb10* in growth of long bones during skeletogenesis.

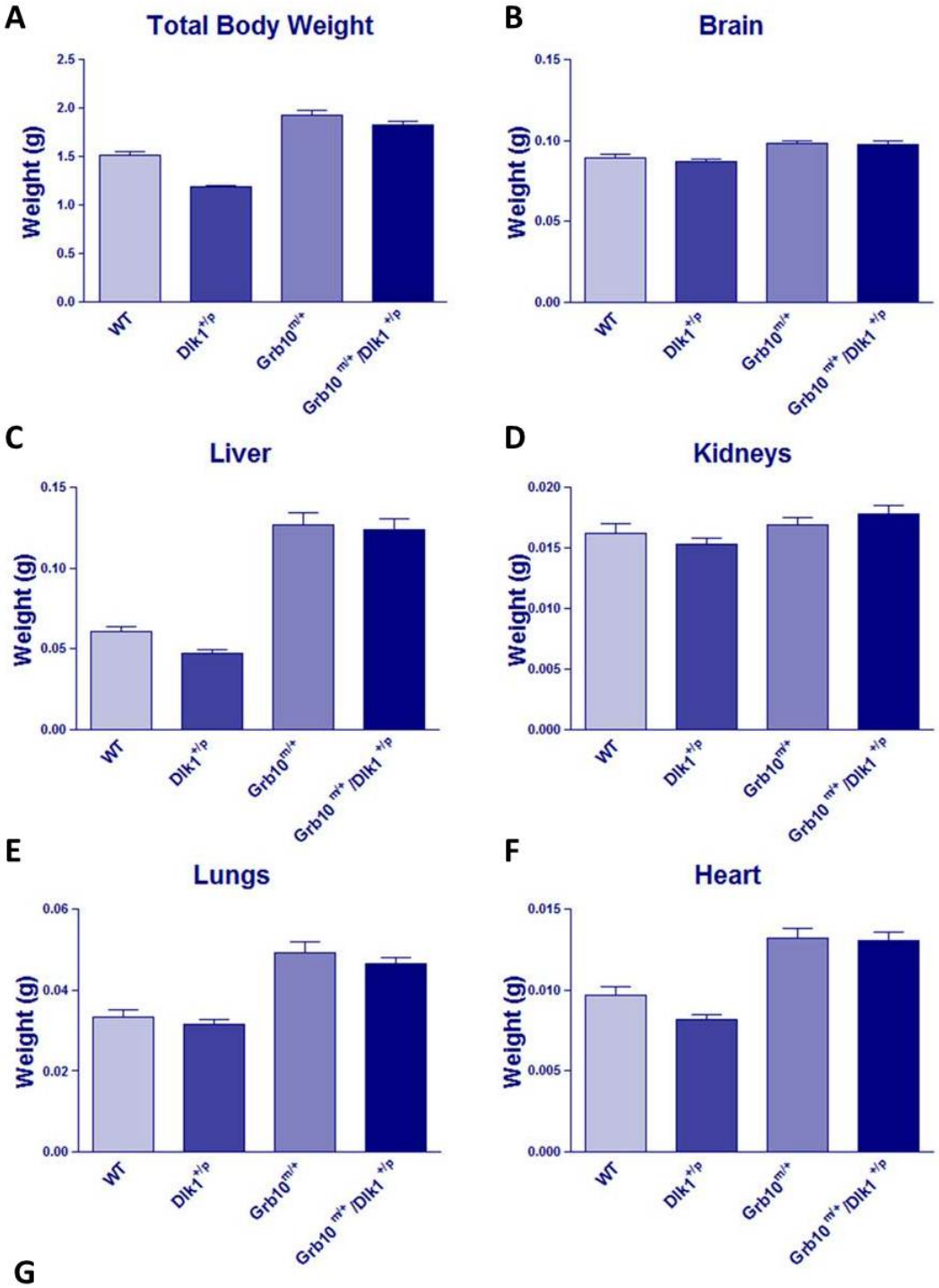

G

	Total body weight	Brain	Liver	Kidneys	Lungs	Heart
WT vs Grb10$^{m/+}$	***	*	***	ns	***	***
WT vs Dlk1$^{+/p}$	***	ns	ns	ns	ns	ns
WT vs Grb10$^{m/+}$/Dlk1$^{+/p}$	***	*	***	ns	***	***
Grb10$^{m/+}$ vs Dlk1$^{+/p}$	***	***	***	ns	***	***
Grb10$^{m/+}$ vs Grb10$^{m/+}$/Dlk1$^{+/p}$	ns	ns	ns	ns	ns	ns
Dlk1$^{+/p}$ vs Grb10$^{m/+}$/Dlk1$^{+/p}$	***	***	***	*	***	***

Figure 4.1 Whole body and organ wet weight analysis of wild type, *Dlk1*$^{+/p}$, *Grb10*$^{m/+}$ and *Grb10*$^{m/+}$/*Dlk1*$^{+/p}$ neonates.

A) *Dlk1*$^{+/p}$ mice were significantly growth retarded (***p<0.001) whereas *Grb10*$^{m/+}$ and *Grb10*$^{m/+}$/*Dlk1*$^{+/p}$ animals demonstrated whole body overgrowth (***p<0.001) when compared to wild type and *Dlk1*$^{+/p}$ mice. **B)** *Grb10*$^{m/+}$ and *Grb10*$^{m/+}$/*Dlk1*$^{+/p}$ mice had overgrown brains when compared to wild type (*p<0.05) and *Dlk1*$^{+/p}$ (***p<0.001) animals. **C)** Significant enlargement of the livers was noted in *Grb10*$^{m/+}$ and *Grb10*$^{m/+}$/*Dlk1*$^{+/p}$ mice compared to wild type (***p<0.001) and *Dlk1*$^{+/p}$ (***p<0.001) animals. **D)** Significant overgrowth of kidneys has been noted in *Grb10*$^{m/+}$/*Dlk1*$^{+/p}$ mice compared to *Dlk1*$^{+/p}$ (*p<0.05). **E)** Significant enlargement of the lungs was observed in *Grb10*$^{m/+}$ and *Grb10*$^{m/+}$/*Dlk1*$^{+/p}$ mice compared to wild type (***p<0.001) and *Dlk1*$^{+/p}$ (***p<0.001) animals. F**)** *Grb10*$^{m/+}$ and *Grb10*$^{m/+}$/*Dlk1*$^{+/p}$ mice exhibited significantly enlarged hearts compared to wild type (***p<0.001) and *Dlk1*$^{+/p}$ (***p<0.001) animals. **G)** Table summarising results of statistical analysis. All values represent means ± SEM, analysed using one way ANOVA with Tukey's post-hoc analysis. WT n=19, *Dlk1*$^{+/p}$ n=36, *Grb10*$^{m/+}$ n=23, *Grb10*$^{m/+}$/*Dlk1*$^{+/p}$ n=22.

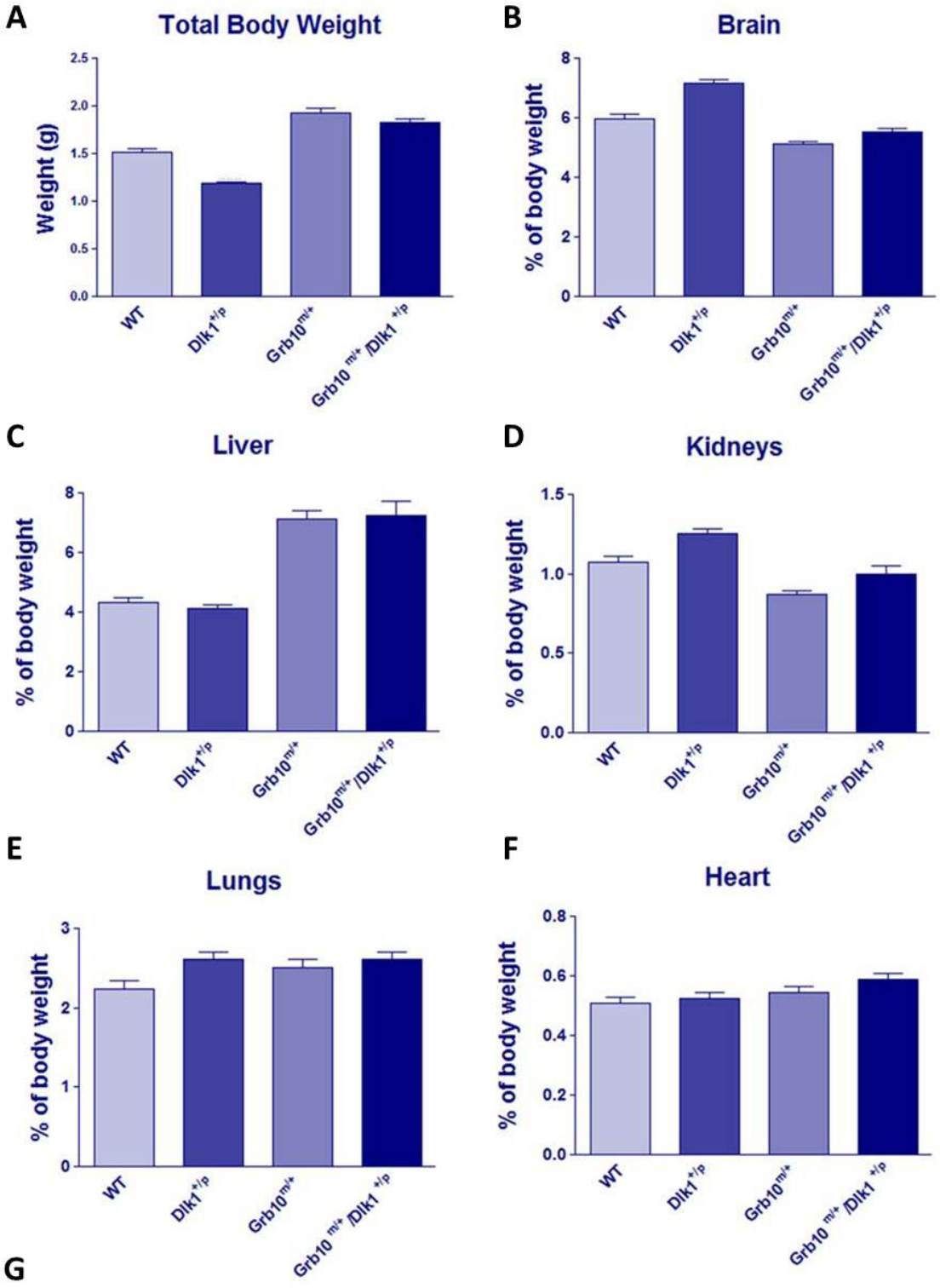

G

	Brain	Liver	Kidneys	Lungs	Heart
WT vs Grb10$^{m/+}$	***	***	***	ns	ns
WT vs Dlk1$^{+/p}$	***	ns	**	*	ns
WT vs Grb10$^{m/+}$/Dlk1$^{+/p}$	ns	***	ns	ns	ns
Grb10$^{m/+}$ vs Dlk1$^{+/p}$	***	***	***	ns	ns
Grb10$^{m/+}$ vs Grb10$^{m/+}$/Dlk1$^{+/p}$	ns	ns	ns	ns	ns
Dlk1$^{+/p}$ vs Grb10$^{m/+}$/Dlk1$^{+/p}$	***	***	***	ns	ns

Figure 4.2 Whole body and relative organ weight analysis of wild type, *Dlk1*$^{+/p}$, *Grb10*$^{m/+}$ and *Grb10*$^{m/+}$/*Dlk1*$^{+/p}$ neonates.

A) *Dlk1*$^{+/p}$ mice were significantly growth retarded (***p<0.001) whereas *Grb10*$^{m/+}$ and *Grb10*$^{m/+}$/*Dlk1*$^{+/p}$ animals demonstrated whole body overgrowth (***p<0.001) when compared to wild type and *Dlk1*$^{+/p}$ mice. **B)** Cranial sparing was seen in *Dlk1*$^{+/p}$ mice in *Grb10*$^{m/+}$ compared to wild type (***p<0.001) and *Dlk1*$^{+/p}$ (***p<0.001) mice and similar results were seen in *Grb10*$^{m/+}$/*Dlk1*$^{+/p}$ animals compared to *Dlk1*$^{+/p}$ mice (***p<0.001); *Dlk1*$^{+/p}$ had enlarged brains in comparison to wild type mice (***p<0.001) **C)** *Grb10*$^{m/+}$ and *Grb10*$^{m/+}$/*Dlk1*$^{+/p}$ mice had disproportionally overgrown livers when compared to wild type (***p<0.001) and *Dlk1*$^{+/p}$ (***p<0.001) animals. **D)** Kidney sparing was seen in *Grb10*$^{m/+}$ compared to wild type (***p<0.001) and *Dlk1*$^{+/p}$ (***p<0.001) mice and opposite growth effect was seen in *Dlk1*$^{+/p}$ (***p<0.001) animals. **E)** Proportionate growth of hearts was seen in all the analysed genotypes. F**)** Overgrowth of lungs was noted in *Dlk1*$^{+/p}$ mice compared to wild type (*p<0.05) mice. **G)** Table summarising results of statistical analysis. All values represent means ± SEM, analysed using one way ANOVA with Tukey's post-hoc analysis. WT n=19, *Dlk1*$^{+/p}$ n=36, *Grb10*$^{m/+}$ n=23, *Grb10*$^{m/+}$/*Dlk1*$^{+/p}$ n=22.

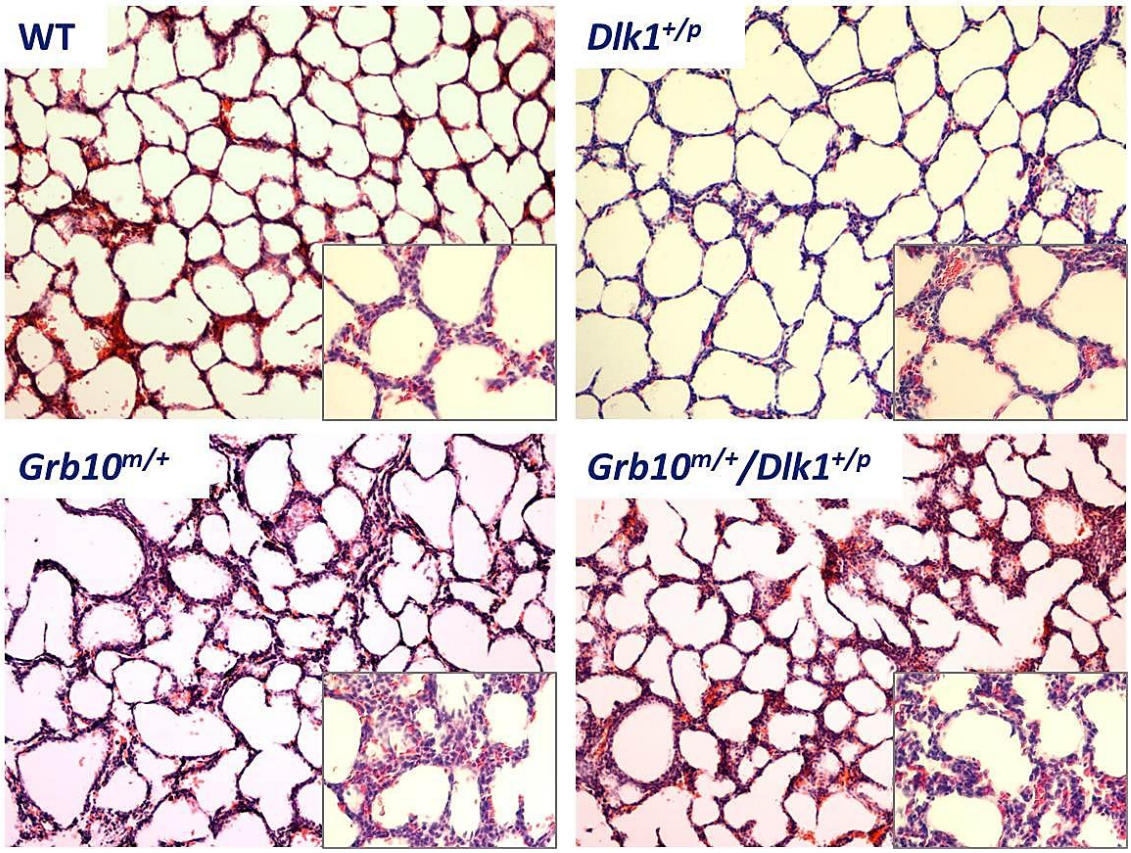

Figure 4.3 H&E stained neonatal lungs of wild type, *Dlk1*$^{+/p}$, *Grb10*$^{m/+}$ and *Grb10*$^{m/+}$*/Dlk1*$^{+/p}$ mice under 100x magnification with 400x magnification insets in bottom right corners .

Thickened epithelial walls were noticed in *Grb10*$^{m/+}$ and *Grb10*$^{m/+}$*/Dlk1*$^{+/p}$ lungs while *Dlk1*$^{+/p}$ lungs appeared to display normal histology. The presented images are representative sections for each of the analysed genotypes. WT n=5, *Dlk1*$^{+/p}$=5, *Grb10*$^{m/+}$ n=5 and *Grb10*$^{m/+}$*/Dlk1*$^{+/p}$ n=5.

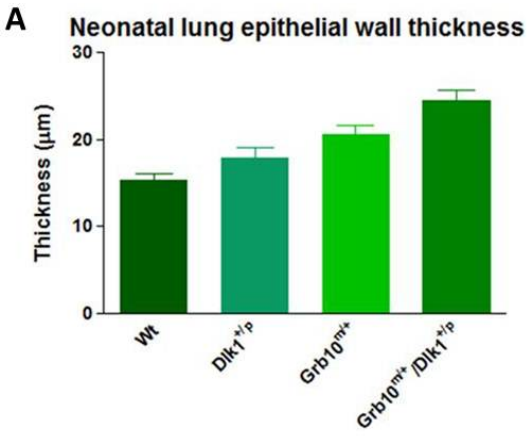

B

	Lung thickness
Wt vs Grb10$^{m/+}$	*
Wt vs Dlk1$^{+/p}$	ns
Wt vs Grb10$^{m/+}$/Dlk1$^{+/p}$	***
Grb10$^{m/+}$ vs Dlk1$^{+/p}$	ns
Grb10$^{m/+}$ vs Grb10$^{m/+}$/Dlk1$^{+/p}$	ns
Dlk1$^{+/p}$ vs Grb10$^{m/+}$/Dlk1$^{+/p}$	***

Figure 4.4 Comparison of epithelial wall thickness in neonatal wild type, *Dlk1$^{+/p}$*, *Grb10$^{m/+}$* and *Grb10$^{m/+}$/Dlk1$^{+/p}$* mice.

A) Morphometric analysis of the epithelial walls thickness revealed a significant increase in thickness in neonatal *Grb10$^{m/+}$* (*p<0.05) compared to wild type mice and *Grb10$^{m/+}$/Dlk1$^{+/p}$* (***p<0.001) compared to wild type and *Dlk1$^{+/p}$* mice, with no differences in *Dlk1$^{+/p}$* lungs compared to wild type. **B)** Table summarising results of statistical analysis. All values represent means ± SEM, analysed using one way ANOVA with Tukey's post-hoc analysis. WT n=5, *Dlk1$^{+/p}$*=5, *Grb10$^{m/+}$* n=5 and *Grb10$^{m/+}$/Dlk1$^{+/p}$* n=5.

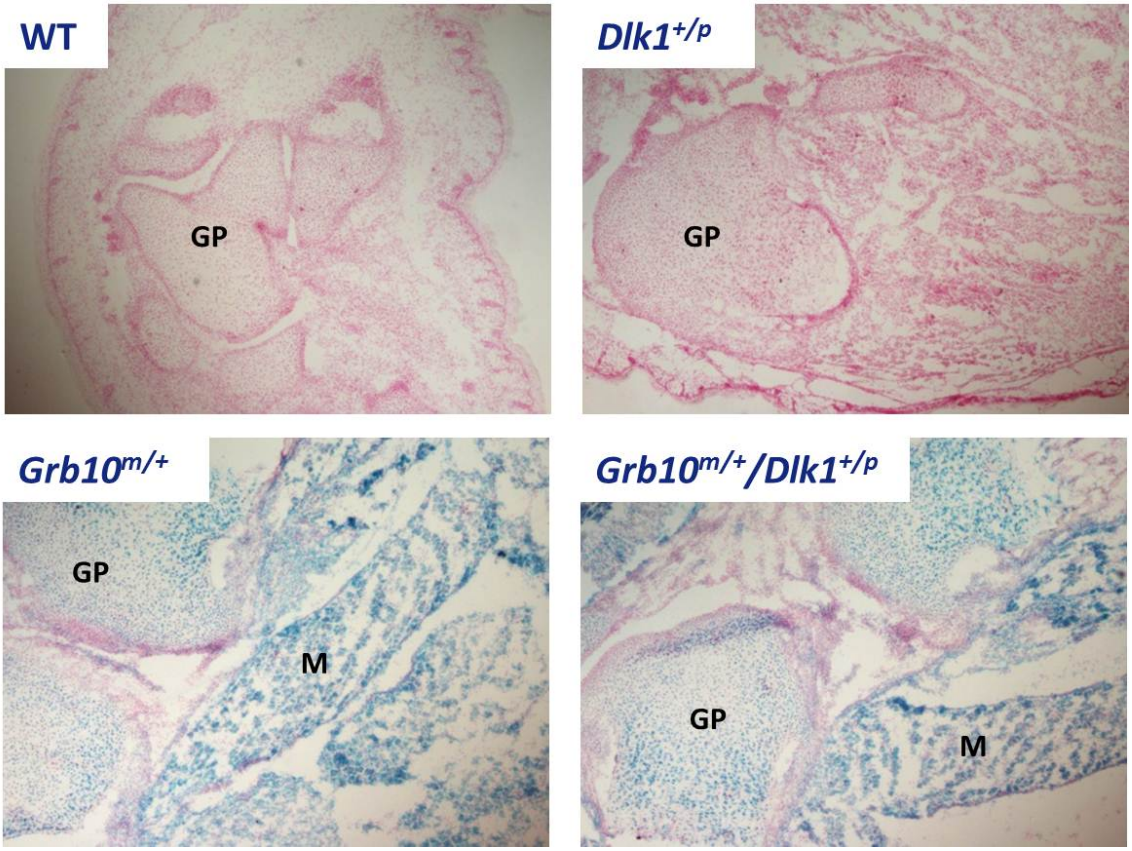

Figure 4.5 *LacZ* stained neonatal wild type, *Dlk1*$^{+/p}$, *Grb10*$^{m/+}$ and *Grb10*$^{m/+}$*/Dlk1*$^{+/p}$ femur bones under 40x magnification.

LacZ (blue) staining was detected in *Grb10*$^{m/+}$ and *Grb10*$^{m/+}$*/Dlk1*$^{+/p}$ neonatal bones, specifically in growth plates and muscle tissue adjacent to the long bones. The images show the distal growth plate (GP) of the femur, with associated muscle (M) and in some cases the knee joint and adjacent growth plate of the tibia. Presented images show representative sections for each of the analysed genotypes. WT n=5, *Dlk1*$^{+/p}$=5, *Grb10*$^{m/+}$ n=5 and *Grb10*$^{m/+}$*/Dlk1*$^{+/p}$ n=5.

4.2.2 Characterisation of 1-2 week old *Dlk1*$^{+/p}$, *Grb10*$^{m/+}$ and *Grb10*$^{m/+}$/*Dlk1*$^{+/p}$ mice.

4.2.2.1 Body and organ weight analysis

To investigate if the identified body weight differences detected at birth would persist into postnatal life we next analysed wild type, *Grb10*$^{m/+}$, *Dlk1*$^{+/p}$ and *Grb10*$^{m/+}$/*Dlk1*$^{+/p}$ mice at 1 week after birth. We compared their body weights and also performed an analysis of liver weights (**Figure** 4.6), as it was the organ exhibiting the most pronounced overgrowth immediately after birth. At 1 week of age, persistent overgrowth was seen in *Grb10*$^{m/+}$ and *Grb10*$^{m/+}$/*Dlk1*$^{+/p}$ knockout mice. Wet weights of the *Grb10*$^{m/+}$ and *Grb10*$^{m/+}$/*Dlk1*$^{+/p}$ livers also stayed significantly elevated until this stage. However, when liver weights were expressed as percentages of the total body weights, no significant differences between the genotypes were found, indicating a shift from the disproportional overgrowth seen at birth to a proportional increase in liver weight in *Grb10*$^{m/+}$ and *Grb10*$^{m/+}$/*Dlk1*$^{+/p}$ mice.

4.2.2.2 Investigation of possible skeletal anomalies

Prompted by the previous report of skeletal abnormalities in *Dlk1* knockout mice (Moon et al., 2002), we observed that one particular litter of mice at 2 weeks of age consisted of individual animals notably different from normal in length and appearance (**Figure** 4.7). Upon sacrifice, Alcian Blue/Alizarin Red bone and cartilage staining was carried out on animals from this litter to identify any potential skeletal malformations. Defects previously described for *Dlk1* knockout mice included asymmetrical attachment of ribs to the sternum, fusion of ribs and also fusion of the vertebrae. In **Figure** 4.8 the carcasses of Alcian Blue/Alizarin Red stained 2 week old mice are presented. Except for the previously noted significant overgrowth (in the case of *Grb10*$^{m/+}$ and *Grb10*$^{m/+}$/*Dlk1*$^{+/p}$ animals) and growth retardation (in the case of *Dlk1*$^{+/p}$) no other differences were evident in the bone and cartilage of analysed skeletons.

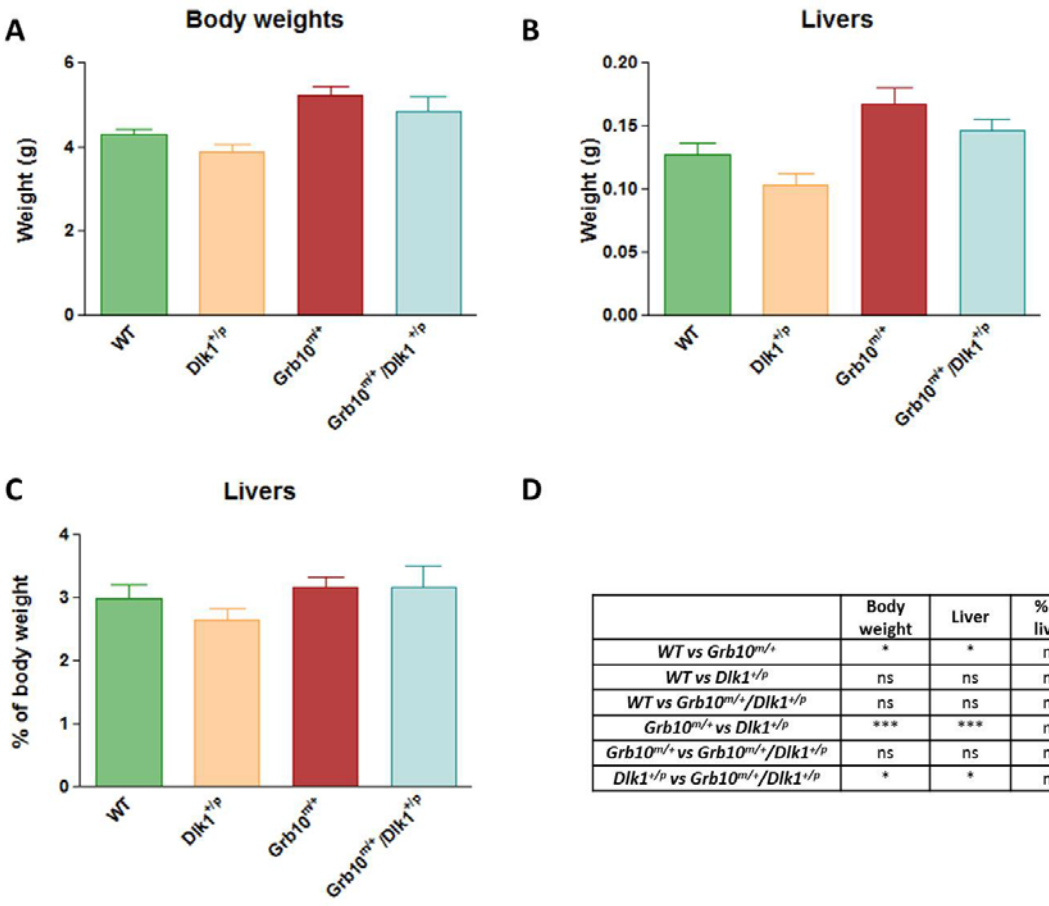

	Body weight	Liver	% of liver
WT vs Grb10$^{m/+}$	*	*	ns
WT vs Dlk1$^{+/p}$	ns	ns	ns
WT vs Grb10$^{m/+}$/Dlk1$^{+/p}$	ns	ns	ns
Grb10$^{m/+}$ vs Dlk1$^{+/p}$	***	***	ns
Grb10$^{m/+}$ vs Grb10$^{m/+}$/Dlk1$^{+/p}$	ns	ns	ns
Dlk1$^{+/p}$ vs Grb10$^{m/+}$/Dlk1$^{+/p}$	*	*	ns

Figure 4.6 Whole body, liver wet weight and relative liver weight analysis of wild type, *Dlk1$^{+/p}$*, *Grb10$^{m/+}$* and *Grb10$^{m/+}$/Dlk1$^{+/p}$* 1 week old mice.

A) Significantly increased body weights were noted in *Grb10$^{m/+}$* compared to wild type (*p<0.05) and *Dlk1$^{+/p}$* (*** p<0.001) and in *Grb10$^{m/+}$/Dlk1$^{+/p}$* compared to *Dlk1$^{+/p}$* (* p<0.05) mice whereas weights of *Dlk1$^{+/p}$* animals did not differ from wild types. **B)** Analysis of wet weights of the livers revealed significant enlargement in *Grb10$^{m/+}$* compared to wild type (*p<0.05) and *Dlk1$^{+/p}$* (***p<0.001) mice and in *Grb10$^{m/+}$/Dlk1$^{+/p}$* compared to *Dlk1$^{+/p}$* (*p<0.05) animals. **C)** No differences were found in relative liver weights. **D)** Table summarising results of statistical analysis. All values represent means ± SEM, analysed using one way ANOVA with Tukey's post-hoc analysis. WT n=10, *Dlk1$^{+/p}$* n=9, *Grb10$^{m/+}$* n=15, *Grb10$^{m/+}$/Dlk1$^{+/p}$* n=8.

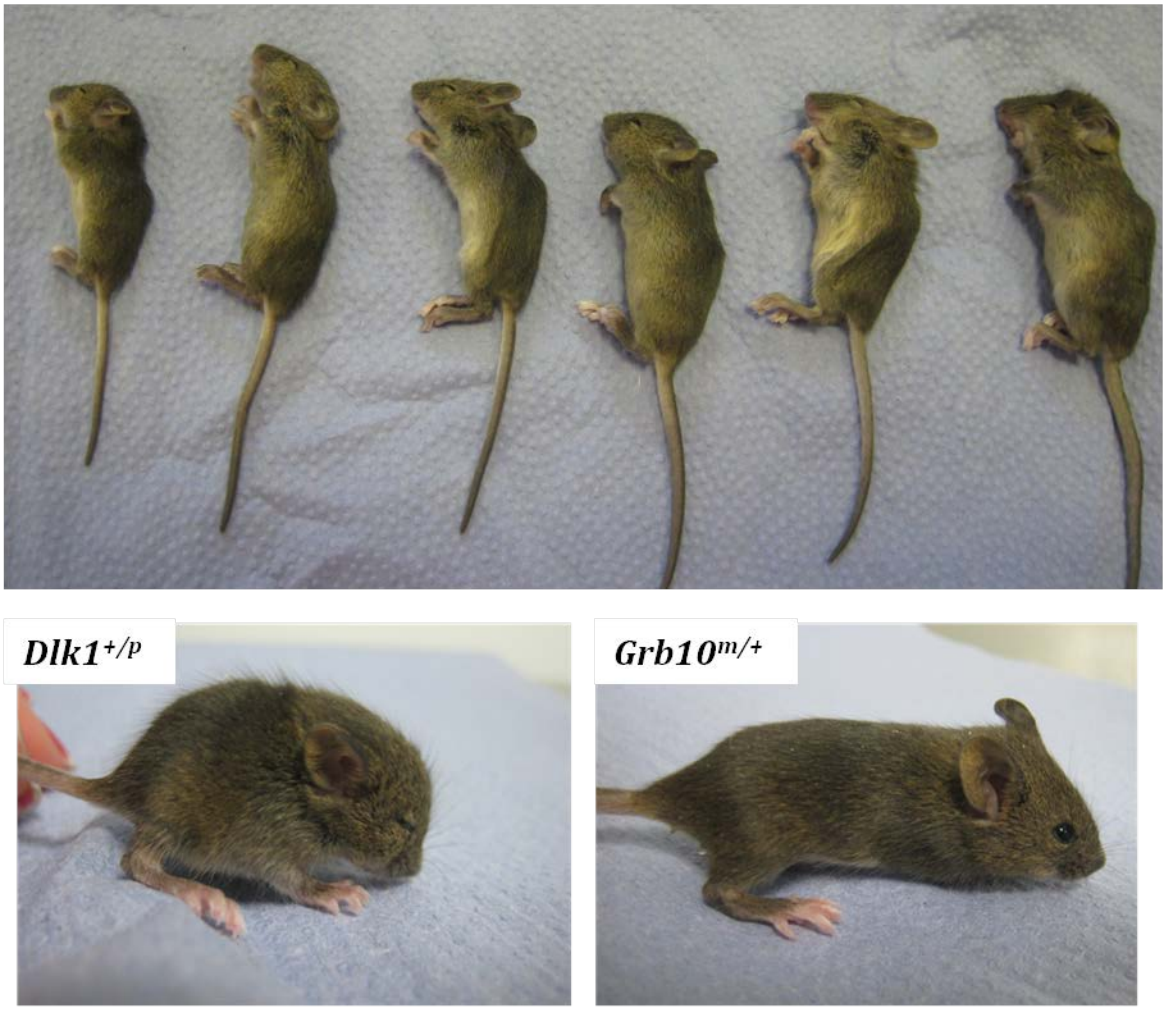

Figure 4.7 2 week old mice exhibiting potential skeletal anomalies, including wild type, *Dlk1*$^{+/p}$. *Grb10*$^{m/+}$ and *Grb10*$^{m/+}$*/Dlk1*$^{+/p}$ animals.

Genotypes of mice presented in top picture, from left to right: *Dlk1*$^{+/p}$, *Grb10*$^{m/+}$, *Dlk1*$^{+/p}$, wild type, *Dlk1*$^{+/p}$ and *Grb10*$^{m/+}$*/Dlk1*$^{+/p}$. Bottom pictures show comparison in appearance of *Grb10*$^{m/+}$and *Dlk1*$^{+/p}$ mice. There were evident size differences between the two genotypes, along with associated differences in posture.

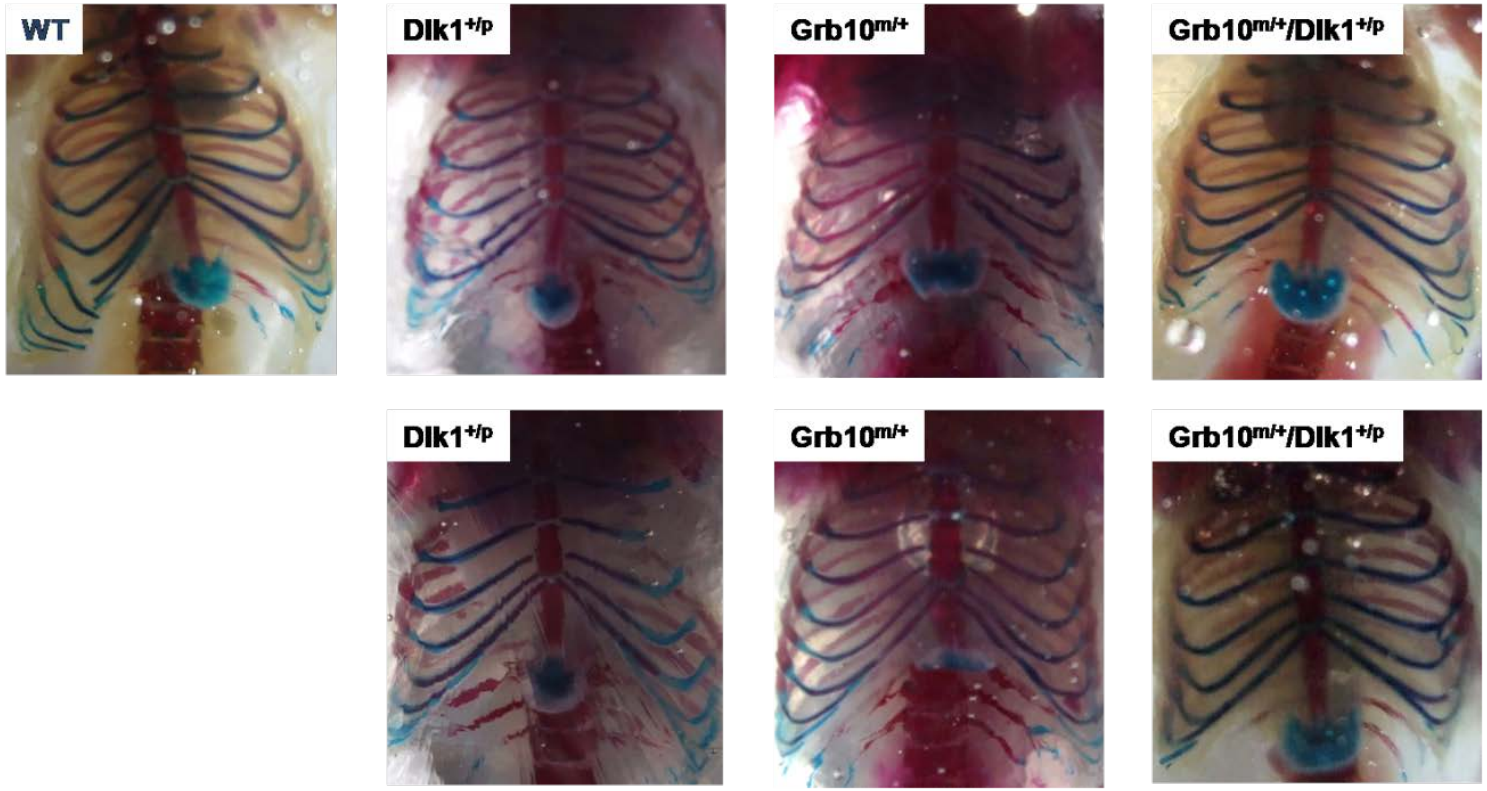

Figure 4.8 Alcian Blue/ Alizarin Red stained 2 weeks old carcasses of wild type, *Dlk1*$^{+/p}$, *Grb10*$^{m/+}$ and *Grb10*$^{m/+}$*/Dlk1*$^{+/p}$ mice.

Analysis of carcasses of 2 weeks old wild type, *Dlk1*$^{+/p}$, *Grb10*$^{m/+}$ and *Grb10*$^{m/+}$*/Dlk1*$^{+/p}$ mice with previously noted abnormal growth/posture (as presented in **Figure** 4.7) revealed no obvious differences in skeletal components, including the ribs and sternum previously reported to be affected in *Dlk1* knockout mice (Moon et al., 2002).

4.2.3 Characterisation of adult *Dlk1*$^{+/p}$, *Grb10*$^{m/+}$ and *Grb10*$^{m/+}$/*Dlk1*$^{+/p}$ mice.

4.2.3.1 Body and organ weight analysis

Given the previously described effects of ablation of the *Dlk1* and *Grb10* genes on growth at the early stages of postnatal development, further investigation of growth in 3-6 month old as well as 7-9 month old mice of both genders was performed. Total body weights along with wet weights of several organs were analysed. Relative organ weights (expressed as percentages of total body weights) were also studied.

Results obtained for 3-6 month male animals are presented in **Figures** 4.9 and 4.10. There were no appreciable differences in whole body weights but a significant increase in wet weights of pancreas was noted in *Grb10*$^{m/+}$ and *Grb10*$^{m/+}$/*Dlk1*$^{+/p}$ when compared to *Dlk1*$^{+/p}$ (**Figure** 4.9). Significantly smaller testes were a feature found in *Dlk1*$^{+/p}$ mice when compared to wild types and *Grb10*$^{m/+}$ animals. Additionally, significant reduction in in kidney weights was found in *Grb10*$^{m/+}$ as well as *Grb10*$^{m/+}$/*Dlk1*$^{+/p}$ mice. Analysis of relative weights (**Figure** 4.10) revealed significantly smaller *Grb10*$^{m/+}$and *Grb10*$^{m/+}$/*Dlk1*$^{+/p}$ livers compared to *Dlk1*$^{+/p}$ along with significantly enlarged pancreas weights in *Grb10*$^{m/+}$/*Dlk1*$^{+/p}$ mice and also a similar, but non-significant, trend observed in *Grb10*$^{m/+}$ mice.

Whole body weights of 7-9 month male mice did not differ significantly between all analysed genotypes (**Figure** 4.11), but significantly larger testes were observed in *Grb10*$^{m/+}$ mice when compared to wild type and *Dlk1*$^{+/p}$. Significantly smaller kidney weights were noted in *Grb10*$^{m/+}$ and *Grb10*$^{m/+}$/*Dlk1*$^{+/p}$ animals when compared to wild type controls. Analysis of relative organ weights (**Figure** 4.12) showed significantly smaller kidneys in *Grb10*$^{m/+}$and *Grb10*$^{m/+}$/*Dlk1*$^{+/p}$ animals, whereas the rest of the analysed organs stayed proportional to total body weights.

Examination of total body and wet organ weights in 3-6 month female mice (**Figure** 4.13) showed significant overgrowth of *Grb10*$^{m/+}$ mice when compared to wild type and *Dlk1*$^{+/p}$ along with increased pancreas weights. Significantly smaller gonadal fat pads were observed in *Grb10*$^{m/+}$/*Dlk1*$^{+/p}$ mice compared to *Dlk1*$^{+/p}$ and *Dlk1*$^{+/p}$ animals had enlarged renal fat pads in comparison to all other genotypes. *Grb10*$^{m/+}$ also showed significant overgrowth of gastrocnemius muscle when compared to wild type and *Dlk1*$^{+/p}$.

Analysis of relative weights (**Figure** 4.14) revealed significant overgrowth of pancreas in *Grb10*$^{m/+}$ and *Grb10*$^{m/+}$*/Dlk1*$^{+/p}$ mice when compared to *Dlk1*$^{+/p}$ and significantly smaller gonadal fat pad mass in *Grb10*$^{m/+}$*/Dlk1*$^{+/p}$ animals which was statistically different to *Dlk1*$^{+/p}$. On the other hand, the size of renal fat pads of *Dlk1*$^{+/p}$ was increased and statistically different to wild type whilst the size of renal fat pads of *Grb10*$^{m/+}$ and *Grb10*$^{m/+}$*/Dlk1*$^{+/p}$ was significantly smaller when compared to *Dlk1*$^{+/p}$.

Body weights, and in most cases organ weights, of 7-9 month old female mice did not vary significantly between genotypes (**Figure** 4.15), however pancreas weights of *Grb10*$^{m/+}$*/Dlk1*$^{+/p}$ females were significantly higher than those of *Dlk1*$^{+/p}$. *Grb10*$^{m/+}$ mice displayed significantly reduced weights of gonadal fat pads in comparison to wild type animals. Relative pancreas weights of *Grb10*$^{m/+}$*/Dlk1*$^{+/p}$ mice were significantly higher than those of *Dlk1*$^{+/p}$ mice (**Figure** 16), but no other significant differences in relative weight were found.

In summary, we found that several of the analysed organs consistently showed profound differences in weights between genotypes, these included pancreata, kidneys, livers, testes and fat pads. Among them, largely similar growth trends between *Grb10*$^{m/+}$ and *Grb10*$^{m/+}$*/Dlk1*$^{+/p}$ mice have been noted in pancreata, kidneys, livers, and fat pads.

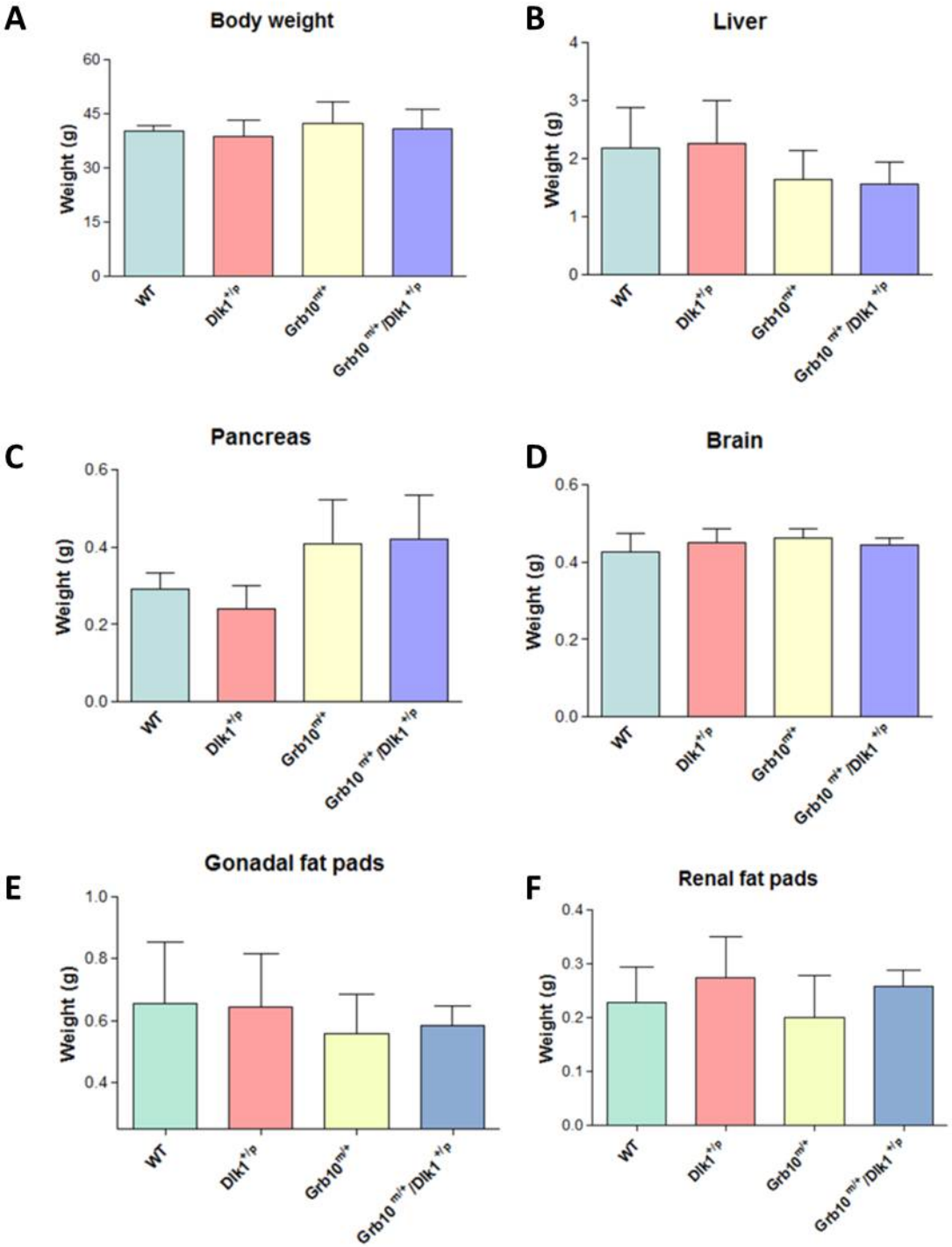
A
Body weight
Weight (g)
60
45
30
15
0
WT
Dlk1+/p
Grb10m+
Grb10 m+ /Dlk1 +/p
B
Liver
Weight (g)
4
3
2
1
0
WT
Dlk1+/p
Grb10m+
Grb10 m+ /Dlk1 +/p
C
Pancreas
Weight (g)
0.6
0.4
0.2
0.0
WT
Dlk1+/p
Grb10m+
Grb10 m+ /Dlk1 +/p
D
Brain
Weight (g)
0.6
0.4
0.2
0.0
WT
Dlk1+/p
Grb10m+
Grb10 m+ /Dlk1 +/p
E
Gonadal fat pads
Weight (g)
1.0
0.8
0.6
0.4
WT
Dlk1+/p
Grb10m+
Grb10 m+ /Dlk1 +/p
F
Renal fat pads
Weight (g)
0.4
0.3
0.2
0.1
0.0
WT
Dlk1+/p
Grb10m+
Grb10 m+ /Dlk1 +/p

G

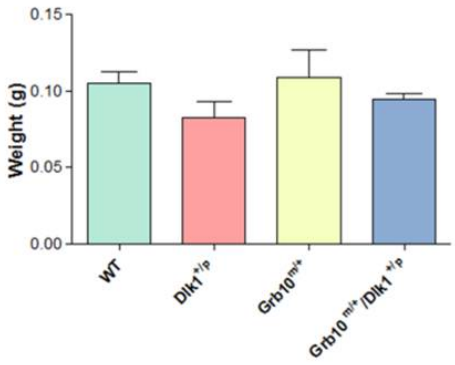

H

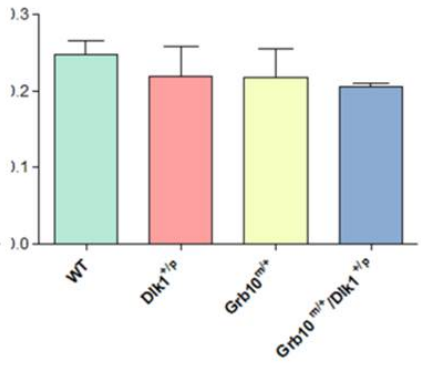

I

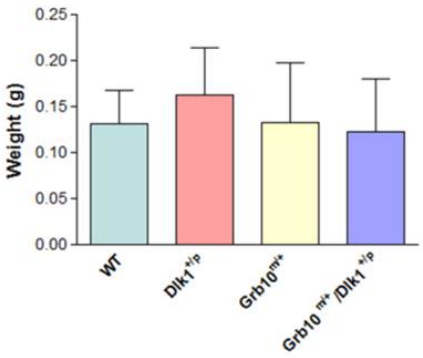

J

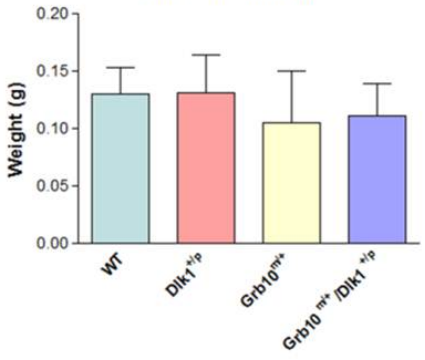

K

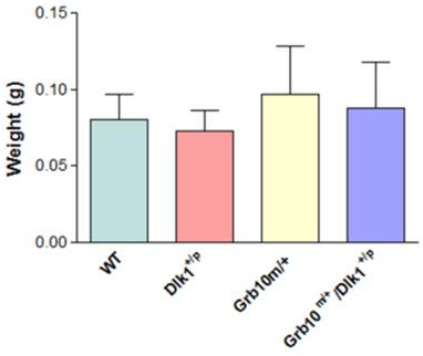

L

	Body weight	Liver	Pancreas	Brain	Gonadal fat pads	Renal fat pads
WT vs Grb10$^{m/+}$	ns	ns	ns	ns	ns	ns
WT vs Dlk1$^{+/p}$	ns	ns	ns	ns	ns	ns
WT vs Grb10$^{m/+}$/Dlk1$^{+/p}$	ns	ns	ns	ns	ns	ns
Grb10$^{m/+}$ vs Dlk1$^{+/p}$	ns	ns	*	ns	ns	ns
Grb10$^{m/+}$ vs Grb10$^{m/+}$/Dlk1$^{+/p}$	ns	ns	ns	ns	ns	ns
Dlk1$^{+/p}$ vs Grb10$^{m/+}$/Dlk1$^{+/p}$	ns	ns	**	ns	ns	ns

	Testes	Kidneys	Gastrocnemius muscle	Masseter muscle	Tongue
WT vs Grb10$^{m/+}$	ns	*	ns	ns	ns
WT vs Dlk1$^{+/p}$	***	ns	ns	ns	ns
WT vs Grb10$^{m/+}$/Dlk1$^{+/p}$	ns	**	ns	ns	ns
Grb10$^{m/+}$ vs Dlk1$^{+/p}$	***	ns	ns	ns	ns
Grb10$^{m/+}$ vs Grb10$^{m/+}$/Dlk1$^{+/p}$	ns	ns	ns	ns	ns
Dlk1$^{+/p}$ vs Grb10$^{m/+}$/Dlk1$^{+/p}$	ns	ns	ns	ns	ns

Figure 4.9 Weight analysis of 3-6 month old male wild type, *Dlk1*$^{+/p}$, *Grb10*$^{m/+}$ and *Grb10*$^{m/+}$*/Dlk1*$^{+/p}$ mice.

No significant differences were found in **A)** total body weights and weights of **B)** livers, **D)** brains, **E)** gonadal fat pads, **F)** renal fat pads, **I)** gastrocnemius muscles, **J)** masseter muscles and **K)** tongues. **C)** A significant increase in pancreas weight was noted in *Grb10*$^{m/+}$ (*p<0.05) and *Grb10*$^{m/+}$*/Dlk1*$^{+/p}$ (**p<0.01) when compared to *Dlk1*$^{+/p}$ mice. **G)** Significant testes growth reduction was observed in *Dlk1*$^{+/p}$ when compared to WT mice (***p<0.001) and the contrasting result of significant testes overgrowth was noted in *Grb10*$^{m/+}$ animals when compared to *Dlk1*$^{+/p}$ (***p<0.001). **H)** Significant decreases in kidney weights were found in *Grb10*$^{m/+}$ (*p<0.05) and *Grb10*$^{m/+}$*/Dlk1*$^{+/p}$ (**p<0.01) mice. **L)** Tables summarising results of statistical analysis. All values represent means ± SEM, analysed by one way ANOVA with post hoc Tukey's analysis. WT n=7, *Dlk1*$^{+/p}$=6, *Grb10*$^{m/+}$ n=6 and *Grb10*$^{m/+}$*/Dlk1*$^{+/p}$ n=6.

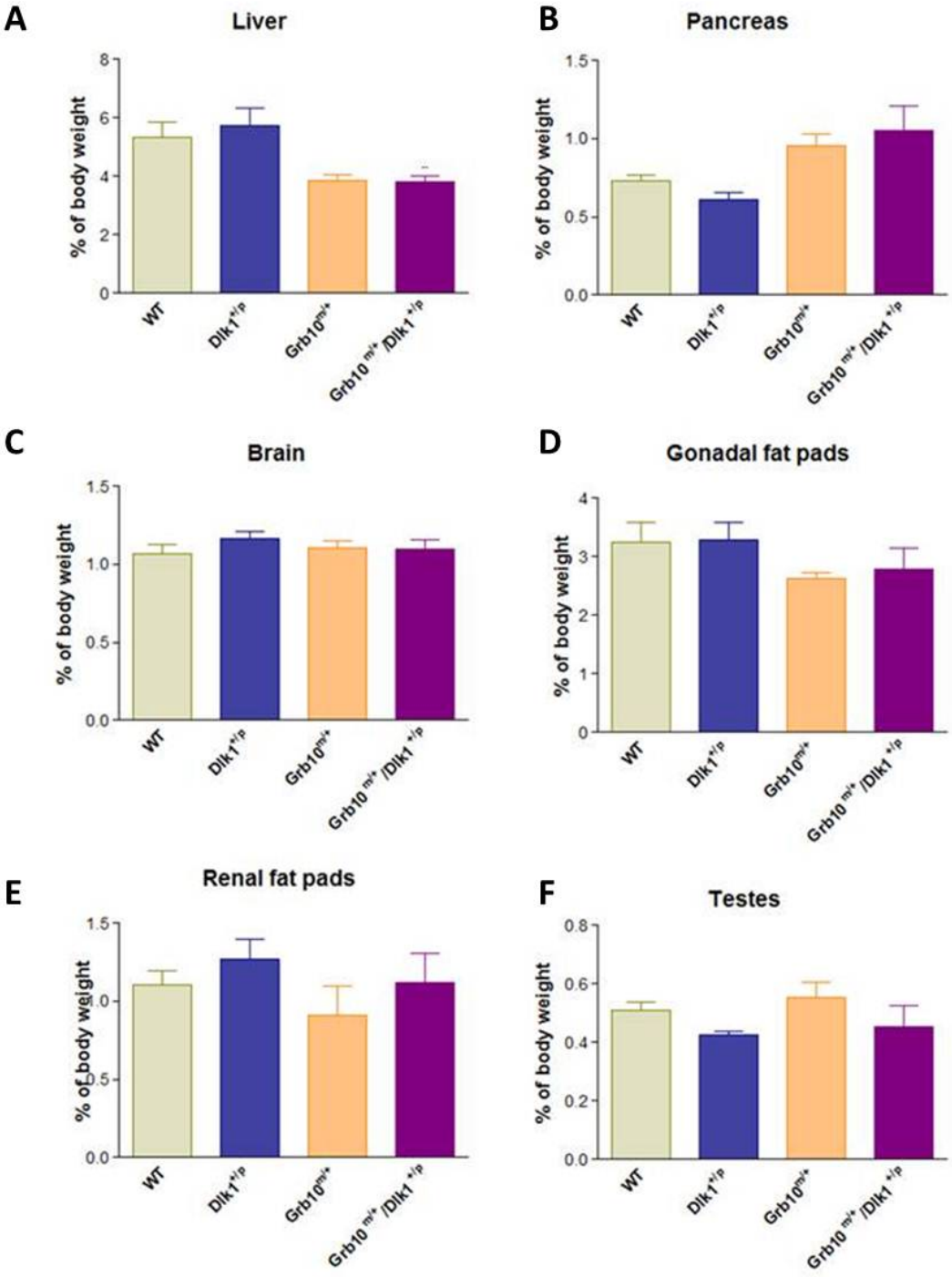
A
Liver
% of body weight
0
2
4
6
8
WT
Dlk1+/p
Grb10m/+
Grb10 m/+ /Dlk1 +/p
B
Pancreas
% of body weight
0.0
0.5
1.0
1.5
WT
Dlk1+/p
Grb10m/+
Grb10 m/+ /Dlk1 +/p
C
Brain
% of body weight
0.0
0.5
1.0
1.5
WT
Dlk1+/p
Grb10m/+
Grb10 m/+ /Dlk1 +/p
D
Gonadal fat pads
% of body weight
0
1
2
3
4
WT
Dlk1+/p
Grb10m/+
Grb10 m/+ /Dlk1 +/p
E
Renal fat pads
% of body weight
0.0
0.5
1.0
1.5
WT
Dlk1+/p
Grb10m/+
Grb10 m/+ /Dlk1 +/p
F
Testes
% of body weight
0.0
0.2
0.4
0.6
0.8
WT
Dlk1+/p
Grb10m/+
Grb10 m/+ /Dlk1 +/p

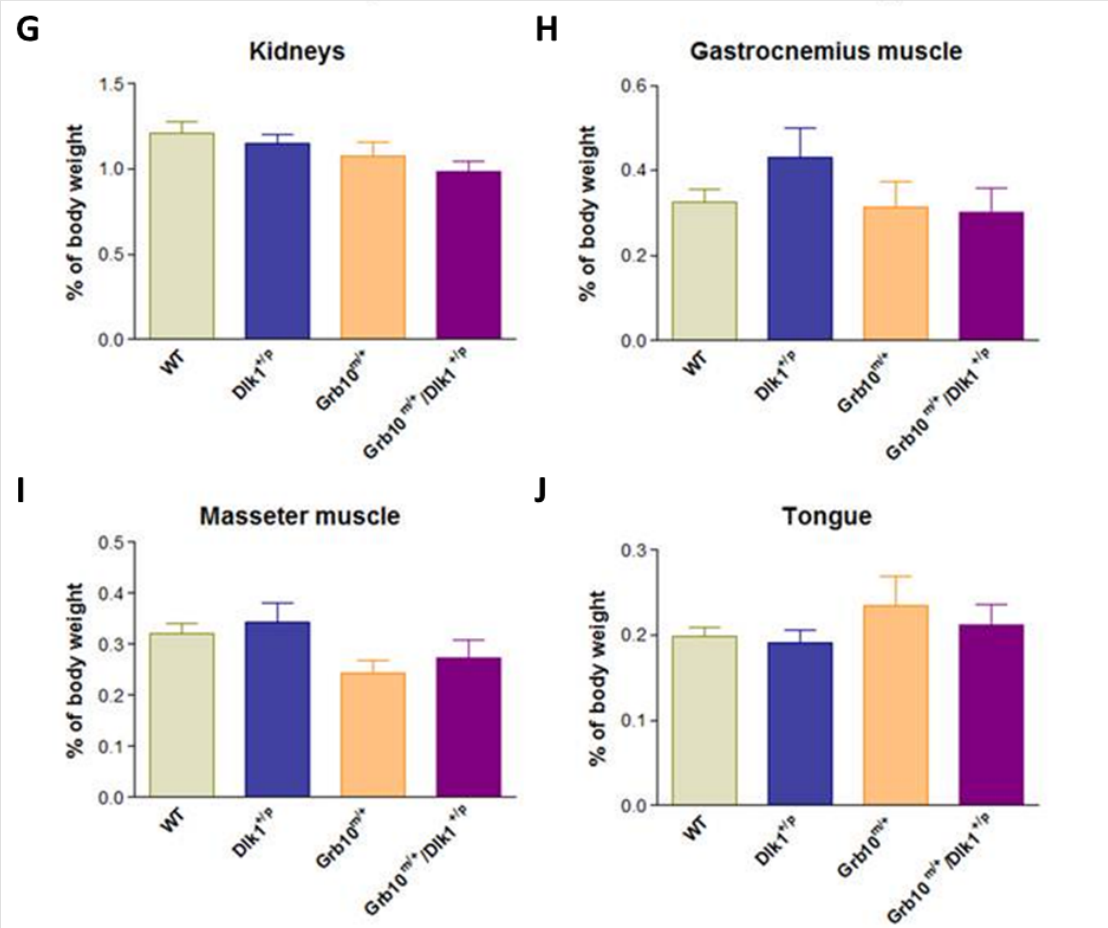

K

	Liver	Pancreas	Brain	Gonadal fat pads	Renal fat pads
WT vs Grb10$^{m/+}$	ns	ns	ns	ns	ns
WT vs Dlk1$^{+/p}$	ns	ns	ns	ns	ns
WT vs Grb10$^{m/+}$/Dlk1$^{+/p}$	ns	ns	ns	ns	ns
Grb10$^{m/+}$ vs Dlk1$^{+/p}$	*	ns	ns	ns	ns
Grb10$^{m/+}$ vs Grb10$^{m/+}$/Dlk1$^{+/p}$	ns	ns	ns	ns	ns
Dlk1$^{+/p}$ vs Grb10$^{m/+}$/Dlk1$^{+/p}$	*	**	ns	ns	ns

	Testes	Kidneys	Gastrocnemius muscle	Masseter muscle	Tongue
WT vs Grb10$^{m/+}$	ns	ns	ns	ns	ns
WT vs Dlk1$^{+/p}$	ns	ns	ns	ns	ns
WT vs Grb10$^{m/+}$/Dlk1$^{+/p}$	ns	ns	ns	ns	ns
Grb10$^{m/+}$ vs Dlk1$^{+/p}$	ns	ns	ns	ns	ns
Grb10$^{m/+}$ vs Grb10$^{m/+}$/Dlk1$^{+/p}$	ns	ns	ns	ns	ns
Dlk1$^{+/p}$ vs Grb10$^{m/+}$/Dlk1$^{+/p}$	ns	ns	ns	ns	ns

Figure 4.10 Proportionate weight analysis of 3-6 month old male wild type, *Dlk1*$^{+/p}$, *Grb10*$^{m/+}$ and *Grb10*$^{m/+}$*/Dlk1*$^{+/p}$ mice.

Weights of whole animals and selected organs were recorded and organ weights expressed as a percentage of total body weights. No significant differences were found in weights of **C)** brains, **D)** gonadal fat pads, **E)** renal fat pads, **F)** testes, **G)** kidneys, **H)** gastrocnemius muscles, **I)** masseter muscles and **J)** tongues. **A)** Both *Grb10*$^{m/+}$ and *Grb10*$^{m/+}$*/Dlk1*$^{+/p}$ mice exhibited a significant decrease in relative liver weights (*$p<0.05$) when compared to *Dlk1*$^{+/p}$ mice. **B)** Significantly elevated relative pancreas mass was noted in *Grb10*$^{m/+}$*/Dlk1*$^{+/p}$ animals which was statistically different to *Dlk1*$^{+/p}$ (**$p<0.01$). **K)** Tables summarising results of statistical analysis. All values represent means ± SEM, analysed by one way ANOVA with post hoc Tukey's analysis. WT n=7, *Dlk1*$^{+/p}$=6, *Grb10*$^{m/+}$ n=6 and *Grb10*$^{m/+}$*/Dlk1*$^{+/p}$ n=6.

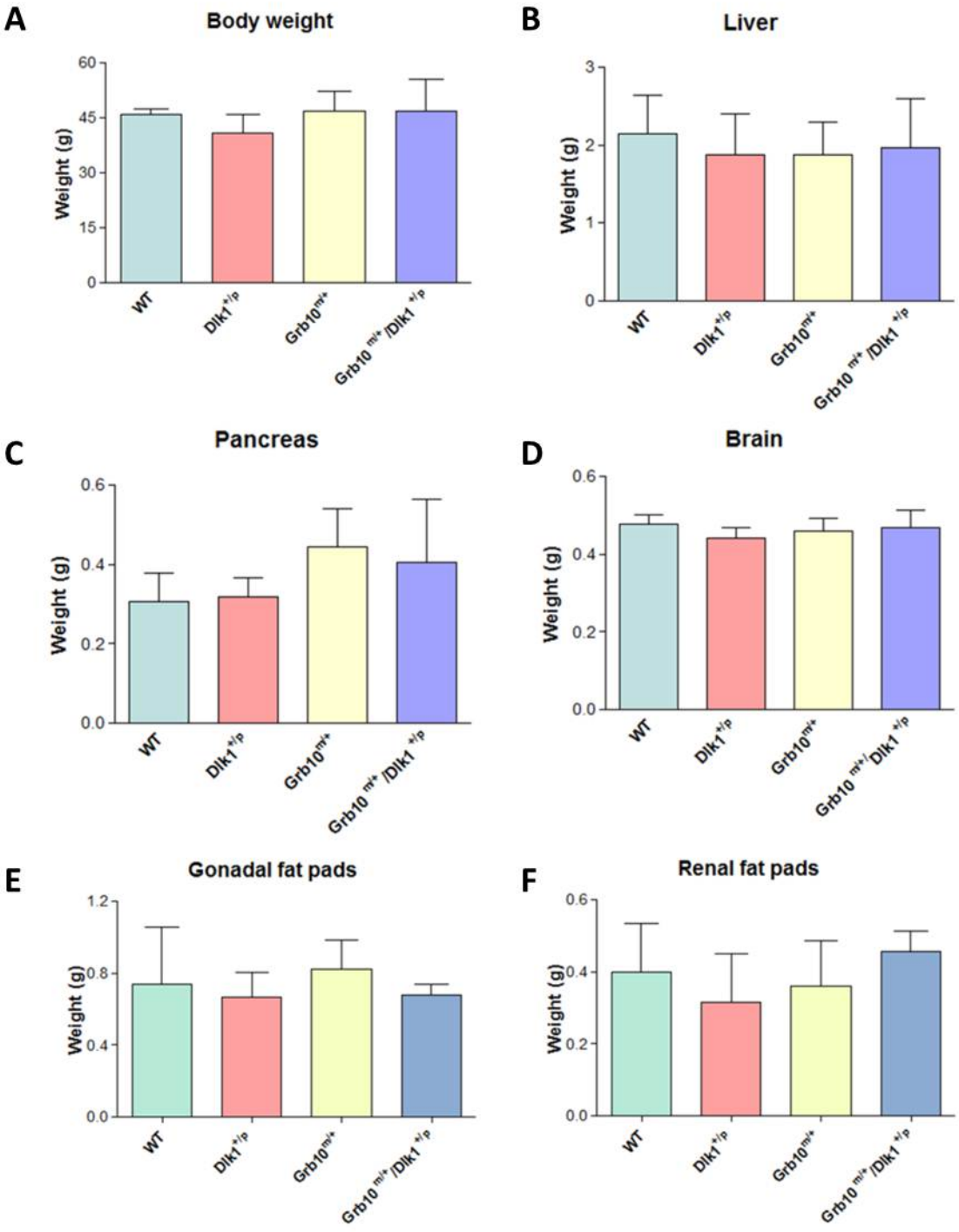
A
Body weight
Weight (g)
60
45
30
15
0
WT
Dlk1+/p
Grb10m+
Grb10 m+ /Dlk1 +/p
B
Liver
Weight (g)
3
2
1
0
WT
Dlk1+/p
Grb10m+
Grb10 m+ /Dlk1 +/p
C
Pancreas
Weight (g)
0.6
0.4
0.2
0.0
WT
Dlk1+/p
Grb10m+
Grb10 m+ /Dlk1 +/p
D
Brain
Weight (g)
0.6
0.4
0.2
0.0
WT
Dlk1+/p
Grb10m+
Grb10 m+/Dlk1 +/p
E
Gonadal fat pads
Weight (g)
1.2
0.8
0.4
0.0
WT
Dlk1+/p
Grb10m+
Grb10 m+ /Dlk1 +/p
F
Renal fat pads
Weight (g)
0.6
0.4
0.2
0.0
WT
Dlk1+/p
Grb10m+
Grb10 m+ /Dlk1 +/p

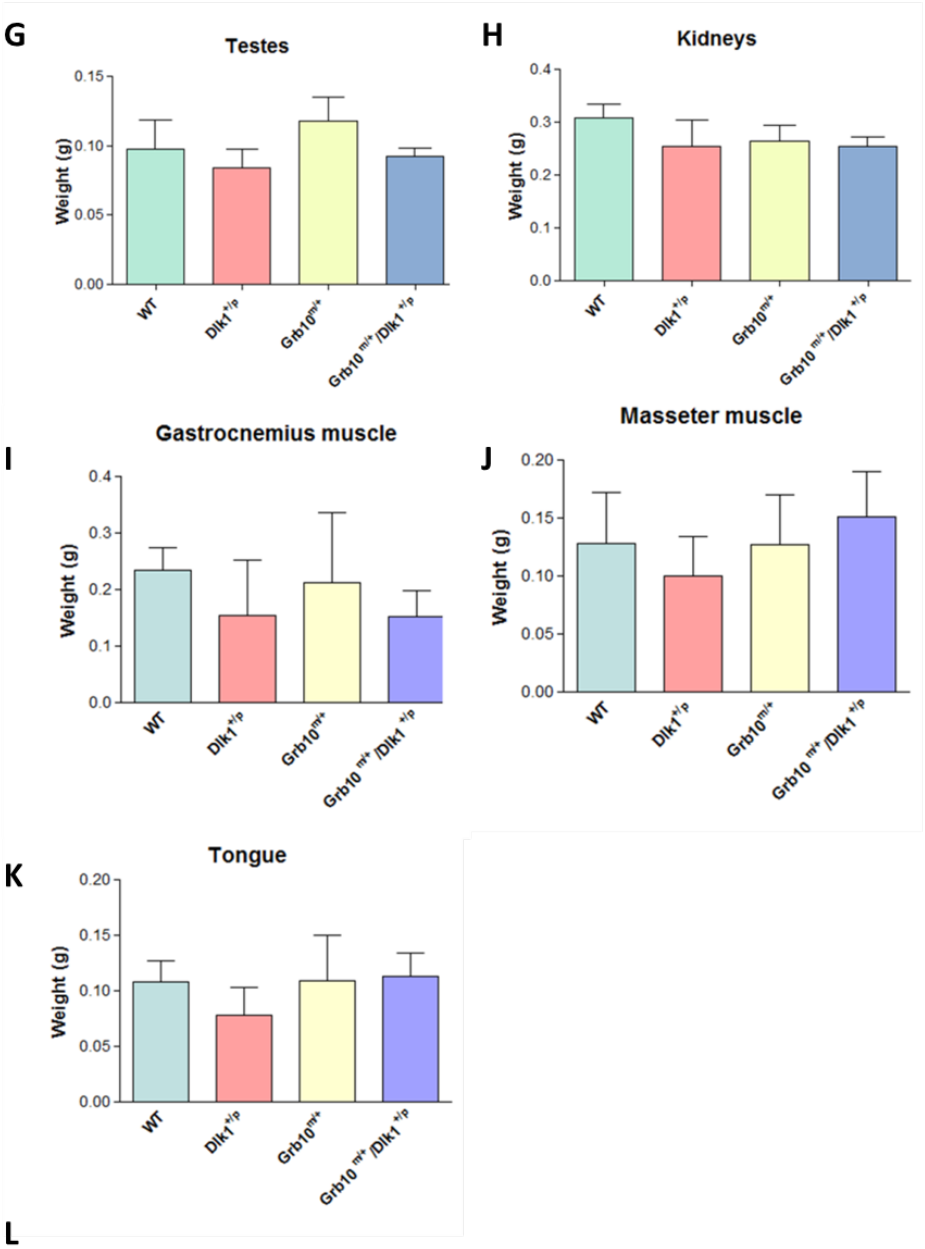

L

	Body weight	Liver	Pancreas	Brain	Gonadal fat pads	Renal fat pads
WT vs Grb10$^{m/+}$	ns	ns	ns	ns	ns	ns
WT vs Dlk1$^{+/p}$	ns	ns	ns	ns	ns	ns
WT vs Grb10$^{m/+}$/Dlk1$^{+/p}$	ns	ns	ns	ns	ns	ns
Grb10$^{m/+}$ vs Dlk1$^{+/p}$	ns	ns	ns	ns	ns	ns
Grb10$^{m/+}$ vs Grb10$^{m/+}$/Dlk1$^{+/p}$	ns	ns	ns	ns	ns	ns
Dlk1$^{+/p}$ vs Grb10$^{m/+}$/Dlk1$^{+/p}$	ns	ns	ns	ns	ns	ns

	Testes	Kidneys	Gastrocnemius muscle	Masseter muscle	Tongue
WT vs Grb10$^{m/+}$	*	*	ns	ns	ns
WT vs Dlk1$^{+/p}$	ns	ns	ns	ns	ns
WT vs Grb10$^{m/+}$/Dlk1$^{+/p}$	ns	*	ns	ns	ns
Grb10$^{m/+}$ vs Dlk1$^{+/p}$	***	Ns	ns	ns	ns
Grb10$^{m/+}$ vs Grb10$^{m/+}$/Dlk1$^{+/p}$	ns	Ns	ns	ns	ns
Dlk1$^{+/p}$ vs Grb10$^{m/+}$/Dlk1$^{+/p}$	ns	Ns	ns	ns	ns

Figure 4.11 Weight analysis of 7-9 month old male wild type, *Dlk1*$^{+/p}$, *Grb10*$^{m/+}$ and *Grb10*$^{m/+}$*/Dlk1*$^{+/p}$ mice.

Weights of whole animals and selected organs were recorded. No significant differences were found in **A)** total body weights and weights of **B)** livers, **C)** pancreata, **D)** brains, **E)** gonadal fat pads, **F)** renal fat pads, **I)** gastrocnemius muscles, **J)** masseter muscles and **K)** tongues. **G)** Significantly enlarged testes were observed in *Grb10*$^{m/+}$ mice when compared to wild type (*p<0.05) and *Dlk1*$^{+/p}$ (***p<0.001) animals. **H)** Kidney weights were significantly reduced in *Grb10*$^{m/+}$ and *Grb10*$^{m/+}$*/Dlk1*$^{+/p}$ mice in comparison to wild type controls (*p<0.05). **L)** Tables summarising results of statistical analysis. All values represent means ± SEM, analysed by one way ANOVA with post hoc Tukey's analysis. WT n=7, *Dlk1*$^{+/p}$=6, *Grb10*$^{m/+}$ n=6 and *Grb10*$^{m/+}$*/Dlk1*$^{+/p}$ n=6.

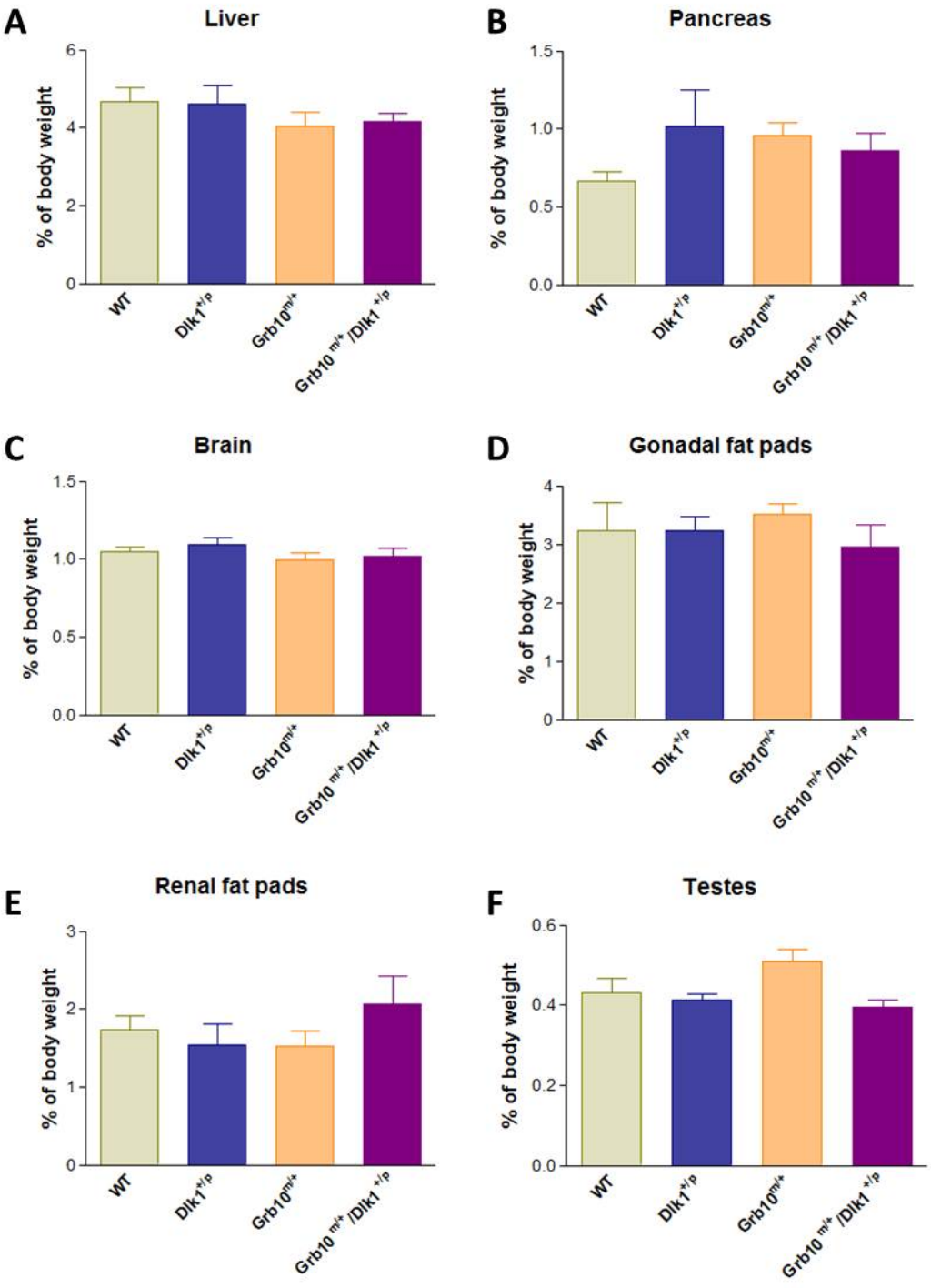
A
Liver
% of body weight
6
4
2
0
WT
Dlk1+/p
Grb10m/+
Grb10 m/+ /Dlk1 +/p
B
Pancreas
% of body weight
1.5
1.0
0.5
0.0
WT
Dlk1+/p
Grb10m/+
Grb10 m/+ /Dlk1 +/p
C
Brain
% of body weight
1.5
1.0
0.5
0.0
WT
Dlk1+/p
Grb10m/+
Grb10 m/+ /Dlk1 +/p
D
Gonadal fat pads
% of body weight
4
3
2
1
0
WT
Dlk1+/p
Grb10m/+
Grb10 m/+ /Dlk1 +/p
E
Renal fat pads
% of body weight
3
2
1
0
WT
Dlk1+/p
Grb10m/+
Grb10 m/+ /Dlk1 +/p
F
Testes
% of body weight
0.6
0.4
0.2
0.0
WT
Dlk1+/p
Grb10m/+
Grb10 m/+ /Dlk1 +/p

G

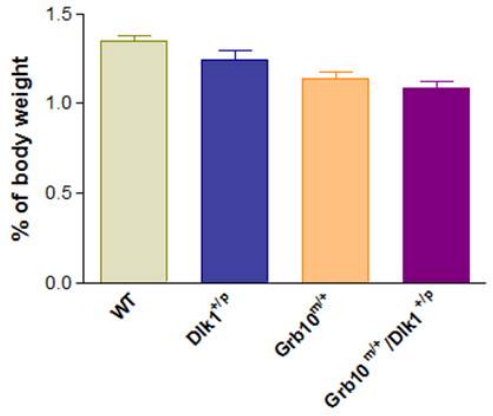

H

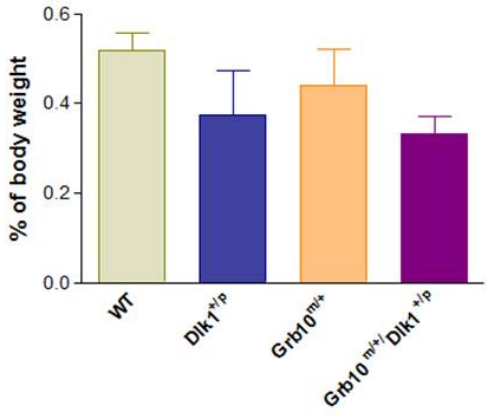

I

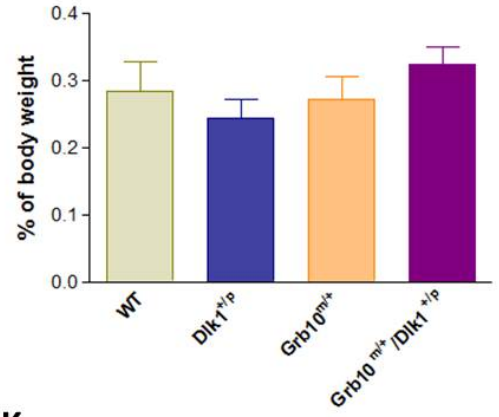

J

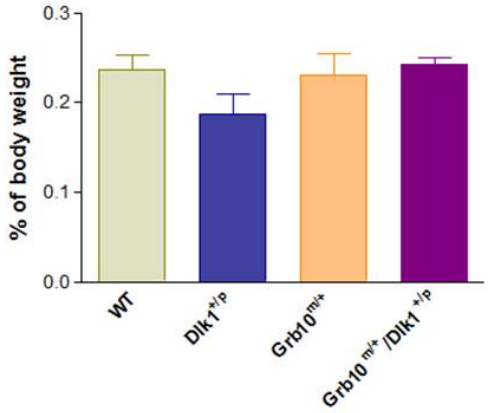

K

	Liver	Pancreas	Brain	Gonadal fat pads	Renal fat pads
WT vs Grb10$^{m/+}$	ns	ns	ns	ns	ns
WT vs Dlk1$^{+/p}$	ns	ns	ns	ns	ns
WT vs Grb10$^{m/+}$/Dlk1$^{+/p}$	ns	ns	ns	ns	ns
Grb10$^{m/+}$ vs Dlk1$^{+/p}$	ns	ns	ns	ns	ns
Grb10$^{m/+}$ vs Grb10$^{m/+}$/Dlk1$^{+/p}$	ns	ns	ns	ns	ns
Dlk1$^{+/p}$ vs Grb10$^{m/+}$/Dlk1$^{+/p}$	ns	ns	ns	ns	ns

	Testes	Kidneys	Gastrocnemius muscle	Masseter muscle	Tongue
WT vs Grb10$^{m/+}$	ns	**	ns	ns	ns
WT vs Dlk1$^{+/p}$	ns	ns	ns	ns	ns
WT vs Grb10$^{m/+}$/Dlk1$^{+/p}$	ns	***	ns	ns	ns
Grb10$^{m/+}$ vs Dlk1$^{+/p}$	ns	ns	ns	ns	ns
Grb10$^{m/+}$ vs Grb10$^{m/+}$/Dlk1$^{+/p}$	ns	ns	ns	ns	ns
Dlk1$^{+/p}$ vs Grb10$^{m/+}$/Dlk1$^{+/p}$	ns	ns	ns	ns	ns

Figure 4.12 Proportionate weight analysis of 7-9 month old male wild type, *Dlk1*$^{+/p}$, *Grb10*$^{m/+}$ and *Grb10*$^{m/+}$*/Dlk1*$^{+/p}$ mice.

Weights of whole animals and selected organs were recorded and organ weights expressed as percentage of total body weights. No significant differences were found in weights of **A)** livers, **B)** pancreata, **C)** brains, **D)** gonadal fat pads, **E)** renal fat pads, **F)** testes, **H)** gastrocnemius muscles **I)** masseter muscles and **J)** tongues. **G)** *Grb10*$^{m/+}$ and *Grb10*$^{m/+}$*/Dlk1*$^{+/p}$ mice exhibited a significant decrease in kidney weights compared to wild type animals (**p<0.01 and ***p<0.001, respectively). **K)** Tables summarising results of statistical analysis. All values represent means ± SEM, analysed by one way ANOVA with post hoc Tukey's analysis. WT n=7, *Dlk1*$^{+/p}$=6, *Grb10*$^{m/+}$ n=6 and *Grb10*$^{m/+}$*/Dlk1*$^{+/p}$ n=6.

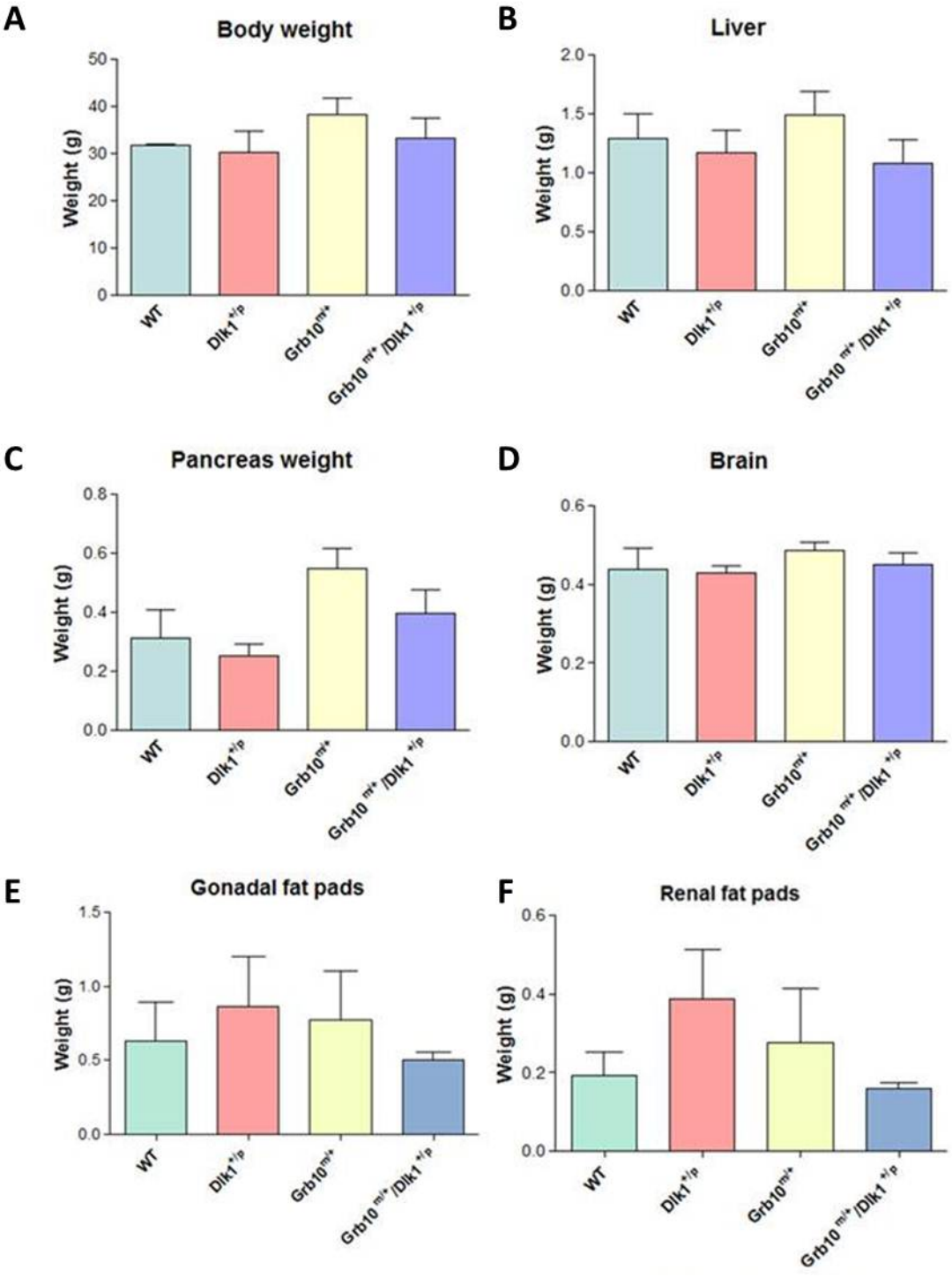
A
Body weight
Weight (g)
50
40
30
20
10
0
WT
Dlk1 +/p
Grb10 m/+
Grb10 m/+ /Dlk1 +/p
B
Liver
Weight (g)
2.0
1.5
1.0
0.5
0.0
WT
Dlk1 +/p
Grb10 m/+
Grb10 m/+ /Dlk1 +/p
C
Pancreas weight
Weight (g)
0.8
0.6
0.4
0.2
0.0
WT
Dlk1 +/p
Grb10 m/+
Grb10 m/+ /Dlk1 +/p
D
Brain
Weight (g)
0.6
0.4
0.2
0.0
WT
Dlk1 +/p
Grb10 m/+
Grb10 m/+ /Dlk1 +/p
E
Gonadal fat pads
Weight (g)
1.5
1.0
0.5
0.0
WT
Dlk1 +/p
Grb10 m/+
Grb10 m/+ /Dlk1 +/p
F
Renal fat pads
Weight (g)
0.6
0.4
0.2
0.0
WT
Dlk1 +/p
Grb10 m/+
Grb10 m/+ /Dlk1 +/p

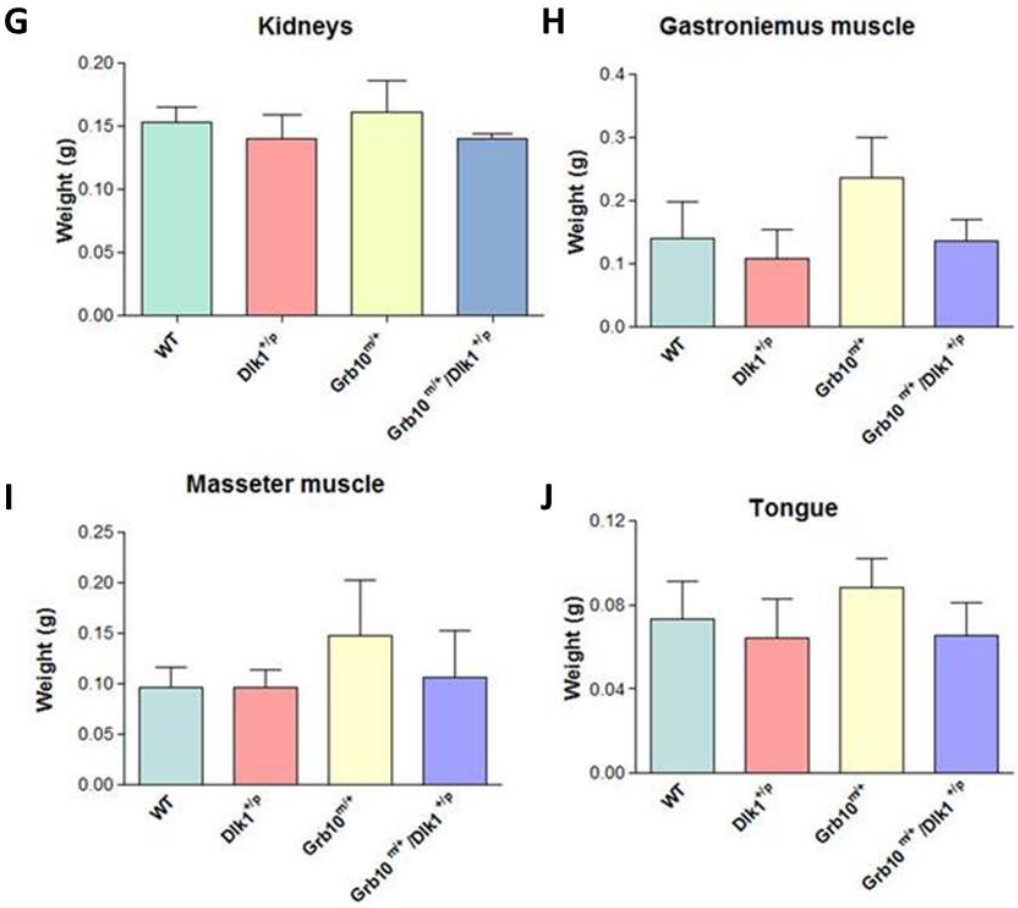

K

	Body weight	Liver	Pancreas	Brain	Gonadal fat pads	Renal fat pads
WT vs Grb10$^{m/+}$	*	ns	***	ns	ns	ns
WT vs Dlk1$^{+/p}$	ns	ns	ns	ns	ns	***
WT vs Grb10$^{m/+}$/Dlk1$^{+/p}$	ns	ns	**	ns	ns	ns
Grb10$^{m/+}$ vs Dlk1$^{+/p}$	**	ns	***	ns	ns	***
Grb10$^{m/+}$ vs Grb10$^{m/+}$/Dlk1$^{+/p}$	ns	ns	ns	ns	ns	ns
Dlk1$^{+/p}$ vs Grb10$^{m/+}$/Dlk1$^{+/p}$	ns	ns	***	ns	*	***

	Kidneys	Gastrocnemius muscle	Masseter muscle	Tongue
WT vs Grb10$^{m/+}$	ns	*	ns	ns
WT vs Dlk1$^{+/p}$	ns	ns	ns	ns
WT vs Grb10$^{m/+}$/Dlk1$^{+/p}$	ns	ns	ns	ns
Grb10$^{m/+}$ vs Dlk1$^{+/p}$	ns	**	ns	ns
Grb10$^{m/+}$ vs Grb10$^{m/+}$/Dlk1$^{+/p}$	ns	ns	ns	ns
Dlk1$^{+/p}$ vs Grb10$^{m/+}$/Dlk1$^{+/p}$	ns	ns	ns	ns

Figure 4.13 Weight analysis of 3-6 month old female wild type, *Dlk1*$^{+/p}$, *Grb10*$^{m/+}$ and *Grb10*$^{m/+}$*/Dlk1*$^{+/p}$ mice.

Weights of whole animals and selected organs were recorded. **A)** Analysis of total body weights revealed that *Grb10*$^{m/+}$ animals were significantly larger than wild type (*p<0.05) and *Dlk1*$^{+/p}$ (**p<0.01) mice. No significant differences were found in weights of: **B)** livers, **D)** brains, **G)** kidneys, **I)** masseter muscles and **J)** tongues. **C)** *Grb10*$^{m/+}$ animals exhibited increased pancreas weights when compared to wild type (***p<0.001) and *Dlk1*$^{+/p}$ (***p<0.001) animals; significantly overgrown pancreata were also found in *Grb10*$^{m/+}$*/Dlk1*$^{+/p}$ mice when compared to wild type (**p<0.01) and *Dlk1*$^{+/p}$ (***p<0.001) animals. **E)** Significantly smaller gonadal fat pads were noted in *Grb10*$^{m/+}$*/Dlk1*$^{+/p}$ mice compared to *Dlk1*$^{+/p}$ (*p<0.05). **F)** *Dlk1*$^{+/p}$ animals had elevated renal fat pad mass when compared to all other genotypes (***p<0.001). **H)** *Grb10*$^{m/+}$ displayed significant increase in gastrocnemius muscle mass when compared to wild type (*p<0.05) and *Dlk1*$^{+/p}$ (**p<0.01) mice. **K)** Tables summarising results of statistical analysis. All values represent means ± SEM, analysed by one way ANOVA with post hoc Tukey's analysis. WT n=7, *Dlk1*$^{+/p}$=6, *Grb10*$^{m/+}$ n=6 and *Grb10*$^{m/+}$*/Dlk1*$^{+/p}$ n=7.

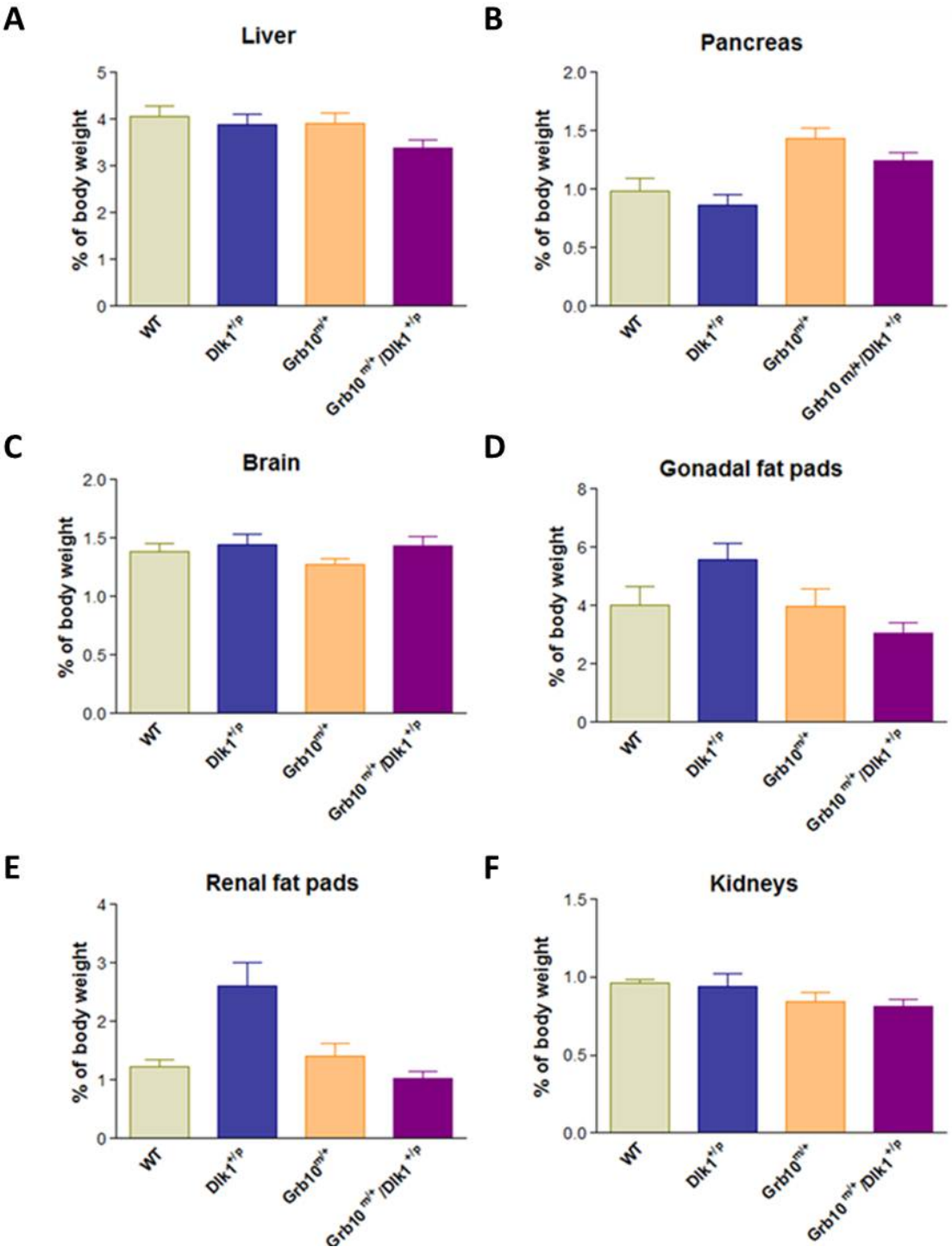
A
Liver
% of body weight
0
1
2
3
4
5
WT
Dlk1+/p
Grb10m/+
Grb10 m/+/Dlk1 +/p
B
Pancreas
% of body weight
0.0
0.5
1.0
1.5
2.0
WT
Dlk1+/p
Grb10m/+
Grb10 m/+/Dlk1 +/p
C
Brain
% of body weight
0.0
0.5
1.0
1.5
2.0
WT
Dlk1+/p
Grb10m/+
Grb10 m/+ /Dlk1 +/p
D
Gonadal fat pads
% of body weight
0
2
4
6
8
WT
Dlk1+/p
Grb10m/+
Grb10 m/+ /Dlk1 +/p
E
Renal fat pads
% of body weight
0
1
2
3
4
WT
Dlk1+/p
Grb10m/+
Grb10 m/+ /Dlk1 +/p
F
Kidneys
% of body weight
0.0
0.5
1.0
1.5
WT
Dlk1+/p
Grb10m/+
Grb10 m/+ /Dlk1 +/p

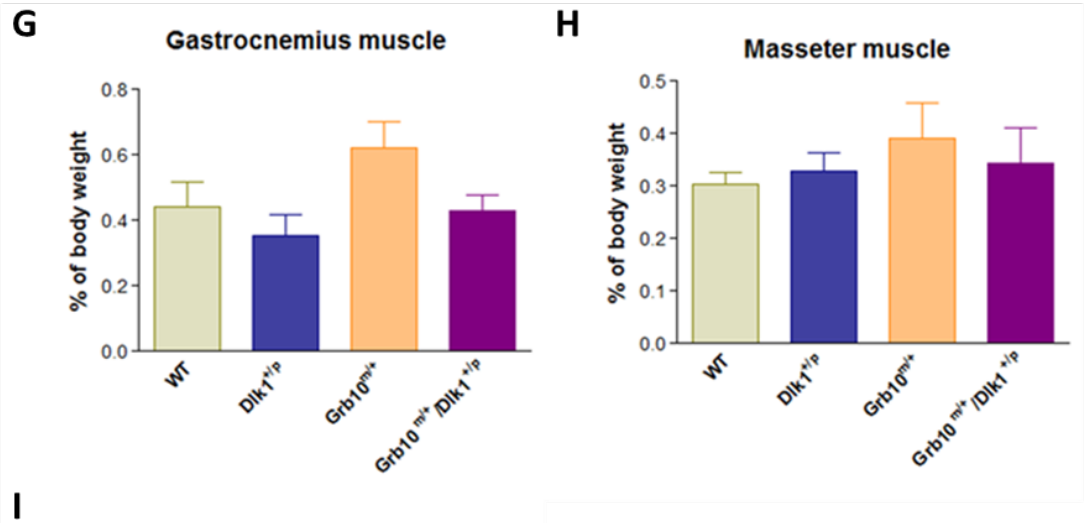

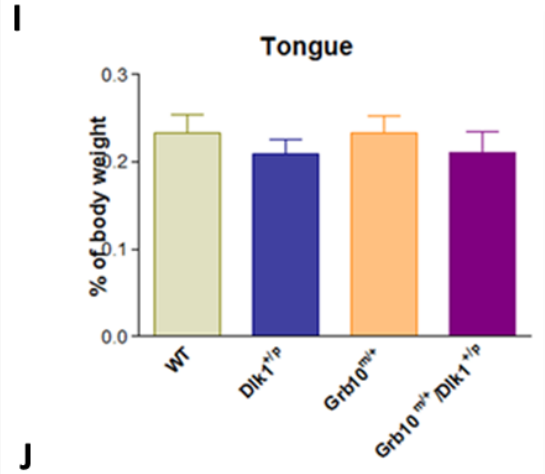

J

	Liver	Pancreas	Brain	Gonadal fat pads	Renal fat pads
WT vs Grb10$^{m/+}$	ns	*	ns	ns	ns
WT vs Dlk1$^{+/p}$	ns	ns	ns	ns	**
WT vs Grb10$^{m/+}$/Dlk1$^{+/p}$	ns	ns	ns	ns	ns
Grb10$^{m/+}$ vs Dlk1$^{+/p}$	ns	**	ns	ns	*
Grb10$^{m/+}$ vs Grb10$^{m/+}$/Dlk1$^{+/p}$	ns	ns	ns	ns	ns
Dlk1$^{+/p}$ vs Grb10$^{m/+}$/Dlk1$^{+/p}$	ns	*	ns	*	***

	Kidneys	Gastrocnemius muscle	Masseter muscle	Tongue
WT vs Grb10$^{m/+}$	ns	ns	ns	ns
WT vs Dlk1$^{+/p}$	ns	ns	ns	ns
WT vs Grb10$^{m/+}$/Dlk1$^{+/p}$	ns	ns	ns	ns
Grb10$^{m/+}$ vs Dlk1$^{+/p}$	ns	ns	ns	ns
Grb10$^{m/+}$ vs Grb10$^{m/+}$/Dlk1$^{+/p}$	ns	ns	ns	ns
Dlk1$^{+/p}$ vs Grb10$^{m/+}$/Dlk1$^{+/p}$	ns	ns	ns	ns

Figure 4.14 Proportionate weight analysis of 3-6 month old female wild type, *Dlk1*$^{+/p}$, *Grb10*$^{m/+}$ and *Grb10*$^{m/+}$*/Dlk1*$^{+/p}$ mice.

Weights of whole animals and selected organs were recorded and organ weights expressed as percentage of total body weights. No significant differences were found in weights of **A)** livers, **C)** brains, **F)** kidneys, **G)** gastrocnemius muscles, **H)** masseter muscles and **I)** tongues; **B)** *Grb10*$^{m/+}$ and *Grb10*$^{m/+}$*/Dlk1*$^{+/p}$ mice displayed significantly elevated pancreas mass (**p<0.01 for *Grb10*$^{m/+}$ and *p<0.05 for *Grb10*$^{m/+}$*/Dlk1*$^{+/p}$) when compared to *Dlk1*$^{+/p}$ mice. **D)** Significant decrease in gonadal fat pad mass was noted in *Grb10*$^{m/+}$*/Dlk1*$^{+/p}$ animals compared to *Dlk1*$^{+/p}$ (*p<0.05). **E)** Renal fat pads of *Dlk1*$^{+/p}$ animals were enlarged and statistically different to wild type (**p<0.01) whereas renal fat pads of *Grb10*$^{m/+}$ (*p<0.05) and *Grb10*$^{m/+}$*/Dlk1*$^{+/p}$ (***p<0.001) mice were significantly smaller when compared to those of *Dlk1*$^{+/p}$. **J)** Tables summarising results of statistical analysis. All values represent means ± SEM, analysed by one way ANOVA with post hoc Tukey's analysis. WT n=7, *Dlk1*$^{+/p}$=6, *Grb10*$^{m/+}$ n=6 and *Grb10*$^{m/+}$*/Dlk1*$^{+/p}$ n=7.

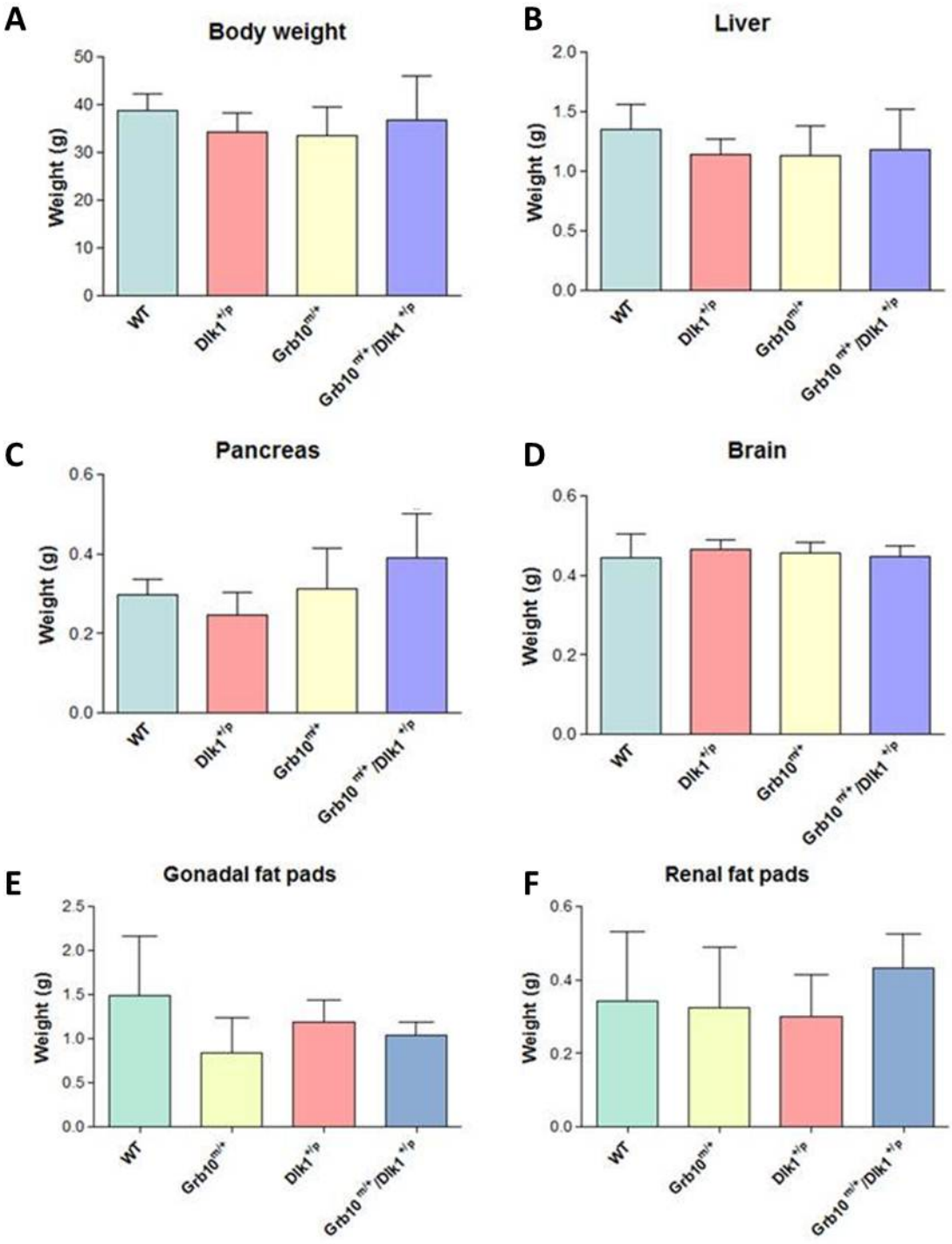
A
Body weight
Weight (g)
50
40
30
20
10
0
WT
Dlk1 +/p
Grb10 m/+
Grb10 m/+ /Dlk1 +/p
B
Liver
Weight (g)
2.0
1.5
1.0
0.5
0.0
WT
Dlk1 +/p
Grb10 m/+
Grb10 m/+ /Dlk1 +/p
C
Pancreas
Weight (g)
0.6
0.4
0.2
0.0
WT
Dlk1 +/p
Grb10 m/+
Grb10 m/+ /Dlk1 +/p
D
Brain
Weight (g)
0.6
0.4
0.2
0.0
WT
Dlk1 +/p
Grb10 m/+
Grb10 m/+ /Dlk1 +/p
E
Gonadal fat pads
Weight (g)
2.5
2.0
1.5
1.0
0.5
0.0
WT
Grb10 m/+
Dlk1 +/p
Grb10 m/+ /Dlk1 +/p
F
Renal fat pads
Weight (g)
0.6
0.4
0.2
0.0
WT
Grb10 m/+
Dlk1 +/p
Grb10 m/+ /Dlk1 +/p

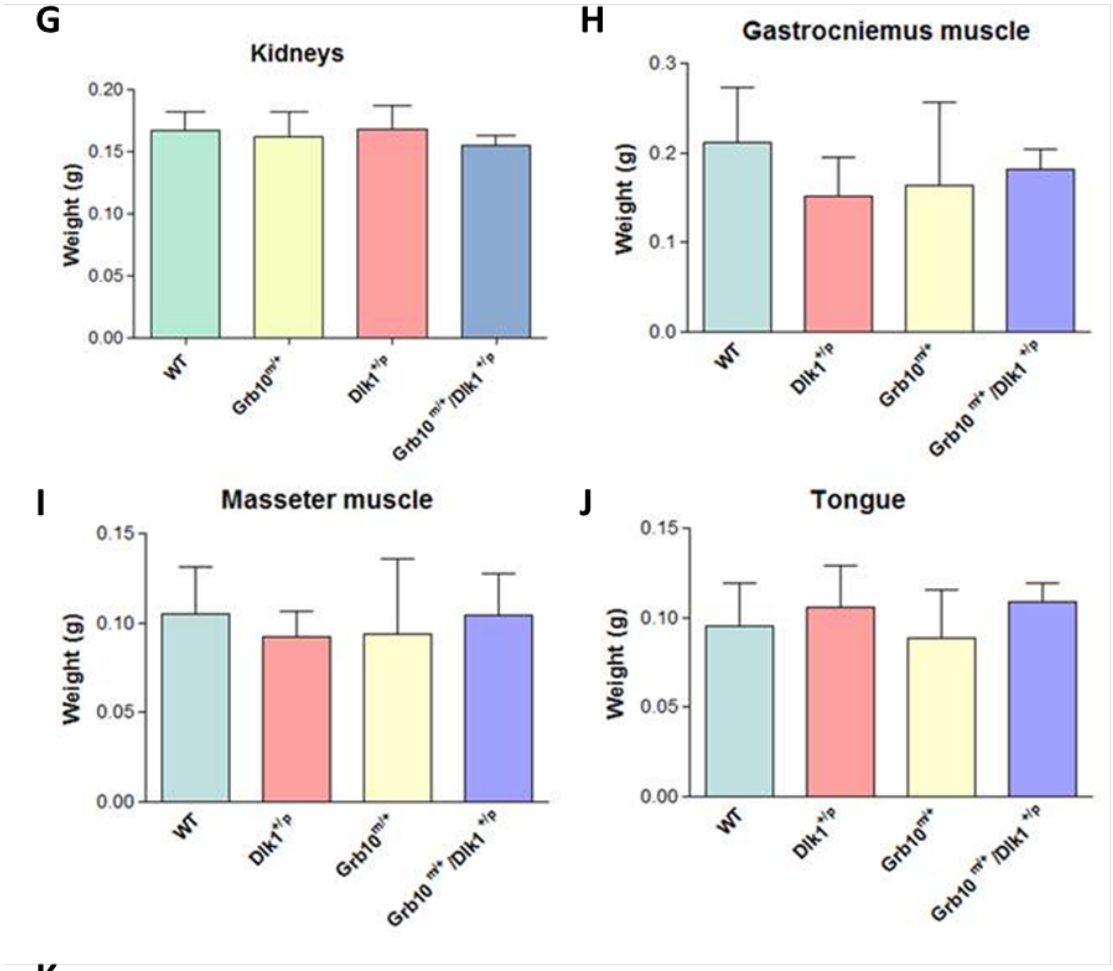

K

	Body weight	Liver	Pancreas	Brain	Gonadal fat pads	Renal fat pads
WT vs Grb10$^{m/+}$	ns	ns	ns	ns	**	ns
WT vs Dlk1$^{+/p}$	ns	ns	ns	ns	ns	ns
WT vs Grb10$^{m/+}$/Dlk1$^{+/p}$	ns	ns	ns	ns	ns	ns
Grb10$^{m/+}$ vs Dlk1$^{+/p}$	ns	ns	ns	ns	ns	ns
Grb10$^{m/+}$ vs Grb10$^{m/+}$/Dlk1$^{+/p}$	ns	ns	ns	ns	ns	ns
Dlk1$^{+/p}$ vs Grb10$^{m/+}$/Dlk1$^{+/p}$	ns	ns	*	ns	ns	ns

	Kidneys	Gastrocnemius muscle	Masseter muscle	Tongue
WT vs Grb10$^{m/+}$	ns	ns	ns	ns
WT vs Dlk1$^{+/p}$	ns	ns	ns	ns
WT vs Grb10$^{m/+}$/Dlk1$^{+/p}$	ns	ns	ns	ns
Grb10$^{m/+}$ vs Dlk1$^{+/p}$	ns	ns	ns	ns
Grb10$^{m/+}$ vs Grb10$^{m/+}$/Dlk1$^{+/p}$	ns	ns	ns	ns
Dlk1$^{+/p}$ vs Grb10$^{m/+}$/Dlk1$^{+/p}$	ns	ns	ns	ns

Figure 4.15 Weight analysis of 7-9 month old female wild type, *Dlk1*$^{+/p}$, *Grb10*$^{m/+}$ and *Grb10*$^{m/+}$*/Dlk1*$^{+/p}$ mice.

Weights of whole animals and selected organs were recorded. No significant differences were found in **A)** total body weights and weights of **B)** livers, **D)** brains, **F)** renal fat pads, **G)** kidneys, **H)** gastrocnemius muscles, **I)** masseter muscles and **J)** tongues. **C)** *Grb10*$^{m/+}$*/Dlk1*$^{+/p}$ pancreata were significantly larger when compared to *Dlk1*$^{+/p}$ (*p<0.05). **E)** *Grb10*$^{m/+}$ mice had significantly smaller gonadal fat pads in comparison to wild type animals (**p<0.01). **K)** Tables summarising results of statistical analysis. All values represent means ± SEM, analysed by one way ANOVA with post hoc Tukey's analysis. WT n=6, *Dlk1*$^{+/p}$=6, *Grb10*$^{m/+}$ n=6 and *Grb10*$^{m/+}$*/Dlk1*$^{+/p}$ n=5.

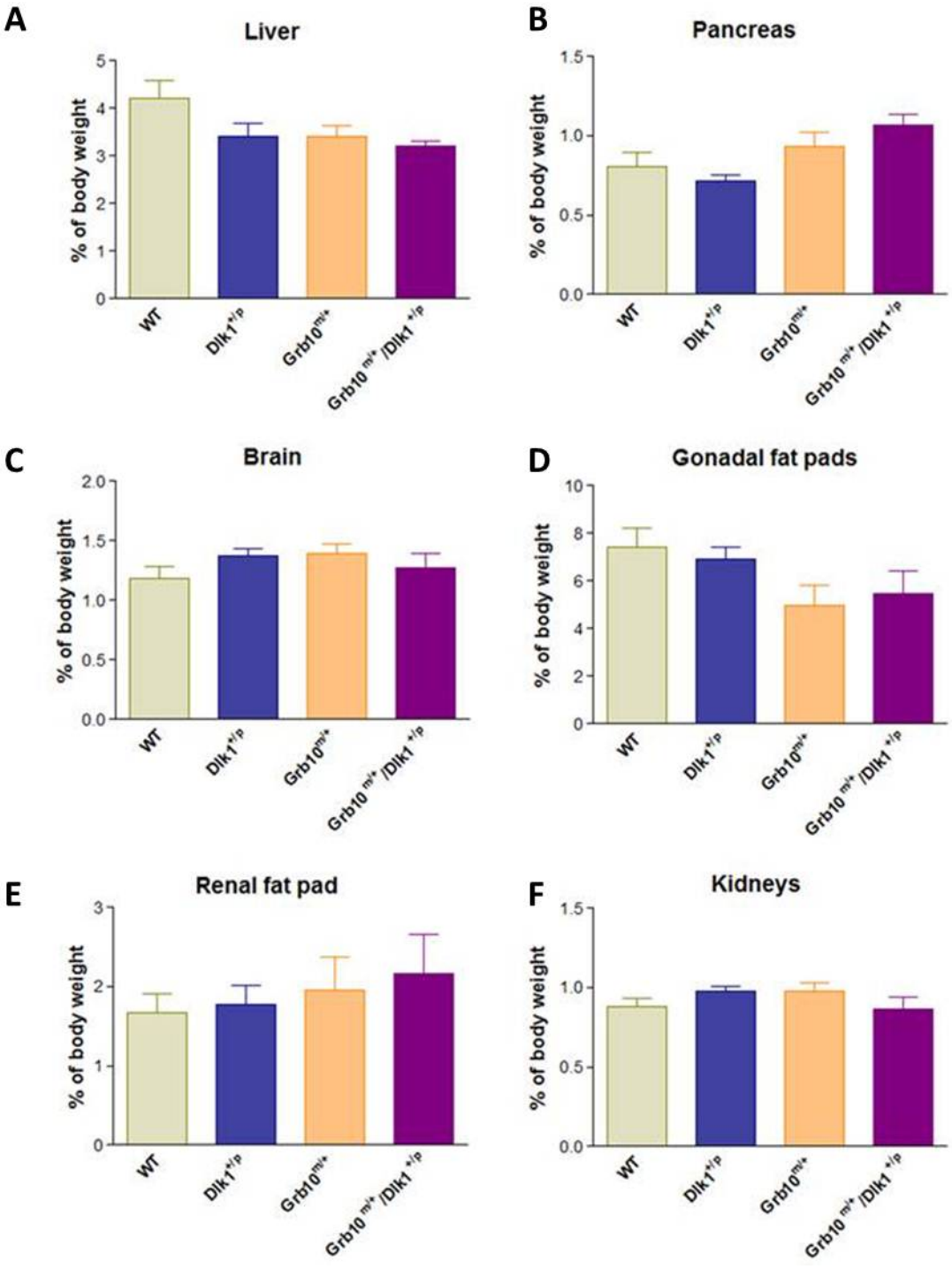
A
Liver
% of body weight
5
4
3
2
1
0
WT
Dlk1+/p
Grb10m/+
Grb10 m/+ /Dlk1 +/p
B
Pancreas
% of body weight
1.5
1.0
0.5
0.0
WT
Dlk1+/p
Grb10m/+
Grb10 m/+ /Dlk1 +/p
C
Brain
% of body weight
2.0
1.5
1.0
0.5
0.0
WT
Dlk1+/p
Grb10m/+
Grb10 m/+ /Dlk1 +/p
D
Gonadal fat pads
% of body weight
10
8
6
4
2
0
WT
Dlk1+/p
Grb10m/+
Grb10 m/+ /Dlk1 +/p
E
Renal fat pad
% of body weight
3
2
1
0
WT
Dlk1+/p
Grb10m/+
Grb10 m/+ /Dlk1 +/p
F
Kidneys
% of body weight
1.5
1.0
0.5
0.0
WT
Dlk1+/p
Grb10m/+
Grb10 m/+ /Dlk1 +/p

G

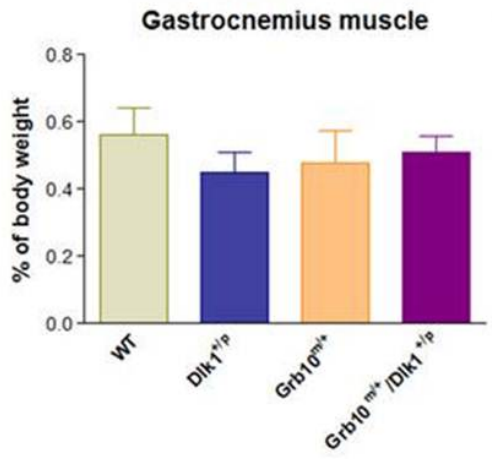

H

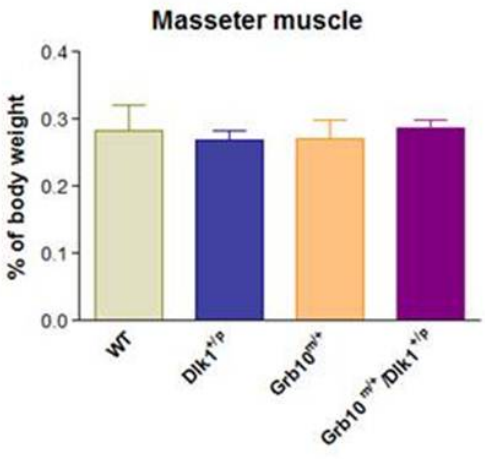

I

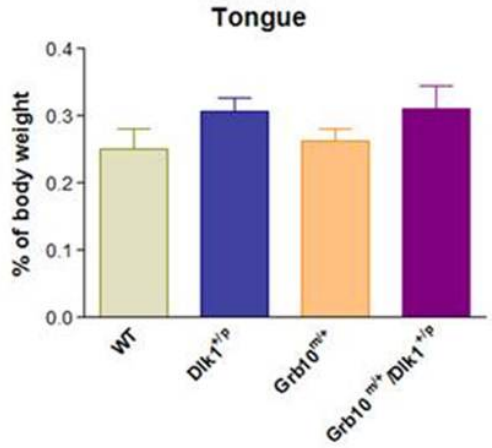

J

	Liver	Pancreas	Brain	Gonadal fat pads	Renal fat pads
WT vs Grb10$^{m/+}$	ns	ns	ns	ns	ns
WT vs Dlk1$^{+/p}$	ns	ns	ns	ns	ns
WT vs Grb10$^{m/+}$/Dlk1$^{+/p}$	ns	ns	ns	ns	ns
Grb10$^{m/+}$ vs Dlk1$^{+/p}$	ns	ns	ns	ns	ns
Grb10$^{m/+}$ vs Grb10$^{m/+}$/Dlk1$^{+/p}$	ns	ns	ns	ns	ns
Dlk1$^{+/p}$ vs Grb10$^{m/+}$/Dlk1$^{+/p}$	ns	*	ns	ns	ns

	Kidneys	Gastrocnemius muscle	Masseter muscle	Tongue
WT vs Grb10$^{m/+}$	ns	ns	ns	ns
WT vs Dlk1$^{+/p}$	ns	ns	ns	ns
WT vs Grb10$^{m/+}$/Dlk1$^{+/p}$	ns	ns	ns	ns
Grb10$^{m/+}$ vs Dlk1$^{+/p}$	ns	ns	ns	ns
Grb10$^{m/+}$ vs Grb10$^{m/+}$/Dlk1$^{+/p}$	ns	ns	ns	ns
Dlk1$^{+/p}$ vs Grb10$^{m/+}$/Dlk1$^{+/p}$	ns	ns	ns	ns

Figure 4.16 Proportionate weight analysis of 7-9 month old female wild type, *Dlk1*$^{+/p}$, *Grb10*$^{m/+}$ and *Grb10*$^{m/+}$*/Dlk1*$^{+/p}$ mice.

Weights of whole animals and internal organs were recorded and organ weights expressed as a percentage of total body weights. No significant differences were found in weights of **A)** livers, **C)** brains, **D)** gonadal fat pads, **E)** renal fat pads, **F)** kidneys, **G)** gastrocnemius muscles, **H)** masseter muscles and **I)** tongues. **B)** *Grb10*$^{m/+}$*/Dlk1*$^{+/p}$ mice had significantly increased pancreas mass (*$p<0.05$) when compared to *Dlk1*$^{+/p}$. **J)** Tables summarising results of statistical analysis. All values represent means ± SEM, analysed by one way ANOVA with post hoc Tukey's analysis. WT n=6, *Dlk1*$^{+/p}$=6, *Grb10*$^{m/+}$ n=6 and *Grb10*$^{m/+}$*/Dlk1*$^{+/p}$ n=5.

4.2.4 Histological and morphometric analyses of *Dlk1*$^{+/p}$, *Grb10*$^{m/+}$ and *Grb10*$^{m/+}$/*Dlk1*$^{+/p}$ mice.

Earlier we made an observation that *Grb10*$^{m/+}$and *Grb10*$^{m/+}$/*Dlk1*$^{+/p}$ neonatal lungs had thicker epithelial walls than wild type and *Dlk1*$^{+/p}$ mice (Section 4.2.1.2), therefore we decided to carry out an investigation whether this effect persisted until adulthood. H&E stained sections of adult lungs revealed no obvious abnormalities between genotypes (**Figure** 4.17) and morphometric study of the adult lungs from all the genotypes (**Figure** 4.18) confirmed that there were essentially no differences in epithelial wall thickness, in contrast to the results seen in neonatal *Grb10*$^{m/+}$and *Grb10*$^{m/+}$/*Dlk1*$^{+/p}$ mice.

The wet weights of neonatal kidneys (presented in Section 4.2.1.1) seemed to be comparable between the genotypes regardless of changes in total body weights. As a result, when presented as relative weights, the weights of kidneys in *Grb10*$^{m/+}$and *Grb10*$^{m/+}$/*Dlk1*$^{+/p}$ mice were significantly decreased. Similarly, we have found several significant weight differences in adult kidneys, especially in *Grb10*$^{m/+}$and *Grb10*$^{m/+}$/*Dlk1*$^{+/p}$ knockout mice (**Figures** 4.9 to 4.16). Previous reports demonstrated *Grb10* kidney expression during early development (Charalambous et al., 2003; Lui et al., 2008), prompting an investigation of the *Grb10* expression in the adult kidneys. Since it has been confirmed that expression of the *LacZ* reporter in *Grb10*$^{m/+}$ mice generally recapitulates the endogenous expression of the *Grb10* gene we performed *LacZ* staining on cryosections from adult kidneys (**Figure** 4.19). By looking at *Grb10*$^{m/+}$and *Grb10*$^{m/+}$/*Dlk1*$^{+/p}$ kidneys, we found that *Grb10* expression was present in the brush borders of proximal tubules. The evident expression of *Grb10* in kidneys, together with the proportional changes of kidney weights according to body weights encouraged us to perform further histological analysis of adult kidneys stained with PAS (**Figure** 4.20). No obvious histological differences were noted between kidneys from mice of the four different genotypes and, additionally, morphometric analysis of glomerulus numbers showed no statistically significant differences (**Figure** 4.21). To gain insight into correct kidney function we analysed the protein content of urine samples from 3 month old male mice and ran them on the SDS-PAGE gel. This analysis did not reveal any unexpected proteins in any of the analysed samples, indicating normal kidney function in mice of all the analysed genotypes, however for this experiment to be more convincing it should be repeated whilst using a positive control and quantification analysis.

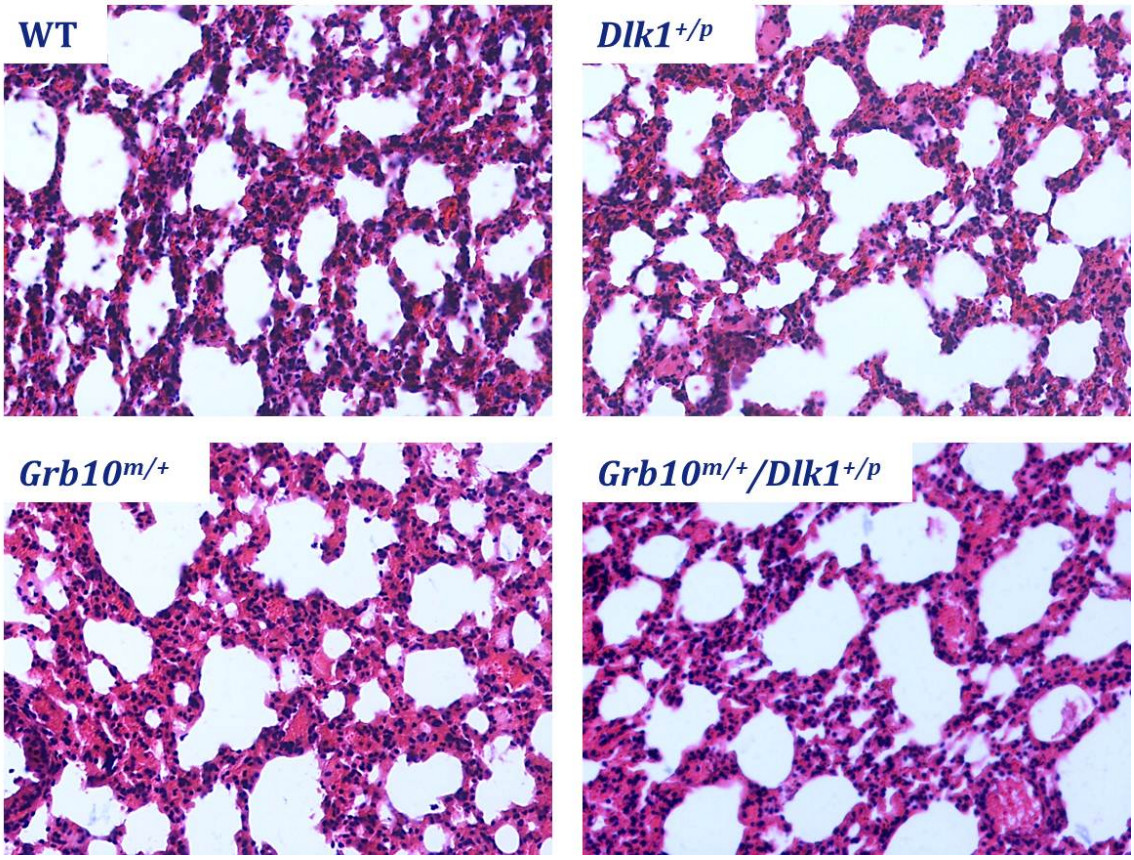

Figure 4.17 H&E stained adult wild type, *Dlk1*$^{+/p}$, *Grb10*$^{m/+}$ and *Grb10*$^{m/+}$/*Dlk1*$^{+/p}$ lungs under 100x magnification.

Histological analysis of lungs from 3 month old male mice revealed no abnormalities in any of the studied genotypes. Presented images show representative sections for each of the analysed genotypes. WT n=5, *Dlk1*$^{+/p}$=5, *Grb10*$^{m/+}$ n=5 and *Grb10*$^{m/+}$/*Dlk1*$^{+/p}$ n=5.

A

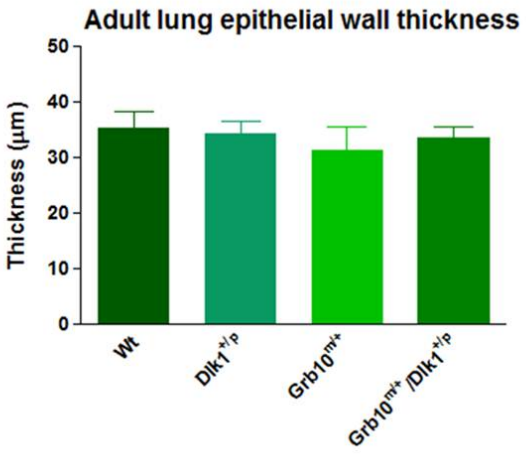

B

	Lung thickness
Wt vs Grb10$^{m/+}$	ns
Wt vs Dlk1$^{+/p}$	ns
Wt vs Grb10$^{m/+}$/Dlk1$^{+/p}$	ns
Grb10$^{m/+}$ vs Dlk1$^{+/p}$	ns
Grb10$^{m/+}$ vs Grb10$^{m/+}$/Dlk1$^{+/p}$	ns
Dlk1$^{+/p}$ vs Grb10$^{m/+}$/Dlk1$^{+/p}$	ns

Figure 4.18 Comparison of epithelial wall thickness in adult wild type, *Dlk1$^{+/p}$*, *Grb10$^{m/+}$* and *Grb10$^{m/+}$/Dlk1$^{+/p}$* mice.

A) Morphometric analysis of adult lung epithelial wall thickness revealed no significant differences for any of the analysed genotypes. **B)** Table summarising results of statistical analysis. All values represent means ± SEM, analysed by one way ANOVA with post hoc Tukey's analysis. WT n=5, *Dlk1$^{+/p}$*=5, *Grb10$^{m/+}$* n=5 and *Grb10$^{m/+}$/Dlk1$^{+/p}$* n=5.

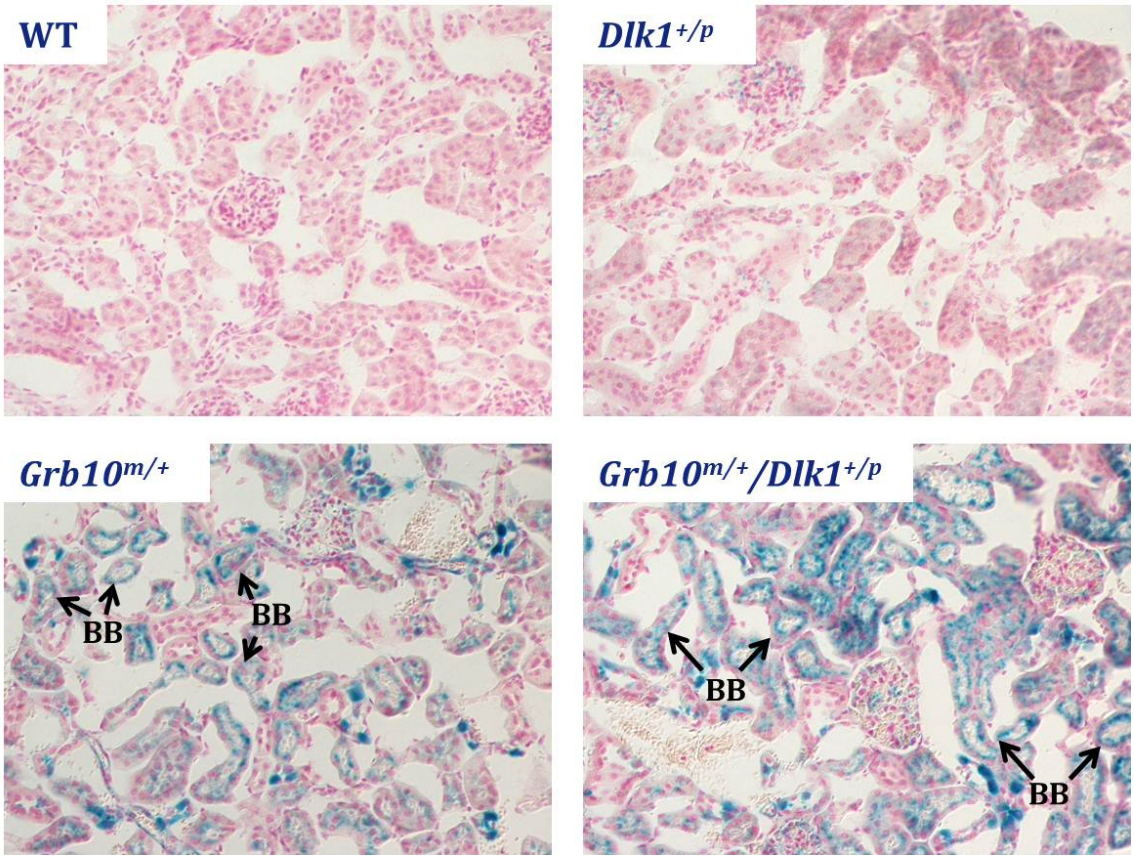

Figure 4.19 *LacZ* stained adult wild type, *Dlk1*$^{+/p}$, *Grb10*$^{m/+}$ and *Grb10*$^{m/+}$*/Dlk1*$^{+/p}$ kidneys, counterstained with eosin under 200x magnification.

Distinctive blue *LacZ* staining was observed in *Grb10*$^{m/+}$ and *Grb10*$^{m/+}$*/Dlk1*$^{+/p}$ kidneys in brush borders of the adult proximal tubules. Presented images show representative sections for each of the analysed genotypes. BB: brush border. WT n=5, *Dlk1*$^{+/p}$=5, *Grb10*$^{m/+}$ n=5 and *Grb10*$^{m/+}$*/Dlk1*$^{+/p}$ n=5.

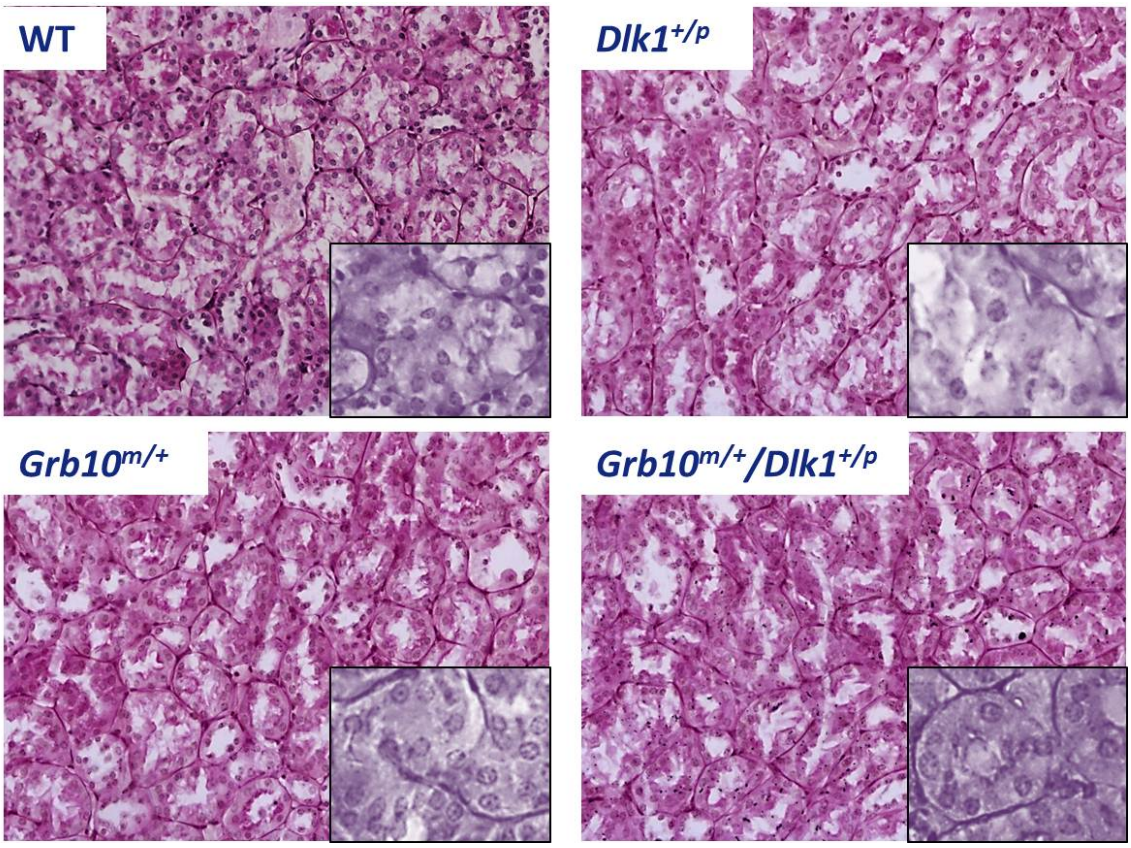

Figure 4.20 H&E stained adult wild type, *Dlk1*$^{+/p}$, *Grb10*$^{m/+}$ and *Grb10*$^{m/+}$*/Dlk1*$^{+/p}$ kidneys under 200x magnification with 400x magnification insets in bottom right corners.

No obvious abnormalities were identified through the histological analysis of kidneys from 3 month old male mice. To account for possible changes within intra-cellular spaces and glomerulus numbers morphometric analysis has been performed (**Figure** 4.21). Presented images show representative sections for each of the analysed genotypes. WT n=5, *Dlk1*$^{+/p}$=5, *Grb10*$^{m/+}$ n=5 and *Grb10*$^{m/+}$*/Dlk1*$^{+/p}$ n=5.

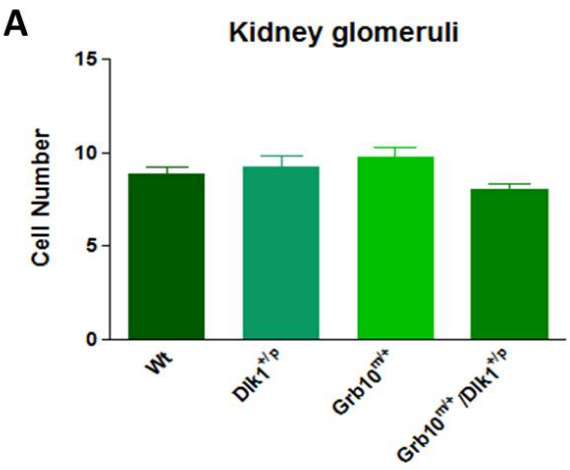

B

	Glomerulus numbers
Wt vs Grb10$^{m/+}$	ns
Wt vs Dlk1$^{+/p}$	ns
Wt vs Grb10$^{m/+}$/Dlk1$^{+/p}$	ns
Grb10$^{m/+}$ vs Dlk1$^{+/p}$	ns
Grb10$^{m/+}$ vs Grb10$^{m/+}$/Dlk1$^{+/p}$	ns
Dlk1$^{+/p}$ vs Grb10$^{m/+}$/Dlk1$^{+/p}$	ns

Figure 4.21 Glomerulus numbers in adult wild type, *Dlk1$^{+/p}$*, *Grb10$^{m/+}$* and *Grb10$^{m/+}$/Dlk1$^{+/p}$* kidneys.

A) Morphometric analysis of 3 month old male kidneys revealed no significant differences between glomerulus numbers among all the analysed genotypes. **B)** Table summarising results of statistical analysis. All values represent means ± SEM, analysed by one way ANOVA with post hoc Tukey's analysis. WT n=5, *Dlk1$^{+/p}$*=5, *Grb10$^{m/+}$* n=5 and *Grb10$^{m/+}$/Dlk1$^{+/p}$* n=5.

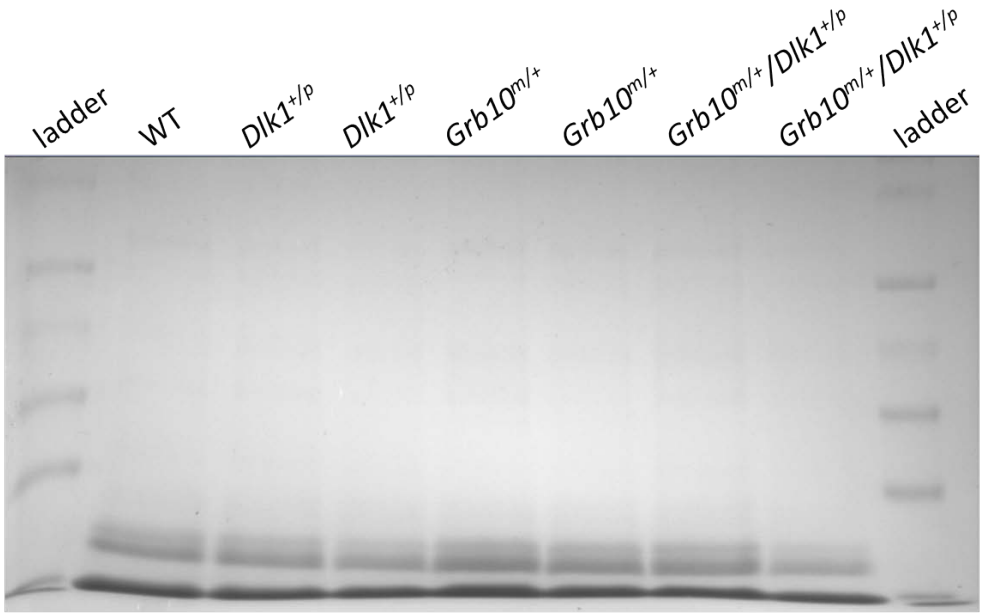

Figure 4.22 Representative SDS-PAGE gel with urine samples from wild type, *Dlk1*$^{+/p}$, *Grb10*$^{m/+}$ and *Grb10*$^{m/+}$*/Dlk1*$^{+/p}$ mice.

Visual inspection did not reveal any apparent changes in protein content in urine samples from 3 month old males of any of the analysed genotypes. WT n=5, *Dlk1*$^{+/p}$=5, *Grb10*$^{m/+}$ n=5 and *Grb10*$^{m/+}$*/Dlk1*$^{+/p}$ n=5.

4.3 Discussion

Different groups of imprinted genes might be controlled by various mechanisms in order to be able to play distinct roles in prenatal development and postnatal physiology. It is a challenging task to distinguish between the specific postnatal effects of imprinted genes and consequences of fetal programming, as early developmental changes can have a great influence on various aspects of postnatal life. In this chapter, we have provided a study of postnatal features of mice lacking the *Grb10* and *Dlk1* genes, both of which are known to function pre- and post-natally. We therefore believe that our investigation of the knockout phenotypes improves understanding of the potential link between these genes and provides more information on the postnatal effects of *Grb10* and *Dlk1* ablation, resulting either from fetal programming or directly from lack of *Grb10* and/or *Dlk1* expression in specific tissues. However, it can be difficult to firmly establish the underlying sources of observed phenotypic changes.

Although both *Grb10* and *Dlk1* have been studied in a number of biochemical and *in vitro* experiments and have been implicated as members of several signalling pathways, their interactions and physiological impact *in vivo* need to be explored in more detail. Shortfalls of *in vitro* studies are exemplified by conflicting evidence regarding the *Grb10* role in insulin signalling, which has been reported both to be negative (Langlais et al., 2004; Mori et al., 2005; Smith et al., 2007; Wang et al., 2007) as well as positive (O'Neill et al., 1996; Wang et al., 1999; Deng et al., 2003). As previously mentioned, employing *in vivo* models has allowed the identification of important roles for both *Grb10* and *Dlk1* in influencing embryonic growth but also in causing several postnatal phenotypic abnormalities. In both cases, the early developmental growth effects were persistent, but less prominent, following birth. The phenotypic variance and coefficient of variation for mouse body weight increase from birth to approximately 28 to 35 days of age, followed by a decrease and eventual stabilisation (Eisen, 1976). The comparison of body weight alterations with age along with changes in body composition (specifically fat and lean tissue content) were previously assessed and compared between different mouse strains, and the results of comparison of 3 and 6 month old C57BL/6 female and male mice showed variation of 19.8 ± 1.16 g in female and 25.8 ± 1.62 g in male 3 month old animals against 23.8 ± 1.50 g and 29.9 ± 1.14 g in 6 month old female and male animals, respectively (Mouse Phenome Database; http://phenome.jax.org). For the purpose of our allometric analysis of adult mice we decided to pool together 3-6 and 7-9 month old mice, as we did not observe significant variations in weights between 3 and 6 and also between

7 and 9 month old animals. In order to perform more specific analysis, allometric examination of specifically 3, 6, 7 and 9 month old mice should be performed to discard any potential discrepancies in the total body and organ weights due to use of animals that were not strictly age-matched.

Allometric studies presented in this chapter confirm previously published findings, demonstrating significant overgrowth of *Grb10*$^{m/+}$ knockout (Charalambous et al., 2003; Smith et al., 2007) and growth retardation of *Dlk1* knockout (Moon et al., 2002) neonatal mice. Our primary interest, however, was to analyse the postnatal growth phenotype of *Grb10*$^{m/+}$*/Dlk1*$^{+/p}$ double knockout mice. *Grb10*$^{m/+}$*/Dlk1*$^{+/p}$ neonates displayed a growth phenotype that resembled that observed for *Grb10*$^{m/+}$ single knockout mice, being significantly overgrown on the day of birth. The examination of mice at 1 week of age confirmed the persistent overgrowth in *Grb10*$^{m/+}$ and *Grb10*$^{m/+}$*/Dlk1*$^{+/p}$ animals, although the overgrowth was less prominent in *Grb10*$^{m/+}$*/Dlk1*$^{+/p}$ double knockout mice. Analysis of total body weights of 3-6 and 7-9 months old male and female mice revealed no obvious abnormalities with the exception of 3-6 month female *Grb10*$^{m/+}$ animals that were 21% heavier than wild type mice. Previous studies have also reported that the overgrowth phenotype of *Grb10*$^{m/+}$ knockout mice diminished with time, but was persistent until at least 6 months of age when *Grb10*$^{m/+}$ animals were still 13% larger than their wild type counterparts (Smith et al., 2007). Thus, in the present study there was either a more rapid or complete diminution of the increased mass of *Grb10*$^{m/+}$*/Dlk1*$^{+/p}$ animals, as well as male and older female *Grb10*$^{m/+}$ knockout mice, possibly due to the different genetic background that resulted from crossing *Grb10*$^{m/+}$ with *Dlk1*$^{+/p}$ knockout animals.

In addition to the examination of total body weights, organs from neonatal and adult animals were subject to allometric analysis. Assessment of neonatal organ weights revealed that in accordance with changes in total body size, there were proportional differences in weights of hearts and lungs in transgenic animals of each of the mutant genotypes, so these organs were enlarged in *Grb10*$^{m/+}$ and *Grb10*$^{m/+}$*/Dlk1*$^{+/p}$ and reduced in size in *Dlk1*$^{+/p}$ neonates. In contrast, sparing was noted in kidneys from *Grb10*$^{m/+}$ and *Grb10*$^{m/+}$*/Dlk1*$^{+/p}$ animals since their wet weights remained comparable to wild type and, consequently, relative kidney weights of *Grb10*$^{m/+}$ and *Grb10*$^{m/+}$*/Dlk1*$^{+/p}$ were significantly reduced whereas relative kidney weights of *Dlk1*$^{+/p}$ neonates were significantly elevated. In adulthood, no alterations were found in female kidney weights, however in the case of males the trend of significantly smaller wet kidney weights was noted in *Grb10*$^{m/+}$ and *Grb10*$^{m/+}$*/Dlk1*$^{+/p}$ along with decreased relative

kidney weights in *Grb10*$^{m/+}$ and *Grb10*$^{m/+}$*/Dlk1*$^{+/p}$ 7-9 months male mice (approximately 16% smaller for *Grb10*$^{m/+}$ and 20% for *Grb10*$^{m/+}$*/Dlk1*$^{+/p}$). Interestingly, there has been some evidence provided for *Grb10* expression in kidney tubules (Smith, 2004) and by looking at *LacZ* staining in kidneys of adult *Grb10*$^{m/+}$ and *Grb10*$^{m/+}$*/Dlk1*$^{+/p}$ mice we found that it was largely concentrated in proximal convoluted tubules. Control and regulation of arterial blood pressure is associated with the function of kidneys in maintaining water and salt homeostasis. More than 20 years ago it has been proposed that reduced nephron number could lead to higher risk of developing adult hypertension (Brenner et al., 1988), which has since been supported by experimental and clinical data. Examination of cases of intrauterine growth restriction in Aboriginal children showed that postnatal hypertension might be a consequence of abnormal fetal development (Spencer et al., 2001), most possibly as a result of a reduction in nephron number, and other human studies have also highlighted the association between the nephron number and hypertension (Keller et al., 2003; Douglas-Denton et al., 2006). Moreover, a decrease in nephron number as well as reduction in kidney size have been noted in mice overexpressing the *Ret* (REarranged during Transfection) kinase receptor (Yu et al., 2004), required for proliferation, migration and differentiation of neural crest cells and for kidney organogenesis in the developing urinary tract and kidney (Pachnis et al., 1993). The evidence of interaction between *Ret* and *Grb10* (Pandey et al., 1995), together with the role of *Grb10* in inhibiting receptor tyrosine kinase signalling, suggests that changes in this interaction may lead to the observed kidney phenotype that we found in *Grb10*$^{m/+}$ and *Grb10*$^{m/+}$*/Dlk1*$^{+/p}$ mice. Therefore, it would be interesting to investigate in the future Ret protein levels in these mice and look for any associated abnormalities.

Fetal programming can potentially influence the postnatal phenotype, and it is largely possible that in the case of kidneys the fetal programming effect of neonatal under/over-growth of these organs in proportion to overall body size might lead to serious cardiovascular malfunctions in later life. To investigate the adult kidney morphology, we performed histological analysis along with an assessment of glomerulus numbers in 3 month old male kidneys. We did not find any histological differences in examined kidneys, and morphometric analysis provided evidence that there were no significant discrepancies in the overall glomerulus numbers between mice of all genotypes. Additionally, urine analysis aimed at investigating potential kidney malfunctions revealed no incidence of proteinurea in any of the genotypes, indicating that kidney function was normal in studied animals, regardless of their genotype. However, it would still be interesting to examine blood pressure in *Dlk1*$^{+/p}$, *Grb10*$^{m/+}$ and *Grb10*$^{m/+}$*/Dlk1*$^{+/p}$ mice as a measure of another major aspect of kidney function and to

undertake an analysis of histology, morphometry and function of neonatal kidneys to investigate the possibility of kidney anomalies at the neonatal stage that might be resolved during the course of postnatal life.

Studies of Silver-Russell syndrome patients demonstrate that cranial sparing is a frequent feature of this disorder (Price et al., 1999). Interestingly, a similar effect of cranial sparing in *Grb10*$^{m/+}$ and *Grb10*$^{m/+}$*/Dlk1*$^{+/p}$ neonates, along with relative brain overgrowth in *Dlk1*$^{+/p}$ neonates, was noted during allometric analysis of the brain. No modifications in wet and relative brain weights were identified in the adult animals, despite confirmed expression from the paternal *Grb10* allele in the developing and postnatal brain (Garfield et al., 2011). Absence of maternal *Grb10* expression in fetal CNS and a distinct pattern of paternal *Grb10* expression from fetal life into adulthood have been recently reported by our group (Garfield et al., 2011). Ablation of the paternal *Grb10* copy has led to changes in some aspects of social behaviour, primarily increased social dominance. These observations have established *Grb10* as the first example of an imprinted gene whose monoallelic expression from each of the parental alleles in a tissue-specific manner is able to control distinct physiological and behavioural processes. Maternal *Grb10* controls fetal growth along with postnatal metabolism (Charalambous et al., 2003; Smith et al., 2007; Garfield et al., 2011) and paternal *Grb10* controls aspects of social behaviour, highlighting complex mechanisms of action and roles for imprinted genes that go far beyond only affecting early development.

One of the most interesting phenotypic features found during the study presented in this chapter was the growth of the livers, which was significantly different between genotypes and was also dependent on the stage of development. Neonatal *Grb10*$^{m/+}$ liver overgrowth has already been reported (Charalambous et al., 2003), and liver overgrowth in *Grb10*$^{m/+}$ and *Grb10*$^{m/+}$*/Dlk1*$^{+/p}$ during fetal development has been shown in Section 3.2.1. *Grb10*$^{m/+}$ and *Grb10*$^{m/+}$*/Dlk1*$^{+/p}$ neonates displayed significantly increased wet and relative liver weights, whereas liver weights of *Dlk1*$^{+/p}$ mice were slightly (but not significantly) reduced, even in proportion to the reduced total body weights of these animals. At 1 week of age, both *Grb10*$^{m/+}$ and *Grb10*$^{m/+}$*/Dlk1*$^{+/p}$ wet liver weights were still significantly increased but this was not the case for relative liver weights. Interestingly, we found that at 3-6 months of age *Grb10*$^{m/+}$ male mice had significantly smaller relative liver wet weights, whereas liver wet weights from *Grb10*$^{m/+}$ 3-6 months old females were significantly higher, but this trend disappeared in relative liver weights. This suggests that liver weights in this case changed in proportion to total body weights which were also increased in *Grb10*$^{m/+}$ and *Grb10*$^{m/+}$*/Dlk1*$^{+/p}$

3-6 month old female mice. Taken together, it seems that the liver enlargement in *Grb10*$^{m/+}$ and *Grb10*$^{m/+}$*/Dlk1*$^{+/p}$ mice that is prominent during later stages of fetal development persists until the day of birth and then diminishes with time during postnatal life, which appears to be in line with strong *Grb10* expression during gestation that diminishes with time from the day of birth (Lui et al., 2008), so that lack of *Grb10* in postnatal life leads to significant reduction in adult liver weight. The nature of changes in liver composition that could account for these variations in liver mass will be discussed further in the following chapter.

The expression of *Grb10* in adult pancreas is restricted to the endocrine part of this organ. Our lab has previously found that *Grb10*$^{m/+}$ E14.5 pancreata were significantly overgrown (Smith, 2004). Here we report that relative pancreas weights of 3-6 month old *Grb10*$^{m/+}$ and *Grb10*$^{m/+}$*/Dlk1*$^{+/p}$ males were increased, becoming significantly larger for *Grb10*$^{m/+}$*/Dlk1*$^{+/p}$ animals. In both 3-6 month and 7-9 month old females wet and relative weights of *Grb10*$^{m/+}$ and *Grb10*$^{m/+}$*/Dlk1*$^{+/p}$ pancreata were significantly enlarged. Postnatal pancreas overgrowth in *Grb10*$^{m/+}$ 3 month old animals has been noted previously (Smith, 2004; Garfield, 2007), although this phenotypic feature did not persist until 6 months of age in these earlier studies. Former examination of pancreatic tissues from 3 weeks old *Grb10*$^{m/+}$ mice revealed no endocrine hyperplasia or hypertrophy, thus it has been concluded that increased exocrine tissue is responsible for the apparent pancreatic overgrowth (Smith, 2004), which was a surprising finding due to the lack of *Grb10* expression in this tissue. Further morphological and immunohistochemical investigation, and possibly investigation of pancreatic progenitor cell number during fetal development, are required to confirm the exact nature of the observed pancreatic overgrowth during pre- and post-natal life, along with an assessment of neonatal pancreatic weights and their morphology.

It has been suggested that the pancreatic overgrowth could also occur as a consequence of the liver overgrowth even though liver overgrowth is not maintained in *Grb10*$^{m/+}$ and *Grb10*$^{m/+}$*/Dlk1*$^{+/p}$ animals between 3-9 months of age. The explanation for this could be based on simultaneous overgrowth of both of these organs during early development, which stops at the time of birth when *Grb10* expression decreases and so does the liver size, whilst pancreas size does not. Reduction of liver size might also be influenced by other factors (such as changes within lipid and glucose storage), while pancreas remains overgrown. The possibility of liver and pancreas interacting with each other in some way during development could be investigated by culturing *Grb10*$^{m/+}$ and *Grb10*$^{m/+}$*/Dlk1*$^{+/p}$ pancreatic and liver buds separately *in vitro* and observing if without any signals from the other organ they both show enhanced

growth when compared to wild type controls. The results ought to show if the growth changes in these two organs result from two independent mechanisms or there are some common factors acting simultaneously in both liver and pancreas. It has also been argued, that, unlike liver, the size of pancreas correlates with the progenitor cell pool present during the development of the pancreatic bud (Stanger et al., 2007), suggesting that the organ size can be determined by the progenitor cell number rather than depend on the regulation by growth factors.

Dlk1 is known to be expressed in multipotent mesenchymal stem cells (MSC) that are able to differentiate into a number of cell types, such as chondrocytes, adipocytes and osteoblasts. Even though there is a relatively large number of studies on the role of *Dlk1* in adipogenesis (Smas et al., 1998; Mei et al., 2002; Moon et al., 2002; Lee et al., 2003), its role in chondrogenesis has not been analysed in such detail. A recent study has shown that Dlk1 along with secreted frizzled-related protein 1 (sFRP-1) are secreted in the bone marrow environment and control osteoblastogenesis and adipogenesis by mediating cross-talk between lineage committed cell populations along with governing differentiation choices of multipotent MSCs (Abdallah and Kassem, 2011).

Sox9, a *Dlk1* target, has been found to play a crucial role in skeletogenesis and in addition its downregulation proved to be necessary for adipocyte differentiation, as recent study suggested that *Dlk1* is responsible for inhibition of adipocyte differentiation by upregulating *Sox9* expression (Wang and Sul, 2009). It has also been shown that by induction of *Sox9* *Dlk1* is able to enhance chondrogenic induction of mesenchymal cells and simultaneously inhibit chondrocyte maturation and osteoblast differentiation (Wang and Sul, 2009). Studies of *Sox9* in chondrogenesis showed that the active form of *Sox9* is vital for cartilage formation in mice (reviewed in de Crombrugghe et al., 2001), and mice with *Sox9* ablation and *Sox9* overexpression exhibit similar skeletal phenotypes to the ones observed in *Dlk1* knockout mice (Moon et al., 2002)and animals with *Dlk1* overexpression (Lee et al., 2003), respectively. *Dlk1* is able to inhibit osteoblast differentiation of human bone marrow stromal cells (Abdallah et al., 2004) and also to prevent the downregulation of *Sox9*, therefore inhibiting osteoblast differentiation as well as expression of the osteogenic transcription factor *Runx2* (Wang and Sul, 2009). Co-expression of *Sox9* and *Runx2* has been detected in progenitor cells in early mesenchymal condensations. *Runx2* has been identified as a osteogenesis promoter and enhancer of chondrocyte maturation (Takeda et al., 2001) and it seems to be able to fully function only in case of *Sox9* downregulation in hypertrophic chondrocytes or in

osteoblasts. Additionally, recent *in vitro* study of *Dlk1* overexpression in mouse cells identified *Dlk1* as a novel factor able to control chondrogenesis through inhibiting PI3k/Akt pathways and subsequently inhibiting chondrogenesis (Chen et al., 2011).

DLK1 contribution to normal human physiology is exemplified by the human syndrome with silent *DLK1* (mUPD14), characterised by obesity, hypotonia, premature puberty, macrocephaly, short stature, and small hands (Berends et al., 1999; Kotzot, 1999). The contrasting syndrome of pUPD14 with *DLK1* overexpression results in narrow thorax with abnormally-shaped ribs, facial dysmorphism and mild hypoplasia of the ilia (Berends et al., 1999; Kotzot, 1999). These phenotypic abnormalities are largely associated with skeletal malformations and indicate a crucial role for *DLK1* in normal osteo- and possibly also chondro-genesis.

Gsα, one of the protein products of another paternally imprinted locus *Gnas,* has also been found to be important in bone development and inhibition of ectopic ossification. The most dramatic phenotypic features of mice with local Cre-mediated inactivation of *Gsα* are skeletal malformations of the forelimbs due to shortened and fused extremity bones (Castrop et al., 2007). Loss-of-function mutations of *Gsα* in humans are linked to numerous developmental abnormalities, including phenotypes such as Albright's hereditary osteodystrophy (AHO) and progressive osseous heteroplasia (POH), both associated with bone-related symptoms.

Bearing in mind the roles of imprinted genes in normal skeletal development, we decided to examine in detail the skeletons of one particular litter with individual mice of visible atypical postures (hunched and abnormally small versus large and elongated), although usually we saw no obvious signs of skeletal abnormalities in mice of any genotype. This analysis did not lead to the identification of previously reported malformations, such as rib fusion, fusion of vertebrae or asymmetrical rib fusion to the sternum (Moon et al., 2002). Rather, we concluded that $Dlk1^{+/p}$ animals were visibly smaller, and presented a 'hunched' posture, whereas, as expected, $Grb10^{m/+}$ and $Grb10^{m/+}/Dlk1^{+/p}$ mice were much larger than their wild type counterparts. It would be of interest to conduct bone/cartilage staining on larger cohorts of neonatal mice in order to look for any subtle skeletal abnormalities which might have been previously overlooked. In addition, analysis of the length of long bones in mice at the beginning of postnatal development would be informative if the growth differences are associated only with alterations in the weights of some organs or also with changes in body size due to elongated bones. Axial lengths of $Grb10^{m/+}$ neonatal mice were previously

investigated in our lab (M. Cowley, data not published) and revealed significantly greater nose-rump lengths of male and female animals in comparison to wild type littermates. Lengths of *Grb10*$^{m/+}$ mice of both genders normalised to wild type littermates by around day 11-12. This finding is encouraging for further analysis of bone lengths in *Dlk1*$^{+/p}$, *Grb10*$^{m/+}$ and *Grb10*$^{m/+}$*/Dlk1*$^{+/p}$ mice, as our examination of 2 weeks skeletons suggests once again a similar growth phenotype of *Grb10*$^{m/+}$ and *Grb10*$^{m/+}$*/Dlk1*$^{+/p}$ mice and this could be further confirmed by detailed analyses of axial and bone length in mice of all four genotypes.

The differential expression of *Grb10* and *Dlk1*, among several other imprinted genes, has been reported in the growth plate of rat bones during postnatal growth (Andrade et al., 2009). The expression of growth promoting *Dlk1* ceased towards adulthood whereas the expression of growth inhibiting *Grb10* increased with time, in agreement with the possibility that the developmental processes related to differential expression patterns of growth promoting and growth inhibiting genes are responsible for the decrease in the growth of longitudinal bone over time. In order to investigate this ourselves, we have tracked *LacZ* expression in neonatal long bones of *Grb10*$^{m/+}$ and *Grb10*$^{m/+}$*/Dlk1*$^{+/p}$ animals and found that *LacZ* expression was restricted to the growth plate regions of the bones and, as expected, to associated skeletal muscle tissue. Further analysis, in particular of the expression in adult bones is under way. It will be informative of possible expression changes of *Grb10* from neonatal to postnatal life, leading to the restriction of long bone growth. The comparison of long bone length and expression patterns in embryos at the later stages of gestation (for example at E17.5) could also be potentially useful in determining *Grb10* and *Dlk1* function in skeletal growth and development.

Despite the general assumption of adipose tissue as a passive energy reservoir, it is in fact an active metabolic and endocrine organ with a dynamic role in energy metabolism. Adipose tissue is subject to signals from the CNS but at the same time it is responsible for secretion of adipokines, bioactive peptides involved in processes such as lipid metabolism, insulin sensitivity and energy homeostasis. In addition, brown adipose tissue (BAT), is able to accumulate triglycerides and acts as an effector organ for non-shivering thermogenesis. Therefore, it is not surprising that proliferation and differentiation of adipocytes are closely linked to the development of obesity. Several imprinted genes have so far been implicated in adipocyte metabolism, and these include *Dlk1, Peg1* and *Ndn* (*Necdin*). *Peg1* white adipose tissue (WAT) mRNA levels are increased in mice with high fat diet-induced, and genetically induced, obesity (Takahashi et al., 2005). Transgenic mice overexpressing *Peg1* suffer from

obesity and associated adipose cell hypertrophy, and ectopic expression of *Peg1* leads to elevated levels of adipocyte marker expression *in vivo* and *in vitro* (Takahashi et al., 2005). Additionally, it has been suggested that increased organ and body weight in mouse interspecies hybrids might be due to loss of imprinting of *Peg1,* causing biallelic expression of this gene (Shi et al., 2004). The importance of this gene in the regulation of fat metabolism has also been highlighted by study in which increased levels of *Peg1* were found in adipose tissue of inbred mouse predisposed to diet-induced obesity (Koza et al., 2006).

NDN, a transcriptional regulator of the melanoma-associated antigen (MAGE) protein family coded in the PWS region, has been demonstrated to act as a potent growth inhibitor regulating differentiation and survival of neurons (Taniura et al., 1998). NDN also has demonstrated expression in adipocytes and differential expression in white and brown preadipocytes (Gerard et al., 1999; Boeuf et al., 2001). Mice lacking *Ndn* gene did not exhibit features of obesity (Tsai et al., 1999), even though evidence has been provided of a role for *Ndn* in suppression of brown adipocyte differentiation through downregulation of *Dlk1* and *Wnt10a* expression (Tseng et al., 2005), implying that Dlk1 is able to inhibit brown adipogenesis downstream of Necdin.

Dlk1 is used as a preadipocytes marker as it reflects a level of adipocyte differentiation *in vitro* and *in vivo* (Shimomura et al., 1998; Fox et al., 2006; Wang et al., 2006; Rodeheffer et al., 2008; Wang et al., 2008). Various studies have shown that Dlk1 has an inhibitory role in adipocyte differentiation (Wolfrum et al., 2003; Wang et al., 2006) and that differentiation of 3T3-L1 preadipocytes to adipocytes *in vitro* requires the downregulation of *Dlk1* activity (Smas and Sul, 1993; Smas et al., 1999). Paternal transmission of the null allele of *Dlk1* leads to moderate increase in fat pad weight on a normal diet and a significant 30% increase on a high-fat diet, resulting from adipocyte hypertrophy (Moon et al., 2002). Overexpression of a soluble isoform of *Dlk1* in white adipose tissue leads to reduction of adipocyte cell size along with reduced fat pad mass and decreased expression of adipocyte marker genes (Moon et al., 2002). A wide range of metabolic changes, including hypertriglyceridemia, impaired glucose tolerance, and reduced insulin sensitivity, have been noted in transgenic mice exhibiting considerably reduced adipose tissue content (Lee et al., 2003). *Dlk1* is downregulated in most tissues postnatally, but its overexpression during the prenatal period can still result in a postnatal decrease in adiposity (da Rocha et al., 2009), suggesting that the dosage of *Dlk1* in prenatal life can influence postnatal white adipose tissue energy storage.

Overexpression of *GRB10* protein in adipose cell lines results in inhibition of insulin stimulation of the mitogen-activated protein kinases pathway (Langlais et al., 2004). Increased lean mass and reduced adiposity postnatally are amongst the phenotypic consequences of *Grb10* deficiency in mice (Smith et al., 2007). In light of unambiguous roles of *Dlk1* and *Grb10* genes in maintenance of correct adipose and lean tissue content we have performed weight analysis of several types of fat pads and muscles in 3-6 and 7-9 month old mice of both sexes. We found that 3-6 month old $Grb10^{m/+}$ female mice had significantly increased wet weights of gastrocnemius muscle, while analyses of fat pads revealed a significant increase in wet and relative renal fat content for $Dlk1^{+/p}$ animals as well as elevated gonadal fat content in $Dlk1^{+/p}$ mice when compared to $Grb10^{m/+}/Dlk1^{+/p}$. We also found significantly reduced wet weight of gonadal fat pads in 7-9 month old $Grb10^{m/+}$ female mice, which was not identified during relative weight analysis. The fact that no alternations have been found in male mice along with differences between results obtained for both female age groups could be associated with the relatively large variance in weight within the analysed groups, evidenced by quite high error bars. To overcome this issue and more explicitly pinpoint any real trends, further analyses with expanded numbers of mice would be required. The observation that there was no obvious increase in adipose tissue mass of male $Dlk1^{+/p}$ animals could be explained by the fact that the authors who first reported a relationship between lack of *Dlk1* and elevated adiposity (Moon et al., 2002) made their observations in high fat diet fed animals. Therefore, our data is consistent with increased adipose tissue content in $Dlk1^{+/p}$ mice being diet-dependent. Thus, it would be of interest to carry out similar adipose and muscle tissue weight analyses in $Grb10^{m/+}$, $Dlk1^{+/p}$ and $Grb10^{m/+}/Dlk1^{+/p}$ mice fed on high fat diet when the predispositions to obesity are expected to be elevated.

Obvious indications of *Grb10* and *Dlk1* roles in the regulation of adipogenesis provided by *in vitro* studies as well as *in vivo* characterisation of phenotypic features in mouse models give clear indications for further investigation of these two genes in this particular tissue in $Grb10^{m/+}/Dlk1^{+/p}$ animals. Examination of *Grb10* and *Dlk1* expression in different types of adipose tissue at various developmental stages with expanded mouse cohort numbers will help to delineate roles of these genes in adipose tissue. Investigation of any potential changes indicating on these two genes interacting in the same genetics pathway could tell us more about their mode of action in this particular tissue. More experiments that address *Grb10* and *Dlk1* influence on lipid metabolism will be discussed in Chapter 5.

A previously reported incidence of approximately 12% perinatal lethality amongst *Grb10*$^{m/+}$ animals was linked to blood-filled alveoli and trachea (Charalambous et al., 2003), with abnormal lung development indicated as a cause of death by suffocation among these animals. Moreover, *Dlk1* expression has been implicated to mark developing endothelium and sites of branching morphogenesis in the mouse embryo and placenta, and relatively high levels of *Dlk1* expression have been demonstrated in developing lungs (Yevtodiyenko and Schmidt, 2006). The Notch signalling pathway is necessary for branching morphogenesis and maturation of the lungs, and perinatal lethality due to lung hypotrophy can be a potential consequence of disrupting this pathway (reviewed in Collins et al., 2004). We therefore decided to undertake a histological and morphometric analysis of both neonatal and adult lungs of mice of all four genotypes. Histological examination of neonatal lungs revealed potentially thicker epithelial walls in *Grb10*$^{m/+}$ and *Grb10*$^{m/+}$*/Dlk1*$^{+/p}$ knockout mice when compared to wild type and surprisingly, *Dlk1*$^{+/p}$ animals in which Moon et al (2002) have previously reported pulmonary defects and pointed at them as one of the sources of observed increase in lethality. This result has been confirmed by morphometric assessment of neonatal lung epithelial wall thickness, which showed that indeed *Grb10*$^{m/+}$ and *Grb10*$^{m/+}$*/Dlk1*$^{+/p}$ neonates had significantly thicker epithelial walls. A similar examination was also undertaken in adult mice and at this stage no differences were found between the genotypes. These findings could indicate an important role of *Grb10*$^{m/+}$ in normal lung development, as its absence leads to abnormalities during the perinatal period that possibly result in cases of lethality. However, it seems that in the majority of cases these lung malformations are overcome and most *Grb10*$^{m/+}$ animals survive and go on to reach adulthood, when changes in lung morphology are no longer evident. This is consistent with the timing of *Grb10* expression, which is high and widespread during embryonic development (Lui et al., 2008) and highly restricted in adulthood. Further study of neonatal along with late embryonic lungs should be undertaken to identify the first time point during development at which significantly thicker lung epithelium appears. Dlk1-specific antibodies could be used to determine differences in lung expression of *Grb10*$^{m/+}$*/Dlk1*$^{+/p}$ double knockout mice and *Grb10*$^{m/+}$ single knockout neonates and embryos.

Aside from the obvious effects of imprinted genes in mother-offspring interface, there are potential secondary effects of imprinted genes seen in postnatal life. In light of established roles of *Grb10* and *Dlk1* genes in fetal growth and development along with the *Grb10*$^{m/+}$*/Dlk1*$^{+/p}$ embryonic growth phenotype being similar to *Grb10*$^{m/+}$ knockout, as described in the previous chapter, we undertook analyses of postnatal growth and characteristics of *Grb10*$^{m/+}$*/Dlk1*$^{+/p}$ mice. We aimed to investigate potential influence of both

Dlk1 and *Grb10* genes on proportionate growth and phenotypes of several organs following birth. Our study of neonatal and adult *Grb10*$^{m/+}$*/Dlk1*$^{+/p}$ mice revealed similarities between them and *Grb10*$^{m/+}$single knockout animals, which is in consistence with results obtained for prenatal growth and development discussed in Chapter 3. Whether identified postnatal consequences of *Dlk1* and *Grb10* ablation are direct effects of these imprinted genes on postnatal phenotype or whether they result from modified mother/offspring interactions in early development remains to be established. Even though further investigation is needed to gain more insight into the true nature of the identified phenotypic malformations, it seems plausible to suggest that our hypothesis of *Grb10* and *Dlk1* genes acting epistatically in the same genetic pathway is largely confirmed by studies of *Grb10*$^{m/+}$*/Dlk1*$^{+/p}$ postnatal phenotype, as most of the identified postnatal differences were shared between *Grb10*$^{m/+}$*/Dlk1*$^{+/p}$ and *Grb10*$^{m/+}$animals.

CHAPTER 5

5 Metabolic characterisation of *Grb10*$^{m/+}$*/Dlk1*$^{+/p}$ double knockout mice

5.1 Introduction

Increasing number of imprinted genes has been implicated in governing behaviour (Isles et al., 2006; Davies et al., 2007; Garfield et al., 2011) and postnatal metabolism (Da Costa et al., 1994; Lee et al., 2003; Plagge et al., 2004; Chen et al., 2005; Smith et al., 2006; Smith et al., 2007; Yamamoto et al., 2008), the latter suggesting crucial roles in maintaining correct overall metabolic status in both mice and humans. Many human disorders associated with impairment of glucose-related metabolic processes have been linked to changes in expression of imprinted genes (**Table** 5.1) (reviewed in Smith et al., 2006). It is likely that disrupted metabolic homeostasis can influence growth and, in a similar manner, altered growth can have an impact on metabolic homeostasis. Imprinted genes might provide a link between embryonic growth and metabolic functions, although it is difficult to distinguish between primary and secondary effects of imprinted genes in mice, the latter potentially being a result of disrupted early stage development. So far, expression of a single parental allele has not been specifically linked to metabolic effects, as both maternally and paternally imprinted genes can influence glucose-regulated and lipid metabolism with no consistent antagonism between the two parental genomes (**Table** 5.1).

The role of imprinted genes in the regulation of adult metabolic status is complex and not well understood, as adult metabolic phenotypes could be the results of direct effects of gene expression in adult tissues or indirectly be consequences of disrupted embryonic development that may lead to altered metabolic health status in later life. Many epidemiological studies demonstrated that a restricted maternal diet during pregnancy causes a higher risk of developing various disorders in offspring's postnatal life, such as metabolic syndrome, diabetes, hypertension, cardiovascular disease and obesity (reviewed in McMillen and Robinson, 2005), for example clinically growth restricted human babies were found to be more prone to adult hypertension and diabetes (Malamitsi-Puchner et al., 2006). A recent study suggested that maternal high fat diet during embryonic development initiates the misregulation of imprinted gene clusters crucial in regulation of various metabolic, cellular and physiological functions (Gallou-Kabani et al., 2010). The study investigated the influence of HFD during pregnancy on the expression of 20 imprinted genes, as well as the DNA methylation status of the whole genome and in DMRs of imprinted genes in embryos of both sexes. *Dlk1* was among six genes that showed an altered expression pattern in E15.5 placentae when the mother was fed a HFD, and this effect was much more pronounced in female placentae (Gallou-Kabani et al., 2010), however the details of any role for *Dlk1* in placenta remain unknown.

Gene	Expressed allele	Gene manipulation	Metabolic phenotype	Reference
Igf2	Paternal	Overexpression	reduced adiposity	(Da Costa et al., 1994)
		Knockout (brain)	increased adiposity, occasional obesity and hypophagic	(Jones et al., 2001)
Gnas(E2)	Maternal	Knockout	increased adiposity, hypometabolic, increased insulin sensitivity	(Yu et al., 1998; Yu et al., 2000; Yu et al., 2001)
	Paternal	Knockout	reduced adiposity, hypermetabolic, increased insulin sensitivity	
Dlk1	Paternal	Knockout	increased adiposity, elevated lipid metabolite level, adult fatty livers	(Moon et al., 2002)
		Overexpression	reduced adiposity, hyperglycemia, hyperinsulinemia, insulin resistance	(Lee et al., 2003)
Rasgrf1	Paternal	Knockout	reduced adiposity, hypoinsulinemia, glucose intolerance	(Font de Mora et al.,2003)
Grb10	Maternal	Knockout	reduced adiposity, improved glucose clearance and insulin sensitivity	(Smith et al., 2007; Wang et al., 2007)
		Overexpression	hyperinsulinemia, increased adiposity, impaired glucose tolerance	(Shiura et al., 2005; Yamamoto et al., 2008)
Gnas	Paternal	Knockout	reduced adiposity, hypoglycemia, hypoinsulinemia	(Plagge et al., 2004)
Zac1/Hyma1	Paternal	Overexpression	hyperglycemia, impaired glucose tolerance	(Ma et al., 2004)

Table 5.1 Imprinted genes with roles in adiposity and glucose-regulated metabolism.

The fetal programming hypothesis suggests that environmental factors acting during vital developmental periods can have permanent effects on normal development and function of

an organism (Drake and Walker, 2004). Numerous studies in both sexes in various human populations have provided evidence for a relationship between reduced growth during gestation and early postnatal development and subsequent adult consequences in the form of type 2 diabetes, hypertension, hyperlipidaemia, cardiovascular disease and insulin resistance. Proposed mechanisms of fetal programming include: the role of fetal undernutrition permanently decreasing number of cells and affecting growth and organ function, as well as altered DNA methylation and gene expression during embryogenesis leading to permanent changes within an organism (Drake and Walker, 2004). As epigenotype establishment during fetal development can be influenced by environmental factors, it has also been proposed that the epigenetic regulation of gene expression provides a link between fetal nutrition, gene expression and health status (Jirtle and Skinner, 2007). Nevertheless, the exact molecular mechanisms behind fetal programming remain to be established (McMillen et al., 2008).

Several hypotheses attempt to explain the fact that the fetal nourishment results in permanent programming of metabolism and abnormal phenotype postnatally due to a mismatch between fetal and adult environmental conditions. One of the possible explanations is based on epigenetic alterations as causes for maternal diet having life-long effects on gene expression in progeny (Ozanne and Constancia, 2007). The main hypotheses trying to explain how adult metabolic disorders might originate from early development include the following: the 'Thrifty Metabolic State', a hypothesis which states that genes that help survival will be selected due to natural selection acting over long periods of irregular and poor nutrition (Neel, 1962); the 'Predictive Adaptive Response' hypothesis which states that 'Developmental induction' or programming is not a sign of pathophysiological processes, but instead it is a result of an organisms ability to adapt to their phenotype during fetal and postnatal development to better adjust to a specific environment and thereby achieve maximal fitness (Gluckman and Hanson, 2006); and finally, the 'Thrifty phenotype' hypothesis which suggests that permanent changes in metabolic programming result from exposures *in utero* and that embryonic malnutrition leads to adopting a survival approach under poor postnatal nutrition conditions (Hales and Barker, 1992). This hypothesis has been proposed in order to account for the relationship between reduced fetal and early postnatal growth and subsequent higher risk of developing impaired glucose tolerance (Hales et al., 1991) along with metabolic syndrome (Barker et al., 1993) in adulthood. According to the thrifty phenotype hypothesis, altered postnatal metabolism is an adaptive response to poor fetal nutrition, which could be beneficial when poor nutrition is persistent into adult life but can have severe effects when there is an inconsistence between fetal and adult environments. Taking into account

insulin's role as one of the most important fetal growth hormones, it is not surprising that poor fetal growth, although not very frequently, has been related to impaired insulin secretion resulting from genetic causes (Frayling and Hattersley, 2001). Frayling and Hattersley (2001) suggested the existence of 'thrifty phenotype' as a consequence of thrifty genotype, and that changes in fetal growth and type 2 diabetes might result as two different phenotypes of the same genotype.

A strong association of birth weight and the occurrence of metabolic syndrome has been discovered, when men with smallest birth weights were eighteen times more likely to develop the metabolic syndrome than those with high birth weight (Barker et al., 1993). Metabolic syndrome, as recognised by the World Health Organisation is characterised by the following criteria: insulin resistance (type 2 diabetes, impaired fasting glucose or glucose tolerance) and any two of the following symptoms: high blood pressure, increased levels of plasma triglycerides, high density lipoprotein cholesterol, increased Body Mass Index and high urinary albumin.

A variety of metabolic disorders have been associated with misregulation of imprinted genes (**Table** 5.1), for example the *Gnas* locus on mouse chromosome 2 is a cluster containing three imprinted, protein-coding genes (*Gsα*, *Gnasxl* and *Nesp55*) with crucial roles in maintenance of metabolic homeostasis (Plagge and Kelsey, 2006). Owing to distinct maternally and paternally expressed gene products of *Gnas*, maternal or paternal inheritance of an exon 2 deletion leads to opposite physiological and metabolic phenotypes resulting from simultaneous loss of *Gsα* and *Gnasxl* transcripts (Yu et al., 1998). Mice with disruption of the maternal allele are obese and hypometabolic, while those with an ablated paternal allele are lean and hypermetabolic. Enhanced insulin sensitivity has been noted regardless of the parental origin of the mutation (Yu et al., 1998; Yu et al., 2000; Yu et al., 2001). Disruption of the *Gnasxl* transcript in mice caused decreased adiposity, hypoglycaemia, hypoinsulinemia, inactivity and mild postnatal growth retardation, a phenotype largely similar to that of mice with paternal *Gnas* exon 2 deletion (Plagge et al., 2004). On the other hand, *Gsα* knockout mice were obese and insulin resistant, resembling the phenotypic features previously noted in mice lacking maternal *Gnas* exon 2 (Chen et al., 2005). *Gsα* and *Gnasxl* seem to exert reciprocal effects on glucose-related and lipid metabolism. Pseudohypoparathyroidism type Ia (PHP-Ia) and Albright hereditary osteodystrophy (AHO), characterised by short stature and obesity, are human disorders associated with *GNAS* (Plagge and Kelsey, 2006). Maternal transmission of a mutated *Gsα* allele causes AHO and paternal transmission results in PHP1a, which is in

agreement with the phenotypes described previously resulting from either paternal and maternal loss, respectively, of mouse *Gsα*.

Another extensively studied imprinted gene with known role in control of metabolism is paternally expressed *Igf2*. Mice with a knockout of the paternal copy of a maternally imprinted *Igf2* gene show only 60% of normal growth on the day of birth, while those with an ablated maternal copy exhibit normal growth (DeChiara et al., 1990; DeChiara et al., 1991). Increased oxidation of fat in adipose tissue caused a lean phenotype in transgenic mice with elevated serum Igf2 levels (Da Costa et al., 1994; Rogler et al., 1994). Conversely, Jones et al. (2001) showed that lower *Igf2* expression in the brain, caused by a deletion of a putative gene regulatory element located mid-way between *Igf2* and *H19,* was associated with weight gain due to raised fat deposition, occasionally resulting in obesity. Obese animals were found to be hypophagic, which pointed at the increase in fat accumulation being a result of altered fat metabolism, rather than an increase in appetite or food intake (Jones et al., 2001).

Maternally imprinted and postnatally expressed *Rasgrf1* also affects normal growth and metabolic status, as its loss leads to growth retardation, reduced adiposity, hypoinsulinemia and glucose intolerance (Itier et al., 1998; Font de Mora et al., 2003). In contrast to that, disruption of *Peg3,* another imprinted, paternally expressed gene*,* resulted in increased adiposity and hypometabolism, which was associated with perturbed hypothalamic function (Curley et al., 2005). *ZAC1* and *HYMA1* are overlapping, paternally expressed genes situated within a region usually connected to transient neonatal diabetes mellitus (TNDM). The symptoms of this rare disease include intrauterine growth retardation and insulin dependence. Transgenic mice carrying human TNDM locus following paternal transmission exhibit hyperglycemia and disrupted impaired glucose tolerance (Ma et al., 2004).

The significance of the imprinted *Grb10* and *Dlk1* genes not only in growth and development, but also in various aspects of maintaining correct metabolic status, has been highlighted by *in vitro* studies (reviewed in Holt and Siddle, 2005; Ceccarelli and Sicheri, 2009; Sul, 2009) but also by characterisation of transgenic animal models (Lee et al., 2003; Smith et al., 2007; Wang et al., 2007; Yamamoto et al., 2008), providing information about their functions in a physiological context.

Grb10 has a somewhat controversial role in insulin signalling, with the majority of studies showing an inhibitory role but some indicating stimulatory effects (Wang et al., 1999; Deng et al., 2003). Interaction of the Grb10 adapter protein with a variety of receptor tyrosine kinases (RTKs) is possible through its BPS and SH2 domains (He et al., 1998; Hagan et al., 2009) and

Grb10 has the ability to bind IR and Igf1r (Dey et al., 1996; Hansen et al., 1996; Morrione et al., 1996; O'Neill et al., 1996; He et al., 1998). Grb10 acts as a potential tumour suppressor that inhibits RTKs signalling upon phosphorylation by mTORC1 in a negative feedback loop (Hsu et al., 2011; Yu et al., 2011).

Studies of mouse models provided evidence that *Grb10* regulates postnatal glucose metabolism and related physiological processes. Transgenic mice with ectopic *Grb10* expression displayed growth retardation at 4 weeks after birth and 10-15% weight reduction at the age of 4 months (Shiura et al., 2005) along with insulin resistance and inability to clear a glucose load (Yamamoto et al., 2008), suggesting that *Grb10* mutant animals share common characteristics with human type 2 diabetes. *Grb10* transgenic mice also had significantly decreased levels of blood urea nitrogen, and conversely significantly higher levels of plasma triglyceride, insulin, adiponectin and resistin. In addition, significantly decreased body, visceral fat and liver weights along with 60% higher incidence of type 2 diabetes following high fat diet were observed in *Grb10* mutants (Yamamoto et al., 2008). These results, however, should be interpreted with care, as possibly *Grb10* transgenic mice did not in fact mirror the real expression profile of *Grb10* gene during development due to the transgene coupled with heterogenous promoter causing ectopic *Grb10* expression that might have produced artifactual effects.

In order to overcome this limitation, another model expressing a double dose of *Grb10* transcripts in the correct organs and specific tissues has been generated by deletion of the imprinting control centre, *Grb10*- DMR (Shiura et al., 2009). The growth retardation phenotype in these mice resembled that observed in mice with maternal disomy Chromosome 11 (MatDi(11)) and maternally duplicated proximal Chromosome 11 (MatDp(prox11)). By comparison of two strains of mice with *Grb10*-DMR deletion, ones with and without neomycin resistance genes in the deletion construct, the authors concluded that increased *Grb10* expression was a major factor that influenced fetal and neonatal growth in the examined mice (Shiura et al., 2009). They also implied that the double dosage of *Grb10* was sufficient to cause pre- and postnatal growth retarded phenotypes in MatDi(11) and MatDp(prox11) mice.

Knockout mice generated by the incorporation of a gene-trap cassette in the endogenous *Grb10* locus displayed overgrowth of embryos and placenta and were 30% heavier than their wild type littermates on the day of birth (Charalambous et al., 2003). Due to the previously established ability of Grb10 to interact with both IR and Igf1r it would be most plausible to suggest that the overgrowth phenotype of *Grb10* knockout mice is the result of an inhibitory interaction of *Grb10* with the *Igf1r*, especially considering that the magnitude of the

overgrowth seen in *Grb10* knockout animals is similar to the growth retardation of animals lacking genes in the IGF pathway (Efstratiadis, 1998). However, it has been proven genetically that *Grb10* must be acting independent of this pathway (Charalambous et al., 2003). *Grb10* knockout mice displayed some key changes in normal metabolic characteristics, such as insulin-induced tyrosine phosphorylation of IRS-1, and associated IR hypophosphorylation, in muscle and white adipose tissue (Smith et al., 2007). Increased muscle mass and subsequent reduction in adiposity was found by Dual X-ray absorptiometry (DXA) analysis carried out on 6 months old animals, which was confirmed by examination of wet weights of individual muscles and fat depots. In addition, *Grb10* knockout mice showed improved whole-body glucose homeostasis and insulin sensitivity, most likely associated with a slightly improved insulin action in skeletal muscle and adipose tissue, along with a significantly enlarged skeletal muscle mass (Smith et al., 2007). In consistence with these results, a different strain of *Grb10*-deficient mice exhibited skeletal muscle and adipose tissue-specific enhanced insulin-induced activation of Akt and Erk, as well as increased insulin sensitivity in skeletal muscle (Wang et al., 2007). Another study of a compound *Grb10/Grb14* mice showed double knockout animals having an increased lean mass comparable to *Grb10* knockout mice, implying that this is an effect specific to *Grb10* (Holt et al., 2009). This study did not identify any additive effects of *Grb10* and *Grb14* genes on insulin signalling and body composition in *Grb10/Grb14* knockout mice, but showed that double knockout animals were immune to high fat diet-induced impaired glucose tolerance, a result not identified in single knockout animals.

Dlk1 is known as a potent regulator of adipogenesis and has numerous metabolic-related functions (reviewed in Sul, 2009). *Dlk1* expression is high in preadipocytes but diminishes during adipogenesis (Smas and Sul, 1993; Wang et al., 2006). Various studies utilising *in vitro* approaches have evidenced Dlk1 role in adipocyte differentiation, for example by demonstrating that Dlk1 responsible for inhibiting differentiation of 3T3-L1 preadipocytes into adipocytes (Smas and Sul, 1993; Smas and Sul, 1997; Smas et al., 1998). It has been reported that *Dlk1* inhibits adipocyte differentiation by preventing downregulation of *Sox9* that usually occurs during differentiation (Wang and Sul, 2009) and that bone morphogenetic protein 7 (*BMP7*) could directly inhibit *Dlk1* expression, allowing for adipogenesis initiation (Zhang et al., 2010).

Mice with a disrupted *Dlk1* gene not only showed reduction in weight at birth and at weaning, but also later on in life they exhibited diet-dependent increased adiposity together with elevated levels of serum lipid metabolites, such as triglycerides, cholesterol and free fatty acids (Moon et al., 2002). Histological analysis of fat depots from knockout animals suggested

adipocyte cell hypertrophy associated with an increase in both fat cell maturation and differentiation that contributed to elevated fat tissue mass in *Dlk1* knockout mice. mRNA levels of FAS and SCD-1 (late adipocyte differentiation markers) were increased in fat pads and in enlarged fatty livers of *Dlk1* knockout mice (Moon et al., 2002). Mice overexpressing a *Dlk1* transgene exhibited reduced adipose tissue mass with smaller adipocyte cells, hypertriglyceridemia, hyperinsulinemia and insulin resistance (Lee et al., 2003), again indicating an important role for *Dlk1* in adipose tissue content and development of diabetes-like syndromes. Consistent with mouse metabolic phenotype, the role of *Dlk1* in human metabolic diseases has been highlighted by various studies, for example recently *Dlk1* expression has been associated adverse effects of severe obesity (O'Connell et al., 2011) and altered marrow adiposity and bone mineral density in women suffering from *Anorexia Nervosa* (Fazeli et al., 2009).

Predisposition to type 2 diabetes and metabolic syndrome has been associated with adipogenic capacity, suggesting that altered expression of adipogenic genes might control susceptibility to diet-induced metabolic syndrome. As an adipogenesis inhibitor, the *Dlk1* gene seems to be an appropriate candidate for this kind of function, as it has been shown to cause insulin resistance and simultaneously prevent diet-induced obesity and also had 6-fold higher expression in *db/db* mice resistant to obesity (Wang et al., 2008). These results raise a possibility of *Dlk1* having a role in the regulation of adipogenic response to chronic overnutrition and susceptibility to metabolic syndrome.

Both *Grb10* and *Dlk1* show pronounced expression in skeletal muscle during early development (see **Table** 1.3 in Section 1.4). *Dlk1* overexpression has been indicated as the cause of *callipyge* (*clpg*) phenotype in sheep (Charlier et al., 2001; Fleming-Waddell et al., 2009) associated with hypertrophic muscles, possibly resulting from an antiadipogenic function of *Dlk1* gene. Conditional knockout and overexpression studies in mice suggested a fundamental role for *Dlk1* in muscle development and regeneration (Waddell et al., 2010).

As *Grb10* has a confirmed role in insulin signalling and *Dlk1* a role in antiadipogenic action, experiments presented in this chapter were aimed at addressing the roles of *Grb10* and *Dlk1* in the maintenance of both glucose and lipid homeostasis *in vivo*. To elucidate contributions of *Grb10* and *Dlk1* to correct metabolic status in mice, we have performed a range of metabolic analyses on animals with knockouts of either *Grb10*, *Dlk1* or both of these genes. Analysis of feeding behaviour was undertaken along with an assessment of lean and fat tissue content by Dual X-ray absorptiometry. Mice have undergone glucose tolerance tests and, in addition, the levels of circulating blood glucose in fed and fasted mice were measured, together with levels

of triglycerides in blood serum. The histology of livers from mice of various ages was studied, together with white adipose tissue and potential changes in adipocyte cell size and/or number. Previous examinations of *Grb10 (*Charalambous et al., 2003; Smith et al., 2007) and *Dlk1* (Moon et al., 2002) knockout mice have shown that lack of either of these genes results in reciprocal metabolic phenotypes. Therefore, it was of interest to examine metabolic features of *Grb10*$^{m/+}$*/Dlk1*$^{+/p}$ double knockout mice and investigate if their phenotype resembles either of the single knockouts. The aim of these studies was to determine whether *Grb10* and *Dlk1* might influence metabolism by acting in a common pathway and, more generally, to provide additional information on how these imprinted genes influence metabolism *in vivo*.

5.2 Results

5.2.1 Feeding behaviour of *Dlk1*$^{+/p}$, *Grb10*$^{m/+}$ and *Grb10*$^{m/+}$/*Dlk1*$^{+/p}$ mice

Due to the previously described marked reduction in body fat of *Grb10*$^{m/+}$ knockout animals (Smith et al., 2007) and diet-dependent predisposition to increased adiposity in *Dlk1* knockout mice (Moon et al., 2002) a study of feeding behaviour was undertaken in *Grb10*$^{m/+}$, *Dlk1*$^{+/p}$ and *Grb10*$^{m/+}$/*Dlk1*$^{+/p}$ mice. In order to investigate the influence of both *Grb10* and *Dlk1* genes on feeding behaviour, the amount of food consumed and the fluctuations in body weights of individually caged animals were monitored over a period of 2 weeks. In addition, the food consumption rates for all genotypes were calculated using a ratio of 2/3 as a scaling component (White and Seymour, 2003) and compared to total body weights. Feeding behaviour was examined for animals of 2 different age groups (3-6 and 7-9 months) and both sexes, but as the results for both age groups showed similar trends (showed in Appendix 1) the data has been pooled together.

The total amount of consumed food over the analysed period of time is presented in **Figure** 5.1 A and B. The statistical analysis revealed no significant differences between the amounts of consumed food by males and females of any genotype. Also the food consumption rates (**Figure** 5.1 C and D) proved to be similar between all the genotypes and for both sexes.

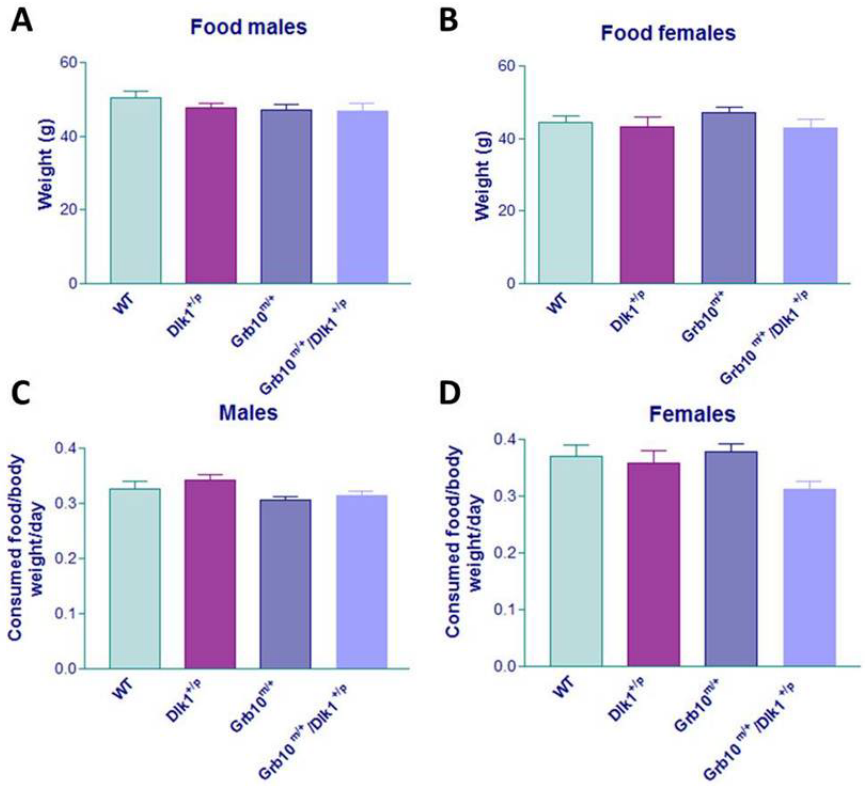

E

	Food males	Food females	Consumption rate males	Consumption rate females
WT vs Grb10$^{m/+}$	ns	ns	ns	ns
WT vs Dlk1$^{+/p}$	ns	ns	ns	ns
WT vs Grb10$^{m/+}$/Dlk1$^{+/p}$	ns	ns	ns	ns
Grb10$^{m/+}$ vs Dlk1$^{+/p}$	ns	ns	ns	ns
Grb10$^{m/+}$ vs Grb10$^{m/+}$/Dlk1$^{+/p}$	ns	ns	ns	ns
Dlk1$^{+/p}$ vs Grb10$^{m/+}$/Dlk1$^{+/p}$	ns	ns	ns	ns

Figure 5.1 Analysis of feeding behaviour in wild type, *Grb10$^{m/+}$*, *Dlk1$^{+/p}$* and *Grb10$^{m/+}$/Dlk1$^{+/p}$* mice.

Food intake was monitored over a period of two weeks. Food consumption rates have been calculated as food consumed per gram of animal body weight per day to the power of 2/3. **A)** Total amount of consumed food by males. **B)** Total amount of consumed food by females. **C)** Male consumption rates: total weight of food consumed by males per gram of body weight per day to the power of 2/3. **D)** Female consumption rates: total weight of food consumed by females per gram of body weight per day to the power of 2/3. There were no significant changes neither in the amounts of consumed food or in food consumption rates of transgenic mice when compared to wild type controls. **E)** Table summarising results of statistical analysis. All values represent means ± SEM and have been subject to one way ANOVA with post hoc Tukey's analysis. Males: WT n=14, *Dlk1$^{+/p}$*=12, *Grb10$^{m/+}$* n=12 and *Grb10$^{m/+}$/Dlk1$^{+/p}$* n=13; females: WT n=13, *Dlk1$^{+/p}$*=12, *Grb10$^{m/+}$* n=12 and *Grb10$^{m/+}$/Dlk1$^{+/p}$* n=12.

5.2.2 Glucose tolerance tests of *Dlk1*$^{+/p}$, *Grb10*$^{m/+}$ and *Grb10*$^{m/+}$/*Dlk1*$^{+/p}$ mice

Several imprinted genes have been implicated in maintenance of metabolic homeostasis (see Section 5.1). Glucose metabolism is of a vital importance in sustaining the correct metabolic body functions, therefore any abnormalities in glucose tolerance or clearance could have potentially detrimental effects on the overall fitness of an animal. Recently, some evidence has been provided for the role of *Grb10* in glucose homeostasis (Smith et al., 2007; Wang et al., 2007; Yamamoto et al., 2008), supported by experiments showing *Grb10* interactions with the insulin receptor (O'Neill et al., 1996; He et al., 1998). Our lab has reported that *Grb10*$^{m/+}$ mice clear glucose more rapidly when compared to wild type littermates (Smith et al., 2007). As a result we decided to use glucose tolerance tests (GTT) to establish whether *Grb10*$^{m/+}$/*Dlk1*$^{+/p}$ mice might show the same trend.

Male and female mice aged 3-9 months were subject to glucose tolerance tests as described in Section 2.5.4. Animals were pooled together as both age groups displayed similar trends (showed in Appendix 2). Consistent with insulin mediated glucose uptake, increased glucose levels were observed 15 min after glucose injection, with a subsequent gradual decrease in glucose concentration over time. The shapes of glucose curves differed slightly between sexes, but they were consistent with previously described results for *Grb10*$^{m/+}$ mice (Smith et al., 2007). Our results showed that from 15 up to 90 minutes post injection both male and female *Grb10*$^{m/+}$ and *Grb10*$^{m/+}$/*Dlk1*$^{+/p}$ mice showed significantly improved abilities to clear a glucose load when compared to *Dlk1*$^{+/p}$ littermates (**Figure** 5.2 A and B), as assessed by analysis of the incremental areas under curves (**Figure** 5.2 C and D). In contrast, the trend of impaired ability to clear glucose load was noted in *Dlk1*$^{+/p}$, however it did not become statistically significant.

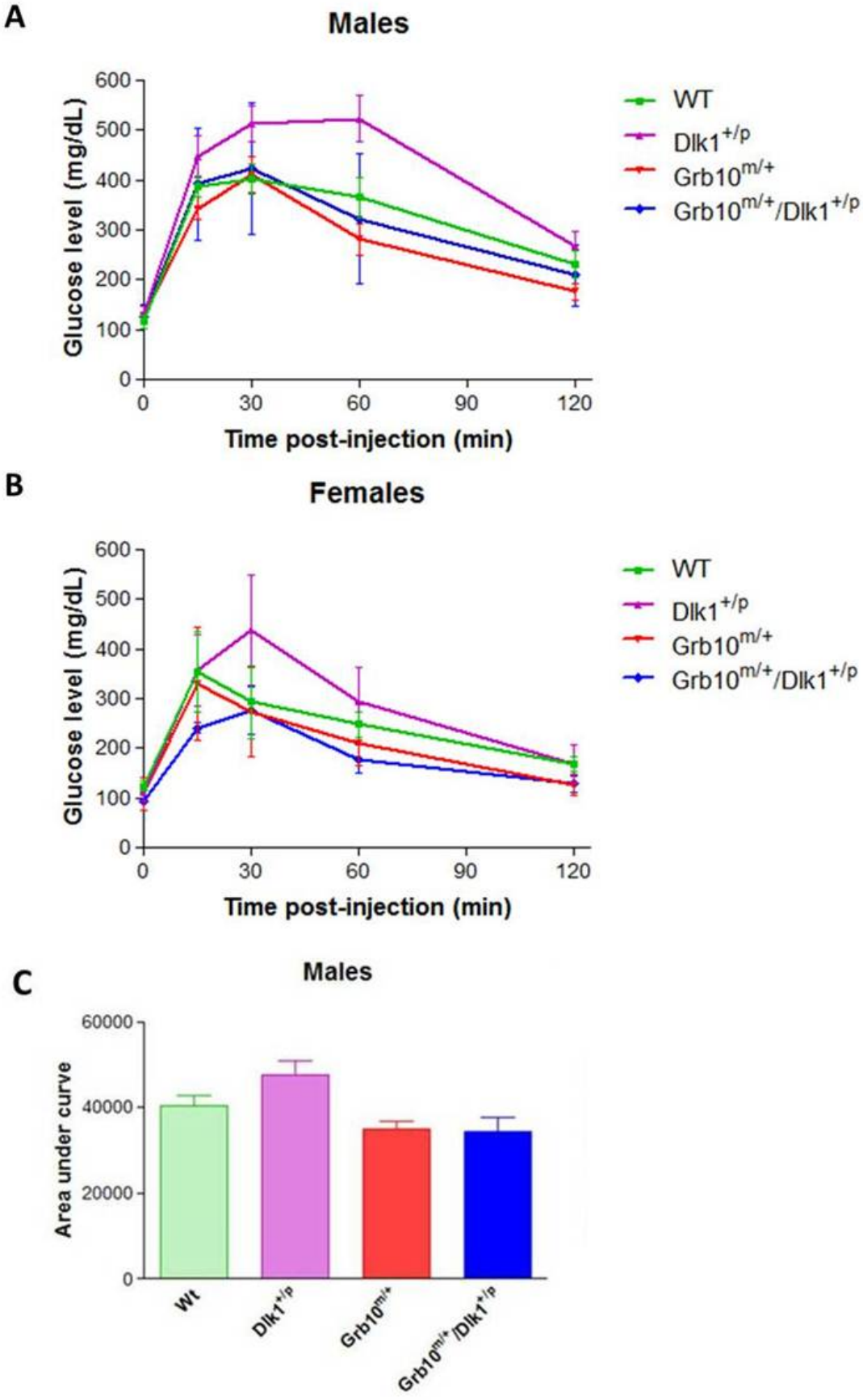
A
Males
Glucose level (mg/dL)
600
500
400
300
200
100
0
0
30
60
90
120
Time post-injection (min)
WT
Dlk1+/p
Grb10m/+
Grb10m/+/Dlk1+/p
B
Females
Glucose level (mg/dL)
600
500
400
300
200
100
0
0
30
60
90
120
Time post-injection (min)
WT
Dlk1+/p
Grb10m/+
Grb10m/+/Dlk1+/p
C
Males
Area under curve
60000
40000
20000
0
Wt
Dlk1+/p
Grb10m/+
Grb10m/+/Dlk1+/p

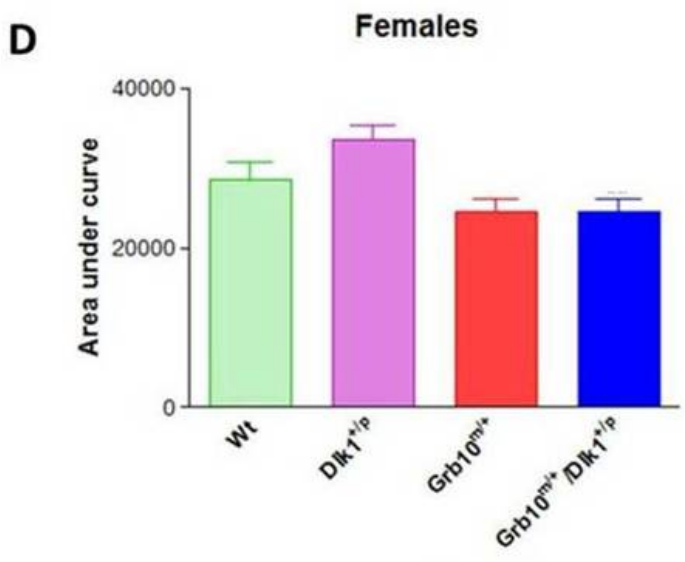

E

	Males	Females
WT vs Grb10$^{m/+}$	ns	ns
WT vs Dlk1$^{+/p}$	ns	ns
WT vs Grb10$^{m/+}$/Dlk1$^{+/p}$	ns	ns
Grb10$^{m/+}$ vs Dlk1$^{+/p}$	**	**
Grb10$^{m/+}$ vs Grb10$^{m/+}$/Dlk1$^{+/p}$	ns	ns
Dlk1$^{+/p}$ vs Grb10$^{m/+}$/Dlk1$^{+/p}$	**	**

Figure 5.2 Glucose tolerance in male and female wild type, *Grb10$^{m/+}$*, *Dlk1$^{+/p}$* and *Grb10$^{m/+}$/Dlk1$^{+/p}$* mice.

Male and female 3-9 months old mice were examined for their ability to clear an intraperitoneal dose of glucose. **A)** and **B)** Results from glucose tolerance tests for male and female mice. **C)** and **D)** Histograms representing areas under glucose curves for male and female mice. Analysis of areas under glucose curves revealed that *Grb10$^{m/+}$* and *Grb10$^{m/+}$/Dlk1$^{+/p}$* mice of both sexes cleared glucose significantly faster than *Dlk1$^{+/p}$* (**p<0.01) animals. **E)** Table summarising results of statistical analysis. All values represent means ± SEM and have been subject to one way ANOVA with post hoc Tukey's analysis. Males: WT n=14, *Dlk1$^{+/p}$*=12, *Grb10$^{m/+}$* n=12 and *Grb10$^{m/+}$/Dlk1$^{+/p}$* n=13; females: WT n=13, *Dlk1$^{+/p}$*=12, *Grb10$^{m/+}$* n=12 and *Grb10$^{m/+}$/Dlk1$^{+/p}$* n=12.

5.2.3 Glucose levels in fed and fasted mice of *Dlk1*$^{+/p}$, *Grb10*$^{m/+}$ and *Grb10*$^{m/+}$/*Dlk1*$^{+/p}$ mice

In order to examine levels of blood glucose in fasted (with food removed for 16 hours including the overnight period) and fed (fed regular diet available *ad libitum*) mice of all four genotypes, tail blood was collected as described in Section 2.5.5.

The obtained results pointed towards slightly elevated glucose levels in both fed and fasted *Dlk1*$^{+/p}$ male mice (**Figure** 5.3 A and B), although they did not translate into significant differences. On the other hand, fed basal serum glucose levels in female mice indicated that *Grb10*$^{m/+}$/*Dlk1*$^{+/p}$ and *Grb10*$^{m/+}$ knockout female mice became significantly hypoglycaemic when compared to wild type control littermates (**Figure** 5.3 D). There was a slight, but non-significant, trend in the same direction for *Grb10*$^{m/+}$/*Dlk1*$^{+/p}$ and *Grb10*$^{m/+}$ male mice (**Figure** 5.3 C).

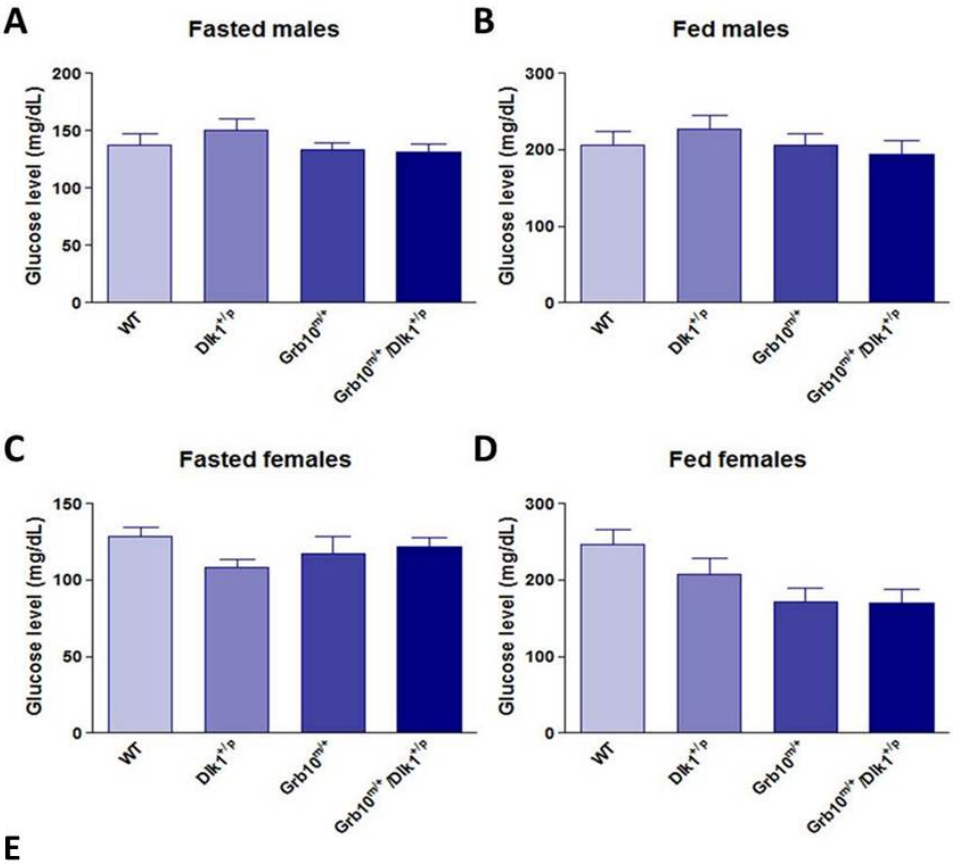

E

	Fasted males	Fed males	Fasted females	Fed females
WT vs Grb10$^{m/+}$	ns	ns	ns	*
WT vs Dlk1$^{+/p}$	ns	ns	ns	ns
WT vs Grb10$^{m/+}$/Dlk1$^{+/p}$	ns	ns	ns	*
Grb10$^{m/+}$ vs Dlk1$^{+/p}$	ns	ns	ns	ns
Grb10$^{m/+}$ vs Grb10$^{m/+}$/Dlk1$^{+/p}$	ns	ns	ns	ns
Dlk1$^{+/p}$ vs Grb10$^{m/+}$/Dlk1$^{+/p}$	ns	ns	ns	ns

Figure 5.3. Analysis of basal glucose levels in fed and fasted wild type, *Grb10$^{m/+}$*, *Dlk1$^{+/p}$* and *Grb10$^{m/+}$/Dlk1$^{+/p}$* mice.

Concentration of serum glucose from tail blood was analysed using a glucometer in female and male mice. Fasted glucose readings were taken from animals without access to food for a period of 16 hours. Fed glucose readings were taken from animals receiving food *ad libitum.* **A)** and **B)** Male animals showed no deviation from WT glucose levels in either fed or fasted state. **C)** Female mutant mice showed no deviation from WT glucose levels in a fasted state. **D)** Female *Grb10$^{m/+}$* and *Grb10$^{m/+}$/Dlk1$^{+/p}$* animals were significantly hypoglycaemic in a fed state compared to WT controls (*p<0.05). **E)** Table summarising results of statistical analysis. All values represent means ± SEM and have been subject to one way ANOVA with post hoc Tukey's analysis. Males: WT n=14, *Dlk1$^{+/p}$*=12, *Grb10$^{m/+}$* n=12 and *Grb10$^{m/+}$/Dlk1$^{+/p}$* n=13; females: WT n=13, *Dlk1$^{+/p}$*=12, *Grb10$^{m/+}$* n=12 and *Grb10$^{m/+}$/Dlk1$^{+/p}$* n=12.

5.2.4 Triglyceride levels in blood serum in *Dlk1*$^{+/p}$, *Grb10*$^{m/+}$ and *Grb10*$^{m/+}$/*Dlk1*$^{+/p}$ mice

In addition to glucose, various other metabolic compounds are known to be crucial in maintenance of metabolic homeostasis. Triglyceride levels affect many basic body functions and *Dlk1* knockout mice have been previously reported to show elevated levels of serum triglycerides (Moon et al., 2002). The concentration of triglycerides was measured and compared for all four genotypes (**Figure** 5.4). *Dlk1*$^{+/p}$ mice had significantly higher levels of triglycerides in their blood stream when compared to *Grb10*$^{m/+}$ animals which were showing an opposite trend, however, neither increased triglyceride levels in *Dlk1*$^{+/p}$ mice nor lower triglyceride levels in *Grb10*$^{m/+}$ were significantly different from those of wild type controls. In *Grb10*$^{m/+}$/*Dlk1*$^{+/p}$ animals the triglyceride levels were also comparable to those of wild type animals.

A

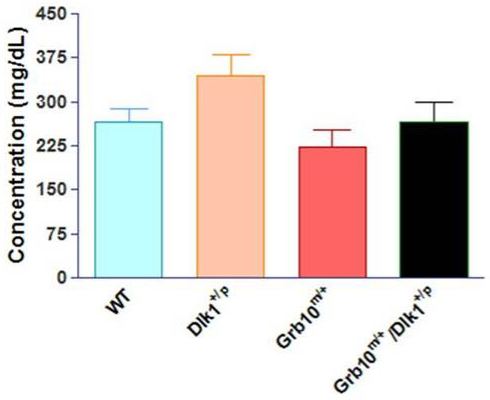

B

	Triglyceride concentration
Wt vs Grb10$^{m/+}$	ns
Wt vs Dlk1$^{+/p}$	ns
Wt vs Grb10$^{m/+}$/Dlk1$^{+/p}$	ns
Grb10$^{m/+}$ vs Dlk1$^{+/p}$	*
Grb10$^{m/+}$ vs Grb10$^{m/+}$/Dlk1$^{+/p}$	ns
Dlk1$^{+/p}$ vs Grb10$^{m/+}$/Dlk1$^{+/p}$	ns

Figure 5.4 Levels of triglycerides in mouse blood serum of wild type, *Grb10$^{m/+}$*, *Dlk1$^{+/p}$* and *Grb10$^{m/+}$/Dlk1$^{+/p}$* mice.

A) Triglyceride levels in blood serum were measured in 3 month old male mice. *Dlk1$^{+/p}$* mice were found to have significantly elevated (*p<0.05) levels of triglycerides in blood serum in comparison to *Grb10$^{m/+}$*. **B)** Table summarising results of statistical analysis. All values represent means ± SEM and have been subject to one way ANOVA with post hoc Tukey's analysis. WT n=6, *Dlk1$^{+/p}$*=6, *Grb10$^{m/+}$* n=6 and *Grb10$^{m/+}$/Dlk1$^{+/p}$* n=6.

5.2.5 Dual energy X-ray absorptiometry analysis of *Dlk1*$^{+/p}$, *Grb10*$^{m/+}$ and *Grb10*$^{m/+}$/*Dlk1*$^{+/p}$ mice

Previous experiments showed that ablation of the *Grb10* and *Dlk1* genes had essentially opposite effects on adipose tissue content in corresponding knockout mice. Adult *Grb10*$^{m/+}$ knockout mice displayed decreased levels of adipose tissue (Smith et al., 2007) while *Dlk1* knockout mice exhibited increased adiposity when fed a high fat diet (Moon et al., 2002). Therefore, it was of interest to investigate if *Grb10*$^{m/+}$/*Dlk1*$^{+/p}$ knockout mice might resemble any of the previously identified phenotypes or follow the adiposity pattern of wild type control mice.

To identify and compare physiological differences between mice of different genotypes we performed Dual energy X-ray absorptiometry (DXA) analysis of carcasses of animals previously used for study of food consumption and GTTs. Measured parameters included bone mineral density (BMD), bone mineral content (BMC) and lean and fat tissue content.

No differences in bone mineral density and bone mineral content were identified in male mice (**Figure** 5.5 A and B), which suggested that there was no change in bone quantity and composition. We also did not find any alterations in bone mineral density in female mice (**Figure** 5.6 A), however *Dlk1*$^{+/p}$ female mice showed significantly decreased bone mineral content in comparison to wild types (**Figure** 5.6 B).

Lean tissue content was significantly increased for *Grb10*$^{m/+}$ male mice when compared to wild type and *Dlk1*$^{+/p}$ mice and it was also higher in *Grb10*$^{m/+}$/*Dlk1*$^{+/p}$ mice when compared to *Dlk1*$^{+/p}$ (**Figure** 5.5 C). In addition, *Grb10*$^{m/+}$ female mice had significantly higher content of lean tissue when compared to *Dlk1*$^{+/p}$ (**Figure** 5.6 C). *Grb10*$^{m/+}$ mice also exhibited significantly increased percentage of lean mass compared to *Dlk1*$^{+/p}$ (for males **Figure** 5.5 E and for females **Figure** 5.6 E). No abnormalities were found in fat tissue content for any of the sexes (**Figure** 5.5 D and **Figure** 5.6 D), although a significantly reduced percentage of fat mass was noted in *Grb10*$^{m/+}$ compared to *Dlk1*$^{+/p}$ animals (for males, **Figure** 5.5 F and for females, **Figure** 5.6 F).

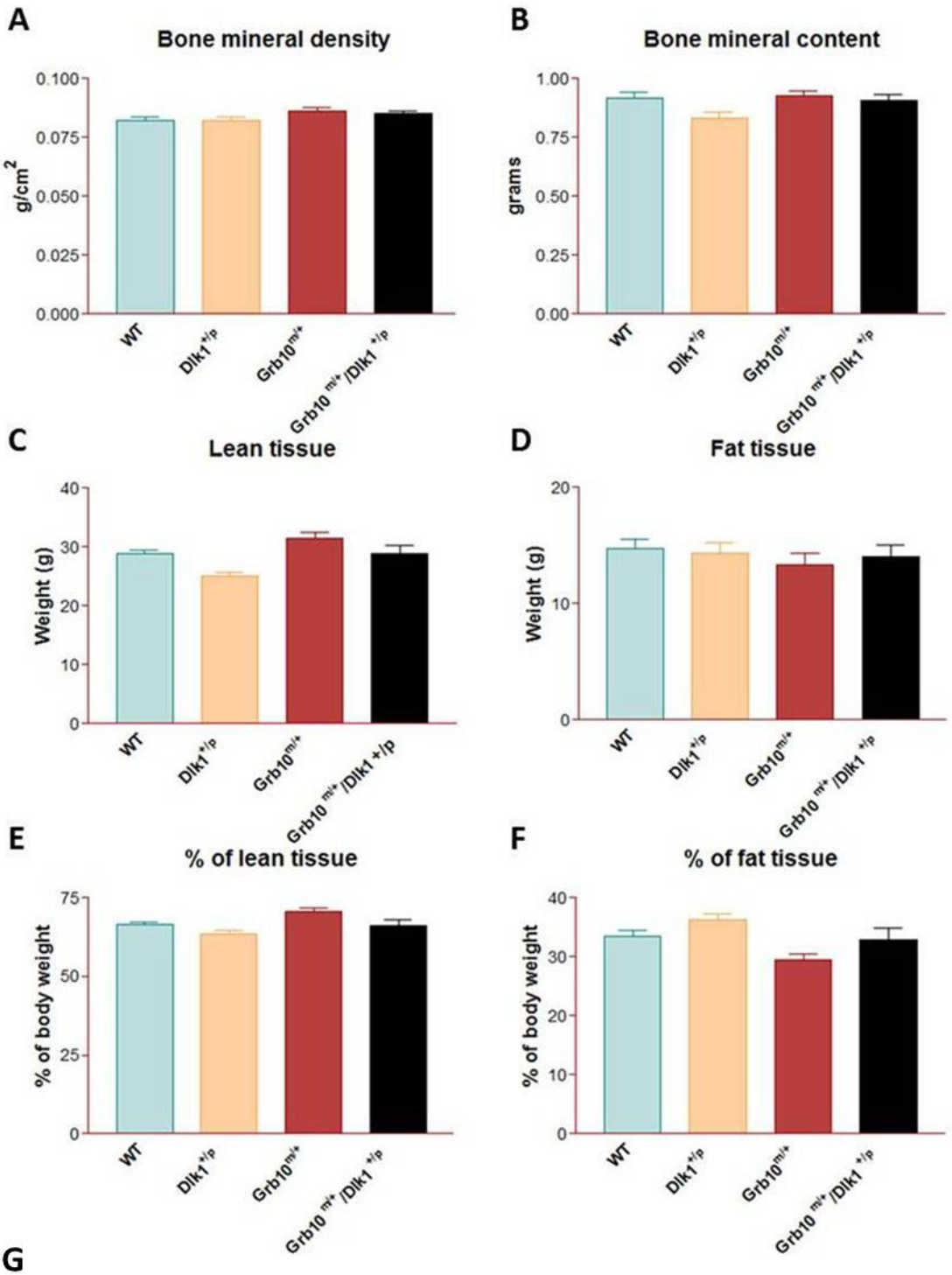

G

	BMD	BMC	Lean tissue	Fat tissue	% of lean tissue	% of fat tissue
WT vs Grb10$^{m/+}$	ns	ns	*	ns	ns	ns
WT vs Dlk1$^{+/p}$	ns	ns	ns	ns	ns	ns
WT vs Grb10$^{m/+}$/Dlk1$^{+/p}$	ns	ns	ns	ns	ns	ns
Grb10$^{m/+}$ vs Dlk1$^{+/p}$	ns	ns	***	ns	**	*
Grb10$^{m/+}$ vs Grb10$^{m/+}$/Dlk1$^{+/p}$	ns	ns	ns	ns	ns	ns
Dlk1$^{+/p}$ vs Grb10$^{m/+}$/Dlk1$^{+/p}$	ns	ns	*	ns	ns	ns

Figure 5.5 DXA analysis of adult wild type, *Grb10*$^{m/+}$, *Dlk1*$^{+/p}$ and *Grb10*$^{m/+}$/*Dlk1*$^{+/p}$ male mice.
Carcasses of male animals were analysed by Dual X-ray absorptiometry to examine various parameters of body composition. **A)** and **B)** No differences were seen in bone mineral density (BMD) or bone mineral content (BMC). **C)** Total lean tissue mass was significantly elevated in *Grb10*$^{m/+}$ animals when compared to wild type (*p<0.05) and *Dlk1*$^{+/p}$ mice (***p<0.001) and in *Grb10*$^{m/+}$/*Dlk1*$^{+/p}$ animals when compared to *Dlk1*$^{+/p}$ (*p<0.05) **D)** No alterations were observed in total fat tissue content. **E)** Percentage of lean mass was significantly increased (***p*<0.01) in *Grb10*$^{m/+}$ mice in comparison to *Dlk1*$^{+/p}$ mice. **F)** Percentage of fat mass was significantly reduced (**p*<0.05) in *Grb10*$^{m/+}$ mice in comparison to *Dlk1*$^{+/p}$ mice. **G)** Table summarising results of statistical analysis. All values represent means ± SEM and have been subject to one way ANOVA with post hoc Tukey's analysis. WT n=14, *Dlk1*$^{+/p}$=12, *Grb10*$^{m/+}$ n=12 and *Grb10*$^{m/+}$/*Dlk1*$^{+/p}$ n=12.

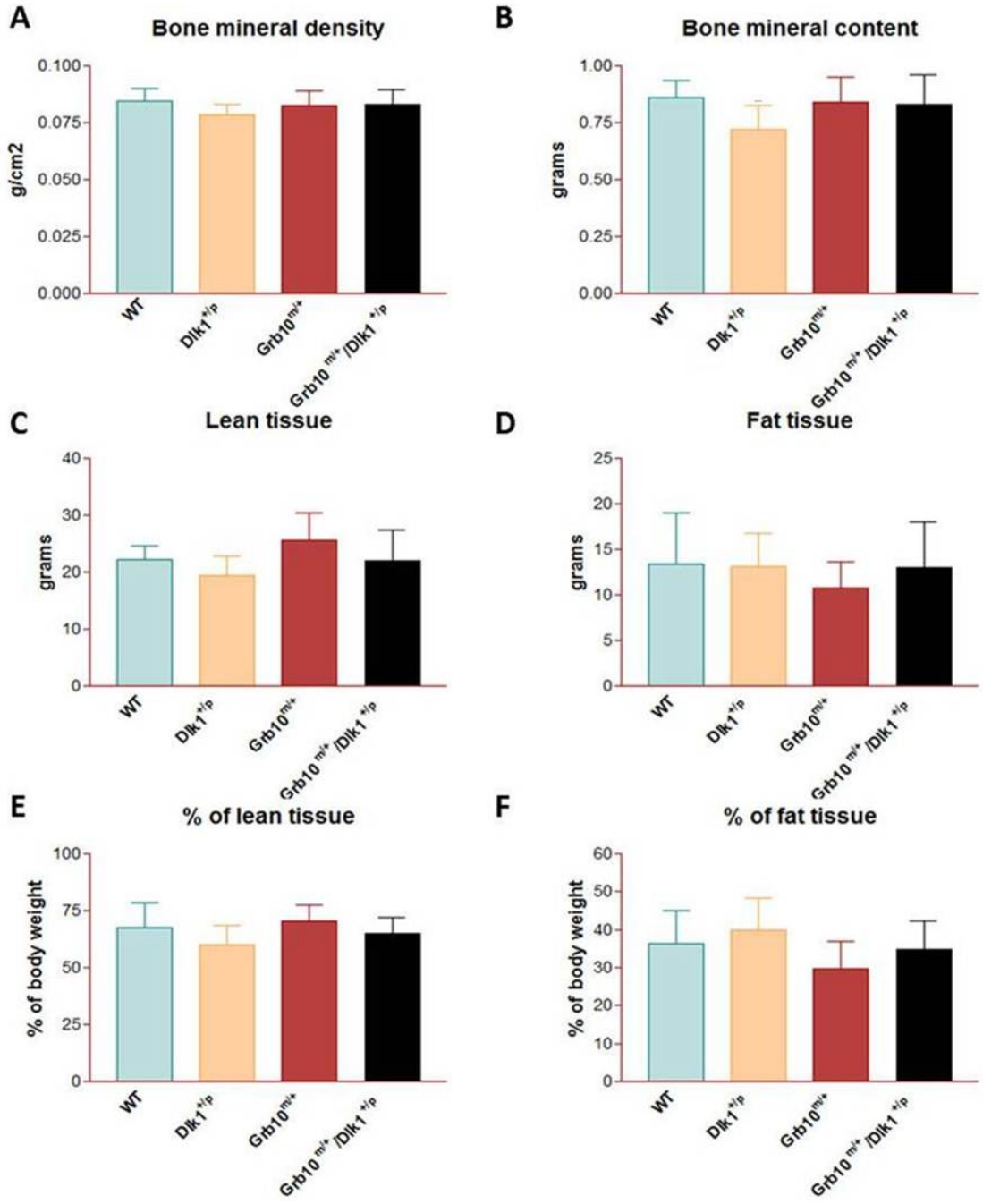

G

	BMD	BMC	Lean tissue	Fat tissue	% of lean tissue	% of fat tissue
WT vs Grb10$^{m/+}$	ns	ns	ns	ns	ns	ns
WT vs Dlk1$^{+/p}$	ns	*	ns	ns	ns	ns
WT vs Grb10$^{m/+}$/Dlk1$^{+/p}$	ns	ns	ns	ns	ns	ns
Grb10$^{m/+}$ vs Dlk1$^{+/p}$	ns	ns	**	ns	*	*
Grb10$^{m/+}$ vs Grb10$^{m/+}$/Dlk1$^{+/p}$	ns	ns	ns	ns	ns	ns
Dlk1$^{+/p}$ vs Grb10$^{m/+}$/Dlk1$^{+/p}$	ns	ns	ns	ns	ns	ns

Figure 5.6 DXA analysis of adult wild type, *Grb10*$^{m/+}$, *Dlk1*$^{+/p}$ and *Grb10*$^{m/+}$/*Dlk1*$^{+/p}$ female mice.

Carcasses of female animals were analysed by Dual X-ray absorptiometry to examine various parameters of body composition. **A)** No differences were found in bone mineral density (BMD). **B)** Bone mineral content was significantly reduced in *Dlk1*$^{+/p}$ mice in comparison to wild type (*p<0.05). **C)** Total lean tissue mass was significantly elevated in *Grb10*$^{m/+}$ animals (**p<0.001) when compared to *Dlk1*$^{+/p}$. **D)** No changes were seen in total fat tissue content. **E)** Percentage of lean mass was significantly increased (**p*<0.05) in *Grb10*$^{m/+}$ mice in comparison to *Dlk1*$^{+/p}$ mice. **F)** Percentage of fat mass was significantly reduced (**p*<0.05) in *Grb10*$^{m/+}$ mice when compared to *Dlk1*$^{+/p}$. **G)** Table summarising results of statistical analysis. All values represent means ± SEM and have been subject to one way ANOVA with post hoc Tukey's analysis. WT n=13, *Dlk1*$^{+/p}$=12, *Grb10*$^{m/+}$ n=12 and *Grb10*$^{m/+}$/*Dlk1*$^{+/p}$ n=12.

5.2.6 Liver lipid content in *Dlk1*$^{+/p}$, *Grb10*$^{m/+}$ and *Grb10*$^{m/+}$/*Dlk1*$^{+/p}$ mice

Lipid metabolism is strictly associated with maintenance of energy homeostasis and liver is known to play a key role in energy homeostasis of lipid metabolism. In vertebrate species liver is the typical site for fatty acid synthesis and lipid circulation through lipoprotein synthesis. Any discrepancies in lipid synthesis, storage or circulation might have significant effects on overall body health status and lead to serious diseases such as hepatic steatosis or fatty liver disease (Nguyen et al., 2008).

In light of genotype-related liver weight discrepancies reported in previous chapters we performed histological analyses of livers from mice of various ages in order to investigate any potential morphological differences that might be associated with the identified growth phenotypes. No obvious differences were found in E14.5 embryonic livers stained with H&E (**Figure** 5.7), however, the presence of white, round spaces was noted in neonatal *Grb10*$^{m/+}$ and *Grb10*$^{m/+}$/*Dlk1*$^{+/p}$ livers (**Figure** 5.8). These spaces were also present in approximately half of examined *Grb10*$^{m/+}$ and *Grb10*$^{m/+}$/*Dlk1*$^{+/p}$ livers from 1 week old mice (**Figure** 5.9). in contrast to that *Grb10*$^{m/+}$ and *Grb10*$^{m/+}$/*Dlk1*$^{+/p}$ livers from 3 month old male mice looked comparable to wild type, but at this stage *Dlk1*$^{+/p}$ livers were found to have an abnormal accumulation of white, round spaces (**Figure** 5.10). To investigate the nature of the observed white structures, we carried out Periodic acid-Schiff (PAS) staining on neonatal old livers in order to learn if the abnormal appearance of these organs is the result of increased accumulation of glycogen. The result from PAS staining was negative, no differences were found between genotypes, suggesting that histological differences were not due to altered levels in glycogen content between genotypes (**Figure** 5.11). We then stained cryosections from neonatal livers with Oil Red O, an indicator of the presence of lipid droplets that stain red. Cryosections from *Grb10*$^{m/+}$ and *Grb10*$^{m/+}$/*Dlk1*$^{+/p}$ neonatal livers indeed showed increased accumulation of red lipid droplets (**Figure** 5.12). In keeping with results previously described for H&E staining, there was an increased red lipid droplet accumulation in *Dlk1*$^{+/p}$ but not in *Grb10*$^{m/+}$ and *Grb10*$^{m/+}$/*Dlk1*$^{+/p}$ adult livers (**Figure** 5.13).

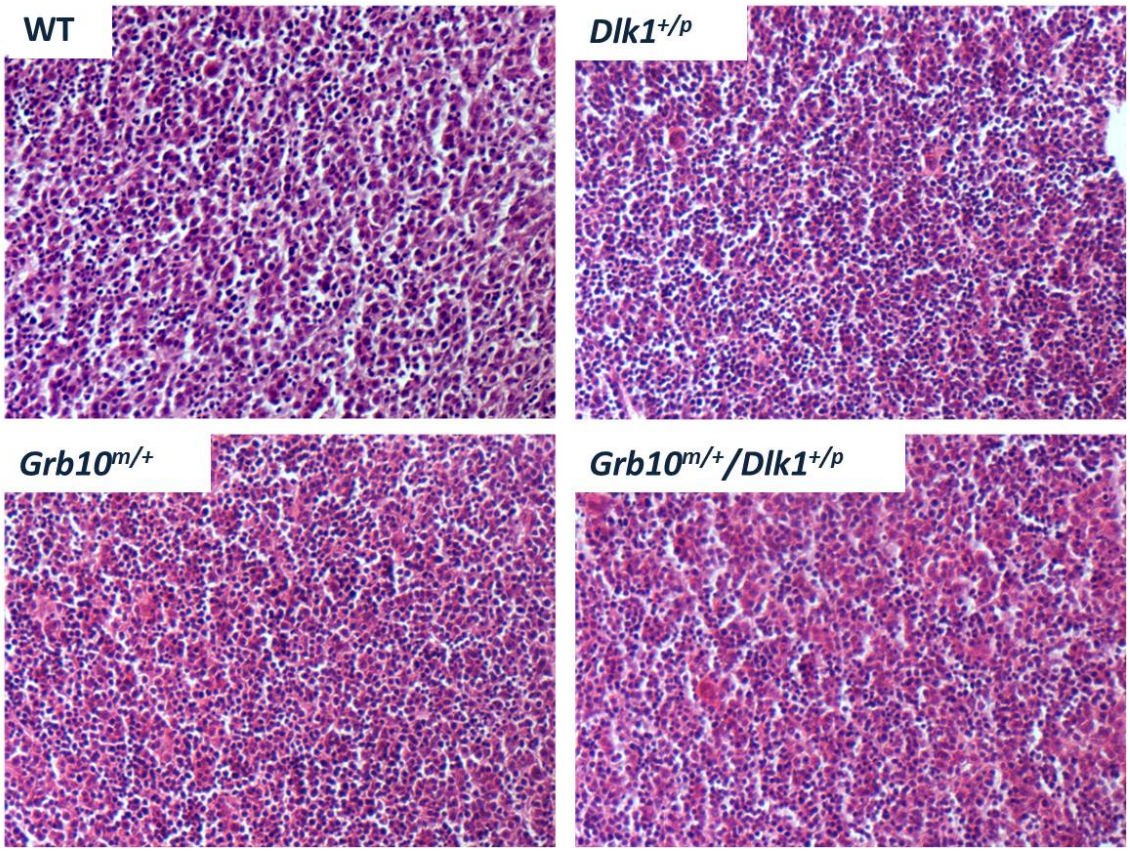

Figure 5.7 H&E stained liver sections of wild type, *Grb10*$^{m/+}$, *Dlk1*$^{+/p}$ and *Grb10*$^{m/+}$/*Dlk1*$^{+/p}$ E14.5 embryos under 200x magnification.

Livers were stained with H&E and representative sections are shown. No differences in liver histology were apparent among the analysed genotypes. WT n=5, *Dlk1*$^{+/p}$=5, *Grb10*$^{m/+}$ n=5 and *Grb10*$^{m/+}$/*Dlk1*$^{+/p}$ n=5.

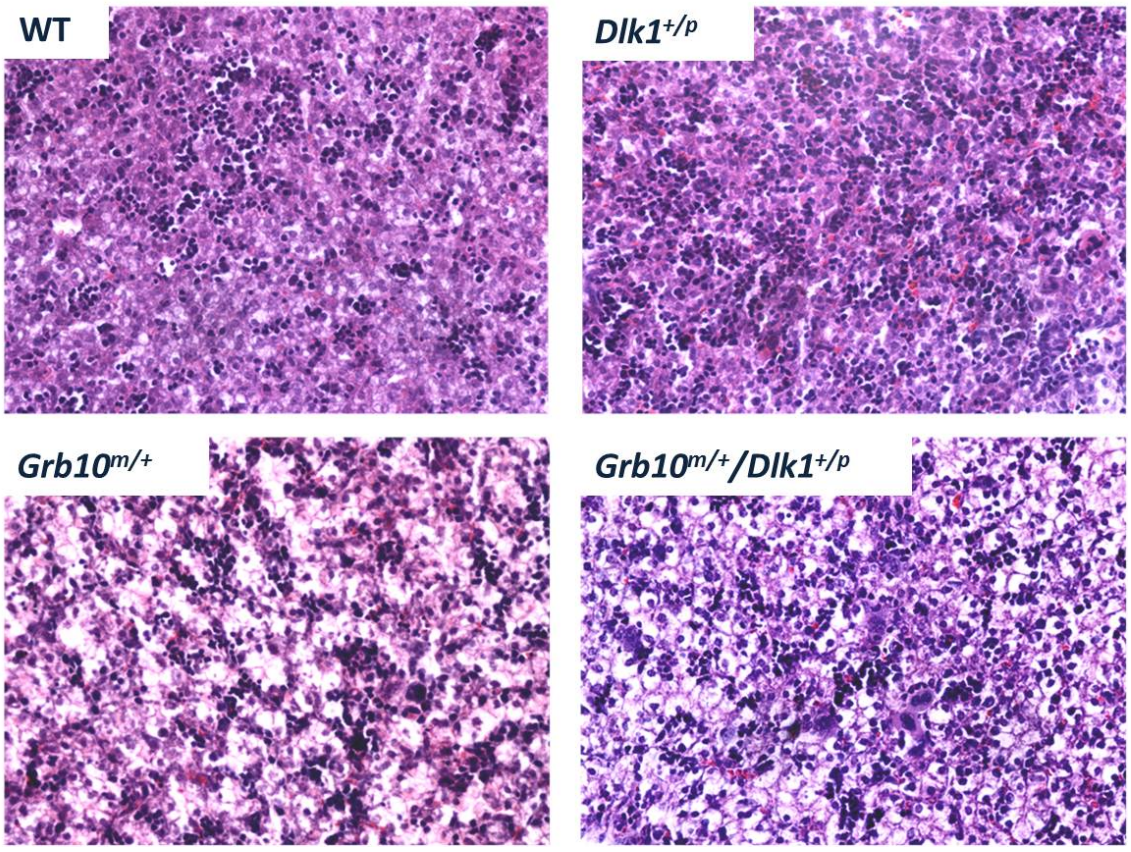

Figure 5.8 H&E stained liver sections of neonatal wild type, *Grb10*$^{m/+}$, *Dlk1*$^{+/p}$ and *Grb10*$^{m/+}$/*Dlk1*$^{+/p}$ mice under 200x magnification.

Livers from 1 day old mice were stained with H&E. *Dlk1*$^{+/p}$ sections were indistinguishable from wild type, but *Grb10*$^{m/+}$ and *Grb10*$^{m/+}$/*Dlk1*$^{+/p}$ livers showed the presence of large numbers of white, round spaces. Presented images show representative sections for each of the analysed genotypes. WT n=5, *Dlk1*$^{+/p}$=5, *Grb10*$^{m/+}$ n=5 and *Grb10*$^{m/+}$/*Dlk1*$^{+/p}$ n=5.

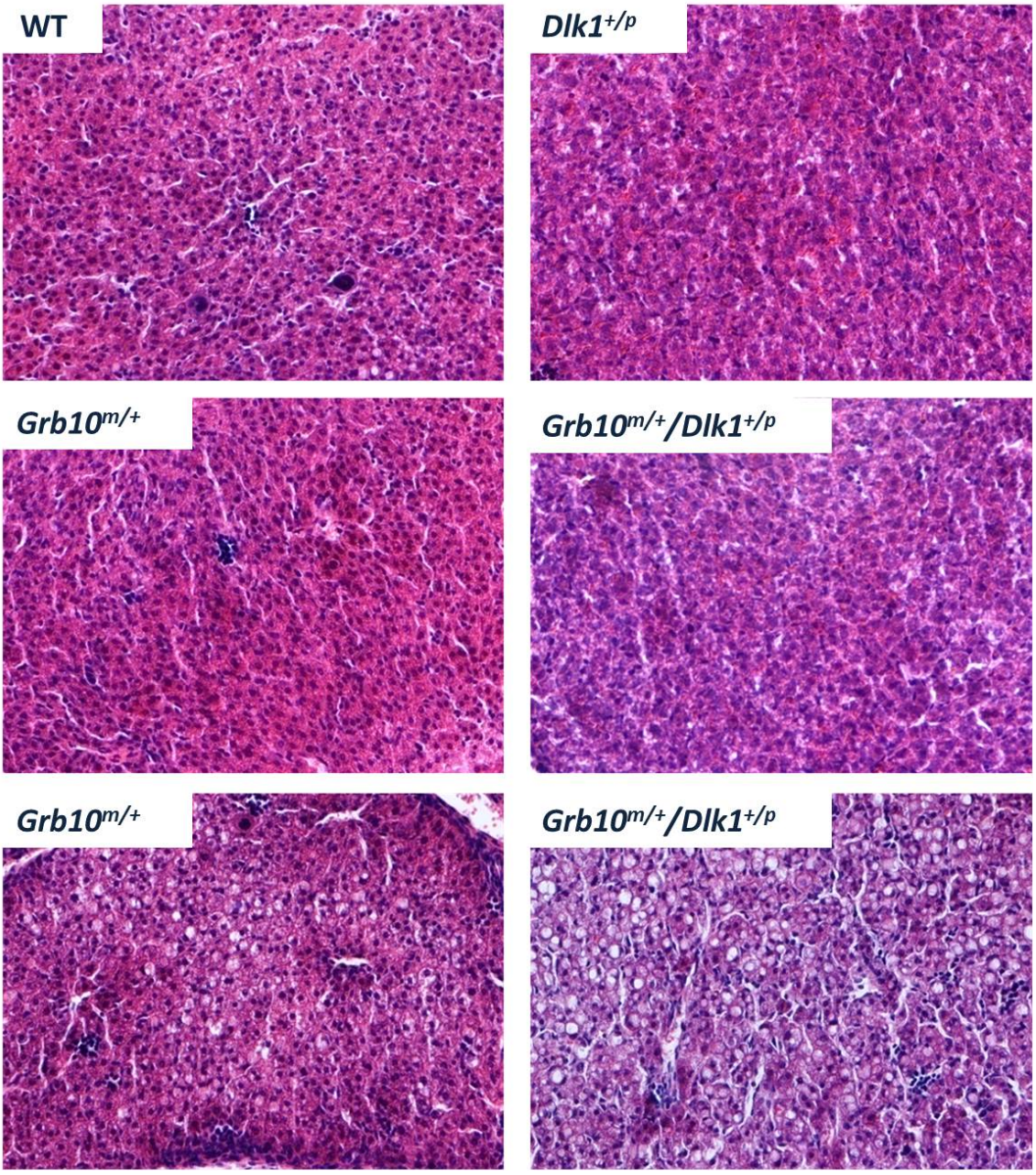

Figure 5.9 H&E stained liver sections of wild type, *Grb10*$^{m/+}$, *Dlk1*$^{+/p}$ and *Grb10*$^{m/+}$/*Dlk1*$^{+/p}$ 1 week old mice under 200x magnification.

Livers from 1 week old mice were stained with H&E. In wild type and *Dlk1*$^{+/p}$ no differences in histology were observed. This was also the case for some *Grb10*$^{m/+}$ and *Grb10*$^{m/+}$/*Dlk1*$^{+/p}$ (middle panel) livers but in other cases (bottom panel) the presence of white, round spaces was noted. Presented images show representative sections for each of the analysed genotypes. WT n=6, *Dlk1*$^{+/p}$=6, *Grb10*$^{m/+}$ n=6 and *Grb10*$^{m/+}$/*Dlk1*$^{+/p}$ n=6.

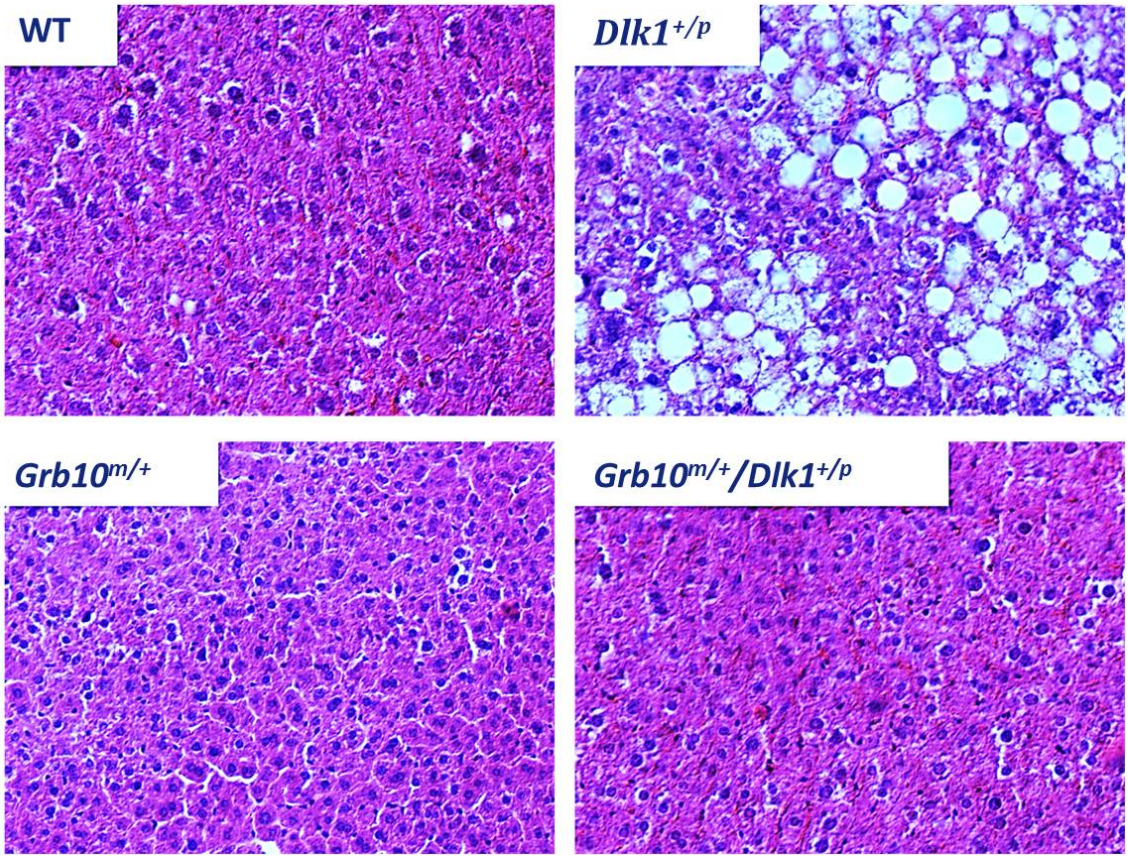

Figure 5.10 H&E stained liver sections of wild type, *Grb10$^{m/+}$*, *Dlk1$^{+/p}$* and *Grb10$^{m/+}$/Dlk1$^{+/p}$* 3 month old mice under 200x magnification.

Livers from 3 month old male mice were stained with H&E. In wild type, *Grb10$^{m/+}$* and *Grb10$^{m/+}$/Dlk1$^{+/p}$* no differences in histology were observed, however the presence of abundant white, round spaces was noted in *Dlk1$^{+/p}$* livers. Presented images show representative sections for each of the analysed genotypes. WT n=5, *Dlk1$^{+/p}$*=5, *Grb10$^{m/+}$* n=5 and *Grb10$^{m/+}$/Dlk1$^{+/p}$* n=5.

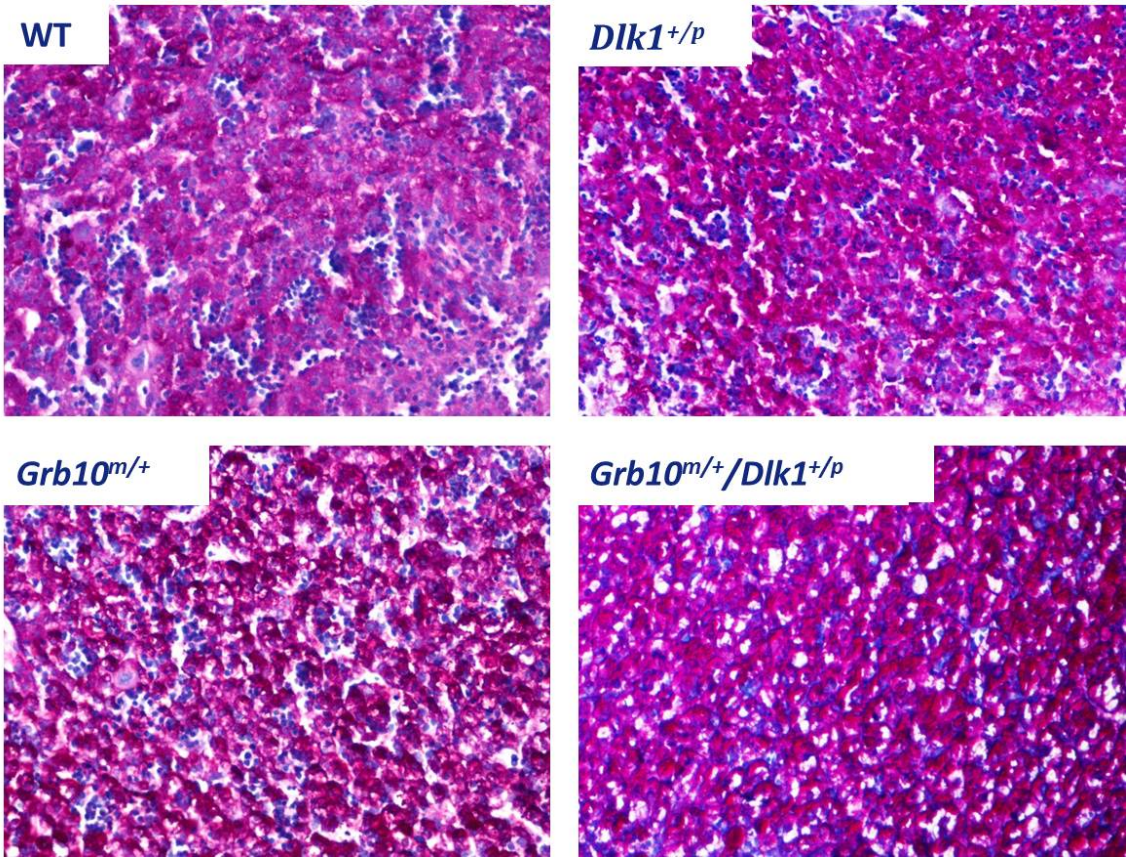

Figure 5.11 PAS stained liver sections of neonatal wild type, *Grb10*$^{m/+}$, *Dlk1*$^{+/p}$ and *Grb10*$^{m/+}$/*Dlk1*$^{+/p}$ neonatal old mice under 200x magnification.

Livers from 1 day old mice were stained with PAS. No differences in liver histology were apparent among the analysed genotypes. Presented images show representative sections for each of the analysed genotypes. WT n=5, *Dlk1*$^{+/p}$=5, *Grb10*$^{m/+}$ n=5 and *Grb10*$^{m/+}$/*Dlk1*$^{+/p}$ n=5.

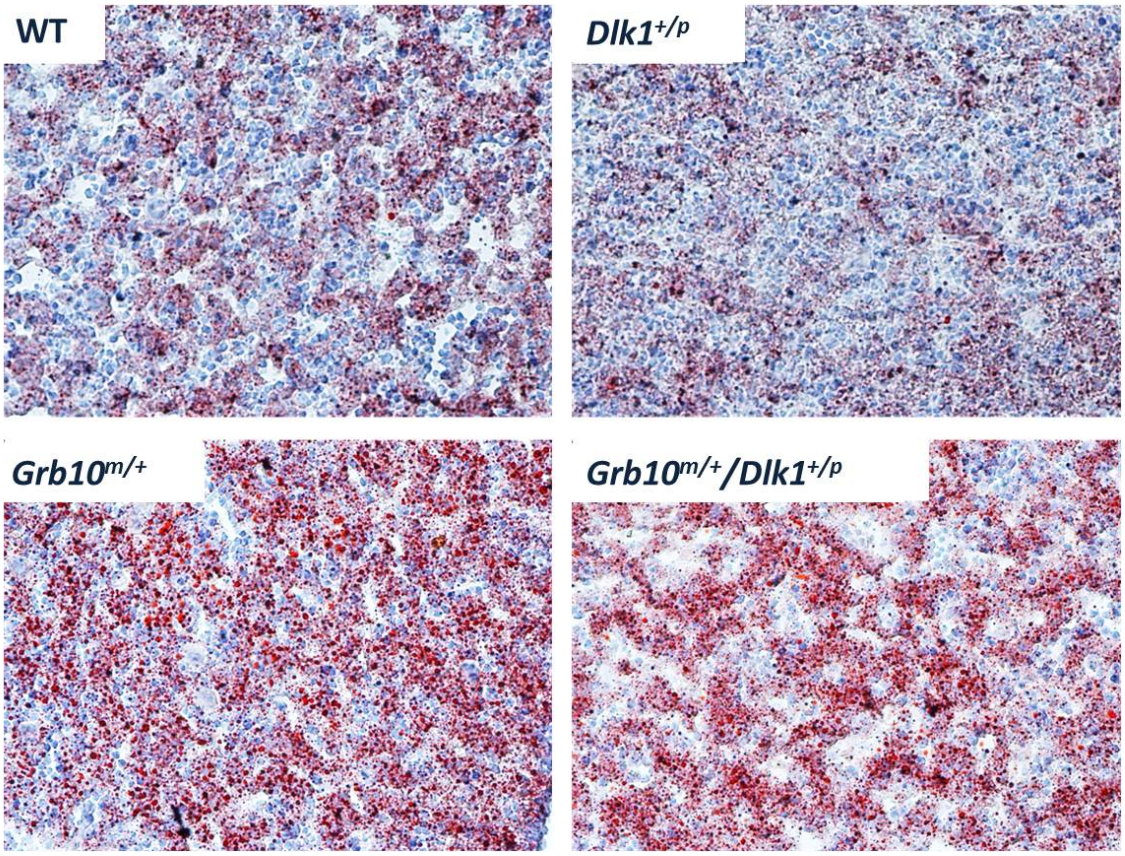

Figure 5.12 Oil Red O stained liver cryosections of neonatal wild type, *Grb10*$^{m/+}$, *Dlk1*$^{+/p}$ and *Grb10*$^{m/+}$/*Dlk1*$^{+/p}$ mice under 200x magnification.

Livers from 1 day old mice were cryosectioned and stained with Oil Red O for the presence of lipid droplets. An increased number of lipid droplets was observed in both *Grb10*$^{m/+}$ and *Grb10*$^{m/+}$/*Dlk1*$^{+/p}$ livers. Presented images show representative sections for each of the analysed genotypes. WT n=5, *Dlk1*$^{+/p}$=5, *Grb10*$^{m/+}$ n=5 and *Grb10*$^{m/+}$/*Dlk1*$^{+/p}$ n=5.

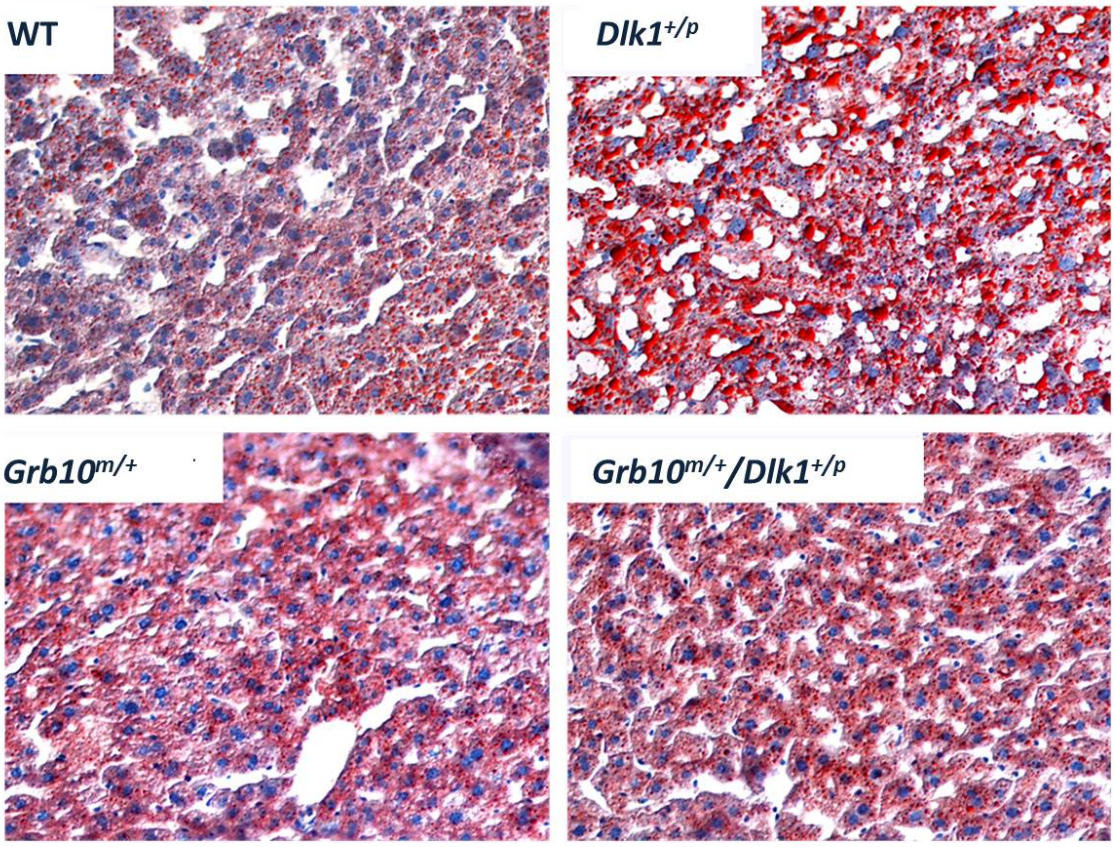

Figure 5.13 Oil Red O stained liver cryosections of 3 month old wild type, *Grb10*$^{m/+}$, *Dlk1*$^{+/p}$ and *Grb10*$^{m/+}$/*Dlk1*$^{+/p}$ mice under 200x magnification.

Livers from 3 months old male mice were cryosectioned and stained with Oil Red O for the presence of lipid droplets. An increased number of lipid droplets was observed in *Dlk1*$^{+/p}$ knockout mice. Presented images show representative sections for each of the analysed genotypes. WT n=5, *Dlk1*$^{+/p}$=5, *Grb10*$^{m/+}$ n=5 and *Grb10*$^{m/+}$/*Dlk1*$^{+/p}$ n=5.

5.2.7 Analysis of adipocyte cell size and number distribution in *Dlk1*$^{+/p}$, *Grb10*$^{m/+}$ and *Grb10*$^{m/+}$/*Dlk1*$^{+/p}$ mice

Previous phenotypic analysis of *Dlk1* mice revealed high fat diet-related increased adipose tissue content (Moon et al., 2002). Consequently, Moon et al (2002) investigated if this was a result of adipocyte hypertrophy or hyperplasia. They found abnormalities in fat cell size distribution resulting in elevated cell size, indicating adipocyte hypertrophy in *Dlk1* knockout animals as a potential cause of increased adiposity (Moon et al., 2002). Although DXA analysis described in the previous section showed only limited significant changes within fat tissue content in *Grb10*$^{m/+}$ compared to *Dlk1*$^{+/p}$ animals, we decided to examine if the fat cell size distribution in mutant animals is in keeping with normal fat tissue.

Abdominal fat pads from 3 month old male mice were sectioned and stained with H&E (**Figure** 5.14) and we did not note any obvious histological differences between the genotypes. Further morphometric analysis of adipocyte cells was performed as described in Section 2.4.8 in order to investigate in detail any potential discrepancies in cell size or number distribution. Parameters including adipocyte mean and maximum width, adipocyte areas and numbers in field of view were recorded (**Figure** 5.15), but no significant differences were found between genotypes.

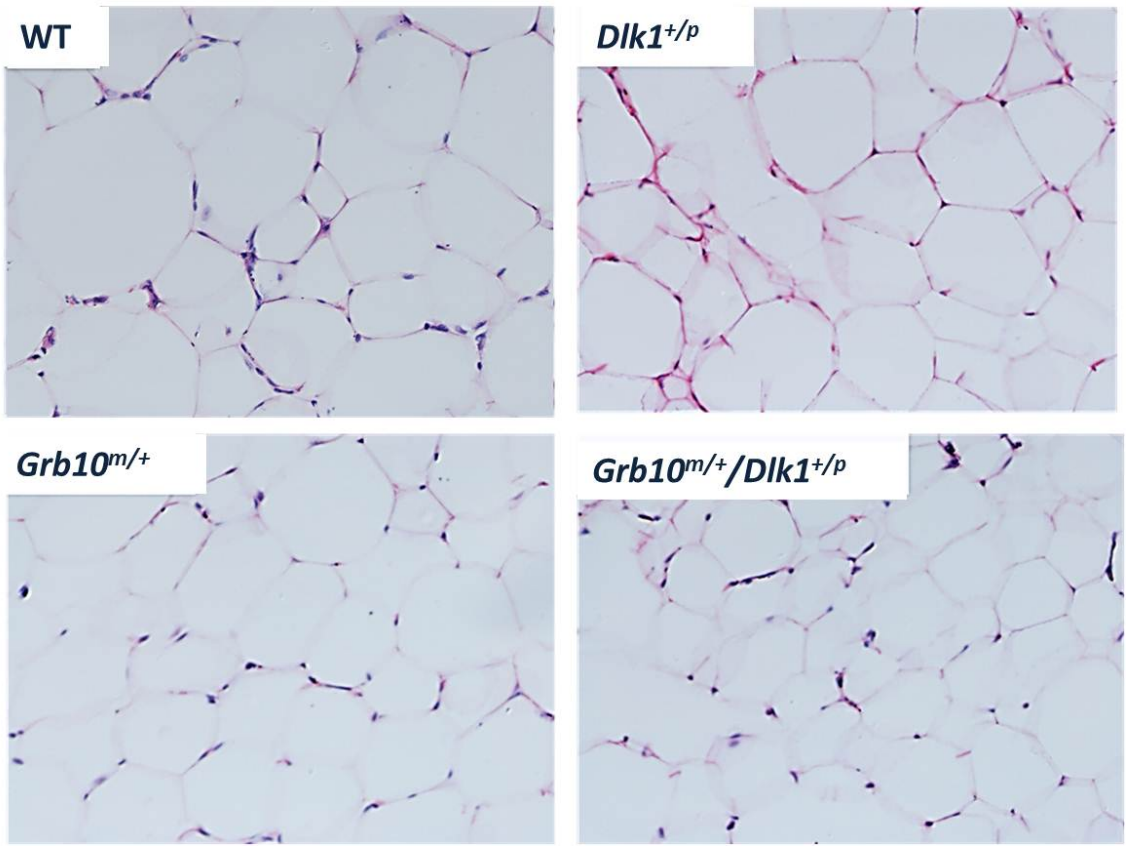

Figure 5.14 H&E stained white adipose tissue sections of wild type, *Grb10*$^{m/+}$, *Dlk1*$^{+/p}$ and *Grb10*$^{m/+}$*/Dlk1*$^{+/p}$ 3 months old adult old mice under 100x magnification.

H&E stained sections of white adipose tissue. No obvious differences were noted between any of the analysed genotypes. Presented images show representative sections for each of the analysed genotypes. WT n=5, *Dlk1*$^{+/p}$=5, *Grb10*$^{m/+}$ n=5 and *Grb10*$^{m/+}$*/Dlk1*$^{+/p}$ n=5.

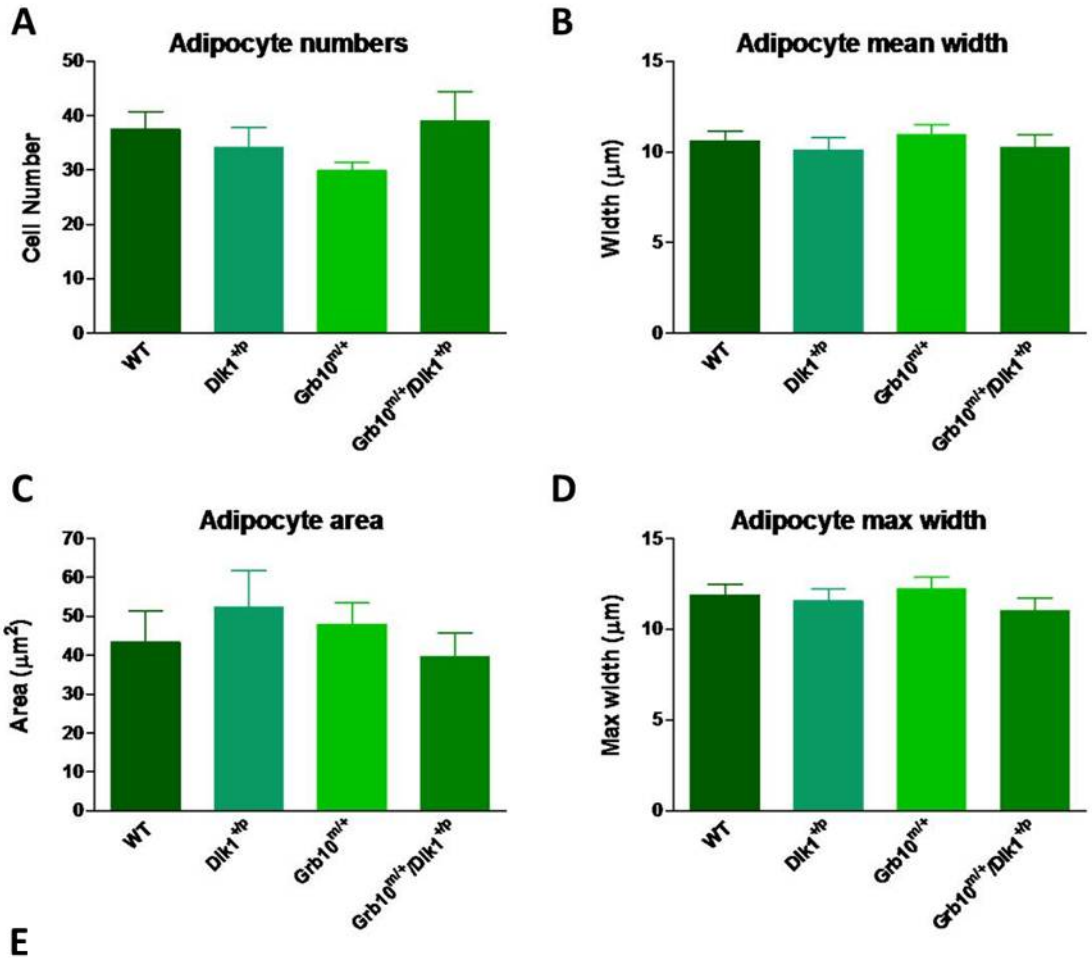

E

	Adipocyte numbers	Adipocyte area	Adipocyte max width	Adipocyte min width
WT vs Grb10$^{m/+}$	ns	ns	ns	ns
WT vs Dlk1$^{+/p}$	ns	ns	ns	ns
WT vs Grb10$^{m/+}$/Dlk1$^{+/p}$	ns	ns	ns	ns
Grb10$^{m/+}$ vs Dlk1$^{+/p}$	ns	ns	ns	ns
Grb10$^{m/+}$ vs Grb10$^{m/+}$/Dlk1$^{+/p}$	ns	ns	ns	ns
Dlk1$^{+/p}$ vs Grb10$^{m/+}$/Dlk1$^{+/p}$	ns	ns	ns	ns

Figure 5.15 Measurements of adipocyte numbers, mean and maximum width and areas in white adipose tissue of wild type, *Grb10$^{m/+}$*, *Dlk1$^{+/p}$* and *Grb10$^{m/+}$/Dlk1$^{+/p}$* mice.

Morphometric analysis has been used to analyse the numbers (**A**), mean (**B**) and maximum areas (**C**), as well as widths (**D**) of adipocyte cells in sections of white adipose tissue. No significant differences were found for any of the analysed parameters in tissues from animals of all four genotypes. **E)** Table summarising results of statistical analysis. All values represent means ± SEM and have been subject to one way ANOVA with post hoc Tukey's analysis. WT n=5, *Dlk1$^{+/p}$*=5, *Grb10$^{m/+}$* n=5 and *Grb10$^{m/+}$/Dlk1$^{+/p}$* n=5.

5.3 Discussion

Fetal growth and adult metabolism are closely linked and frequently the same genes or genetic pathways play parts in regulating both processes. Abnormalities during embryonic development have long been associated with postnatal disorders and epigenetic regulation of metabolic genes has been linked to nutritional influences during development (reviewed in Waterland and Jirtle, 2004), in a process known as fetal programming. Various imprinted genes are able to influence growth, metabolism and energy homeostasis, among them *Grb10* and *Dlk1* exerting roles in growth regulation and the maintenance of correct metabolic status (Moon et al., 2002; Lee et al., 2003; Smith et al., 2007; Wang et al., 2007). The mode of action for both genes might be based on direct control of metabolism or alternatively they could cause specific alterations during early development that influence the metabolic functions in postnatal life. Moreover, as various imprinted genes, including *Grb10*, have established roles in regulation of insulin signalling, any changes in their function might alter insulin signalling and have an effect on metabolism. Taking into account previous reports of *Dlk1* and *Grb10* influence on adipocyte differentiation and insulin signalling, in this chapter we have studied consequences of *Grb10* and *Dlk1* ablation on glucose and lipid-related metabolism, as representative aspects of correct metabolic status.

Grb10$^{m/+}$ knockout mice have previously been reported to have a lean phenotype (Charalambous et al., 2003; Smith et al., 2007) and *Dlk1* knockout mice to have increased adipose tissue mass when fed on high fat diet (Moon et al., 2002). One obvious explanation for any differences in body composition or overall body mass would be altered feeding behaviour, therefore we initially decided to check for hypophagia (reduced food consumption) or hyperphagia (increased food consumption), but statistical analysis revealed no differences in feeding behaviour in any of the analysed genotypes. Analysis of separate age groups (3-6 and 7-9 month old male and female mice) revealed similar trends therefore the results pooled together for 3-9 month old male and female mice has been shown. These results indicate that any discrepancies in body composition of mice lacking *Grb10*, *Dlk1* or both of these genes are not due to differences in feeding behaviour, but rather are results of metabolic changes.

Previous analysis of feeding behaviour in *Grb10*$^{m/+}$ knockout mice, which still displayed increase in body weights, also did not show any alterations from normal (Garfield, 2007). Aside from that, *Grb10*$^{m/+}$ serum leptin levels were reduced in proportion with decreased white adipose tissue mass (Smith et al., 2007). This was in agreement with the association between leptin concentration and mass of adipose tissue (Friedman and Halaas, 1998). Loss of correlation between plasma leptin and total body weight in *Grb10*$^{m/+}$ suggested lean mass and

not adipose tissue mass as the main cause of body weight variability in these mice, similar to previous reports for other mouse models and for human patients with reduction in adiposity (Klaman et al., 2000; Bluher et al., 2002).

In order for the brain to be able to control the energy homeostasis, it has to be able to receive signals about peripheral energy stores, specifically adipose tissue mass. Leptin is a widely studied peptide hormone secreted from adipocyte cells (mainly subcutaneous fat mass) acting as an indicator of the body's adiposity status and its levels are correlated with the amount of body fat (Zhang et al., 1994). Insulin and leptin complement each other in regulating food consumption, uptake, and nutrient storage and several human studies indicate that leptin may play a part in insulin resistance in states of chronically elevated leptin levels (Segal et al., 1996; Boden et al., 1997; Ruige et al., 1999). Recent studies in a lean mouse model of type 2 diabetes have highlighted the role of leptin in improving insulin sensitivity in a manner independent of its effects on food intake (Li et al., 2011).

Aside from that, evidence for a leptin-independent programming of adiposity and adult body weight in genetically obese strain of mice has also been provided. Leptin deficient mice with low birth weight managed to rapidly gain body mass during lactation and displayed increased weight in adulthood together with greater adiposity (Cottrell et al., 2011), suggesting that factors other than leptin are also important in energy homeostasis programming. Nevertheless, the level of leptin is still treated as one of the main indicators of body energy homeostasis, therefore it would be of interest to analyse its levels in *Grb10*$^{m/+}$*/Dlk1*$^{+/p}$ double knockout mice and assess any potential changes in these animals resulting from lack of *Grb10* and *Dlk1* genes. This type of analysis would be interesting especially in light of reduced expression of leptin in *Dlk1* transgenic mice (Lee et al., 2003) and a recent report that leptin administration in mice reduced adiposity and decreased expression of adipogenesis-related genes, including *Dlk1* (Ambati et al., 2009). In spite of the well-established role for *Dlk1* in adipocyte differentiation, measurements of leptin levels in *Dlk1*$^{+/p}$ knockout mice have not been previously reported.

An improved ability to clear a glucose load has previously been noted in *Grb10*$^{m/+}$ knockout mice of both sexes, and was associated with an enhancement of insulin signalling efficacy in skeletal muscle and WAT rather than with an increase in circulating insulin levels (Smith et al., 2007). These results suggested that altered insulin signalling was the effect of a lack of *Grb10* inhibitory action. In agreement with this, an opposite, glucose resistant phenotype was reported in transgenic mice ubiquitously overexpressing *Grb10* under the control of a *β-actin* promoter (Shiura et al., 2005). More recent analysis of the same mouse

strain overexpressing *Grb10* showed characteristics of a non-obese mouse model, including insulin resistance, glucose intolerance along with decreased body, visceral fat and liver weights and when fed on high fat diet. The *Grb10* transgenic mice also showed increased plasma triglyceride and insulin levels and other characteristics similar to those seen in human type 2 diabetes (Yamamoto et al., 2008). As mentioned previously, the limitation of this model is associated with an overexpression of *Grb10* in all the tissues (including those that usually are not expressing *Grb10*), which is otherwise highly restricted postnatally, and may result in a non-physiological interactions of Grb10 with signalling components of postnatal growth axes, making it difficult to pinpoint the real *Grb10* function.

An increase in Irs1 phosphorylation and the failure to inhibit dephosphorylation of the Irs1 binding site has been previously suggested as a mechanism through which Grb14 regulates insulin signalling (Cooney et al., 2004; Nouaille et al., 2006) and was therefore also considered a possible mechanism of action for Grb10. The cause for the observed glucose phenotype in $Grb10^{m/+}$ knockout mice could be down to enhanced insulin signalling or, alternatively, increased muscle mass in $Grb10^{m/+}$ knockout animals that could result in greater glucose uptake, causing an enhanced overall insulin response. *Dlk1* can also influence glucose homeostasis, as mice with overexpression of soluble Dlk1 in adipose tissue showed hypertriglyceridemia, impaired glucose tolerance and decreased insulin sensitivity (Lee et al., 2003).

To investigate the ability to clear a glucose load by $Grb10^{m/+}/Dlk1^{+/p}$ double knockout mice, 3-9 month old animals of both sexes were subject to glucose tolerance tests (animals of 3-6 and 7-9 months of age have been pooled together as both cohorts showed similar trends, as presented in Appendix 2). Similar to $Grb10^{m/+}$, $Grb10^{m/+}/Dlk1^{+/p}$ double knockout mice were also able to clear glucose significantly faster when compared to $Dlk1^{+/p}$ knockout mice which showed a trend towards slower glucose clearance. Even though adipose tissue is responsible for approximately 10% of whole body glucose uptake (Golay et al., 1988; Marin et al., 1992), insulin is highly important in promoting adipogenesis, inhibiting lipolysis and stimulating glucose uptake and liposynthesis (Rosen et al., 2000). Previous examination of $Grb10^{m/+}$ knockout mice revealed that enhanced glucose clearance in these animals could not be associated with increased insulin levels and instead indicated there was improved insulin action, which was confirmed by insulin tolerance tests during which $Grb10^{m/+}$ mice showed decreased serum glucose levels upon insulin injection (Smith et al., 2007). Consequently, to investigate the mechanism behind the improved glucose clearance ability in $Grb10^{m/+}/Dlk1^{+/p}$

double knockout mice, insulin tolerance tests (ITTs) and assessment of serum insulin levels could be performed in a similar manner.

Control of glucose homeostasis is one of the major functions of the liver, which is highly regulated by insulin and other hormones. Liver insulin resistance and, more specifically, insulin's inability to suppress glucose production have been associated with fasting hyperglycaemia in type 2 diabetes. Insulin degradation is also one of the liver functions, as insulin removal helps to control the cellular response to the hormone by decreasing availability. Generation of a *Cre/Lox* system under an albumin promoter to drive *Cre* expression only in the liver and tissue-specific inactivation of the *IR* gene in hepatocytes allowed for an examination of the consequences of the lack of direct insulin action in liver (Michael et al., 2000). Liver-specific insulin receptor knockout (LIRKO) mice displayed severe insulin resistance along with glucose intolerance and an inability of insulin to suppress hepatic glucose production and to regulate hepatic gene expression. Another metabolic feature confirmed in LIRKO mice is hyperinsulinemia due to a combination of reduced insulin clearance and enhanced insulin secretion. Over time LIRKO livers undergo changes in morphology (40% size reduction, areas of scattered focal dysplasia, decreased glycogen content, enlarged gall bladders, increased lipid content and enlarged mitochondria) and function (biliary tract dysfunction, hepatocellular damage), and the severity of the metabolic phenotype decreases (Michael et al., 2000). This model established the vital role of insulin receptors in the liver in glucose homeostasis regulation for normal insulin clearance as well as maintenance of a correct liver function, and also confirmed insulin's role as an important metabolic regulator with both direct and indirect effects on majority of tissues.

Only fed *Grb10*$^{m/+}$ and *Grb10*$^{m/+}$*/Dlk1*$^{+/p}$ female mice showed hypoglycaemia, a result difficult to explain, especially in light of the DXA analysis which showed that body composition in these mice was not significantly different to that of wild type animals. The handling of glucose was different between the sexes, as could be observed by comparing the shapes of glucose tolerance curves between males and females. In addition, the measurements of glucose levels in fed mice with constant access to food can be misleading because of lack of knowledge about the exact time at which the animals have eaten. Thus it is important to expand the numbers of analysed mice in order to confirm if the hypoglycaemia confirmed in *Grb10*$^{m/+}$ and *Grb10*$^{m/+}$*/Dlk1*$^{+/p}$ female mice is indeed a biologically meaningful result.

Body composition, specifically lean/fat tissue content can exert dramatic effects on glucose homeostasis and potentially the development of diabetes-like syndromes, as exemplified by serious glucose tolerance defects in *Dlk1* transgenic mice with a substantial

reduction in adipose tissue mass (Lee et al., 2003). Hence we have employed DXA analysis in order to establish the possible foundations of observed changes in glucose homeostasis. Consistent with previous studies, *Grb10*$^{m/+}$ knockout mice of both sexes showed a trend towards reduced relative adipose tissue weight and elevated lean tissue mass when analysed using DXA (Smith et al., 2007). On the other hand, *Dlk1*$^{+/p}$ knockout mice did not display increased adiposity, which has been suggested previously (Moon et al., 2002), but in animals of different genetic background and fed on a high fat diet. The only significant difference found in *Dlk1*$^{+/p}$ mice was decreased lean tissue mass compared to *Grb10*$^{m/+}$ mice. *Grb10*$^{m/+}$*/Dlk1*$^{+/p}$ double knockout mice did not exhibit any lean/fat content alterations compared to wild type mice except for increased lean tissue mass in male mice. These results are in agreement with allometric muscle/fat depots analysis described in the previous chapter which did not reveal any substantial changes within lean/adipose tissue content in analysed mice.

DXA also allowed us to investigate the possible changes within bone mineral density and bone mineral content, as we were very much interested in examining BMD and BMC in *Grb10*$^{m/+}$*/Dlk1*$^{+/p}$, especially in light of the role for *Dlk1* in osteogenesis and normal skeletal development. A recent study has suggested *Dlk1* exerts a negative influence on bone mass, as a negative correlation between serum Dlk1 and BMD has been identified in women suffering from *Anorexia Nervosa* (Fazeli et al., 2009). Examination of mice with osteoblast-specific Dlk1 overexpression has shown Dlk1 as a regulator of bone mass that inhibits bone formation and stimulates bone resorption under estrogen deficiency (Abdallah et al., 2011b). This finding was supported by a report of elevated levels of serum Dlk1 in post-menopausal women that may be mediating the effects of estrogen deficiency on bone turnover (Abdallah et al., 2011a). The proposed molecular mechanism behind Dlk1 action in adipogenesis is that Dlk1 activates the MAPK/ERK pathway and blocks downregulation of Sox9, which in turn inhibits the differentiation of committed MSCs down the osteogenic and adipogenic lineages (reviewed in Sul, 2009).

Previously, ablation of *Grb14* in mice caused hypoinsulinemia and improved glucose tolerance indicative of enhanced insulin sensitivity, as upon *in vivo* insulin stimulation, livers and muscles of *Grb14* knockout mice exhibited enhanced insulin signalling via IRS-1 and Akt and increased incorporation of glucose into glycogen and no changes in insulin action in adipose tissue were identified (Cooney et al., 2004). Improved glucose clearance and tissue-specific changes in insulin-induced Insr and IRS1 tyrosine phosphorylation along with similar changes at the IGF1R and at the level of IRS1 tyrosine phosphorylation in response to IGF1 were detected in *Grb10*$^{m/+}$ mice and IGF1-induced signalling, at least to IRS1, was particularly

increased in muscles of adult *Grb10*-deficient animals (Smith et al., 2007). These results indicated on *Grb10* and *Grb14* being able to inhibit IR/IRS1 signalling in a similar manner but with distinct tissue specificity but *Grb10* also showing an ability to modulate body composition, as the elevated muscles mass in $Grb10^{m/+}$ animals on a whole-body basis could be associated with the improved glucose tolerance at least partly resulting from increased glucose clearance into muscle. The results of glucose tolerance tests and DXA analysis of body composition presented in this chapter showed that $Grb10^{m/+}$ knockout animals, consistent with previous studies, had an increased lean tissue mass and improved glucose tolerance, whilst $Grb10^{m/+}/Dlk1^{+/p}$ knockout animals had an essentially normal body composition but still exhibited improved glucose clearance, indicating on the improved glucose clearance in $Grb10^{m/+}$ and $Grb10^{m/+}/Dlk1^{+/p}$ mice most likely resulting from an enhanced insulin signalling due to the lack of an inhibitory action of *Grb10*. Further work will be necessary to prove if the same changes in IR/IRS1 signalling are the basis for the improved glucose tolerant phenotype noted in $Grb10^{m/+}/Dlk1^{+/p}$ mice.

Moon et al (2002) have reported not only an increase in adipose tissue mass in *Dlk1* knockout mice fed on a high fat diet, but also elevated levels of serum lipid metabolites that included triglycerides, free fatty acids and cholesterol. All three types of metabolites were present at significantly increased levels, with elevated levels of triglycerides being the most pronounced (by 36% and 77% in *Dlk1* knockout female and male mice, respectively). Both hypercholesterolemia and hyperlipidaemia indicated that in *Dlk1* knockout mice lack of *Dlk1* antiadipogenic action results in disrupted lipid metabolism. To investigate if our $Dlk1^{+/p}$ mice also had altered serum triglyceride levels and if $Grb10^{m/+}/Dlk1^{+/p}$ double knockout mice showed a similar trend we measured the levels of triglycerides in blood serum of fasted mice. In keeping with previous reports, $Dlk1^{+/p}$ mice indeed had raised triglyceride levels but only when compared to $Grb10^{m/+}$ mice, indicating opposing effects of these to genes on triglyceride levels. It is possible that the elevated triglyceride levels in $Dlk1^{+/p}$ animals in our study signify the predisposition to accumulating fat, even though increased adiposity was not evident. It has to be taken into account that previous reports of significantly increased triglyceride levels by Moon et al (2002) were based on analysis in animals fed on high fat diet, in contrast to the animals used in our study, therefore any trends towards obesity would be more pronounced in HFD case. It would be of interest to employ a similar high fat diet in $Grb10^{m/+}$, $Dlk1^{+/p}$ and $Grb10^{m/+}/Dlk1^{+/p}$ knockout mice and again assess the levels of triglycerides together with other serum lipid metabolites, such as previously mentioned leptin, adiponectin, FAS (fatty acid synthase),and SCD (stearoyl-CoA desaturase1). These kinds of examination could tell us more

about the predisposition to obesity, or its lack, resulting from ablation of *Grb10* and *Dlk1* as well as providing more information about the metabolic state in the analysed mice. It would be interesting to check if *Grb10*$^{m/+}$mice fed on HFD are protected from diet-induced obesity, as it has been previously shown in other mouse models with low adiposity (e.g. Klaman et al., 2000).

Increased adipose tissue mass might result from an increase in adipocyte cell size alone or together with a rise in adipocyte cell number due to disruption in differentiation from preadipocytes into adipocytes. Previously conducted morphometric analysis of adipocyte cell size, density and morphology in *Dlk1* knockout mice revealed that lack of *Dlk1* resulted in adipocyte hypertrophy in inguinal fat pads with no apparent changes in DNA content which suggested correct cell numbers (Moon et al., 2002). In agreement with that, overexpression of *Dlk1* gene in mice led to a reduction in adipocyte size (Lee et al., 2003).

The differentiation of cells into adipocytes is associated with altered expression of several genes, and the final outcome is a fat cell phenotype and adipocyte function specialised in triglyceride storage. Adipocyte cells secrete a variety of molecules, many of which are involved in energy homeostasis. *In vitro* studies have shown that dexamethasone-mediated repression of *Dlk1* contributes to the mechanisms by which glucocorticoids promote adipogenesis (Smas et al., 1999), whilst constitutive expression of Dlk1 inhibits 3T3-L1 adipogenesis (Smas and Sul, 1993) . Only the large soluble form of Dlk1 is able to inhibit 3T3-L 1 adipocyte differentiation *in vitro* (Mei et al., 2002) and the study of human serum levels of DLK1 revealed increased levels of this soluble protein with obesity and its possible negative influence on insulin sensitivity (Chacon et al., 2008). The mechanism by which Dlk1 inhibits adipocyte differentiation has been investigated by using soluble Dlk1 in mouse embryonic fibroblasts from *Dlk1* knockout embryos. It has been reported that Dlk1 interacts with fibronectin via the Dlk1 juxtamembrane domain and fibronectin C-terminal domain (Wang et al., 2010), which is required for the inhibition of adipocyte differentiation through the activation of extracellular signal-regulated kinase/mitogen-activated protein kinase (MEK/ERK) (Kim et al., 2007) and the subsequent upregulation of Sox9 expression (Wang and Sul, 2009). Following that, *Sox9* directly binds the promoter regions of *C/EBPβ* and *C/EBPδ* to suppress their transcription and in turn inhibits adipocyte differentiation (for details see Section 1.3.1).

The role of *Dlk1* in adipogenesis has also been investigated *in vivo*, by studying mice either overexpressing (Lee et al., 2003) or lacking (Moon et al., 2002) *Dlk1*. Mice overexpressing *Dlk1* exhibited a dramatic decrease in total fat pad weight and reduced expression of adipocyte markers and adipocyte-secreted factors (such as leptin and adiponectin). Animals with

considerable reduction in adiposity also displayed a slower glucose clearance rate together with hypertriglyceridemia and insulin insensitivity (Lee et al., 2003). In the same study, mice expressing a *Dlk1* transgene solely in the liver under the control of an albumin promoter had a reduced amount of adipose tissue mass and adipocyte marker expression, suggesting that Dlk1 may act in an endocrine manner (Lee et al., 2003). Therefore, high expression of *Dlk1* in preadipocytes, diminishing during differentiation, together with its role in correct adipocyte differentiation *in vitro* and *in vivo* have established *Dlk1* as a potent negative regulator of adipogenesis.

Bearing in mind the involvement of *Dlk1* in adipogenesis, together with reports of *Grb10* ablation leading to postnatal overgrowth due to increased lean but not fat tissue mass, it was of interest to examine the consequences of lack of both of these genes on adipose tissue morphology, specifically on adipocyte size and numbers. Surprisingly, we found that, histologically and morphometrically, there were no evident changes in size of adipose cells in any of the analysed genotypes. As mentioned before, we did not see any significant modifications within the lean/fat tissue ratio in $Dlk1^{+/p}$, but it was quite surprising that we also observed no alterations in adipocytes of $Dlk1^{+/p}$ knockout mice in our study, in contrast to a previous report of adipocyte hypertrophy (Moon et al., 2002). The clearly less pronounced metabolic phenotype in $Dlk1^{+/p}$ mice used in this study, in comparison to *Dlk1* knockout animals characterised by Moon et al (2002), once again, highlights the possibility of the previously observed differences being diet-dependent. Future work should involve similar adipocyte cell analyses in $Grb10^{m/+}$, $Dlk1^{+/p}$ and $Grb10^{m/+}/Dlk1^{+/p}$ mice fed on a high fat diet to see if phenotype of $Dlk1^{+/p}$ mice is comparable to that of *Dlk1* knockout mice observed by Moon and colleagues (2002), and to determine whether $Grb10^{m/+}/Dlk1^{+/p}$ mice again resemble the $Grb10^{m/+}$ mice, indicating a genetic interaction between *Grb10* and *Dlk1* genes to control normal lipid metabolism.

In light of significant variations in the pre- and post-natal weights of livers reported in previous chapters and changes in liver histology of *Grb10* and *Dlk1* knockout mice described before (Moon et al., 2002; Charalambous et al., 2003), we have performed histological analysis of livers from mice at E14.5, 1 day, 1 week and at 3 months of age. Liver histology in E14.5 embryos did not reveal any unusual features, however we noted presence of white, round spaces in liver sections from $Grb10^{m/+}$ and $Grb10^{m/+}/Dlk1^{+/p}$ neonatal animals. To investigate the nature of these further, we performed Periodic Acid- Schiff staining on neonatal livers to check for any alterations in glycogen content, as it has been previously suggested to be increased in $Grb10^{m/+}$ animals (Charalambous et al., 2003), but we did not find any differences

between genotypes. In contrast, Oil Red O staining performed on cryosectioned neonatal livers revealed that *Grb10*$^{m/+}$ and *Grb10*$^{m/+}$*/Dlk1*$^{+/p}$ 1 day livers contained an elevated lipid droplet content in comparison to wild type and *Dlk1*$^{+/p}$. This suggests that the overgrown liver phenotype identified in neonatal *Grb10*$^{m/+}$ and *Grb10*$^{m/+}$*/Dlk1*$^{+/p}$ mice (shown in Section 4.2.1) might result from an increased lipid content. To investigate if elevated lipid levels are present in *Grb10*$^{m/+}$ and *Grb10*$^{m/+}$*/Dlk1*$^{+/p}$ livers consistently during postnatal life we histologically examined livers from mice of 1 week and 3 months of age. Only half of the organs from 1 week old mice maintained the unusual accumulation of lipids. The diminishing presence of lipid droplets between birth and 1 week of age could be attributed to rapidly decreasing expression of *Grb10* in the liver during this period (Lui et al., 2008). The majority of imprinted genes, including *Grb10* and *Dlk1,* show the most pronounced expression during fetal development, with a substantial decline during postnatal life simultaneously in multiple organs, suggesting that the decrease of imprinted genes expression might match the decline in somatic growth. Developmental defects were previously reported in both *Grb10* and *Dlk1* knockout livers, as *Grb10* ablation caused significant neonatal liver overgrowth (Charalambous et al., 2003) and lack of *Dlk1* resulted in increased adult liver weight along with elevated total lipid content and enhanced expression of FAS and SCD-1, usually associated with increased hepatic lipogenesis and fat synthesis (Moon et al., 2002). In the previous chapter describing postnatal allometric organ analysis, we noticed a slight trend towards *Dlk1*$^{+/p}$ male liver overgrowth, which became significant during analysis of relative liver weights in 3-6 month old male mice when compared to *Grb10*$^{m/+}$ and *Grb10*$^{m/+}$*/Dlk1*$^{+/p}$ (Section 4.2.3). This interesting finding of fat livers is even more noteworthy due to the fact that it seems to be most pronounced at the time of birth, as analysis of E14.5 did not reveal significant changes in liver histology. It would be of interest to identify the specific time of liver lipid accumulation, especially that the analysis of E17.5 liver wet weights revealed that *Grb10*$^{m/+}$ and *Grb10*$^{m/+}$*/Dlk1*$^{+/p}$ livers were overgrown, possibly suggesting that at this gestational stage the lipid accumulation is already taking place. It would also be interesting to analyse the total lipid content in the livers (extracted by the method of Folch et al, 1957) and compare it between the genotypes and to identify the specific type of lipids accumulated in neonatal *Grb10*$^{m/+}$ and *Grb10*$^{m/+}$*/Dlk1*$^{+/p}$ livers and check for triglyceride, total cholesterol and phospholipid liver content.

Variety of factors is thought to influence development of fatty liver, steatosis or hepatic lipidosis characterised by the abnormal accumulation of triglycerides within hepatocytes. In humans, fatty liver is frequently associated with chronic alcohol ingestion and is common in patients with maturity-onset diabetes mellitus, obesity and hyperlipidaemia. Various rodent

experimental models proved useful in uncovering the mechanisms of fatty liver development and the risk of fatty liver leading to more serious liver diseases, as fatty liver can be experimentally induced by nutritional treatments or by administering drugs such as carbon tetrachloride or ethionine (Farber, 1967; Recknagel, 1967). There are also some models genetically predisposed to develop fatty livers, for example fatty liver formation is frequently observed in mutant obese mouse strains such as *ob/ob, db/db* and *fat/fat* (Coleman and Hummel, 1967; Austin et al., 1984; Naggert et al., 1995), but there is a shortage of animals characterised by spontaneous fatty liver without developing obesity (Reue and Doolittle, 1996), but recently an inbred strain named FLS (fatty liver Shionogi) with spontaneous fatty liver without obesity has been established (Soga et al., 1999). Neonatal FLS mice had hepatocytes filled with fine lipid droplets which increased in size as the mice aged. Prominent fatty liver is also a feature characteristic of fatty liver dystrophy (FLD) mice that carry a recessive mutation that arose spontaneously in an inbred mouse strain (Langner et al., 1989). The formation of fatty liver starts in FLD mice when the newborn animals start suckling milk and is also associated with increased levels of plasma triglycerides, but both abnormalities diminish by the time mutant mice are 2-3 weeks old, at which time they start to suffer from a peripheral neuropathy that persists throughout their lifetime (Langner et al., 1991). The jvs (juvenile visceral steatosis) mice also have fatty livers along with growth retardation, hypoglycaemia and hyperammonemia (Kuwajima et al., 1996).

Hepatic lipid deposition can be associated with deficiency in lipoprotein metabolism, which could be accompanied by altered profiles of plasma lipids or lipoproteins. Therefore, it would be interesting to investigate the levels of blood serum triglyceride content in neonatal *Grb10*$^{m/+}$ and *Grb10*$^{m/+}$*/Dlk1*$^{+/p}$ mice and check if the increased liver adiposity is accompanied by elevated blood triglyceride levels resulting from an increased fatty acid mobilisation from adipocytes into the circulation.

The contents of hepatic lipids at a particular developmental stage result from an equilibrium between a lipid synthesizing activity, the lipid-oxidizing capacity of the liver, lipid uptake by the liver and lipid secretion from the liver as lipoproteins. It is possible that lipid transfer across the placenta from the mother to the *Grb10*$^{m/+}$ and *Grb10*$^{m/+}$*/Dlk1*$^{+/p}$ fetuses is at least in part responsible for the observed increase in the contents of lipids in the fetal livers during late gestation that persists on the day of birth, therefore it would be crucial to examine the livers of E17.5-E18.5 embryos and check their lipid content. Additionally, it is possible that the transfer of dietary lipids through milk to suckling neonatal animals influences the liver lipid storage and also that *Grb10*$^{m/+}$ and *Grb10*$^{m/+}$*/Dlk1*$^{+/p}$ exhibit decreased lipid export from the

liver. Further experiments are needed to explain the mechanisms of fat accumulation in *Grb10*$^{m/+}$ and *Grb10*$^{m/+}$*/Dlk1*$^{+/p}$ neonatal mice.

It is interesting to note that, once again, *Grb10*$^{m/+}$ and *Grb10*$^{m/+}$*/Dlk1*$^{+/p}$ share a phenotypic feature contrasting with the one observed in *Dlk1*$^{+/p}$ mice. During histological analysis we found that adult *Grb10*$^{m/+}$ and *Grb10*$^{m/+}$*/Dlk1*$^{+/p}$ livers were indistinguishable from wild types, whilst *Dlk1*$^{+/p}$ knockout livers had increased lipid droplet content, as confirmed by Oil Red O staining. Liver, an organ of crucial importance in maintenance of correct metabolic state, is a site of a *Grb10* and *Dlk1* embryonic expression which declines upon birth (Lui et al., 2008), but here we report that lack of the *Dlk1* gene affects the postnatal liver phenotype, which is consistent with previous reports (Moon et al., 2002). It would therefore be interesting to conduct a more thorough histological analysis of embryonic and neonatal livers to pinpoint the exact time of unusual lipid accumulation in *Grb10*$^{m/+}$ and *Grb10*$^{m/+}$*/Dlk1*$^{+/p}$ livers. Significantly overgrown *Grb10*$^{m/+}$ and *Grb10*$^{m/+}$*/Dlk1*$^{+/p}$ neonatal livers could be a result of increased lipid accumulation and/or changes in hepatocyte size/numbers, however previous examination demonstrated that hepatocyte size was not affected following *Grb10* ablation (Charalambous et al., 2003). We could also use Western Blot analysis of embryonic livers to more directly investigate the possible molecular interaction between *Grb10* and *Dlk1* genes in this organ, as it is a site of prominent expression for both genes.

Work in this chapter demonstrates the importance of imprinted genes, *Grb10* and *Dlk1*, in the maintenance of metabolic homeostasis. We hypothesised that reciprocal metabolic phenotypes of *Grb10* (increased lean mass, reduced adiposity, improved glucose tolerance) and *Dlk1* (elevated adipose tissue mass, slight obesity, raised blood serum triglyceride levels) knockout mice would allow us to dissect if these two genes are potentially interacting with each other in the same genetic pathway in regulating postnatal metabolism. By characterising the phenotype of *Grb10*$^{m/+}$*/Dlk1*$^{+/p}$ double knockout animals we aimed to elucidate if these animals share metabolic characteristics with any of the single knockouts, which could indicate that *Grb10* and *Dlk1* are acting antagonistically in the same pathway in order to control metabolic homeostasis. The findings are summarised in **Table** 5.2. Although our metabolic analysis did not show that *Grb10*$^{m/+}$*/Dlk1*$^{+/p}$ double knockout mice and *Grb10*$^{m/+}$ knockout mice are metabolically similar in every aspect, we found some important similarities supporting the possibility of a *Grb10-Dlk1* interaction within a common pathway. The most striking finding was that these two genes might potentially be acting together in order to regulate glucose clearance. Despite having essentially a normal lean tissue content *Grb10*$^{m/+}$*/Dlk1*$^{+/p}$ double knockout animals still exhibited faster glucose clearance, supporting the idea that the reason

for improved glucose tolerance in *Grb10*$^{m/+}$and *Grb10*$^{m/+}$/*Dlk1*$^{+/p}$ animals is mostly due to increased insulin signalling, rather than increased lean tissue mass. Importantly, *Grb10*$^{m/+}$/*Dlk1*$^{+/p}$ did not share any abnormal characteristics found in *Dlk1*$^{+/p}$ mice, for example associated with age-related liver lipid deposition. Further analysis of other metabolic parameters, including insulin tolerance tests or the analysis of adiposity in mice exposed to a high fat diet, will be necessary to fully establish the role of these two genes in specific aspects of metabolism. Given the established functions of *Dlk1* in adiposity and *Grb10* in insulin signalling, gaining more detailed insights into their roles in metabolism could prove useful for future development of for treatments for obesity, diabetes or various other metabolic disorders in humans.

Type of analysis Genotype	Feeding behaviour	Glucose tolerance test	Glucose levels in fed and fasted mice	Triglyceride levels in blood serum	DXA analysis	Liver lipid content	Adipocyte numbers and size distribution
***Dlk1*$^{+/p}$ knockout mice**	No differences	No significant differences but trend to clear glucose slower	No differences	Elevated triglyceride levels	Reduced lean tissue content in males	No changes until adulthood when livers are filled with lipid droplets	No differences
***Grb10*$^{m/+}$ knockout mice**	No differences	Significantly faster glucose clearance	No differences in males, fed females hypoglycaemic	No differences	Significantly increased wet and relative weight of lean tissue and decreased wet and relative weight of fat mass in males and females	No changes at E14.5, neonatal livers filled with lipid droplets that are disappearing by 1 week, no changes in adult livers	No differences
***Grb10*$^{m/+}$*/Dlk1*$^{+/p}$ double knockout mice**	No differences	Significantly faster glucose clearance	No differences in males, fed females hypoglycaemic	No differences	Elevated lean tissue content in males	No changes at E14.5, neonatal livers filled with lipid droplets that are disappearing by 1 week, no changes in adult livers	No differences

Table 5.2 Summary of analyses in wild type, *Grb10*$^{m/+}$, *Dlk1*$^{+/p}$ and *Grb10*$^{m/+}$/*Dlk1*$^{+/p}$ mice of glucose-regulated metabolism and insulin-responsive tissues.

CHAPTER 6

6 Final discussion

The advantage of diploidy over haploidy is evident, as diploid organisms are less prone to deleterious effects of mutations due the presence of two active chromosomal copies. Therefore, it remains one of the most intriguing issues why did complex organisms, such as seed plants and mammals, evolve to contain a subset of genes with monoallelic expression. There is no doubt over the crucial roles of these so-called imprinted genes, clearly evidenced by lethality as well as fetal and placental growth malformations in androgenetic and parthenogenetic mouse embryos (Barton et al., 1984; Mann and Lovell-Badge, 1984; McGrath and Solter, 1984; Surani et al., 1984; Barton et al., 1985). Various hypotheses have been proposed to explain the driving forces behind the evolution of genomic imprinting, these include a host-defence mechanism to protect the mammalian genome against the integration of foreign DNA (Barlow et al., 1991), prevention of parthenogenesis and aneuploidy (Thomas, 1995) and also protection of the female against invasive trophoblastic tumours (Varmuza and Mann, 1994), although arguments against each of these hypothesis have been provided. Haig and Westoby (1989) proposed the most widely accepted theory explaining the genomic imprinting phenomenon, termed the parental conflict hypothesis. According to this hypothesis, imprinting evolved as a result of the parental conflict over the allocation of maternal resources. Many aspects of imprinted gene actions might be explained by this hypothesis, especially in the case of growth and metabolic effects. For example, the *Grb10* gene, predominantly expressed from the maternal allele, acts as a growth suppressor and is primarily involved in maintaining not only the optimal fitness of offspring, but also of the mother. Maternally expressed imprinted genes are therefore thought to prevent excessive fetal growth that could disrupt delivery and have detrimental consequences for the mother (Henriksen, 2008). The reciprocally expressed *Dlk1* promotes the growth of offspring, apparently regardless of potential deleterious effects on the mother's fitness.

So far none of the proposed hypotheses for imprinting evolution can explain all aspects of the imprinting phenomenon. The remaining questions about the reasons for imprinting genes evolution and their regulation are handled by an abundance of studies of specific imprinted clusters, the relationships between specific imprinted genes and by analysing their function (notably in knockout mice and human disorders associated with mutations, or epimutations, at imprinted loci). Three primary characteristics of imprinted genes include: monoallelic expression from a specific parental allele, clustering in evolutionarily conserved imprinted domains, and parental-allele-specific methylation. Epigenetic modifications, among them histone modifications and DNA methylation have been indicated as the bases for the different epigenetic state on the two parental alleles (Ferguson-Smith, 2011).

Imprinted genes are capable of affecting growth and differentiation along with mediating postnatal metabolism and behaviour (reviewed in Charalambous et al., 2007; Wilkinson et al., 2007). Studies in mice and humans revealed that all these functions are affected following disruption of either *Grb10* or the *Dlk1-Dio3* locus, which both show complex modes of regulation. Therefore, better understanding of regulation and function of *Grb10* and *Dlk1* and their domains, especially in light of their established roles as tumour suppressors and growth regulators, has important implications for human disorders and cancer. Thus, the study of these and other imprinted genes holds not only fundamental scientific interest, but also medical interest.

Epistasis is the masking of one mutant phenotype by the phenotype of a mutation at a different locus, and as such it can be useful in identification of a functional order of action of two genes. Even though epistatic analysis can be used irrespective of the direction, or order, of the interaction between the two genes, it is most instructive in the case of two genes regulating a common process as it can confirm the findings from phenotypic analysis or suggest a sequence of events. A typical regulatory gene pathway involves genes that can be switched on or off, so that their different states result in different outcomes of the pathway. The crucial requirement is that genes involved in this pathway result in reciprocal phenotypes and also are able to bypass the requirement for upstream genes. Therefore, the generation of double mutants is informative in determining the relationship between two genes, as the epistatic mutation is the one resulting in the phenotype of a double mutant which resembles one of the single mutant phenotypes.

It was surprising that in spite of the known biochemical interaction between *Grb10* and *IGF1R*, through the generation of double knockout mutants our lab has demonstrated a non-epistatic relationship of *Grb10* and *Igf2* (Charalambous et al., 2003), implying that IGF signalling is not the axis through which *Grb10* is able to mediate embryonic and placental growth. This was further supported by generation of *Grb10/Igf1r* double mutant mice and the discovery of a lack of an epistatic association between *Grb10* and *Igf1r*. Furthermore, studies of *Grb10* interaction with *IR in vivo* have indicated *Grb10* as an inhibitor of *IR* in the liver but not generally in controlling fetal or placental growth (Smith, 2004). Failure to identify the *Grb10* genetic pathway up until now has encouraged further investigation of possible *Grb10* interacting partners involved in the growth regulatory function of Grb10.

Ablation of *Grb10* or *Dlk1* leads to reciprocal phenotypic outcomes in mice (Moon et al., 2002; Charalambous et al., 2003). We proposed a hypothesis that these two genes may act

antagonistically in a common genetic pathway. Availability of mouse models lacking each of the genes of interest permitted the generation and characterisation of *Grb10*$^{m/+}$/*Dlk1*$^{+/p}$ double knockout animals in order to address the possible epistatic relationship between the *Grb10* and *Dlk1* genes. Here we report the results of prenatal, postnatal and metabolic characterisation of *Grb10*$^{m/+}$/*Dlk1*$^{+/p}$ double knockout mice and suggest that *Grb10* might indeed be acting epistatically to *Dlk1* in the same genetic pathway in order to regulate some aspects of growth and metabolism (**Figure** 6.1).

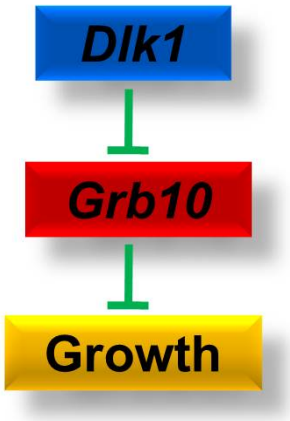

Figure 6.1 The possible genetic pathway for *Dlk1* and *Grb10* action as concluded from results presented in this study.

The proposed epistatic pathway shows *Dlk1* acting as a *Grb10* inhibitor, whilst simultaneously *Grb10* is exerting inhibitory effects on growth and other phenotypic aspects, such as glucose homeostasis. Whether the interaction between *Dlk1* and *Grb10* is direct or indirect remains to be elucidated.

In light of previous reports of *Grb10* and *Dlk1* opposite effects on prenatal growth and development, along with several sites of imprinted co-expression and similar time of action, we have characterised *Grb10*$^{m/+}$/*Dlk1*$^{+/p}$ double knockout conceptuses to analyse the consequences of *Grb10* and *Dlk1* ablation on embryogenesis. *Grb10*$^{m/+}$/*Dlk1*$^{+/p}$ embryos showed significant overgrowth similar to *Grb10*$^{m/+}$ embryos from E12.5 onwards and placental overgrowth from E14.5. Our results for E17.5 which also showed *Grb10*$^{m/+}$/*Dlk1*$^{+/p}$ and *Grb10*$^{m/+}$ embryonic and placental overgrowth along with increased placental efficiency, should however be further supported by extending the size of the analysed cohort. It was exciting to see that *Grb10*$^{m/+}$/*Dlk1*$^{+/p}$ shared the phenotype of *Grb10*$^{m/+}$ embryos, possibly suggesting an epistatic relationship between *Grb10* and *Dlk1* to control embryonic development. However, the important issue to consider before interpreting results obtained during this study involves

the maternal genotype (*Grb10*$^{m/+}$) possibly influencing development and growth of the offspring of all four genotypes, therefore in the future use of *Grb10*$^{m/p}$ dams should be considered as the main point of our study was to compare the phenotype of *Grb10*$^{m/+}$/*Dlk1*$^{+/p}$ animals to the phenotypes of *Grb10*$^{m/+}$ and *Dlk1*$^{+/p}$ single knockout animals.

The co-localisation analysis of reciprocally imprinted genes during embryonic development has been used as a useful approach in identifying different mechanisms underlying imprinting mechanisms in different imprinted clusters, as exemplified by analyses of *Igf2/H19* (Ohlsson et al., 1994), *Nespas* within the *Gnas* locus (Ball et al., 2001), as well as *Dlk1* and *Gtl2* (da Rocha et al., 2007). It would therefore be informative to carry out similar analysis of *Grb10* and *Dlk1* co-expression during embryogenesis as both genes show their most pronounced expression during this time of development.

Extensive *Grb10* expression from the maternal allele has been reported in several organs of *Grb10*$^{m/+}$ E14.5 embryos, including various muscle tissues, lung bronchioles, liver, adrenal gland and pancreatic bud as well as developing tubules and the mesenchyme of the kidneys (Charalambous et al., 2003). Furthermore, expression has been noted in cartilage primordia including those of the atlas, ribs and long bones. On the other hand, paternal *Grb10* expression has been noted in the developing CNS and, in parallel with maternal expression, in cartilage tissue (Charalambous et al., 2003). One of the most prominent sites of *Dlk1* expression in the brain is the developing pituitary gland, along with the dermomyotome, myotome and sclerotome of the somites at E10, and afterwards skeletal muscle along with the primordial cartilage of different types of bones (da Rocha et al., 2007). Prominent *Dlk1* expression has also been noted in the preadipocytes, cortex of the adrenal gland and pancreas, and the expression in both of these organs persisted until adulthood. *Dlk1* is also expressed in the cytoplasm of some fetal hepatic cells, ducts of salivary glands and segmental bronchi of the lungs, where it is suspected to play a role in branching morphogenesis (Yevtodiyenko and Schmidt, 2006). Therefore, there are several sites of *Grb10-Dlk1* co-expression, notably in the liver, lung, adrenal gland, skeletal muscle and cartilage.

Embryonic growth is largely influenced by correct function of the placenta, an organ that evolved in eutherian mammals to provide nutrients for the developing embryo. Various imprinted genes have been postulated to mediate a network of supply and demand factors *in utero*, for example the *Igf2* gene (Coan et al., 2008), which, however has been shown to not interact with *Grb10* in the same genetic pathway (Charalambous et al., 2003)

Extraembryonic *Dlk1* expression has been demonstrated in all three layers of the placenta: (labyrinth zone, junctional zone and decidua basalis), chorionic plate and yolk sac (Yevtodiyenko and Schmidt, 2006; da Rocha et al., 2007). The *Dlk1* expression within the labyrinth zone decreases with time and it is confined to the membrane of the fetal capillary endothelium, whereas in the junctional zone and decidua basalis it is found within the glycogen cells (Yevtodiyenko and Schmidt, 2006; da Rocha et al., 2007). Furthermore, predominantly maternal *Grb10* expression has also been reported in the labyrinth compartment of the placenta, more specifically in the fetal endothelium and in at least one of the three trophoblast layers of the labyrinth (Charalambous et al., 2010). The labyrinth zone of the placenta is a site of the nutrient exchange between mother and offspring, which occurs by passive diffusion and active transport (Sibley et al., 1997). *Grb10* has been reported as the unique imprinted gene not only able to influence the size (Charalambous et al., 2003) but also the efficiency of the placenta (Charalambous et al., 2010), although previous reports of changes within placental efficiency (Constancia et al., 2002) or size (Frank et al., 2002) affected by imprinted genes exist. Co-localised expression of *Grb10* and *Dlk1* in the placental labyrinth zone suggests each could function in mediating maternal-nutrient exchange, which could influence fetal growth, as exemplified by genetic studies (Moon et al., 2002; Charalambous et al., 2003; Charalambous et al., 2010). Therefore it was of interest to analyse the effects of *Grb10* and *Dlk1* ablation on growth of *Grb10*$^{m/+}$*/Dlk1*$^{+/p}$ placentae. Our results showing similar overgrowth in *Grb10*$^{m/+}$and *Grb10*$^{m/+}$*/Dlk1*$^{+/p}$ E14.5 placentae could possibly support the hypothesis of *Grb10-Dlk1* interaction in extraembryonic tissues that influences the embryonic growth, and results obtained for E17.5 show a similar trend but they need to be further confirmed using larger sample size. It also needs to be taken into account that alternative explanation for the observed overgrowth in *Grb10*$^{m/+}$*/Dlk1*$^{+/p}$ embryos may be provided by the highly increased efficiency of nutrient supply by the *Grb10*$^{m/+}$*/Dlk1*$^{+/p}$ placentae. Therefore, more detailed stereological measurements, including percentage volume fractions of junctional and labyrinth zones, the surface areas within the labyrinth zone (fetal capillaries and maternal blood spaces), and the interhemal membrane thickness will be applied in order to analyse the morphology and function of *Grb10*$^{m/+}$*/Dlk1*$^{+/p}$ placenta in comparison with *Grb10*$^{m/+}$ and *Dlk1*$^{+/p}$ placentae. It will also be interesting to study the details of nutrient transfer in *Grb10*$^{m/+}$, *Grb10*$^{m/+}$*/Dlk1*$^{+/p}$ and *Dlk1*$^{+/p}$ placentae check if, especially in light of shortage of information on *Dlk1*$^{+/p}$ placentae characteristics. These kinds of studies are important as deregulation of supply and demand affects fetal growth and can have detrimental consequences on health in the neonatal period and, as a result of fetal programming, in adulthood.

We have used *in vitro* analysis to investigate the cellular basis for the enhanced growth in *Grb10*$^{m/+}$*/Dlk1*$^{+/p}$ conceptuses, as we studied the proliferation rates in pMEFs derived from E14.5 embryos and discovered that *Grb10*$^{m/+}$*/Dlk1*$^{+/p}$ and *Grb10*$^{m/+}$ cells proliferated significantly faster than wild type and *Dlk1*$^{+/p}$ cells, findings in agreement with significant embryonic overgrowth in mice of the former genotypes. Again, the identified similarity in phenotype between *Grb10*$^{m/+}$*/Dlk1*$^{+/p}$ and *Grb10*$^{m/+}$ cells further supports the possible epistatic action of *Grb10* to *Dlk1*. This is the first report of the growth rates of *Dlk1*$^{+/p}$ pMEFs, which proliferated at a lower rate than *Grb10*$^{m/+}$*/Dlk1*$^{+/p}$ and *Grb10*$^{m/+}$ pMEFs, but not significantly slower than wild type cells. This is consistent with results from allometric analyses which showed *Dlk1*$^{+/p}$ embryos being smaller than those of other the other analysed genotypes, but the differences did not become significant until birth.

To further examine the nature of *Grb10*$^{m/+}$*/Dlk1*$^{+/p}$ and *Grb10*$^{m/+}$ embryonic overgrowth, we used FACS analysis to determine cell size and cycle kinetics in cells derived from E11.5 embryos and in E14.5 pMEFs. No apparent hypertrophy has been observed in *Grb10*$^{m/+}$*/Dlk1*$^{+/p}$ and *Grb10*$^{m/+}$ cells, however results from this experiment need to be interpreted with great care due to the unspecific gating of the singlet and dublet cells that might have influenced and covered the real results. Therefore, the analysis of the results from this experiment should be repeated and gating carried out in the same manner as performed during cell cycle analysis. The examination of cell cycle phases revealed a shortened S-phase and elongated G2-phase with in these cells, which is in agreement with previous reports of the hyperproliferative nature of *Grb10*$^{m/+}$ cells that was not associated with changes in intrinsic apoptosis or with altered cell size (Garfield, 2007). This suggests that *Grb10* acts as a repressor of cell cycle progression (most possibly during S and G2 phases) and that its lack causes cell hyperproliferation resulting in somatic overgrowth. Some features observed in mice with ablation of *Grb10* resemble characteristics of patients suffering from Silver-Russell syndrome, although there is a shortage of firm evidence for its role in this disease. Whilst several clinical studies have implicated *Grb10* in SRS cases (Joyce et al., 1999; Hannula et al., 2001), others have argued against its role in this disorder (McCann et al., 2001). Nonetheless, it is still possible that *Grb10* plays a role in the aetiology of other disorders associated with growth, such as mUPD7. Taken together, these results indicate that *Dlk1* and *Grb10* possibly interact with each other to provide an optimal size of the developing embryo at birth, at least in part, by regulating cell proliferation rates during embryogenesis.

The effects of *Grb10* on placental and embryonic growth are potentially consistent with both parental conflict and coadaptation theories of imprinted gene evolution. The recent

discovery by our lab that the *Grb10* gene is most likely involved in a coadaptive strategy to influence the maintenance of optimal offspring fitness (Cowley et al., submitted) has led us to reconsider the driving forces that have resulted in evolution of imprinting at this locus.

Allometric analysis revealed that significant overgrowth of *Grb10*$^{m/+}$*/Dlk1*$^{+/p}$ and *Grb10*$^{m/+}$ mice during embryogenesis persisted until birth, but was not evident in the adulthood, in contrast to the previously described *Grb10*$^{m/+}$ overgrowth that persisted until the age of 6 months (Smith et al., 2007). The explanation for the diminished increase of total body weights in *Grb10*$^{m/+}$ mice could be provided by the different genetic background that resulted from crossing *Grb10*$^{m/+}$ with *Dlk1*$^{+/p}$ knockout animals, as *Dlk1*$^{+/p}$ animals were of C57BL/6 background whereas *Grb10*$^{m/+}$mice were maintained on a mixed C57BL/6/CBA background, which also needs to be taken into consideration when comparing the growth of these animals. Similarly, the use of animals that were not strictly age-matched (3-6 and 7-9 month old) could potentially influence the results of allometric analyses of total body and organ weights in studied animals, therefore future examination should be based on the use of mouse cohorts of more similar ages.

We observed that neonatal *Grb10*$^{m/+}$*/Dlk1*$^{+/p}$ and *Grb10*$^{m/+}$ mice displayed significantly elevated relative liver weights and cranial and kidney sparing. The cranial sparing, previously observed in *Grb10*$^{m/+}$ neonates (Charalambous et al., 2003; Garfield, 2007), could be explained by limited maternal *Grb10* expression within the developing CNS. Although neonatal lung weights changed proportionally to changes of total body weights, their histological analysis revealed abnormalities in *Grb10*$^{m/+}$*/Dlk1*$^{+/p}$ and *Grb10*$^{m/+}$ mice. Previous reports of pulmonary defects in *Dlk1* knockout mice as well as incidence of *Grb10* knockout perinatal lethality due to blood-filled lung alveoli encouraged us to investigate in more detail the lung morphology in *Grb10*$^{m/+}$*/Dlk1*$^{+/p}$ knockout mice. In neonatal, but not adult, *Grb10*$^{m/+}$*/Dlk1*$^{+/p}$ and *Grb10*$^{m/+}$ mice, we identified thickened lung epithelial walls and reduced airway spaces, which could reduce the oxygen exchange area and consequently lead to impaired breathing efficiency. It was interesting and somewhat surprising that we did not find any abnormalities within *Dlk1*$^{+/p}$ lungs, especially in light of a demonstrated strong *Dlk1* expression in segmental bronchi of the lungs (Yevtodiyenko and Schmidt, 2006; da Rocha et al., 2007), where it might influence the process of lung branching morphogenesis. In addition, altered lung morphology in *Grb10*$^{m/+}$*/Dlk1*$^{+/p}$ and *Grb10*$^{m/+}$ neonates did not persist until adulthood, suggesting that possible perinatal lung dysfunctions have been overcome postnatally.

Recent studies have demonstrated that Grb10 has a capacity to inhibit RTKs, including insulin receptor, through acting in a negative feedback loop upon phosphorylation by mTORC1 (**Figure** 6.2; Hsu et al., 2011; Yu et al., 2011). Mammalian target of rapamycin (mTOR) is known as an important effector of cell growth, protein synthesis and proliferation. It functions by integrating various signals expected to change during late gestation, the birth process, and the neonatal period, including amino acid and energy availability, hormonal levels and changes in pO_2 (reviewed in Martin and Hall, 2005). A recent study has aimed to investigate mTOR signalling in translational regulation in the developing rat lung and at birth (Otulakowski et al., 2009). Otulakowski et al (2009) provided evidence that mTOR functions in perinatal lung physiology, as mTOR signalling was found to control protein synthesis in perinatal rat lung, causing a substantial increase in protein synthesis following birth. Disruption of a downstream effector of mTOR, *S6K1,* causes growth reduction in mice, whereas double knockout of *S6K1* and its homolog *S6K2* leads to a high incidence of perinatal lethality, indicating the importance of these genes in normal fetal growth and particularly the transition from fetal to postnatal life (Pende et al., 2004). This raises a possibility that as another identified mTOR downstream target Grb10 could have similar function and influence adaptation from fetal to postnatal life by influencing the lung physiology.

Dlk1 expression has been reported in hepatoblasts and immature hepatocytes (Tanimizu et al., 2003), where it has been confined to cytoplasm of the majority of hepatic cells in mouse embryos (da Rocha et al., 2007). *Grb10* expression in developing liver has also been noted (Charalambous et al., 2003), although liver expression of both *Grb10* and *Dlk1* genes significantly declines after birth (Lui et al., 2008). Here we used histological analyses to look for abnormalities that could account for differences in liver weights postnatally. Abnormally high accumulation of lipids was noted in all neonatal and half of 1 week old $Grb10^{m/+}/Dlk1^{+/p}$ and $Grb10^{m/+}$ livers, along with similar lipid accumulation in overgrown adult $Dlk1^{+/p}$ livers, and at the same time we have observed the increased growth of these livers during allometric analysis. It was interesting to note that at the stage of E14.5 $Grb10^{m/+}/Dlk1^{+/p}$ and $Grb10^{m/+}$ livers did not show any discrepancies from wild type histology, indicating at the later gestational stages or day of birth that could possibly mark the start of the abnormal lipid accumulation. Thus it would be of interest to histologically examine livers of $Grb10^{m/+}/Dlk1^{+/p}$ and $Grb10^{m/+}$ embryos during late fetal development. Similarly, investigation of the types of lipids accumulated in $Grb10^{m/+}/Dlk1^{+/p}$ and $Grb10^{m/+}$ livers along with total liver lipid content and examination of blood lipid levels in neonatal mice should clarify the nature of the observed $Grb10^{m/+}/Dlk1^{+/p}$ and $Grb10^{m/+}$ fatty livers. The significant neonatal liver overgrowth

would require further investigation through morphometric analysis of hepatocyte numbers to check if high adiposity could solely account for the observed overgrowth phenotype or there are also other factors that play part in it, as previous analysis has shown that hepatocyte size was not altered in *Grb10*$^{m/+}$ neonatal livers (Charalambous et al., 2003).

Neonatal hepatic steatosis is a fatal condition associated with a rapid microvesicular fat infiltration and enhanced growth of the liver, and subsequent early postnatal mortality (Satran et al., 1969). Impaired mitochondrial function related to hepatic steatosis has been previously associated with genetic defects in the oxidation of fatty acids (Boles et al., 1998), with inhibition of oxidation by drugs (Fromenty et al., 1997; Fromenty and Pessayre, 1997), with defective carnitine-dependent transport of fatty acids (Brivet et al., 1999), with an impaired production of ATP (Krahenbuhl, 1993) and with a deficit in adenosine-dependent metabolism (Boison et al., 2002). Mice carrying disrupted Adenosine Kinase (*Adk*) gene displayed normal embryonic development but within 4 days after birth they showed microvesicular hepatic steatosis and lethality within 2 weeks after birth, at which stage they also had fatty livers (Boison et al., 2002). Histological analysis of the livers from *Adk* mutant mice and wild type littermates performed at different perinatal time points (E17.5, P0.5, P2, P4, P6 and P14) did not reveal any morphological abnormalities in the livers of *Adk* mice at E17.5, but 12 h after birth (P0.5) the first morphological differences were observed in the form of microvesicular steatosis. The development of macrovesicular steatosis started at P2 as the entire cytoplasm was often occupied by lipids and the nucleus was frequently moved to the cell periphery. Eventually, a homogenous mixture of micro- and macrovesicular steatosis without any lobular predominance was observed at day P4 in the *Adk* mutant livers (Boison et al., 2002). *Adk* homozygous livers were similar size to wild type despite overall 20% growth reduction in *Adk* mutants, and their livers did not show any alterations in glycogen content as confirmed by PAS staining. Therefore, impaired adenosine metabolism has been implied as a potential source of neonatal hepatic steatosis, as it provided a model for the development of postnatal fatty liver leading to early mortality. There are similarities between the *Adk* and *Grb10*$^{m/+}$ or *Grb10*$^{m/+}$*/Dlk1*$^{+/p}$ neonatal fatty livers, as in both cases they develop during perinatal period and are not associated with altered liver glycogen content, however further examination of *Grb10*$^{m/+}$ or *Grb10*$^{m/+}$*/Dlk1*$^{+/p}$ late embryonic livers will help to specify if *Grb10*$^{m/+}$ or *Grb10*$^{m/+}$*/Dlk1*$^{+/p}$ mice develop fatty livers specifically upon birth or the liver lipid accumulation begins during late embryogenesis. In addition, unlike in the case of *Adk* mutant mice, neonatal fatty livers of *Grb10*$^{m/+}$ or *Grb10*$^{m/+}$*/Dlk1*$^{+/p}$ did not lead to lethality within first two weeks of life, probably due to the fact that in contrast to progressing hepatic steatosis in *Adk* livers, lipid

content of *Grb10*$^{m/+}$ or *Grb10*$^{m/+}$*/Dlk1*$^{+/p}$ livers appeared to diminish with time, as confirmed by decreased adiposity in *Grb10*$^{m/+}$ or *Grb10*$^{m/+}$*/Dlk1*$^{+/p}$ 1 week old livers compared to neonatal ones. Therefore, it is possible that two different mechanisms are underlying the development of *Grb10*$^{m/+}$ or *Grb10*$^{m/+}$*/Dlk1*$^{+/p}$ and also *Adk* fatty livers, but it still would be of interest to assess the possible contribution of adenosine metabolism to the liver pathology of *Grb10*$^{m/+}$ or *Grb10*$^{m/+}$*/Dlk1*$^{+/p}$ mice.

In contrast to *Adk* mutant mice, fatty liver dystrophy (*fld*) mice are characterised by hypertriglyceridemia and fatty liver during neonatal development that spontaneously resolves between the age of 14–18 days (Rehnmark et al., 1998). It would be of interest to check at specifically what age the fatty livers are not detectable in *Grb10*$^{m/+}$ or *Grb10*$^{m/+}$*/Dlk1*$^{+/p}$ mice and if their increased liver adiposity also resolves at around 2 weeks after birth. Triglyceride accumulation in the *fld* fatty liver has been associated with disrupted expression of proteins involved in fatty acid oxidation as 60% reduction in hepatic fatty acid oxidation has been noted in *fld* neonates but was normal in adult *fld* mice that do not have fatty livers (Rehnmark et al., 1998). Therefore, to investigate the biochemical basis for the increased lipid accumulation in *Grb10*$^{m/+}$ or *Grb10*$^{m/+}$*/Dlk1*$^{+/p}$ neonatal livers, their protein expression patterns could be compared to those of wild type littermates and quantification of rates of fatty acid oxidation could also be performed. An exciting discovery of specifically-neonatal hepatic steatosis in *Grb10*$^{m/+}$ or *Grb10*$^{m/+}$*/Dlk1*$^{+/p}$ livers and identification of the underlying causes could add to our understanding of genes and biochemical mechanisms contributing to fatty liver formation as it becomes clear that steatosis can lead to the development of more advanced liver pathology.

The observation of liver lipid accumulation in adult *Dlk1*$^{+/p}$ mice could be explained by lack of *Dlk1* affecting normal adipocyte differentiation and, subsequently, resulting in abnormal lipid storage, which is further supported by the elevated levels of triglycerides in blood serum of *Dlk1*$^{+/p}$ mice. Both liver lipid accumulation and elevated blood serum triglyceride levels were reported previously (Moon et al., 2002) and associated with lack of normal anti-adipogenic *Dlk1* action. The occurrence and nature of the adult pancreatic overgrowth and its association with liver overgrowth is currently being investigated.

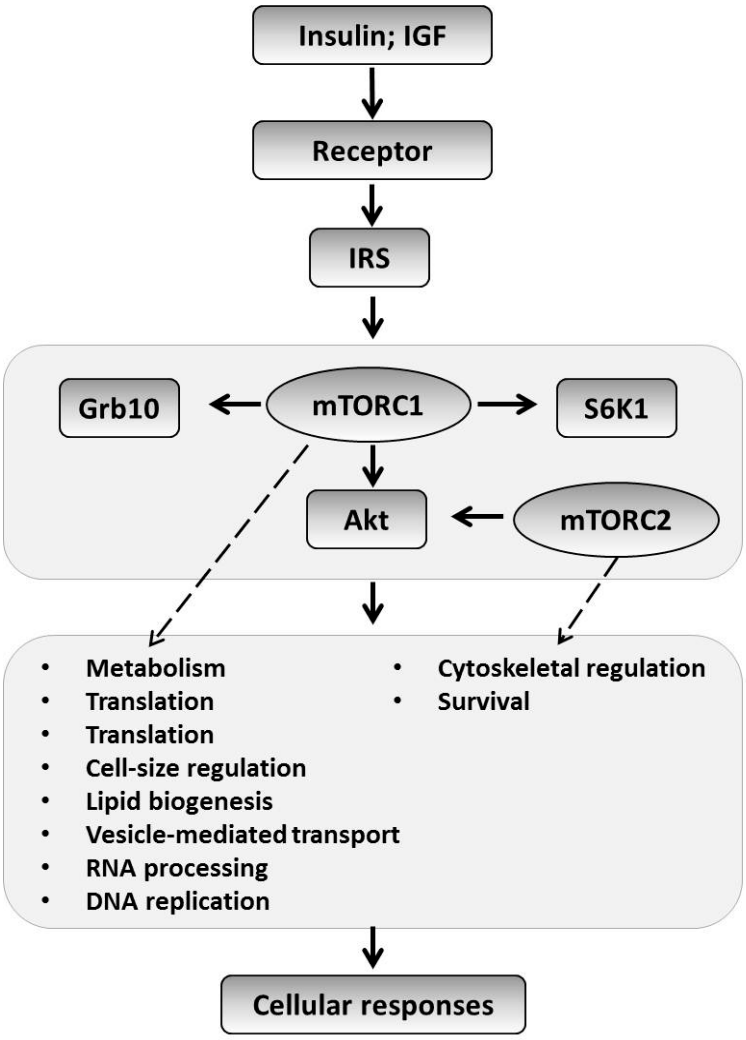

Figure 6.2 mTOR signalling and processes controlled by mTOR. Figure adapted from (Yea and Fruman, 2011).

mTOR functions in two separate protein complexes (mTORC1 and mTORC2), which both act to control the majority of AGC (cAMP-dependent, cGMP-dependent and protein kinase C) protein superfamily members, including Akt and S6K1. mTORC1, which is activated downstream of insulin or IGFs, directly phosphorylates Grb10 and enhances its ability to inhibit signals from insulin and IGF receptors. This negative feedback loop is complementary to another feedback pathway with S6K1 phosphorylating IRS and targeting it for degradation.

Allometric analysis did not show the previously demonstrated reduction of adiposity in *Grb10*$^{m/+}$ or *Grb10*$^{m/+}$/*Dlk1*$^{+/p}$ mice, and incidence of higher fat tissue content was found only in *Dlk1*$^{+/p}$ 3-6 month female mice. DXA analysis of body composition showed opposite trends in lean tissue content of *Grb10*$^{m/+}$ and *Dlk1*$^{+/p}$ mice, with *Grb10*$^{m/+}$ animals having a significantly elevated lean tissue mass. It would be interesting to investigate *Grb10* function as a promoter of proliferation or differentiation of adipocytes by feeding *Grb10*$^{m/+}$ and *Grb10*$^{m/+}$/*Dlk1*$^{+/p}$ mice

on high fat diet, especially in light of previous studies showing opposite results of HFD on the fat tissue content in *Dlk1*$^{+/p}$ and *Grb10*$^{m/+}$ mice, as the former showed significant increase in adipose depots (Moon et al., 2002) whereas the latter displayed significantly smaller fat depots when compared to control animals (Holt et al., 2009). As we did not see any changes in adipose/lean tissue composition of *Grb10*$^{m/+}$*/Dlk1*$^{+/p}$ mice, it would be of interest to study changes within their body composition following high fat diet. Correlation between *Grb10*, *Dlk1* and adipogenesis make them exciting targets in studying obesity.

Grb10$^{m/+}$ adult mice exhibit enhanced glucose metabolism, which has been partly associated with an increased lean/fat ratio (Smith et al., 2007; Wang et al., 2007). Recent study by our lab provided evidence that normal lean/fat ratio requires correct *Grb10* function in both dam and pup, as by controlling supply and demand after birth, *Grb10* regulates body composition (Cowley et al., submitted). This finding further supports a role for *Grb10* in coadaptation between maternal and offspring genomes in order to optimise offspring fitness by influencing correct body proportions. It also indicates a role for *Grb10* in early development programming of adult health status and suggests that adult lean/fat ratio in *Grb10*$^{m/+}$ mice does not represent a postnatal-specific phenotype.

Enhanced insulin signalling has been implicated as a cause of improved whole-body glucose homeostasis in *Grb10* (Smith et al., 2007) and *Grb14* deficient mice (Cooney et al., 2004), but only mice with *Grb10* ablation also exhibited reduced adipose tissue mass. Furthermore, the ablation of *Grb7* likewise resulted in increased glucose tolerance and slightly reduced adiposity, suggesting overlapping roles in glucose-related metabolism for all members of the Grb7 protein family. Largely similar effects of *Grb10* and *Grb14* ablation in mice have encouraged the generation of compound knockout mice (Holt et al., 2009), but surprisingly double knockout animals did not show further increased insulin signalling but rather displayed an increase in lean mass, indicating that this is a function specific to the *Grb10* gene. In spite of that, *Grb10/Grb14* knockout mice were protected from adverse changes in glucose tolerance following feeding on a HFD, a result not observed in animals with the single gene ablations. This suggests Grb10 and Grb14 might not only regulate glucose homeostasis by exerting effects on Irs-1/Akt signalling, but employ some other mechanisms, and implies that genes within the Grb7 family might indeed prove to be excellent therapeutic targets for treatment or prevention of type 2 diabetes and obesity.

Although the imprinting status of *Grb10* and *Dlk1* has been identified more than a decade ago (Miyoshi et al., 1998; Schmidt et al., 2000), the details of their regulation and modes of

action are yet to be determined, and with every new finding they continue to be even more exciting to work on. With time and more intricate studies of the *Grb10* imprinting more interesting features are discovered in this unique gene, which makes it a great model for investigation of imprinted gene function and regulation. *Grb10* is unusual among other imprinted genes, with its reciprocal, parent-of-origin- expression conserved in mice and human (Blagitko et al., 2000; Arnaud et al., 2003; Monk et al., 2009) that regulates entirely distinct physiological processes in a tissue-specific manner (Garfield et al, 2011). Preliminary results showing the function of the two zebrafish *Grb10* orthologs suggest that the growth regulatory function of *Grb10* might be mammal-specific, which is in agreement with the evolution of genomic imprinting in mammals but not fish (Lee, Kelsh and Ward, unpublished data). Although a recent study has proposed a novel mechanism by which tissue-specific imprinting of *Grb10* is controlled (Sanz et al., 2008), the reasons underlying this kind of allele-specific expression remains unknown. Generation of mice with *Grb10* ablation transmitted separately through each of the parental alleles allowed this issue to be addressed by characterising the role of each of the parental *Grb10* alleles in a physiological context. Maternally expressed *Grb10* regulates embryonic growth (Charalambous et al., 2003) and litter size (Charalambous et al., 2010) along with body composition and glucose-regulated metabolism (Smith et al., 2007). Moreover, our lab has recently found that *Grb10* maternal expression in mammary gland during pregnancy influences postnatal nutrient supply and demand, regulating the size of the offspring and that maternal and offspring *Grb10* have distinct consequences on the body composition of the progeny (Cowley et al., submitted). On the other hand, the pattern and role of maternally imprinted *Grb10* is somewhat different, as paternal *Grb10* is mostly expressed in the CNS where it functions to control behaviour, specifically social dominance (Garfield et al., 2011). This is the first example of opposite imprinting within one gene that has evolved according to different, tissue-specific functions, and this situation is likely to be conserved in humans (Blagitko et al., 2000). The ability of *Grb10* to control growth, metabolism and behaviour adds to the complexity and importance of imprinted genes in normal organism function and makes it a unique, exciting gene to study.

Much attention has also been put into investigation of the establishment, function and regulation of the imprinted *Dlk1/Dio3* locus (da Rocha et al., 2008; Edwards et al., 2008; Sato et al., 2011), as its developmental importance has been exemplified by dramatic phenotypes associated with altered dosage of genes within this locus in mice and humans. Impaired expression of genes within the *Dlk1-Dio3* cluster results in a range of phenotypic alterations including growth abnormalities and developmental defects in the embryo and placenta as well

as disrupted adult metabolism and brain function. The *Dlk1-Dio3* imprinted domain has emerged as a useful model for analysing the regulation, function, genomic organisation and evolution of imprinted clusters in mammalian species (reviewed in da Rocha et al., 2008; Edwards et al., 2008).

Dlk1, situated within *Dlk1-Dio3* cluster, is another very exciting gene to study, with its unusual structure and obviously crucial role in normal growth, development and metabolism. *Dlk1* codes for a transmembrane glycoprotein with six EGF-like motifs in the extracellular domain, showing a similar structure to Delta-Notch-Serrate protein family, although it does not possess the DSL domain crucial for interacting with and activating the Notch receptor. Indeed, some studies have reported that Dlk1 can act as a Notch antagonist (Baladron et al., 2005; Nueda et al., 2007; Bray et al., 2008).

Accumulated evidence suggests *Dlk1* roles in a wide range of differentiation processes, including hematopoiesis (Bauer et al., 1998; Kaneta et al., 2000; Sakajiri et al., 2005), chondrogenesis (Chen et al., 2011), osteogenesis (Abdallah et al., 2004; Abdallah and Kassem, 2011) and neuroendocrine (Floridon et al., 2000) and hepatocyte differentiation (Tanimizu et al., 2003). It has also been shown to regulate cell growth and cancer (Laborda et al., 1993; Yin et al., 2004; Kawakami et al., 2006). However, the most widely studied process regulated by *Dlk1* is adipogenesis, as *Dlk1* has been established as a potent inhibitor of adipocyte differentiation *in vitro* (Smas and Sul, 1993; Smas et al., 1998; Garces et al., 1999). Mouse models with *Dlk1* gain and loss of function have unequivocally confirmed a crucial role for *Dlk1* in adipogenesis. *Dlk1* was found to influence adipose tissue content, glucose homeostasis, and circulating levels of triglycerides as well as impaired expression of adipocyte markers and adipocyte-secreted factors (Moon et al., 2002; Lee et al., 2003; Villena et al., 2008). All these findings strongly support *Dlk1* as a potent inhibitor of adipogenesis and indicate its possible roles in obesity (especially due to obesity observed in patients with mUPD14) and lipodystrophy, commonly associated with pathologies including diabetes and cardiovascular diseases.

Aside from developmental roles, correct imprinting status is also crucial in postnatal health, as disrupted imprinted gene expression has been implicated in various diseases pronounced in adulthood, including cancers and neurological disorders such as Angelman and Prader-Willi syndromes (discussed in more detail in Section 1.1.4). Here we have demonstrated that *Grb10* and *Dlk1* ablation leads to number of postnatal phenotypic abnormalities in mice, although it is difficult to firmly state if they are direct consequences of

lack of *Grb10* and *Dlk1* postnatal expression or rather they result from fetal programming of adult growth. As expression of *Grb10* and *Dlk1* upon birth is largely restricted, it could be argued that fetal programming effects could be a more plausible explanation for the observed phenotypes.

It was interesting to find that the embryonic growth similarities between *Grb10*$^{m/+}$*/Dlk1*$^{+/p}$ and *Grb10*$^{m/+}$ mice discussed in Chapter 3 had similar foundations for both genotypes, as we demonstrated that hyperproliferation is the most probable cause of the observed embryonic overgrowth phenotype. Interestingly, growth effects seen during embryogenesis were largely persistent until day of birth, as we revealed significant overgrowth in *Grb10*$^{m/+}$*/Dlk1*$^{+/p}$ and *Grb10*$^{m/+}$ neonates among other changes within neonatal organ weights, including liver overgrowth and cranial sparing discussed in Chapter 4. Aside from that, we also found that *Grb10*$^{m/+}$*/Dlk1*$^{+/p}$ and *Grb10*$^{m/+}$ handled a glucose load in a similar manner, displaying the capacity to clear the glucose significantly faster than control animals (Chapter 5), which indicated that this ability is associated with enhanced insulin signalling rather than increased lean tissue mass, as has previously been suggested for *Grb10*$^{m/+}$ mice. An epistatic interaction between two genes is observed if the combined effects of mutations in both genes are different from the sum of each mutation's individual effects. Better understanding of epistatic genetic interactions is needed to uncover the genotype-phenotype relationships. The generation of *Grb10*$^{m/+}$*/Dlk1*$^{+/p}$ double knockout mice proved to be of a great benefit in investigating the possible epistatic interaction between *Grb10* and *Dlk1* genes, although it was expected that not all aspects of *Grb10*$^{m/+}$and*Dlk1*$^{+/p}$ knockout mice phenotypes will be mirrored by *Grb10*$^{m/+}$*/Dlk1*$^{+/p}$ and explained by their interaction. Here we demonstrate that *Grb10* and *Dlk1* genes can potentially interact with each other in order to regulate embryonic and placental growth, postnatal size and morphology of several organs and some aspects of adult metabolism (summarised in **Table** 6.1). Further investigation, specifically of the details of biochemical basis of *Dlk1-Grb10* interaction is under way, as Western Blot analysis of embryos and mid-gestational livers should provide some further evidence for possible *Grb10* and *Dlk1* interaction.

Prenatal analysis	Postnatal analysis	Metabolic analysis
E12.5, E14.5 and E17.5 embryonic overgrowth	Neonatal body and live overgrowth, cranial and kidney sparing, thicker epithelial walls in neonatal lungs	Significantly improved ability to clear glucose load
E14.5 placental overgrowth	3-6 month old males: increased wet and relative pancreas weights, decreased wet weights of the kidneys and relative liver weights	Lower glucose levels in fed female mice
Higher proliferation rate of E14.5 pMEFs	7-9 month old males: smaller wet and relative kidney weights	Increased liver lipid accumulation in neonatal and 1 week old mice
Shortened S-phase and elongated G2-phase of the cell cycle	3-6 month old females: higher relative pancreas weights decreased renal fat pad weights	

Table 6.1 Summary of the phenotypic features shared between *Grb10*$^{m/+}$/*Dlk1*$^{+/p}$ and *Grb10*$^{m/+}$ mice that were significantly different to those of wild type mice.

To summarise, the studies described here have not only confirmed and widened our knowledge on the crucial roles of *Grb10* and *Dlk1* genes in correct embryonic and postnatal growth and development and adult metabolism, but most importantly provided evidence for a possible interaction between these two genes within the same genetic pathway (**Figure** 6.1). The majority of studies presented here have substantiated the hypothesis that *Grb10* and *Dlk1* form part of an epistatic pathway, in which *Dlk1* inhibits *Grb10* which in turn acts to supress growth and exert other effects on the correct heath status of an organism. Whether this interaction is direct or indirect remains to be determined. The results presented here provide a foundation for future investigations of a novel imprinted gene pathway consisting of genes that are able to influence the crucial sites of imprinted gene action: growth, metabolism and behaviour.

Appendix 1

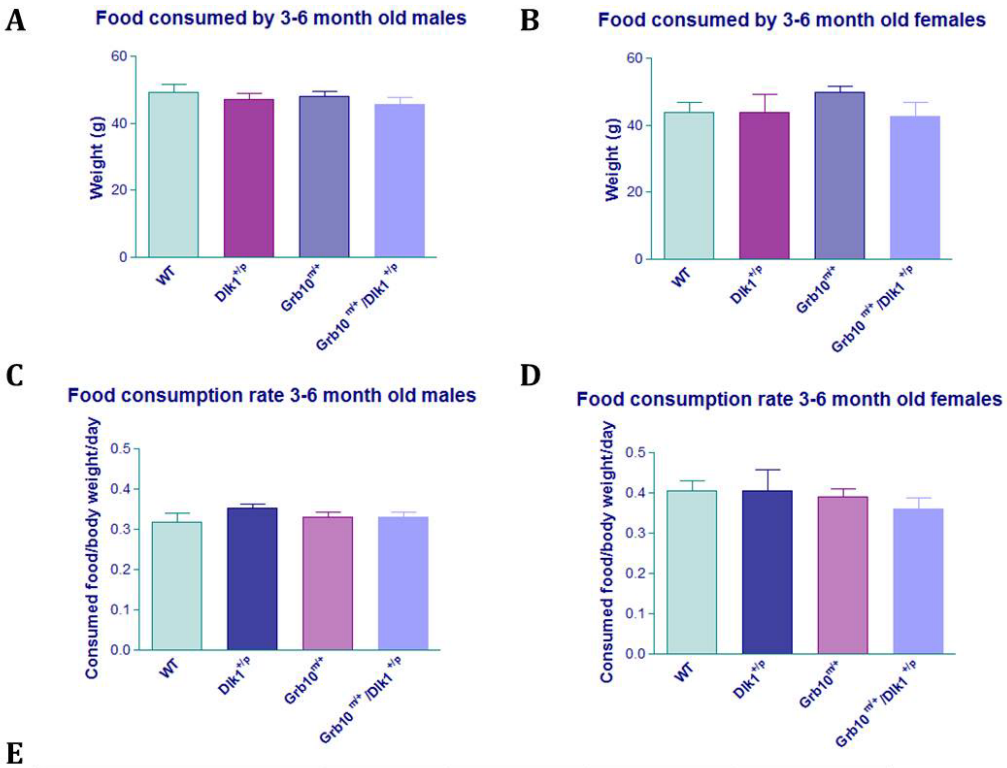

E

	Food males	Food females	Consumption rate males	Consumption rate females
WT vs Grb10$^{m/+}$	ns	ns	ns	ns
WT vs Dlk1$^{+/p}$	ns	ns	ns	ns
WT vs Grb10$^{m/+}$/Dlk1$^{+/p}$	ns	ns	ns	ns
Grb10$^{m/+}$ vs Dlk1$^{+/p}$	ns	ns	ns	ns
Grb10$^{m/+}$ vs Grb10$^{m/+}$/Dlk1$^{+/p}$	ns	ns	ns	ns
Dlk1$^{+/p}$ vs Grb10$^{m/+}$/Dlk1$^{+/p}$	ns	ns	ns	ns

Analysis of feeding behaviour in 3-6 month old wild type, *Grb10$^{m/+}$*, *Dlk1$^{+/p}$* and *Grb10$^{m/+}$/Dlk1$^{+/p}$* mice.

Food intake was monitored over a period of two weeks. Food consumption rates have been calculated as food consumed per gram of animal body weight per day to the power of 2/3. **A)** Total amount of consumed food by males. **B)** Total amount of consumed food by females. **C)** Male consumption rates: total weight of food consumed by males per gram of body weight per day to the power of 2/3. **D)** Female consumption rates: total weight of food consumed by females per gram of body weight per day to the power of 2/3. There were no significant changes neither in the amounts of consumed food or in food consumption rates of transgenic mice when compared to wild type controls. **E)** Table summarising results of statistical analysis. All values represent means ± SEM and have been subject to one way ANOVA with post hoc Tukey's analysis. Males: WT n=7, *Dlk1$^{+/p}$*=7, *Grb10$^{m/+}$* n=6 and *Grb10$^{m/+}$/Dlk1$^{+/p}$* n=7; females: WT n=9, *Dlk1$^{+/p}$*=6, *Grb10$^{m/+}$* n=6 and *Grb10$^{m/+}$/Dlk1$^{+/p}$* n=7.

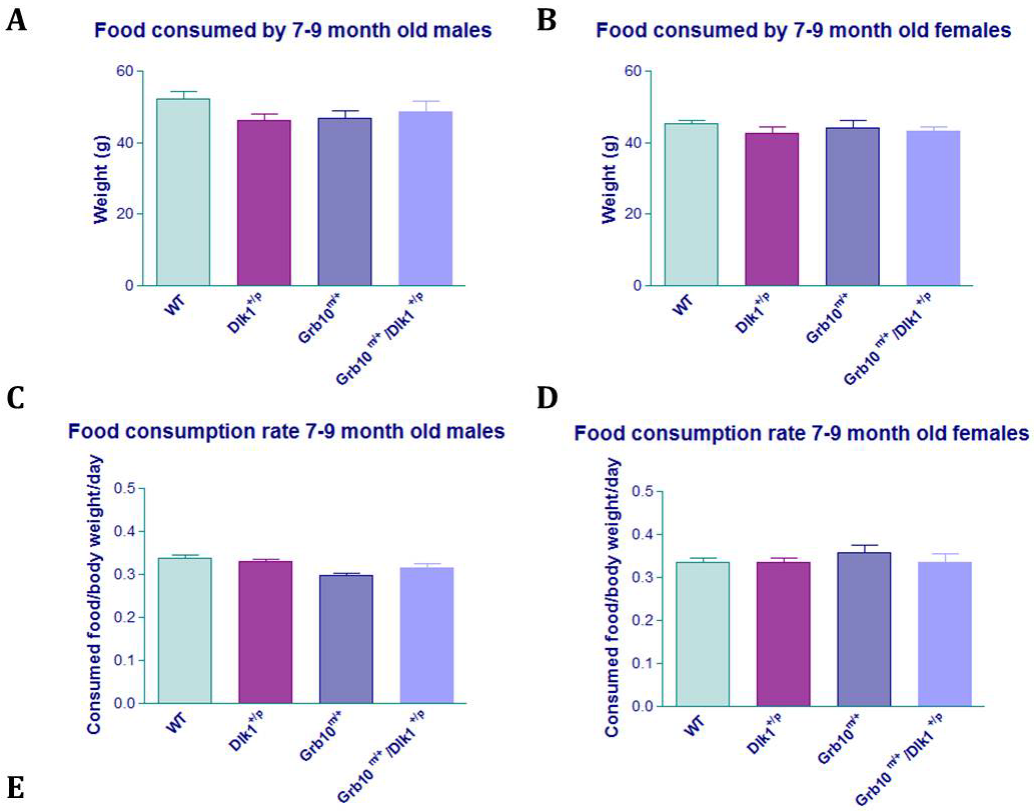

E

	Food males	Food females	Consumption rate males	Consumption rate females
WT vs Grb10$^{m/+}$	ns	ns	ns	ns
WT vs Dlk1$^{+/p}$	ns	ns	ns	ns
WT vs Grb10$^{m/+}$/Dlk1$^{+/p}$	ns	ns	ns	ns
Grb10$^{m/+}$ vs Dlk1$^{+/p}$	ns	ns	ns	ns
Grb10$^{m/+}$ vs Grb10$^{m/+}$/Dlk1$^{+/p}$	ns	ns	ns	ns
Dlk1$^{+/p}$ vs Grb10$^{m/+}$/Dlk1$^{+/p}$	ns	ns	ns	ns

Analysis of feeding behaviour in 7-9 month old wild type, *Grb10$^{m/+}$*, *Dlk1$^{+/p}$* and *Grb10$^{m/+}$/Dlk1$^{+/p}$* mice.

Food intake was monitored over a period of two weeks. Food consumption rates have been calculated as food consumed per gram of animal body weight per day to the power of 2/3. **A)** Total amount of consumed food by males. **B)** Total amount of consumed food by females. **C)** Male consumption rates: total weight of food consumed by males per gram of body weight per day to the power of 2/3. **D)** Female consumption rates: total weight of food consumed by females per gram of body weight per day to the power of 2/3. There were no significant changes neither in the amounts of consumed food or in food consumption rates of transgenic mice when compared to wild type controls. **E)** Table summarising results of statistical analysis. All values represent means ± SEM and have been subject to one way ANOVA with post hoc Tukey's analysis. Males: WT n=7, *Dlk1$^{+/p}$*=6, *Grb10$^{m/+}$* n=6 and *Grb10$^{m/+}$/Dlk1$^{+/p}$* n=6; females: WT n=6, *Dlk1$^{+/p}$*=6, *Grb10$^{m/+}$* n=6 and *Grb10$^{m/+}$/Dlk1$^{+/p}$* n=5.

Appendix 2

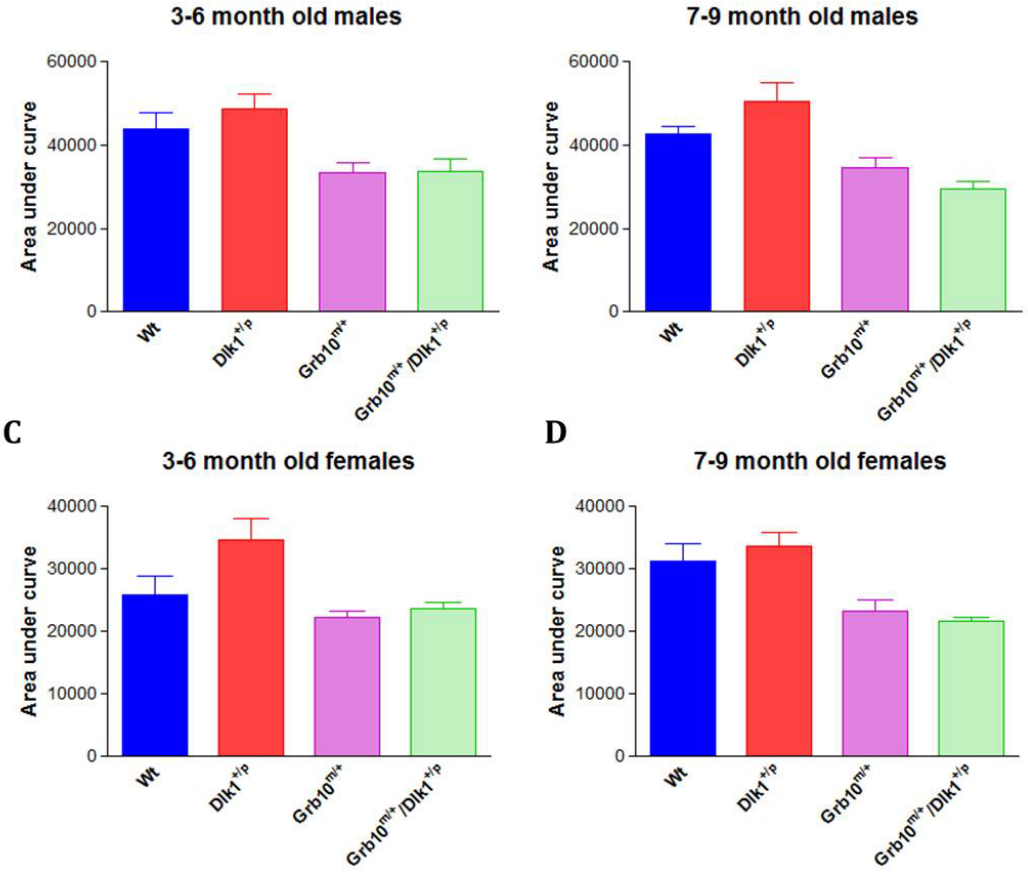

E

	3-6 males	7-9 males	3-6 females	7-9 females
WT vs Grb10$^{m/+}$	ns	ns	ns	ns
WT vs Dlk1$^{+/p}$	ns	ns	ns	ns
WT vs Grb10$^{m/+}$/Dlk1$^{+/p}$	ns	ns	ns	ns
Grb10$^{m/+}$ vs Dlk1$^{+/p}$	*	**	**	*
Grb10$^{m/+}$ vs Grb10$^{m/+}$/Dlk1$^{+/p}$	ns	ns	ns	ns
Dlk1$^{+/p}$ vs Grb10$^{m/+}$/Dlk1$^{+/p}$	*	**	*	**

Glucose tolerance in male and female wild type, *Grb10$^{m/+}$*, *Dlk1$^{+/p}$* and *Grb10$^{m/+}$/Dlk1$^{+/p}$* mice. Male and female 3-9 months old mice were examined for their ability to clear an intraperitoneal dose of glucose. **A)** and **B)** Results from glucose tolerance tests for male and female mice. **C)** and **D)** Histograms representing areas under glucose curves for male and female mice. Analysis of areas under glucose curves revealed that *Grb10$^{m/+}$* and *Grb10$^{m/+}$/Dlk1$^{+/p}$* mice of both sexes cleared glucose significantly faster than *Dlk1$^{+/p}$* (**p<0.01) animals. **E)** Table summarising results of statistical analysis. All values represent means ± SEM and have been subject to one way ANOVA with post hoc Tukey's analysis. Males: WT n=14, *Dlk1$^{+/p}$*=12, *Grb10$^{m/+}$* n=12 and *Grb10$^{m/+}$/Dlk1$^{+/p}$* n=13; females: WT n=13, *Dlk1$^{+/p}$*=12, *Grb10$^{m/+}$* n=12 and *Grb10$^{m/+}$/Dlk1$^{+/p}$* n=12.

References

Abdallah, B. M., Bay-Jensen, A., Srinivasan, B., Tabassi, N. C., Garnero, P., Delaisse, J., Khosla, S. and Kassem, M. (2011a). Estrogen inhibits Dlk1/FA1 production: A potential mechanism for estrogen effects on bone turnover. *J Bone Miner Res*.

Abdallah, B. M., Ding, M., Jensen, C. H., Ditzel, N., Flyvbjerg, A., Jensen, T. G., Dagnaes-Hansen, F., Gasser, J. A. and Kassem, M. (2007). Dlk1/FA1 is a novel endocrine regulator of bone and fat mass and its serum level is modulated by growth hormone. *Endocrinology* **148**, 3111-21.

Abdallah, B. M., Ditzel, N., Mahmood, A., Isa, A., Traustadottir, G. A., Schilling, A. F., Ruiz-Hidalgo, M. J., Laborda, J., Amling, M. and Kassem, M. (2011b). DLK1 is a novel regulator of bone mass that mediates estrogen deficiency-induced bone loss in mice. *J Bone Miner Res* **26**, 1457-71.

Abdallah, B. M., Jensen, C. H., Gutierrez, G., Leslie, R. G., Jensen, T. G. and Kassem, M. (2004). Regulation of human skeletal stem cells differentiation by Dlk1/Pref-1. *J Bone Miner Res* **19**, 841-52.

Abdallah, B. M. and Kassem, M. (2011). New factors controlling the balance between osteoblastogenesis and adipogenesis. *Bone*.

Abuzzahab, M. J., Schneider, A., Goddard, A., Grigorescu, F., Lautier, C., Keller, E., Kiess, W., Klammt, J., Kratzsch, J., Osgood, D. et al. (2003). IGF-I receptor mutations resulting in intrauterine and postnatal growth retardation. *N Engl J Med* **349**, 2211-22.

Ackert-Bicknell, C., Beamer W.G., Rosen, C.J., Sundberg, J.P. Aging study: Bone mineral density and body composition of 32 inbred strains of mice. MPD:Ackert1. Mouse Phenome Database web site, The Jackson Laboratory, Bar Harbor, Maine USA. http://phenome.jax.org, Dec, 2011.

Agrawal, A. F., Brodie, E. D., 3rd and Brown, J. (2001). Parent-offspring coadaptation and the dual genetic control of maternal care. *Science* **292**, 1710-2.

Alves, M. J., Coelho, M. M. and Collares-Pereira, M. J. (2001). Evolution in action through hybridisation and polyploidy in an Iberian freshwater fish: a genetic review. *Genetica* **111**, 375-85.

Ambati, S., Li, Q., Rayalam, S., Hartzell, D. L., Della-Fera, M. A., Hamrick, M. W. and Baile, C. A. (2009). Central leptin versus ghrelin: effects on bone marrow adiposity and gene expression. *Endocrine* **37**, 115-23.

Andersen, D. C., Petersson, S. J., Jorgensen, L. H., Bollen, P., Jensen, P. B., Teisner, B., Schroeder, H. D. and Jensen, C. H. (2009). Characterization of DLK1+ cells emerging during skeletal muscle remodeling in response to myositis, myopathies, and acute injury. *Stem Cells* **27**, 898-908.

Andrade, A. C., Lui, J. C. and Nilsson, O. (2009). Temporal and spatial expression of a growth-regulated network of imprinted genes in growth plate. *Pediatr Nephrol* **25**, 617-23.

Annunziata, M., Granata, R. and Ghigo, E. (2011). The IGF system. *Acta Diabetol* **48**, 1-9.

Araki, E., Lipes, M. A., Patti, M. E., Bruning, J. C., Haag, B., 3rd, Johnson, R. S. and Kahn, C. R. (1994). Alternative pathway of insulin signalling in mice with targeted disruption of the IRS-1 gene. *Nature* **372**, 186-90.

Arima, T., Drewell, R. A., Arney, K. L., Inoue, J., Makita, Y., Hata, A., Oshimura, M., Wake, N. and Surani, M. A. (2001). A conserved imprinting control region at the HYMAI/ZAC domain is implicated in transient neonatal diabetes mellitus. *Hum Mol Genet* **10**, 1475-83.

Arnaud, P., Hata, K., Kaneda, M., Li, E., Sasaki, H., Feil, R. and Kelsey, G. (2006). Stochastic imprinting in the progeny of Dnmt3L-/- females. *Hum Mol Genet* **15**, 589-98.

Arnaud, P., Monk, D., Hitchins, M., Gordon, E., Dean, W., Beechey, C. V., Peters, J., Craigen, W., Preece, M., Stanier, P. et al. (2003). Conserved methylation imprints in the human and mouse GRB10 genes with divergent allelic expression suggests differential reading of the same mark. *Hum Mol Genet* **12**, 1005-19.

Astuti, D., Latif, F., Wagner, K., Gentle, D., Cooper, W. N., Catchpoole, D., Grundy, R., Ferguson-Smith, A. C. and Maher, E. R. (2005). Epigenetic alteration at the DLK1-GTL2 imprinted domain in human neoplasia: analysis of neuroblastoma, phaeochromocytoma and Wilms' tumour. *Br J Cancer* **92**, 1574-80.

Austin, B. P., Garthwaite, T. L., Hagen, T. C., Stevens, J. O. and Menahan, L. A. (1984). Hormonal, metabolic and morphologic studies of aged C57BL/6J obese mice. *Exp Gerontol* **19**, 121-32.

Bai, R. Y., Jahn, T., Schrem, S., Munzert, G., Weidner, K. M., Wang, J. Y. and Duyster, J. (1998). The SH2-containing adapter protein GRB10 interacts with BCR-ABL. *Oncogene* **17**, 941-8.

Baker, J., Liu, J. P., Robertson, E. J. and Efstratiadis, A. (1993). Role of insulin-like growth factors in embryonic and postnatal growth. *Cell* **75**, 73-82.

Baladron, V., Ruiz-Hidalgo, M. J., Nueda, M. L., Diaz-Guerra, M. J., Garcia-Ramirez, J. J., Bonvini, E., Gubina, E. and Laborda, J. (2005). dlk acts as a negative regulator of Notch1 activation through interactions with specific EGF-like repeats. *Exp Cell Res* **303**, 343-59.

Bancroft, J.D. and Gamble, M. (2002) Theory and practice of histological techniques. (5th ed.) Chuirchill Livingston Publication

Ball, S. T., Williamson, C. M., Hayes, C., Hacker, T. and Peters, J. (2001). The spatial and temporal expression pattern of Nesp and its antisense Nespas, in mid-gestation mouse embryos. *Mech Dev* **100**, 79-81.

Barker, D. J., Hales, C. N., Fall, C. H., Osmond, C., Phipps, K. and Clark, P. M. (1993). Type 2 (non-insulin-dependent) diabetes mellitus, hypertension and hyperlipidaemia (syndrome X): relation to reduced fetal growth. *Diabetologia* **36**, 62-7.

Barlow, D. P., Stoger, R., Herrmann, B. G., Saito, K. and Schweifer, N. (1991). The mouse insulin-like growth factor type-2 receptor is imprinted and closely linked to the Tme locus. *Nature* **349**, 84-7.

Baroux, C., Spillane, C. and Grossniklaus, U. (2002). Genomic imprinting during seed development. *Adv Genet* **46**, 165-214.

Bartholdi, D., Krajewska-Walasek, M., Ounap, K., Gaspar, H., Chrzanowska, K. H., Ilyana, H., Kayserili, H., Lurie, I. W., Schinzel, A. and Baumer, A. (2009). Epigenetic mutations of the imprinted IGF2-H19 domain in Silver-Russell syndrome (SRS): results from a large cohort of patients with SRS and SRS-like phenotypes. *J Med Genet* **46**, 192-7.

Bartolomei, M. S. and Ferguson-Smith, A. C. (2011). Mammalian genomic imprinting. *Cold Spring Harb Perspect Biol* **3**.

Bartolomei, M. S., Zemel, S. and Tilghman, S. M. (1991). Parental imprinting of the mouse H19 gene. *Nature* **351**, 153-5.

Barton, S. C., Adams, C. A., Norris, M. L. and Surani, M. A. (1985). Development of gynogenetic and parthenogenetic inner cell mass and trophectoderm tissues in reconstituted blastocysts in the mouse. *J Embryol Exp Morphol* **90**, 267-85.

Barton, S. C., Ferguson-Smith, A. C., Fundele, R. and Surani, M. A. (1991). Influence of paternally imprinted genes on development. *Development* **113**, 679-87.

Barton, S. C., Surani, M. A. and Norris, M. L. (1984). Role of paternal and maternal genomes in mouse development. *Nature* **311**, 374-6.

Bastepe, M. (2008). The GNAS locus and pseudohypoparathyroidism. *Adv Exp Med Biol* **626**, 27-40.

Bauer, S. R., Ruiz-Hidalgo, M. J., Rudikoff, E. K., Goldstein, J. and Laborda, J. (1998). Modulated expression of the epidermal growth factor-like homeotic protein dlk influences stromal-cell-pre-B-cell interactions, stromal cell adipogenesis, and pre-B-cell interleukin-7 requirements. *Mol Cell Biol* **18**, 5247-55.

Berends, M. J., Hordijk, R., Scheffer, H., Oosterwijk, J. C., Halley, D. J. and Sorgedrager, N. (1999). Two cases of maternal uniparental disomy 14 with a phenotype overlapping with the Prader-Willi phenotype. *Am J Med Genet* **84**, 76-9.

Bidwell, C. A., Shay, T. L., Georges, M., Beever, J. E., Berghmans, S. and Cockett, N. E. (2001). Differential expression of the GTL2 gene within the callipyge region of ovine chromosome 18. *Anim Genet* **32**, 248-56.

Blagitko, N., Mergenthaler, S., Schulz, U., Wollmann, H. A., Craigen, W., Eggermann, T., Ropers, H. H. and Kalscheuer, V. M. (2000). Human GRB10 is imprinted and expressed from the paternal and maternal allele in a highly tissue- and isoform-specific fashion. *Hum Mol Genet* **9**, 1587-95.

Bliek, J., Terhal, P., van den Bogaard, M. J., Maas, S., Hamel, B., Salieb-Beugelaar, G., Simon, M., Letteboer, T., van der Smagt, J., Kroes, H. et al. (2006). Hypomethylation of the H19 gene causes not only Silver-Russell syndrome (SRS) but also isolated asymmetry or an SRS-like phenotype. *Am J Hum Genet* **78**, 604-14.

Bluher, M., Unger, R., Rassoul, F., Richter, V. and Paschke, R. (2002). Relation between glycaemic control, hyperinsulinaemia and plasma concentrations of soluble adhesion molecules in patients with impaired glucose tolerance or Type II diabetes. *Diabetologia* **45**, 210-6.

Boden, G., Chen, X., Kolaczynski, J. W. and Polansky, M. (1997). Effects of prolonged hyperinsulinemia on serum leptin in normal human subjects. *J Clin Invest* **100**, 1107-13.

Boeuf, S., Klingenspor, M., Van Hal, N. L., Schneider, T., Keijer, J. and Klaus, S. (2001). Differential gene expression in white and brown preadipocytes. *Physiol Genomics* **7**, 15-25.

Boison, D., Scheurer, L., Zumsteg, V., Rulicke, T., Litynski, P., Fowler, B., Brandner, S. and Mohler, H. (2002). Neonatal hepatic steatosis by disruption of the adenosine kinase gene. *Proc Natl Acad Sci U S A* **99**, 6985-90.

Boles, R. G., Buck, E. A., Blitzer, M. G., Platt, M. S., Cowan, T. M., Martin, S. K., Yoon, H., Madsen, J. A., Reyes-Mugica, M. and Rinaldo, P. (1998). Retrospective biochemical screening of fatty acid oxidation disorders in postmortem livers of 418 cases of sudden death in the first year of life. *J Pediatr* **132**, 924-33.

Boonen, S. E., Porksen, S., Mackay, D. J., Oestergaard, E., Olsen, B., Brondum-Nielsen, K., Temple, I. K. and Hahnemann, J. M. (2008). Clinical characterisation of the multiple maternal hypomethylation syndrome in siblings. *Eur J Hum Genet* **16**, 453-61.

Brandeis, M., Kafri, T., Ariel, M., Chaillet, J. R., McCarrey, J., Razin, A. and Cedar, H. (1993). The ontogeny of allele-specific methylation associated with imprinted genes in the mouse. *EMBO J* **12**, 3669-77.

Bray, S. J., Takada, S., Harrison, E., Shen, S. C. and Ferguson-Smith, A. C. (2008). The atypical mammalian ligand Delta-like homologue 1 (Dlk1) can regulate Notch signalling in Drosophila. *BMC Dev Biol* **8**, 11.

Brenner, B. M., Garcia, D. L. and Anderson, S. (1988). Glomeruli and blood pressure. Less of one, more the other? *Am J Hypertens* **1**, 335-47.

Bressan, F. F., De Bem, T. H., Perecin, F., Lopes, F. L., Ambrosio, C. E., Meirelles, F. V. and Miglino, M. A. (2009). Unearthing the roles of imprinted genes in the placenta. *Placenta* **30**, 823-34.

Brivet, M., Boutron, A., Slama, A., Costa, C., Thuillier, L., Demaugre, F., Rabier, D., Saudubray, J. M. and Bonnefont, J. P. (1999). Defects in activation and transport of fatty acids. *J Inherit Metab Dis* **22**, 428-41.

Buiting, K. (2010). Prader-Willi syndrome and Angelman syndrome. *Am J Med Genet C Semin Med Genet* **154C**, 365-76.

Bullman, H., Lever, M., Robinson, D. O., Mackay, D. J., Holder, S. E. and Wakeling, E. L. (2008). Mosaic maternal uniparental disomy of chromosome 11 in a patient with Silver-Russell syndrome. *J Med Genet* **45**, 396-9.

Burns, J. L. and Hassan, A. B. (2001). Cell survival and proliferation are modified by insulin-like growth factor 2 between days 9 and 10 of mouse gestation. *Development* **128**, 3819-30.

Cao, X. R., Lill, N. L., Boase, N., Shi, P. P., Croucher, D. R., Shan, H., Qu, J., Sweezer, E. M., Place, T., Kirby, P. A. et al. (2008). Nedd4 controls animal growth by regulating IGF-1 signaling. *Sci Signal* **1**, ra5.

Caspary, T., Cleary, M. A., Baker, C. C., Guan, X. J. and Tilghman, S. M. (1998). Multiple mechanisms regulate imprinting of the mouse distal chromosome 7 gene cluster. *Mol Cell Biol* **18**, 3466-74.

Caspary, T., Cleary, M. A., Perlman, E. J., Zhang, P., Elledge, S. J. and Tilghman, S. M. (1999). Oppositely imprinted genes p57(Kip2) and igf2 interact in a mouse model for Beckwith-Wiedemann syndrome. *Genes Dev* **13**, 3115-24.

Castrop, H., Oppermann, M., Mizel, D., Huang, Y., Faulhaber-Walter, R., Weiss, Y., Weinstein, L. S., Chen, M., Germain, S., Lu, H. et al. (2007). Skeletal abnormalities and extra-skeletal ossification in mice with restricted Gsalpha deletion caused by a renin promoter-Cre transgene. *Cell Tissue Res* **330**, 487-501.

Cattanach, B. M., Beechey, C. V., Rasberry, C., Jones, J. and Papworth, D. (1996). Time of initiation and site of action of the mouse chromosome 11 imprinting effects. *Genet Res* **68**, 35-44.

Cattanach, B. M. and Kirk, M. (1985). Differential activity of maternally and paternally derived chromosome regions in mice. *Nature* **315**, 496-8.

Ceccarelli, D. F. and Sicheri, F. (2009). Grb-ing hold of insulin signaling. *Nat Struct Mol Biol* **16**, 803-4.

Chacon, M. R., Miranda, M., Jensen, C. H., Fernandez-Real, J. M., Vilarrasa, N., Gutierrez, C., Naf, S., Gomez, J. M. and Vendrell, J. (2008). Human serum levels of fetal antigen 1 (FA1/Dlk1) increase with obesity, are negatively associated with insulin sensitivity and modulate inflammation in vitro. *Int J Obes (Lond)* **32**, 1122-9.

Chapman, V., Forrester, L., Sanford, J., Hastie, N. and Rossant, J. (1984). Cell lineage-specific undermethylation of mouse repetitive DNA. *Nature* **307**, 284-6.

Charalambous, M., Cowley, M., Geoghegan, F., Smith, F. M., Radford, E. J., Marlow, B. P., Graham, C. F., Hurst, L. D. and Ward, A. (2010). Maternally-inherited Grb10 reduces placental size and efficiency. *Dev Biol* **337**, 1-8.

Charalambous, M., da Rocha, S. T. and Ferguson-Smith, A. C. (2007). Genomic imprinting, growth control and the allocation of nutritional resources: consequences for postnatal life. *Curr Opin Endocrinol Diabetes Obes* **14**, 3-12.

Charalambous, M., Smith, F. M., Bennett, W. R., Crew, T. E., Mackenzie, F. and Ward, A. (2003). Disruption of the imprinted Grb10 gene leads to disproportionate overgrowth by an Igf2-independent mechanism. *Proc Natl Acad Sci U S A* **100**, 8292-7.

Charlier, C., Segers, K., Karim, L., Shay, T., Gyapay, G., Cockett, N. and Georges, M. (2001). The callipyge mutation enhances the expression of coregulated imprinted genes in cis without affecting their imprinting status. *Nat Genet* **27**, 367-9.

Chen, L., Qanie, D., Jafari, A., Taipaleemaki, H., Jensen, C. H., Sanz, M. L., Laborda, J., Abdallah, B. M. and Kassem, M. (2011). Delta-like 1 / fetal antigen-1 (Dlk1/FA1) is a novel regulator of chondrogenic cell differentiation via inhibition of the AKT-dependent pathway. *J Biol Chem*.

Chen, M., Gavrilova, O., Liu, J., Xie, T., Deng, C., Nguyen, A. T., Nackers, L. M., Lorenzo, J., Shen, L. and Weinstein, L. S. (2005). Alternative Gnas gene products have opposite effects on glucose and lipid metabolism. *Proc Natl Acad Sci U S A* **102**, 7386-91.

Choi, J. D., Underkoffler, L. A., Wood, A. J., Collins, J. N., Williams, P. T., Golden, J. A., Schuster, E. F., Jr., Loomes, K. M. and Oakey, R. J. (2005). A novel variant of Inpp5f is

imprinted in brain, and its expression is correlated with differential methylation of an internal CpG island. *Mol Cell Biol* **25**, 5514-22.

Choufani, S., Shuman, C. and Weksberg, R. (2010). Beckwith-Wiedemann syndrome. *Am J Med Genet C Semin Med Genet* **154C**, 343-54.

Coan, P. M., Burton, G. J. and Ferguson-Smith, A. C. (2005). Imprinted genes in the placenta--a review. *Placenta* **26 Suppl A**, S10-20.

Coan, P. M., Fowden, A. L., Constancia, M., Ferguson-Smith, A. C., Burton, G. J. and Sibley, C. P. (2008). Disproportional effects of Igf2 knockout on placental morphology and diffusional exchange characteristics in the mouse. *J Physiol* **586**, 5023-32.

Cockett, N. E., Jackson, S. P., Shay, T. L., Farnir, F., Berghmans, S., Snowder, G. D., Nielsen, D. M. and Georges, M. (1996). Polar overdominance at the ovine callipyge locus. *Science* **273**, 236-8.

Cockett, N. E., Smit, M. A., Bidwell, C. A., Segers, K., Hadfield, T. L., Snowder, G. D., Georges, M. and Charlier, C. (2005). The callipyge mutation and other genes that affect muscle hypertrophy in sheep. *Genet Sel Evol* **37 Suppl 1**, S65-81.

Coelho, C. M. and Leevers, S. J. (2000). Do growth and cell division rates determine cell size in multicellular organisms? *J Cell Sci* **113 (Pt 17)**, 2927-34.

Coleman, D. L. and Hummel, K. P. (1967). Studies with the mutation, diabetes, in the mouse. *Diabetologia* **3**, 238-48.

Collins, B. J., Kleeberger, W. and Ball, D. W. (2004). Notch in lung development and lung cancer. *Semin Cancer Biol* **14**, 357-64.

Conlon, I. J., Dunn, G. A., Mudge, A. W. and Raff, M. C. (2001). Extracellular control of cell size. *Nat Cell Biol* **3**, 918-21.

Constancia, M., Hemberger, M., Hughes, J., Dean, W., Ferguson-Smith, A., Fundele, R., Stewart, F., Kelsey, G., Fowden, A., Sibley, C. et al. (2002). Placental-specific IGF-II is a major modulator of placental and fetal growth. *Nature* **417**, 945-8.

Constancia, M., Kelsey, G. and Reik, W. (2004). Resourceful imprinting. *Nature* **432**, 53-7.

Cooney, G. J., Lyons, R. J., Crew, A. J., Jensen, T. E., Molero, J. C., Mitchell, C. J., Biden, T. J., Ormandy, C. J., James, D. E. and Daly, R. J. (2004). Improved glucose homeostasis and enhanced insulin signalling in Grb14-deficient mice. *EMBO J* **23**, 582-93.

Cooper, G.M. (2000). 'Chapter 14: The Eucaryotic Cell Cycle'. The cell: a molecular approach (2nd ed.). Washington, D.C: ASM Press.

Cottrell, E. C., Martin-Gronert, M. S., Fernandez-Twinn, D. S., Luan, J., Berends, L. M. and Ozanne, S. E. (2011). Leptin-independent programming of adult body weight and adiposity in mice. *Endocrinology* **152**, 476-82.

Cowley, M., Garfield, A.S., Madon, M.M., Charalambous, M., Clarkson, R.W., Heisler, L.K., Moorwood K. and Ward, A. (2011) Imprinted *Grb10* links postnatal nutrient supply and demand with metabolic fitness through coadapted roles in mother and offspring. *Submitted*
Garfield, A.S. (2007) Investigating the roles of mouse Grb10 in the regulation of growth and behaviour. *PhD Thesis, University of Bath*.

Crickmore, M. A. and Mann, R. S. (2008). The control of size in animals: insights from selector genes. *Bioessays* **30**, 843-53.

Curley, J. P., Barton, S., Surani, A. and Keverne, E. B. (2004). Coadaptation in mother and infant regulated by a paternally expressed imprinted gene. *Proc Biol Sci* **271**, 1303-9.

Curley, J. P., Pinnock, S. B., Dickson, S. L., Thresher, R., Miyoshi, N., Surani, M. A. and Keverne, E. B. (2005). Increased body fat in mice with a targeted mutation of the paternally expressed imprinted gene Peg3. *FASEB J* **19**, 1302-4.

D'Souza, B., Miyamoto, A. and Weinmaster, G. (2008). The many facets of Notch ligands. *Oncogene* **27**, 5148-67.

Da Costa, T. H., Williamson, D. H., Ward, A., Bates, P., Fisher, R., Richardson, L., Hill, D. J., Robinson, I. C. and Graham, C. F. (1994). High plasma insulin-like growth factor-II and low lipid content in transgenic mice: measurements of lipid metabolism. *J Endocrinol* **143**, 433-9.

da Rocha, S. T., Charalambous, M., Lin, S. P., Gutteridge, I., Ito, Y., Gray, D., Dean, W. and Ferguson-Smith, A. C. (2009). Gene dosage effects of the imprinted delta-like homologue 1 (dlk1/pref1) in development: implications for the evolution of imprinting. *PLoS Genet* **5**, e1000392.

da Rocha, S. T., Edwards, C. A., Ito, M., Ogata, T. and Ferguson-Smith, A. C. (2008). Genomic imprinting at the mammalian Dlk1-Dio3 domain. *Trends Genet* **24**, 306-16.

da Rocha, S. T., Tevendale, M., Knowles, E., Takada, S., Watkins, M. and Ferguson-Smith, A. C. (2007). Restricted co-expression of Dlk1 and the reciprocally imprinted non-coding RNA, Gtl2: implications for cis-acting control. *Dev Biol* **306**, 810-23.

Davies, W., Isles, A. R., Humby, T. and Wilkinson, L. S. (2007). What are imprinted genes doing in the brain? *Epigenetics* **2**, 201-6.

Davies, W., Smith, R. J., Kelsey, G. and Wilkinson, L. S. (2004). Expression patterns of the novel imprinted genes Nap1l5 and Peg13 and their non-imprinted host genes in the adult mouse brain. *Gene Expr Patterns* **4**, 741-7.

Davis, E., Jensen, C. H., Schroder, H. D., Farnir, F., Shay-Hadfield, T., Kliem, A., Cockett, N., Georges, M. and Charlier, C. (2004). Ectopic expression of DLK1 protein in skeletal muscle of padumnal heterozygotes causes the callipyge phenotype. *Curr Biol* **14**, 1858-62.

Davis, T. L., Yang, G. J., McCarrey, J. R. and Bartolomei, M. S. (2000). The H19 methylation imprint is erased and re-established differentially on the parental alleles during male germ cell development. *Hum Mol Genet* **9**, 2885-94.

Day, T. and Bonduriansky, R. (2004). Intralocus sexual conflict can drive the evolution of genomic imprinting. *Genetics* **167**, 1537-46.

de Crombrugghe, B., Lefebvre, V. and Nakashima, K. (2001). Regulatory mechanisms in the pathways of cartilage and bone formation. *Curr Opin Cell Biol* **13**, 721-7.

DeChiara, T. M., Efstratiadis, A. and Robertson, E. J. (1990). A growth-deficiency phenotype in heterozygous mice carrying an insulin-like growth factor II gene disrupted by targeting. *Nature* **345**, 78-80.

DeChiara, T. M., Robertson, E. J. and Efstratiadis, A. (1991). Parental imprinting of the mouse insulin-like growth factor II gene. *Cell* **64**, 849-59.

Demars, J., Shmela, M. E., Rossignol, S., Okabe, J., Netchine, I., Azzi, S., Cabrol, S., Le Caignec, C., David, A., Le Bouc, Y. et al. (2011). Analysis of the IGF2/H19 imprinting control region uncovers new genetic defects, including mutations of OCT-binding sequences, in patients with 11p15 fetal growth disorders. *Hum Mol Genet* **19**, 803-14.

Deng, Y., Bhattacharya, S., Swamy, O. R., Tandon, R., Wang, Y., Janda, R. and Riedel, H. (2003). Growth factor receptor-binding protein 10 (Grb10) as a partner of phosphatidylinositol 3-kinase in metabolic insulin action. *J Biol Chem* **278**, 39311-22.

Depetris, R. S., Wu, J. and Hubbard, S. R. (2009). Structural and functional studies of the Ras-associating and pleckstrin-homology domains of Grb10 and Grb14. *Nat Struct Mol Biol* **16**, 833-9.

Dey, B. R., Frick, K., Lopaczynski, W., Nissley, S. P. and Furlanetto, R. W. (1996). Evidence for the direct interaction of the insulin-like growth factor I receptor with IRS-1, Shc, and Grb10. *Mol Endocrinol* **10**, 631-41.

Dobashi, Y., Watanabe, Y., Miwa, C., Suzuki, S. and Koyama, S. (2011). Mammalian target of rapamycin: a central node of complex signaling cascades. *Int J Clin Exp Pathol* **4**, 476-95.

Dong, L. Q., Du, H., Porter, S. G., Kolakowski, L. F., Jr., Lee, A. V., Mandarino, L. J., Fan, J., Yee, D. and Liu, F. (1997). Cloning, chromosome localization, expression, and characterization of an Src homology 2 and pleckstrin homology domain-containing insulin receptor binding protein hGrb10gamma. *J Biol Chem* **272**, 29104-12.

Douglas-Denton, R. N., McNamara, B. J., Hoy, W. E., Hughson, M. D. and Bertram, J. F. (2006). Does nephron number matter in the development of kidney disease? *Ethn Dis* **16**, S2-40-5.

Drake, A. J. and Walker, B. R. (2004). The intergenerational effects of fetal programming: non-genomic mechanisms for the inheritance of low birth weight and cardiovascular risk. *J Endocrinol* **180**, 1-16.

Dufresne, A. M. and Smith, R. J. (2005). The adapter protein GRB10 is an endogenous negative regulator of insulin-like growth factor signaling. *Endocrinology* **146**, 4399-409.

Echave, P., Conlon, I. J. and Lloyd, A. C. (2007). Cell size regulation in mammalian cells. *Cell Cycle* **6**, 218-24.

Edwards, C. A. and Ferguson-Smith, A. C. (2007). Mechanisms regulating imprinted genes in clusters. *Curr Opin Cell Biol* **19**, 281-9.

Edwards, C. A., Mungall, A. J., Matthews, L., Ryder, E., Gray, D. J., Pask, A. J., Shaw, G., Graves, J. A., Rogers, J., Dunham, I. et al. (2008). The evolution of the DLK1-DIO3 imprinted domain in mammals. *PLoS Biol* **6**, e135.

Efstratiadis, A. (1998). Genetics of mouse growth. *Int J Dev Biol* **42**, 955-76.

Eggermann, T., Begemann, M., Binder, G. and Spengler, S. (2010). Silver-Russell syndrome: genetic basis and molecular genetic testing. *Orphanet J Rare Dis* **5**, 19.

Eggermann, T., Schonherr, N., Meyer, E., Obermann, C., Mavany, M., Eggermann, K., Ranke, M. B. and Wollmann, H. A. (2006). Epigenetic mutations in 11p15 in Silver-Russell syndrome are restricted to the telomeric imprinting domain. *J Med Genet* **43**, 615-6.

Eggermann, T., Spengler, S., Bachmann, N., Baudis, M., Mau-Holzmann, U. A., Singer, S. and Rossier, E. (2011). Chromosome 11p15 duplication in Silver-Russell syndrome due to a maternally inherited translocation t(11;15). *Am J Med Genet A* **152A**, 1484-7.

Eisen, E. J. (1976). Results of growth curve analyses in mice and rats. *J Anim Sci* **42**, 1008-23.

Eriksson, J. G., Forsen, T., Tuomilehto, J., Osmond, C. and Barker, D. J. (2003). Early adiposity rebound in childhood and risk of Type 2 diabetes in adult life. *Diabetologia* **46**, 190-4.

Espina, A. G., Mendez-Vidal, C., Moreno-Mateos, M. A., Saez, C., Romero-Franco, A., Japon, M. A. and Pintor-Toro, J. A. (2009). Induction of Dlk1 by PTTG1 inhibits adipocyte differentiation and correlates with malignant transformation. *Mol Biol Cell* **20**, 3353-62.

Farber, E. (1967). Ethionine fatty liver. *Adv Lipid Res* **5**, 119-83.

Fazeli, P. K., Bredella, M. A., Misra, M., Meenaghan, E., Rosen, C. J., Clemmons, D. R., Breggia, A., Miller, K. K. and Klibanski, A. (2009). Preadipocyte factor-1 is associated with marrow adiposity and bone mineral density in women with anorexia nervosa. *J Clin Endocrinol Metab* **95**, 407-13.

Feil, R. and Berger, F. (2007). Convergent evolution of genomic imprinting in plants and mammals. *Trends Genet* **23**, 192-9.

Feil, R., Walter, J., Allen, N. D. and Reik, W. (1994). Developmental control of allelic methylation in the imprinted mouse Igf2 and H19 genes. *Development* **120**, 2933-43.

Ferguson-Smith, A. C. (2011). Genomic imprinting: the emergence of an epigenetic paradigm. *Nat Rev Genet* **12**, 565-75.

Ferron, S. R., Charalambous, M., Radford, E., McEwen, K., Wildner, H., Hind, E., Morante-Redolat, J. M., Laborda, J., Guillemot, F., Bauer, S. R. et al. (2011). Postnatal loss of Dlk1 imprinting in stem cells and niche astrocytes regulates neurogenesis. *Nature* **475**, 381-5.

Fleming-Waddell, J. N., Olbricht, G. R., Taxis, T. M., White, J. D., Vuocolo, T., Craig, B. A., Tellam, R. L., Neary, M. K., Cockett, N. E. and Bidwell, C. A. (2009). Effect of DLK1 and RTL1 but not MEG3 or MEG8 on muscle gene expression in Callipyge lambs. *PLoS One* **4**, e7399.

Fleming-Waddell, J. N., Wilson, L. M., Olbricht, G. R., Vuocolo, T., Byrne, K., Craig, B. A., Tellam, R. L., Cockett, N. E. and Bidwell, C. A. (2007). Analysis of gene expression during the onset of muscle hypertrophy in callipyge lambs. *Anim Genet* **38**, 28-36.

Floridon, C., Jensen, C. H., Thorsen, P., Nielsen, O., Sunde, L., Westergaard, J. G., Thomsen, S. G. and Teisner, B. (2000). Does fetal antigen 1 (FA1) identify cells with regenerative, endocrine and neuroendocrine potentials? A study of FA1 in embryonic, fetal, and placental tissue and in maternal circulation. *Differentiation* **66**, 49-59.

Folch, J., Lees, M., & Sloane-stantly, G.H. (1957). A simple method for the isolation and purification of total lipids from animal tissues. *J. Biol. Chem.,* 226, 497-308.

Font de Mora, J., Esteban, L. M., Burks, D. J., Nunez, A., Garces, C., Garcia-Barrado, M. J., Iglesias-Osma, M. C., Moratinos, J., Ward, J. M. and Santos, E. (2003). Ras-GRF1 signaling is required for normal beta-cell development and glucose homeostasis. *EMBO J* **22**, 3039-49.

Fowden, A. L., Coan, P. M., Angiolini, E., Burton, G. J. and Constancia, M. (2011). Imprinted genes and the epigenetic regulation of placental phenotype. *Prog Biophys Mol Biol* **106**, 281-8.

Fox, K. E., Fankell, D. M., Erickson, P. F., Majka, S. M., Crossno, J. T., Jr. and Klemm, D. J. (2006). Depletion of cAMP-response element-binding protein/ATF1 inhibits adipogenic conversion of 3T3-L1 cells ectopically expressing CCAAT/enhancer-binding protein (C/EBP) alpha, C/EBP beta, or PPAR gamma 2. *J Biol Chem* **281**, 40341-53.

Frank, D., Fortino, W., Clark, L., Musalo, R., Wang, W., Saxena, A., Li, C. M., Reik, W., Ludwig, T. and Tycko, B. (2002). Placental overgrowth in mice lacking the imprinted gene Ipl. *Proc Natl Acad Sci U S A* **99**, 7490-5.

Frantz, J. D., Giorgetti-Peraldi, S., Ottinger, E. A. and Shoelson, S. E. (1997). Human GRB-IRbeta/GRB10. Splice variants of an insulin and growth factor receptor-binding protein with PH and SH2 domains. *J Biol Chem* **272**, 2659-67.

Frayling, T. M. and Hattersley, A. T. (2001). The role of genetic susceptibility in the association of low birth weight with type 2 diabetes. *Br Med Bull* **60**, 89-101.

Freking, B. A., Keele, J. W., Nielsen, M. K. and Leymaster, K. A. (1998). Evaluation of the ovine callipyge locus: II. Genotypic effects on growth, slaughter, and carcass traits. *J Anim Sci* **76**, 2549-59.

Freking, B. A., Murphy, S. K., Wylie, A. A., Rhodes, S. J., Keele, J. W., Leymaster, K. A., Jirtle, R. L. and Smith, T. P. (2002). Identification of the single base change causing the callipyge muscle hypertrophy phenotype, the only known example of polar overdominance in mammals. *Genome Res* **12**, 1496-506.

Friedman, J. M. and Halaas, J. L. (1998). Leptin and the regulation of body weight in mammals. *Nature* **395**, 763-70.

Fromenty, B., Berson, A. and Pessayre, D. (1997). Microvesicular steatosis and steatohepatitis: role of mitochondrial dysfunction and lipid peroxidation. *J Hepatol* **26 Suppl 1**, 13-22.

Fromenty, B. and Pessayre, D. (1997). Impaired mitochondrial function in microvesicular steatosis. Effects of drugs, ethanol, hormones and cytokines. *J Hepatol* **26 Suppl 2**, 43-53.

Fundele, R., Howlett, S. K., Kothary, R., Norris, M. L., Mills, W. E. and Surani, M. A. (1991). Developmental potential of parthenogenetic cells: role of genotype-specific modifiers. *Development* **113**, 941-6.

Gallou-Kabani, C., Gabory, A., Tost, J., Karimi, M., Mayeur, S., Lesage, J., Boudadi, E., Gross, M. S., Taurelle, J., Vige, A. et al. (2010). Sex- and diet-specific changes of imprinted gene expression and DNA methylation in mouse placenta under a high-fat diet. *PLoS One* **5**, e14398.

Garces, C., Ruiz-Hidalgo, M. J., Bonvini, E., Goldstein, J. and Laborda, J. (1999). Adipocyte differentiation is modulated by secreted delta-like (dlk) variants and requires the expression of membrane-associated dlk. *Differentiation* **64**, 103-14.

Garces, C., Ruiz-Hidalgo, M. J., Font de Mora, J., Park, C., Miele, L., Goldstein, J., Bonvini, E., Porras, A. and Laborda, J. (1997). Notch-1 controls the expression of fatty acid-activated transcription factors and is required for adipogenesis. *J Biol Chem* **272**, 29729-34.

Gardner, R. J., Mackay, D. J., Mungall, A. J., Polychronakos, C., Siebert, R., Shield, J. P., Temple, I. K. and Robinson, D. O. (2000). An imprinted locus associated with transient neonatal diabetes mellitus. *Hum Mol Genet* **9**, 589-96.

Garfield, A.S. (2007) Investigating the roles of mouse Grb10 in the regulation of growth and behaviour. *PhD Thesis, University of Bath*.

Garfield, A. S., Cowley, M., Smith, F. M., Moorwood, K., Stewart-Cox, J. E., Gilroy, K., Baker, S., Xia, J., Dalley, J. W., Hurst, L. D. et al. (2011). Distinct physiological and behavioural functions for parental alleles of imprinted Grb10. *Nature* **469**, 534-8.

George, L. A., Uthlaut, A. B., Long, N. M., Zhang, L., Ma, Y., Smith, D. T., Nathanielsz, P. W. and Ford, S. P. (2010). Different levels of overnutrition and weight gain during pregnancy have differential effects on fetal growth and organ development. *Reprod Biol Endocrinol* **8**, 75.

Georgiades, P., Chierakul, C. and Ferguson-Smith, A. C. (1998). Parental origin effects in human trisomy for chromosome 14q: implications for genomic imprinting. *J Med Genet* **35**, 821-4.

Georgiades, P., Watkins, M., Burton, G. J. and Ferguson-Smith, A. C. (2001). Roles for genomic imprinting and the zygotic genome in placental development. *Proc Natl Acad Sci U S A* **98**, 4522-7.

Georgiades, P., Watkins, M., Surani, M. A. and Ferguson-Smith, A. C. (2000). Parental origin-specific developmental defects in mice with uniparental disomy for chromosome 12. *Development* **127**, 4719-28.

Gerard, M., Hernandez, L., Wevrick, R. and Stewart, C. L. (1999). Disruption of the mouse necdin gene results in early post-natal lethality. *Nat Genet* **23**, 199-202.

Germain-Lee, E. L., Ding, C. L., Deng, Z., Crane, J. L., Saji, M., Ringel, M. D. and Levine, M. A. (2002). Paternal imprinting of Galpha(s) in the human thyroid as the basis of TSH resistance in pseudohypoparathyroidism type 1a. *Biochem Biophys Res Commun* **296**, 67-72.

Gicquel, C., Rossignol, S., Cabrol, S., Houang, M., Steunou, V., Barbu, V., Danton, F., Thibaud, N., Le Merrer, M., Burglen, L. et al. (2005). Epimutation of the telomeric imprinting center region on chromosome 11p15 in Silver-Russell syndrome. *Nat Genet* **37**, 1003-7.

Giorgetti-Peraldi, S., Murdaca, J., Mas, J. C. and Van Obberghen, E. (2001). The adapter protein, Grb10, is a positive regulator of vascular endothelial growth factor signaling. *Oncogene* **20**, 3959-68.

Giovannone, B., Lee, E., Laviola, L., Giorgino, F., Cleveland, K. A. and Smith, R. J. (2003). Two novel proteins that are linked to insulin-like growth factor (IGF-I) receptors by the Grb10 adapter and modulate IGF-I signaling. *J Biol Chem* **278**, 31564-73.

Gluckman, P. D. and Hanson, M. A. (2006). The consequences of being born small - an adaptive perspective. *Horm Res* **65 Suppl 3**, 5-14.

Golay, A., DeFronzo, R. A., Ferrannini, E., Simonson, D. C., Thorin, D., Acheson, K., Thiebaud, D., Curchod, B., Jequier, E. and Felber, J. P. (1988). Oxidative and non-oxidative glucose metabolism in non-obese type 2 (non-insulin-dependent) diabetic patients. *Diabetologia* **31**, 585-91.

Grandjean, V., Smith, J., Schofield, P. N. and Ferguson-Smith, A. C. (2000). Increased IGF-II protein affects p57kip2 expression in vivo and in vitro: implications for Beckwith-Wiedemann syndrome. *Proc Natl Acad Sci U S A* **97**, 5279-84.

Gregg, C., Zhang, J., Weissbourd, B., Luo, S., Schroth, G. P., Haig, D. and Dulac, C. (2010). High-resolution analysis of parent-of-origin allelic expression in the mouse brain. *Science* **329**, 643-8.

Gubina, E., Ruiz-Hidalgo, M. J., Baladron, V. and Laborda, J. (1999). Assignment of DLK1 to human chromosome band 14q32 by in situ hybridization. *Cytogenet Cell Genet* **84**, 206-7.

Gubina, E., Ruiz-Hidalgo, M. J., Baladron, V. and Laborda, J. (2000). Assignment of dlk (Dlk1) to mouse chromosome band 12E-F1 by in situ hybridization. *Cytogenet Cell Genet* **88**, 322-3.

Guillemot, F., Caspary, T., Tilghman, S. M., Copeland, N. G., Gilbert, D. J., Jenkins, N. A., Anderson, D. J., Joyner, A. L., Rossant, J. and Nagy, A. (1995). Genomic imprinting of Mash2, a mouse gene required for trophoblast development. *Nat Genet* **9**, 235-42.

Hagan, J. P., O'Neill, B. L., Stewart, C. L., Kozlov, S. V. and Croce, C. M. (2009). At least ten genes define the imprinted Dlk1-Dio3 cluster on mouse chromosome 12qF1. *PLoS One* **4**, e4352.

Hager, R. and Johnstone, R. A. (2003). The genetic basis of family conflict resolution in mice. *Nature* **421**, 533-5.

Haig, D. (1994). Refusing the ovarian time bomb. *Trends Genet* **10**, 346-7; author reply 348-9.

Hales, C. N. and Barker, D. J. (1992). Type 2 (non-insulin-dependent) diabetes mellitus: the thrifty phenotype hypothesis. *Diabetologia* **35**, 595-601.

Hales, C. N., Barker, D. J., Clark, P. M., Cox, L. J., Fall, C., Osmond, C. and Winter, P. D. (1991). Fetal and infant growth and impaired glucose tolerance at age 64. *BMJ* **303**, 1019-22.

Hannula, K., Lipsanen-Nyman, M., Kontiokari, T. and Kere, J. (2001). A narrow segment of maternal uniparental disomy of chromosome 7q31-qter in Silver-Russell syndrome delimits a candidate gene region. *Am J Hum Genet* **68**, 247-53.

Hansen, H., Svensson, U., Zhu, J., Laviola, L., Giorgino, F., Wolf, G., Smith, R. J. and Riedel, H. (1996). Interaction between the Grb10 SH2 domain and the insulin receptor carboxyl terminus. *J Biol Chem* **271**, 8882-6.

Hayward, B. E., Barlier, A., Korbonits, M., Grossman, A. B., Jacquet, P., Enjalbert, A. and Bonthron, D. T. (2001). Imprinting of the G(s)alpha gene GNAS1 in the pathogenesis of acromegaly. *J Clin Invest* **107**, R31-6.

He, W., Rose, D. W., Olefsky, J. M. and Gustafson, T. A. (1998). Grb10 interacts differentially with the insulin receptor, insulin-like growth factor I receptor, and epidermal growth factor receptor via the Grb10 Src homology 2 (SH2) domain and a second novel domain located between the pleckstrin homology and SH2 domains. *J Biol Chem* **273**, 6860-7.

Henriksen, T. (2008). The macrosomic fetus: a challenge in current obstetrics. *Acta Obstet Gynecol Scand* **87**, 134-45.

Henry, I., Bonaiti-Pellie, C., Chehensse, V., Beldjord, C., Schwartz, C., Utermann, G. and Junien, C. (1991). Uniparental paternal disomy in a genetic cancer-predisposing syndrome. *Nature* **351**, 665-7.

Hernandez, L., Kozlov, S., Piras, G. and Stewart, C. L. (2003). Paternal and maternal genomes confer opposite effects on proliferation, cell-cycle length, senescence, and tumor formation. *Proc Natl Acad Sci U S A* **100**, 13344-9.

Hikichi, T., Kohda, T., Kaneko-Ishino, T. and Ishino, F. (2003). Imprinting regulation of the murine Meg1/Grb10 and human GRB10 genes; roles of brain-specific promoters and mouse-specific CTCF-binding sites. *Nucleic Acids Res* **31**, 1398-406.

Holmes, R., Williamson, C., Peters, J., Denny, P. and Wells, C. (2003). A comprehensive transcript map of the mouse Gnas imprinted complex. *Genome Res* **13**, 1410-5.

Holt, L. J. and Daly, R. J. (2005). Adapter protein connections: the MRL and Grb7 protein families. *Growth Factors* **23**, 193-201.

Holt, L. J., Lyons, R. J., Ryan, A. S., Beale, S. M., Ward, A., Cooney, G. J. and Daly, R. J. (2009). Dual ablation of Grb10 and Grb14 in mice reveals their combined role in regulation of insulin signaling and glucose homeostasis. *Mol Endocrinol* **23**, 1406-14.

Holt, L. J. and Siddle, K. (2005). Grb10 and Grb14: enigmatic regulators of insulin action--and more? *Biochem J* **388**, 393-406.

Hsu, P. P., Kang, S. A., Rameseder, J., Zhang, Y., Ottina, K. A., Lim, D., Peterson, T. R., Choi, Y., Gray, N. S., Yaffe, M. B. et al. (2011). The mTOR-regulated phosphoproteome reveals a mechanism of mTORC1-mediated inhibition of growth factor signaling. *Science* **332**, 1317-22.

Hu, Z. Q., Zhang, J. Y., Ji, C. N., Xie, Y., Chen, J. Z. and Mao, Y. M. (2010). Grb10 interacts with Bim L and inhibits apoptosis. *Mol Biol Rep* **37**, 3547-52.

Huang, Q. and Szebenyi, D. M. (2010). Structural basis for the interaction between the growth factor-binding protein GRB10 and the E3 ubiquitin ligase NEDD4. *J Biol Chem* **285**, 42130-9.

Hurst, L. D. and McVean, G. T. (1997). Growth effects of uniparental disomies and the conflict theory of genomic imprinting. *Trends Genet* **13**, 436-43.

Hurst, L. D. and McVean, G. T. (1998). Do we understand the evolution of genomic imprinting? *Curr Opin Genet Dev* **8**, 701-8.

Ideraabdullah, F. Y., Vigneau, S. and Bartolomei, M. S. (2008). Genomic imprinting mechanisms in mammals. *Mutat Res* **647**, 77-85.

Isles, A. R., Baum, M. J., Ma, D., Szeto, A., Keverne, E. B. and Allen, N. D. (2002). A possible role for imprinted genes in inbreeding avoidance and dispersal from the natal area in mice. *Proc Biol Sci* **269**, 665-70.

Isles, A. R., Davies, W. and Wilkinson, L. S. (2006). Genomic imprinting and the social brain. *Philos Trans R Soc Lond B Biol Sci* **361**, 2229-37.

Itier, J. M., Tremp, G. L., Leonard, J. F., Multon, M. C., Ret, G., Schweighoffer, F., Tocque, B., Bluet-Pajot, M. T., Cormier, V. and Dautry, F. (1998). Imprinted gene in postnatal growth role. *Nature* **393**, 125-6.

Iwasa, Y. and Pomiankowski, A. (2001). The evolution of X-linked genomic imprinting. *Genetics* **158**, 1801-9.

Jackson, S. P., Miller, M. F. and Green, R. D. (1997). Phenotypic characterization of rambouillet sheep expression the callipyge gene: III. Muscle weights and muscle weight distribution. *J Anim Sci* **75**, 133-8.

Jahn, T., Seipel, P., Urschel, S., Peschel, C. and Duyster, J. (2002). Role for the adaptor protein Grb10 in the activation of Akt. *Mol Cell Biol* **22**, 979-91.

Jensen, C. H., Erb, K., Westergaard, L. G., Kliem, A. and Teisner, B. (1999). Fetal antigen 1, an EGF multidomain protein in the sex hormone-producing cells of the gonads and the microenvironment of germ cells. *Mol Hum Reprod* **5**, 908-13.

Jensen, C. H., Krogh, T. N., Hojrup, P., Clausen, P. P., Skjodt, K., Larsson, L. I., Enghild, J. J. and Teisner, B. (1994). Protein structure of fetal antigen 1 (FA1). A novel circulating human epidermal-growth-factor-like protein expressed in neuroendocrine tumors and its relation to the gene products of dlk and pG2. *Eur J Biochem* **225**, 83-92.

Jensen, C. H., Meyer, M., Schroder, H. D., Kliem, A., Zimmer, J. and Teisner, B. (2001). Neurons in the monoaminergic nuclei of the rat and human central nervous system express FA1/dlk. *Neuroreport* **12**, 3959-63.

Jenzora, A., Behrendt, B., Small, J. V., Wehland, J. and Stradal, T. E. (2006). PREL1 provides a link from Ras signalling to the actin cytoskeleton via Ena/VASP proteins. *FEBS Lett* **580**, 455-63.

Jirtle, R. L. and Skinner, M. K. (2007). Environmental epigenomics and disease susceptibility. *Nat Rev Genet* **8**, 253-62.

Jones, B. K., Levorse, J. and Tilghman, S. M. (2001). Deletion of a nuclease-sensitive region between the Igf2 and H19 genes leads to Igf2 misregulation and increased adiposity. *Hum Mol Genet* **10**, 807-14.

Joyce, C. A., Sharp, A., Walker, J. M., Bullman, H. and Temple, I. K. (1999). Duplication of 7p12.1-p13, including GRB10 and IGFBP1, in a mother and daughter with features of Silver-Russell syndrome. *Hum Genet* **105**, 273-80.

Kagami, M., Nishimura, G., Okuyama, T., Hayashidani, M., Takeuchi, T., Tanaka, S., Ishino, F., Kurosawa, K. and Ogata, T. (2005). Segmental and full paternal isodisomy for chromosome 14 in three patients: narrowing the critical region and implication for the clinical features. *Am J Med Genet A* **138A**, 127-32.

Kagami, M., O'Sullivan, M. J., Green, A. J., Watabe, Y., Arisaka, O., Masawa, N., Matsuoka, K., Fukami, M., Matsubara, K., Kato, F. et al. (2010). The IG-DMR and the MEG3-DMR at human chromosome 14q32.2: hierarchical interaction and distinct functional properties as imprinting control centers. *PLoS Genet* **6**, e1000992.

Kagami, M., Sekita, Y., Nishimura, G., Irie, M., Kato, F., Okada, M., Yamamori, S., Kishimoto, H., Nakayama, M., Tanaka, Y. et al. (2008). Deletions and epimutations affecting the human 14q32.2 imprinted region in individuals with paternal and maternal upd(14)-like phenotypes. *Nat Genet* **40**, 237-42.

Kagitani, F., Kuroiwa, Y., Wakana, S., Shiroishi, T., Miyoshi, N., Kobayashi, S., Nishida, M., Kohda, T., Kaneko-Ishino, T. and Ishino, F. (1997). Peg5/Neuronatin is an imprinted gene located on sub-distal chromosome 2 in the mouse. *Nucleic Acids Res* **25**, 3428-32.

Kalscheuer, V. M., Mariman, E. C., Schepens, M. T., Rehder, H. and Ropers, H. H. (1993). The insulin-like growth factor type-2 receptor gene is imprinted in the mouse but not in humans. *Nat Genet* **5**, 74-8.

Kaneta, M., Osawa, M., Sudo, K., Nakauchi, H., Farr, A. G. and Takahama, Y. (2000). A role for pref-1 and HES-1 in thymocyte development. *J Immunol* **164**, 256-64.

Kastan, M. B. and Bartek, J. (2004). Cell-cycle checkpoints and cancer. *Nature* **432**, 316-23.

Kawakami, T., Chano, T., Minami, K., Okabe, H., Okada, Y. and Okamoto, K. (2006). Imprinted DLK1 is a putative tumor suppressor gene and inactivated by epimutation at the region upstream of GTL2 in human renal cell carcinoma. *Hum Mol Genet* **15**, 821-30.

Keller, G., Zimmer, G., Mall, G., Ritz, E. and Amann, K. (2003). Nephron number in patients with primary hypertension. *N Engl J Med* **348**, 101-8.

Kelsey, G. (2010). Imprinting on chromosome 20: Tissue-specific imprinting and imprinting mutations in the GNAS locus. *Am J Med Genet C Semin Med Genet* **154C**, 377-86.

Khoury, H., Suarez-Saiz, F., Wu, S. and Minden, M. D. (2010). An upstream insulator regulates DLK1 imprinting in AML. *Blood* **115**, 2260-3.

Kim, K. A., Kim, J. H., Wang, Y. and Sul, H. S. (2007). Pref-1 (preadipocyte factor 1) activates the MEK/extracellular signal-regulated kinase pathway to inhibit adipocyte differentiation. *Mol Cell Biol* **27**, 2294-308.

Kim, Y. (2010). The effects of nutrient depleted microenvironments and delta-like 1 homologue (DLK1) on apoptosis in neuroblastoma. *Nutr Res Pract* **4**, 455-61.

Klaman, L. D., Boss, O., Peroni, O. D., Kim, J. K., Martino, J. L., Zabolotny, J. M., Moghal, N., Lubkin, M., Kim, Y. B., Sharpe, A. H. et al. (2000). Increased energy expenditure, decreased adiposity, and tissue-specific insulin sensitivity in protein-tyrosine phosphatase 1B-deficient mice. *Mol Cell Biol* **20**, 5479-89.

Kolliker, M., Brinkhof, M. W., Heeb, P., Fitze, P. S. and Richner, H. (2000). The quantitative genetic basis of offspring solicitation and parental response in a passerine bird with biparental care. *Proc Biol Sci* **267**, 2127-32.

Komatsu, H., Chao, M. Y., Larkins-Ford, J., Corkins, M. E., Somers, G. A., Tucey, T., Dionne, H. M., White, J. Q., Wani, K., Boxem, M. et al. (2008). OSM-11 facilitates LIN-12 Notch signaling during Caenorhabditis elegans vulval development. *PLoS Biol* **6**, e196.

Koohmaraie, M., Shackelford, S. D., Wheeler, T. L., Lonergan, S. M. and Doumit, M. E. (1995). A muscle hypertrophy condition in lamb (callipyge): characterization of effects on muscle growth and meat quality traits. *J Anim Sci* **73**, 3596-607.

Kopan, R. and Ilagan, M. X. (2009). The canonical Notch signaling pathway: unfolding the activation mechanism. *Cell* **137**, 216-33.

Kotzot, D. (1999). Abnormal phenotypes in uniparental disomy (UPD): fundamental aspects and a critical review with bibliography of UPD other than 15. *Am J Med Genet* **82**, 265-74.

Kotzot, D. (2004). Maternal uniparental disomy 14 dissection of the phenotype with respect to rare autosomal recessively inherited traits, trisomy mosaicism, and genomic imprinting. *Ann Genet* **47**, 251-60.

Kotzot, D., Schmitt, S., Bernasconi, F., Robinson, W. P., Lurie, I. W., Ilyina, H., Mehes, K., Hamel, B. C., Otten, B. J., Hergersberg, M. et al. (1995). Uniparental disomy 7 in Silver-Russell syndrome and primordial growth retardation. *Hum Mol Genet* **4**, 583-7.

Koza, R. A., Nikonova, L., Hogan, J., Rim, J. S., Mendoza, T., Faulk, C., Skaf, J. and Kozak, L. P. (2006). Changes in gene expression foreshadow diet-induced obesity in genetically identical mice. *PLoS Genet* **2**, e81.

Kozma, S. C. and Thomas, G. (2002). Regulation of cell size in growth, development and human disease: PI3K, PKB and S6K. *Bioessays* **24**, 65-71.

Krahenbuhl, S. (1993). Alterations in mitochondrial function and morphology in chronic liver disease: pathogenesis and potential for therapeutic intervention. *Pharmacol Ther* **60**, 1-38.

Krause, M., Leslie, J. D., Stewart, M., Lafuente, E. M., Valderrama, F., Jagannathan, R., Strasser, G. A., Rubinson, D. A., Liu, H., Way, M. et al. (2004). Lamellipodin, an Ena/VASP ligand, is implicated in the regulation of lamellipodial dynamics. *Dev Cell* **7**, 571-83.

Kuwajima, M., Lu, K., Harashima, H., Ono, A., Sato, I., Mizuno, A., Murakami, T., Nakajima, H., Miyagawa, J., Namba, M. et al. (1996). Carnitine transport defect in fibroblasts of juvenile visceral steatosis (JVS) mouse. *Biochem Biophys Res Commun* **223**, 283-7.

Laborda, J. (2000). The role of the epidermal growth factor-like protein dlk in cell differentiation. *Histol Histopathol* **15**, 119-29.

Laborda, J., Sausville, E. A., Hoffman, T. and Notario, V. (1993). dlk, a putative mammalian homeotic gene differentially expressed in small cell lung carcinoma and neuroendocrine tumor cell line. *J Biol Chem* **268**, 3817-20.

Lafuente, E. M., van Puijenbroek, A. A., Krause, M., Carman, C. V., Freeman, G. J., Berezovskaya, A., Constantine, E., Springer, T. A., Gertler, F. B. and Boussiotis, V. A. (2004). RIAM, an Ena/VASP and Profilin ligand, interacts with Rap1-GTP and mediates Rap1-induced adhesion. *Dev Cell* **7**, 585-95.

Lampert, K. P. (2008). Facultative parthenogenesis in vertebrates: reproductive error or chance? *Sex Dev* **2**, 290-301.

Langlais, P., Dong, L. Q., Ramos, F. J., Hu, D., Li, Y., Quon, M. J. and Liu, F. (2004). Negative regulation of insulin-stimulated mitogen-activated protein kinase signaling by Grb10. *Mol Endocrinol* **18**, 350-8.

Langner, C. A., Birkenmeier, E. H., Ben-Zeev, O., Schotz, M. C., Sweet, H. O., Davisson, M. T. and Gordon, J. I. (1989). The fatty liver dystrophy (fld) mutation. A new mutant mouse with a developmental abnormality in triglyceride metabolism and associated tissue-specific defects in lipoprotein lipase and hepatic lipase activities. *J Biol Chem* **264**, 7994-8003.

Langner, C. A., Birkenmeier, E. H., Roth, K. A., Bronson, R. T. and Gordon, J. I. (1991). Characterization of the peripheral neuropathy in neonatal and adult mice that are homozygous for the fatty liver dystrophy (fld) mutation. *J Biol Chem* **266**, 11955-64.

Larsen, J. B., Jensen, C. H., Schroder, H. D., Teisner, B., Bjerre, P. and Hagen, C. (1996). Fetal antigen 1 and growth hormone in pituitary somatotroph cells. *Lancet* **347**, 191.

Lau, M. M., Stewart, C. E., Liu, Z., Bhatt, H., Rotwein, P. and Stewart, C. L. (1994). Loss of the imprinted IGF2/cation-independent mannose 6-phosphate receptor results in fetal overgrowth and perinatal lethality. *Genes Dev* **8**, 2953-63.

Laviola, L., Giorgino, F., Chow, J. C., Baquero, J. A., Hansen, H., Ooi, J., Zhu, J., Riedel, H. and Smith, R. J. (1997). The adapter protein Grb10 associates preferentially with the insulin receptor as compared with the IGF-I receptor in mouse fibroblasts. *J Clin Invest* **99**, 830-7.

Lawlor, M. A., Mora, A., Ashby, P. R., Williams, M. R., Murray-Tait, V., Malone, L., Prescott, A. R., Lucocq, J. M. and Alessi, D. R. (2002). Essential role of PDK1 in regulating cell size and development in mice. *EMBO J* **21**, 3728-38.

Leach, N. T., Chudoba, I., Stewart, T. V., Holmes, L. B. and Weremowicz, S. (2007). Maternally inherited duplication of chromosome 7, dup(7)(p11.2p12), associated with mild cognitive deficit without features of Silver-Russell syndrome. *Am J Med Genet A* **143A**, 1489-93.

Lee, J., Inoue, K., Ono, R., Ogonuki, N., Kohda, T., Kaneko-Ishino, T., Ogura, A. and Ishino, F. (2002). Erasing genomic imprinting memory in mouse clone embryos produced from day 11.5 primordial germ cells. *Development* **129**, 1807-17.

Lee, K., Villena, J. A., Moon, Y. S., Kim, K. H., Lee, S., Kang, C. and Sul, H. S. (2003). Inhibition of adipogenesis and development of glucose intolerance by soluble preadipocyte factor-1 (Pref-1). *J Clin Invest* **111**, 453-61.

Lefebvre, L., Viville, S., Barton, S. C., Ishino, F., Keverne, E. B. and Surani, M. A. (1998). Abnormal maternal behaviour and growth retardation associated with loss of the imprinted gene Mest. *Nat Genet* **20**, 163-9.

Leighton, P. A., Saam, J. R., Ingram, R. S., Stewart, C. L. and Tilghman, S. M. (1995). An enhancer deletion affects both H19 and Igf2 expression. *Genes Dev* **9**, 2079-89.

Lewis, A., Mitsuya, K., Umlauf, D., Smith, P., Dean, W., Walter, J., Higgins, M., Feil, R. and Reik, W. (2004). Imprinting on distal chromosome 7 in the placenta involves repressive histone methylation independent of DNA methylation. *Nat Genet* **36**, 1291-5.

Li, L., Forman, S. J. and Bhatia, R. (2005). Expression of DLK1 in hematopoietic cells results in inhibition of differentiation and proliferation. *Oncogene* **24**, 4472-6.

Li, L., Keverne, E. B., Aparicio, S. A., Ishino, F., Barton, S. C. and Surani, M. A. (1999). Regulation of maternal behavior and offspring growth by paternally expressed Peg3. *Science* **284**, 330-3.

Li, X., Wu, X., Camacho, R., Schwartz, G. J. and Leroith, D. (2011). Intracerebroventricular Leptin Infusion Improves Glucose Homeostasis in Lean Type 2 Diabetic MKR Mice via Hepatic Vagal and Non-Vagal Mechanisms. *PLoS One* **6**, e17058.

Lin, S. P., Coan, P., da Rocha, S. T., Seitz, H., Cavaille, J., Teng, P. W., Takada, S. and Ferguson-Smith, A. C. (2007). Differential regulation of imprinting in the murine embryo and placenta by the Dlk1-Dio3 imprinting control region. *Development* **134**, 417-26.

Lin, S. P., Youngson, N., Takada, S., Seitz, H., Reik, W., Paulsen, M., Cavaille, J. and Ferguson-Smith, A. C. (2003). Asymmetric regulation of imprinting on the maternal and paternal chromosomes at the Dlk1-Gtl2 imprinted cluster on mouse chromosome 12. *Nat Genet* **35**, 97-102.

Liu, F. and Roth, R. A. (1995). Grb-IR: a SH2-domain-containing protein that binds to the insulin receptor and inhibits its function. *Proc Natl Acad Sci U S A* **92**, 10287-91.

Liu, J. P., Baker, J., Perkins, A. S., Robertson, E. J. and Efstratiadis, A. (1993). Mice carrying null mutations of the genes encoding insulin-like growth factor I (Igf-1) and type 1 IGF receptor (Igf1r). *Cell* **75**, 59-72.

Liu, L., Luo, G. Z., Yang, W., Zhao, X., Zheng, Q., Lv, Z., Li, W., Wu, H. J., Wang, L., Wang, X. J. et al. (2010). Activation of the imprinted Dlk1-Dio3 region correlates with pluripotency levels of mouse stem cells. *J Biol Chem* **285**, 19483-90.

Lock, J. E., Smiseth, P. T. and Moore, A. J. (2004). Selection, inheritance, and the evolution of parent-offspring interactions. *Am Nat* **164**, 13-24.

Louvi, A., Accili, D. and Efstratiadis, A. (1997). Growth-promoting interaction of IGF-II with the insulin receptor during mouse embryonic development. *Dev Biol* **189**, 33-48.

Ludwig, T., Eggenschwiler, J., Fisher, P., D'Ercole, A. J., Davenport, M. L. and Efstratiadis, A. (1996). Mouse mutants lacking the type 2 IGF receptor (IGF2R) are rescued from perinatal lethality in Igf2 and Igf1r null backgrounds. *Dev Biol* **177**, 517-35.

Lui, J. C., Finkielstain, G. P., Barnes, K. M. and Baron, J. (2008). An imprinted gene network that controls mammalian somatic growth is down-regulated during postnatal growth deceleration in multiple organs. *Am J Physiol Regul Integr Comp Physiol* **295**, R189-96.

Lyulcheva, E., Taylor, E., Michael, M., Vehlow, A., Tan, S., Fletcher, A., Krause, M. and Bennett, D. (2008). Drosophila pico and its mammalian ortholog lamellipodin activate serum response factor and promote cell proliferation. *Dev Cell* **15**, 680-90.

Ma, D., Shield, J. P., Dean, W., Leclerc, I., Knauf, C., Burcelin, R. R., Rutter, G. A. and Kelsey, G. (2004). Impaired glucose homeostasis in transgenic mice expressing the human transient neonatal diabetes mellitus locus, TNDM. *J Clin Invest* **114**, 339-48.

Mackay, D. J., Boonen, S. E., Clayton-Smith, J., Goodship, J., Hahnemann, J. M., Kant, S. G., Njolstad, P. R., Robin, N. H., Robinson, D. O., Siebert, R. et al. (2006). A maternal hypomethylation syndrome presenting as transient neonatal diabetes mellitus. *Hum Genet* **120**, 262-9.

Maher, E. R. and Reik, W. (2000). Beckwith-Wiedemann syndrome: imprinting in clusters revisited. *J Clin Invest* **105**, 247-52.

Malamitsi-Puchner, A., Nikolaou, K. E. and Puchner, K. P. (2006). Intrauterine growth restriction, brain-sparing effect, and neurotrophins. *Ann N Y Acad Sci* **1092**, 293-6.

Malumbres, M. and Barbacid, M. (2001). To cycle or not to cycle: a critical decision in cancer. *Nat Rev Cancer* **1**, 222-31.

Malumbres, M. and Barbacid, M. (2009). Cell cycle, CDKs and cancer: a changing paradigm. *Nat Rev Cancer* **9**, 153-66.

Manjila, S., Wu, O. C., Khan, F. R., Khan, M. M., Arafah, B. M. and Selman, W. R. (2010). Pharmacological management of acromegaly: a current perspective. *Neurosurg Focus* **29**, E14.

Mann, J. R. and Lovell-Badge, R. H. (1984). Inviability of parthenogenones is determined by pronuclei, not egg cytoplasm. *Nature* **310**, 66-7.

Mann, M. R. and Bartolomei, M. S. (1999). Towards a molecular understanding of Prader-Willi and Angelman syndromes. *Hum Mol Genet* **8**, 1867-73.

Mano, H., Ohya, K., Miyazato, A., Yamashita, Y., Ogawa, W., Inazawa, J., Ikeda, U., Shimada, K., Hatake, K., Kasuga, M. et al. (1998). Grb10/GrbIR as an in vivo substrate of Tec tyrosine kinase. *Genes Cells* **3**, 431-41.

Manser, J., Roonprapunt, C. and Margolis, B. (1997). C. elegans cell migration gene mig-10 shares similarities with a family of SH2 domain proteins and acts cell nonautonomously in excretory canal development. *Dev Biol* **184**, 150-64.

Mantovani, G., Ballare, E., Giammona, E., Beck-Peccoz, P. and Spada, A. (2002). The gsalpha gene: predominant maternal origin of transcription in human thyroid gland and gonads. *J Clin Endocrinol Metab* **87**, 4736-40.

Marin, P., Hogh-Kristiansen, I., Jansson, S., Krotkiewski, M., Holm, G. and Bjorntorp, P. (1992). Uptake of glucose carbon in muscle glycogen and adipose tissue triglycerides in vivo in humans. *Am J Physiol* **263**, E473-80.

Martin, D. E. and Hall, M. N. (2005). The expanding TOR signaling network. *Curr Opin Cell Biol* **17**, 158-66.

McCann, J. A., Zheng, H., Islam, A., Goodyer, C. G. and Polychronakos, C. (2001). Evidence against GRB10 as the gene responsible for Silver-Russell syndrome. *Biochem Biophys Res Commun* **286**, 943-8.

McGrath, J. and Solter, D. (1984). Completion of mouse embryogenesis requires both the maternal and paternal genomes. *Cell* **37**, 179-83.

McLaren, A. (1965). Genetic and Environmental Effects on Foetal and Placental Growth in Mice. *J Reprod Fertil* **9**, 79-98.

McMillen, I. C., MacLaughlin, S. M., Muhlhausler, B. S., Gentili, S., Duffield, J. L. and Morrison, J. L. (2008). Developmental origins of adult health and disease: the role of periconceptional and foetal nutrition. *Basic Clin Pharmacol Toxicol* **102**, 82-9.

McMillen, I. C. and Robinson, J. S. (2005). Developmental origins of the metabolic syndrome: prediction, plasticity, and programming. *Physiol Rev* **85**, 571-633.

McPherron, A. C. and Lee, S. J. (2002). Suppression of body fat accumulation in myostatin-deficient mice. *J Clin Invest* **109**, 595-601.

Mei, B., Zhao, L., Chen, L. and Sul, H. S. (2002). Only the large soluble form of preadipocyte factor-1 (Pref-1), but not the small soluble and membrane forms, inhibits adipocyte differentiation: role of alternative splicing. *Biochem J* **364**, 137-44.

Menheniott, T. R., Woodfine, K., Schulz, R., Wood, A. J., Monk, D., Giraud, A. S., Baldwin, H. S., Moore, G. E. and Oakey, R. J. (2008). Genomic imprinting of Dopa decarboxylase in heart and reciprocal allelic expression with neighboring Grb10. *Mol Cell Biol* **28**, 386-96.

Mergenthaler, S., Hitchins, M. P., Blagitko-Dorfs, N., Monk, D., Wollmann, H. A., Ranke, M. B., Ropers, H. H., Apostolidou, S., Stanier, P., Preece, M. A. et al. (2001). Conflicting reports of imprinting status of human GRB10 in developing brain: how reliable are somatic cell hybrids for predicting allelic origin of expression? *Am J Hum Genet* **68**, 543-5.

Mertineit, C., Yoder, J. A., Taketo, T., Laird, D. W., Trasler, J. M. and Bestor, T. H. (1998). Sex-specific exons control DNA methyltransferase in mammalian germ cells. *Development* **125**, 889-97.

Michael, M. D., Kulkarni, R. N., Postic, C., Previs, S. F., Shulman, G. I., Magnuson, M. A. and Kahn, C. R. (2000). Loss of insulin signaling in hepatocytes leads to severe insulin resistance and progressive hepatic dysfunction. *Mol Cell* **6**, 87-97.

Miyoshi, N., Kuroiwa, Y., Kohda, T., Shitara, H., Yonekawa, H., Kawabe, T., Hasegawa, H., Barton, S. C., Surani, M. A., Kaneko-Ishino, T. et al. (1998). Identification of the Meg1/Grb10 imprinted gene on mouse proximal chromosome 11, a candidate for the Silver-Russell syndrome gene. *Proc Natl Acad Sci U S A* **95**, 1102-7.

Monami, G., Emiliozzi, V. and Morrione, A. (2008). Grb10/Nedd4-mediated multiubiquitination of the insulin-like growth factor receptor regulates receptor internalization. *J Cell Physiol* **216**, 426-37.

Moncoq, K., Broutin, I., Larue, V., Perdereau, D., Cailliau, K., Browaeys-Poly, E., Burnol, A. F. and Ducruix, A. (2003). The PIR domain of Grb14 is an intrinsically unstructured protein: implication in insulin signaling. *FEBS Lett* **554**, 240-6.

Monk, D., Arnaud, P., Frost, J., Hills, F. A., Stanier, P., Feil, R. and Moore, G. E. (2009). Reciprocal imprinting of human GRB10 in placental trophoblast and brain: evolutionary conservation of reversed allelic expression. *Hum Mol Genet*.

Monk, D., Smith, R., Arnaud, P., Preece, M. A., Stanier, P., Beechey, C. V., Peters, J., Kelsey, G. and Moore, G. E. (2003). Imprinted methylation profiles for proximal mouse chromosomes 11 and 7 as revealed by methylation-sensitive representational difference analysis. *Mamm Genome* **14**, 805-16.

Moon, Y. S., Smas, C. M., Lee, K., Villena, J. A., Kim, K. H., Yun, E. J. and Sul, H. S. (2002). Mice lacking paternally expressed Pref-1/Dlk1 display growth retardation and accelerated adiposity. *Mol Cell Biol* **22**, 5585-92.

Moore, T. and Haig, D. (1991). Genomic imprinting in mammalian development: a parental tug-of-war. *Trends Genet* **7**, 45-9.

Mori, K., Giovannone, B. and Smith, R. J. (2005). Distinct Grb10 domain requirements for effects on glucose uptake and insulin signaling. *Mol Cell Endocrinol* **230**, 39-50.

Morison, I. M., Paton, C. J. and Cleverley, S. D. (2001). The imprinted gene and parent-of-origin effect database. *Nucleic Acids Res* **29**, 275-6.

Morrione, A. (2003). Grb10 adapter protein as regulator of insulin-like growth factor receptor signaling. *J Cell Physiol* **197**, 307-11.

Morrione, A., Plant, P., Valentinis, B., Staub, O., Kumar, S., Rotin, D. and Baserga, R. (1999). mGrb10 interacts with Nedd4. *J Biol Chem* **274**, 24094-9.

Morrione, A., Valentinis, B., Li, S., Ooi, J. Y., Margolis, B. and Baserga, R. (1996). Grb10: A new substrate of the insulin-like growth factor I receptor. *Cancer Res* **56**, 3165-7.

Morrione, A., Valentinis, B., Resnicoff, M., Xu, S. and Baserga, R. (1997). The role of mGrb10alpha in insulin-like growth factor I-mediated growth. *J Biol Chem* **272**, 26382-7.

Mounier, C., Lavoie, L., Dumas, V., Mohammad-Ali, K., Wu, J., Nantel, A., Bergeron, J. J., Thomas, D. Y. and Posner, B. I. (2001). Specific inhibition by hGRB10zeta of insulin-induced glycogen synthase activation: evidence for a novel signaling pathway. *Mol Cell Endocrinol* **173**, 15-27.

Moutoussamy, S., Renaudie, F., Lago, F., Kelly, P. A. and Finidori, J. (1998). Grb10 identified as a potential regulator of growth hormone (GH) signaling by cloning of GH receptor target proteins. *J Biol Chem* **273**, 15906-12.

Murdaca, J., Treins, C., Monthouel-Kartmann, M. N., Pontier-Bres, R., Kumar, S., Van Obberghen, E. and Giorgetti-Peraldi, S. (2004). Grb10 prevents Nedd4-mediated vascular endothelial growth factor receptor-2 degradation. *J Biol Chem* **279**, 26754-61.

Murphy, S. K., Freking, B. A., Smith, T. P., Leymaster, K., Nolan, C. M., Wylie, A. A., Evans, H. K. and Jirtle, R. L. (2005). Abnormal postnatal maintenance of elevated DLK1 transcript levels in callipyge sheep. *Mamm Genome* **16**, 171-83.

Naggert, J. K., Fricker, L. D., Varlamov, O., Nishina, P. M., Rouille, Y., Steiner, D. F., Carroll, R. J., Paigen, B. J. and Leiter, E. H. (1995). Hyperproinsulinaemia in obese fat/fat mice associated with a carboxypeptidase E mutation which reduces enzyme activity. *Nat Genet* **10**, 135-42.

Nantel, A., Mohammad-Ali, K., Sherk, J., Posner, B. I. and Thomas, D. Y. (1998). Interaction of the Grb10 adapter protein with the Raf1 and MEK1 kinases. *J Biol Chem* **273**, 10475-84.

Nativio, R., Sparago, A., Ito, Y., Weksberg, R., Riccio, A. and Murrell, A. (2011). Disruption of genomic neighbourhood at the imprinted IGF2-H19 locus in Beckwith-Wiedemann syndrome and Silver-Russell syndrome. *Hum Mol Genet* **20**, 1363-74.

Neel, J. V. (1962). Diabetes mellitus: a "thrifty" genotype rendered detrimental by "progress"? *Am J Hum Genet* **14**, 353-62.

Netchine, I., Rossignol, S., Dufourg, M. N., Azzi, S., Rousseau, A., Perin, L., Houang, M., Steunou, V., Esteva, B., Thibaud, N. et al. (2007). 11p15 imprinting center region 1 loss of methylation is a common and specific cause of typical Russell-Silver syndrome: clinical scoring system and epigenetic-phenotypic correlations. *J Clin Endocrinol Metab* **92**, 3148-54.

Neumann, B., Kubicka, P. and Barlow, D. P. (1995). Characteristics of imprinted genes. *Nat Genet* **9**, 12-3.

Nguyen, P., Leray, V., Diez, M., Serisier, S., Le Bloc'h, J., Siliart, B. and Dumon, H. (2008). Liver lipid metabolism. *J Anim Physiol Anim Nutr (Berl)* **92**, 272-83.

Nichols, A. M., Pan, Y., Herreman, A., Hadland, B. K., De Strooper, B., Kopan, R. and Huppert, S. S. (2004). Notch pathway is dispensable for adipocyte specification. *Genesis* **40**, 40-4.

Norbury, C. and Nurse, P. (1992). Animal cell cycles and their control. *Annu Rev Biochem* **61**, 441-70.

Nouaille, S., Blanquart, C., Zilberfarb, V., Boute, N., Perdereau, D., Roix, J., Burnol, A. F. and Issad, T. (2006). Interaction with Grb14 results in site-specific regulation of tyrosine phosphorylation of the insulin receptor. *EMBO Rep* **7**, 512-8.

Nueda, M. L., Baladron, V., Sanchez-Solana, B., Ballesteros, M. A. and Laborda, J. (2007). The EGF-like protein dlk1 inhibits notch signaling and potentiates adipogenesis of mesenchymal cells. *J Mol Biol* **367**, 1281-93.

Nueda, M. L., Garcia-Ramirez, J. J., Laborda, J. and Baladron, V. (2008). dlk1 specifically interacts with insulin-like growth factor binding protein 1 to modulate adipogenesis of 3T3-L1 cells. *J Mol Biol* **379**, 428-42.

O'Connell, J., Lynch, L., Hogan, A., Cawood, T. J. and O'Shea, D. (2011). Preadipocyte factor-1 is associated with metabolic profile in severe obesity. *J Clin Endocrinol Metab* **96**, E680-4.

O'Neill, T. J., Rose, D. W., Pillay, T. S., Hotta, K., Olefsky, J. M. and Gustafson, T. A. (1996). Interaction of a GRB-IR splice variant (a human GRB10 homolog) with the insulin and insulin-

like growth factor I receptors. Evidence for a role in mitogenic signaling. *J Biol Chem* **271**, 22506-13.

Obata, Y., Kaneko-Ishino, T., Koide, T., Takai, Y., Ueda, T., Domeki, I., Shiroishi, T., Ishino, F. and Kono, T. (1998). Disruption of primary imprinting during oocyte growth leads to the modified expression of imprinted genes during embryogenesis. *Development* **125**, 1553-60.

Ohlsson, R., Hedborg, F., Holmgren, L., Walsh, C. and Ekstrom, T. J. (1994). Overlapping patterns of IGF2 and H19 expression during human development: biallelic IGF2 expression correlates with a lack of H19 expression. *Development* **120**, 361-8.

Ohta, T., Gray, T. A., Rogan, P. K., Buiting, K., Gabriel, J. M., Saitoh, S., Muralidhar, B., Bilienska, B., Krajewska-Walasek, M., Driscoll, D. J. et al. (1999). Imprinting-mutation mechanisms in Prader-Willi syndrome. *Am J Hum Genet* **64**, 397-413.

Okamoto, M., Takemori, H., Halder, S. K. and Hatano, O. (1997). Zona glomerulosa-specific factor: cloning and function. *Steroids* **62**, 73-6.

Okano, M., Bell, D. W., Haber, D. A. and Li, E. (1999). DNA methyltransferases Dnmt3a and Dnmt3b are essential for de novo methylation and mammalian development. *Cell* **99**, 247-57.

Olek, A. and Walter, J. (1997). The pre-implantation ontogeny of the H19 methylation imprint. *Nat Genet* **17**, 275-6.

Ono, R., Nakamura, K., Inoue, K., Naruse, M., Usami, T., Wakisaka-Saito, N., Hino, T., Suzuki-Migishima, R., Ogonuki, N., Miki, H. et al. (2006). Deletion of Peg10, an imprinted gene acquired from a retrotransposon, causes early embryonic lethality. *Nat Genet* **38**, 101-6.

Ooi, J., Yajnik, V., Immanuel, D., Gordon, M., Moskow, J. J., Buchberg, A. M. and Margolis, B. (1995). The cloning of Grb10 reveals a new family of SH2 domain proteins. *Oncogene* **10**, 1621-30.

Oswald, J., Engemann, S., Lane, N., Mayer, W., Olek, A., Fundele, R., Dean, W., Reik, W. and Walter, J. (2000). Active demethylation of the paternal genome in the mouse zygote. *Curr Biol* **10**, 475-8.

Otulakowski, G., Duan, W. and O'Brodovich, H. (2009). Global and gene-specific translational regulation in rat lung development. *Am J Respir Cell Mol Biol* **40**, 555-67.

Ozanne, S. E. and Constancia, M. (2007). Mechanisms of disease: the developmental origins of disease and the role of the epigenotype. *Nat Clin Pract Endocrinol Metab* **3**, 539-46.

Pachnis, V., Mankoo, B. and Costantini, F. (1993). Expression of the c-ret proto-oncogene during mouse embryogenesis. *Development* **119**, 1005-17.

Pandey, A., Duan, H., Di Fiore, P. P. and Dixit, V. M. (1995). The Ret receptor protein tyrosine kinase associates with the SH2-containing adapter protein Grb10. *J Biol Chem* **270**, 21461-3.

Pearsall, R. S., Shibata, H., Brozowska, A., Yoshino, K., Okuda, K., deJong, P. J., Plass, C., Chapman, V. M., Hayashizaki, Y. and Held, W. A. (1996). Absence of imprinting in U2AFBPL, a human homologue of the imprinted mouse gene U2afbp-rs. *Biochem Biophys Res Commun* **222**, 171-7.

Pende, M., Um, S. H., Mieulet, V., Sticker, M., Goss, V. L., Mestan, J., Mueller, M., Fumagalli, S., Kozma, S. C. and Thomas, G. (2004). S6K1(-/-)/S6K2(-/-) mice exhibit perinatal lethality and

rapamycin-sensitive 5'-terminal oligopyrimidine mRNA translation and reveal a mitogen-activated protein kinase-dependent S6 kinase pathway. *Mol Cell Biol* **24**, 3112-24.

Perkins, A. C., Kramer, L. N., Spurlock, D. M., Hadfield, T. S., Cockett, N. E. and Bidwell, C. A. (2006). Postnatal changes in the expression of genes located in the callipyge region in sheep skeletal muscle. *Anim Genet* **37**, 535-42.

Plagge, A., Gordon, E., Dean, W., Boiani, R., Cinti, S., Peters, J. and Kelsey, G. (2004). The imprinted signaling protein XL alpha s is required for postnatal adaptation to feeding. *Nat Genet* **36**, 818-26.

Plagge, A., Isles, A. R., Gordon, E., Humby, T., Dean, W., Gritsch, S., Fischer-Colbrie, R., Wilkinson, L. S. and Kelsey, G. (2005). Imprinted Nesp55 influences behavioral reactivity to novel environments. *Mol Cell Biol* **25**, 3019-26.

Plagge, A. and Kelsey, G. (2006). Imprinting the Gnas locus. *Cytogenet Genome Res* **113**, 178-87.

Pollak, M. (2008). Insulin and insulin-like growth factor signalling in neoplasia. *Nat Rev Cancer* **8**, 915-28.

Pollak, M. N., Schernhammer, E. S. and Hankinson, S. E. (2004). Insulin-like growth factors and neoplasia. *Nat Rev Cancer* **4**, 505-18.

Ponting, C. P. and Benjamin, D. R. (1996). A novel family of Ras-binding domains. *Trends Biochem Sci* **21**, 422-5.

Preece, M. A. (2002). The genetics of the Silver-Russell syndrome. *Rev Endocr Metab Disord* **3**, 369-79.

Price, S. M., Stanhope, R., Garrett, C., Preece, M. A. and Trembath, R. C. (1999). The spectrum of Silver-Russell syndrome: a clinical and molecular genetic study and new diagnostic criteria. *J Med Genet* **36**, 837-42.

Qi, X., Chen, Z., Liu, D., Cen, J. and Gu, M. (2008). Expression of Dlk1 gene in myelodysplastic syndrome determined by microarray, and its effects on leukemia cells. *Int J Mol Med* **22**, 61-8.

Raghunandan, R., Ruiz-Hidalgo, M., Jia, Y., Ettinger, R., Rudikoff, E., Riggins, P., Farnsworth, R., Tesfaye, A., Laborda, J. and Bauer, S. R. (2008). Dlk1 influences differentiation and function of B lymphocytes. *Stem Cells and Development* **17**, 495-507.

Ramos, F. J., Langlais, P. R., Hu, D., Dong, L. Q. and Liu, F. (2006). Grb10 mediates insulin-stimulated degradation of the insulin receptor: a mechanism of negative regulation. *Am J Physiol Endocrinol Metab* **290**, E1262-6.

Rapkins, R. W., Hore, T., Smithwick, M., Ager, E., Pask, A. J., Renfree, M. B., Kohn, M., Hameister, H., Nicholls, R. D., Deakin, J. E. et al. (2006). Recent assembly of an imprinted domain from non-imprinted components. *PLoS Genet* **2**, e182.

Recknagel, R. O. (1967). Carbon tetrachloride hepatotoxicity. *Pharmacol Rev* **19**, 145-208.

Rehnmark, S., Giometti, C. S., Slavin, B. G., Doolittle, M. H. and Reue, K. (1998). The fatty liver dystrophy mutant mouse: microvesicular steatosis associated with altered expression levels of peroxisome proliferator-regulated proteins. *J Lipid Res* **39**, 2209-17.

Reik, W., Constancia, M., Fowden, A., Anderson, N., Dean, W., Ferguson-Smith, A., Tycko, B. and Sibley, C. (2003). Regulation of supply and demand for maternal nutrients in mammals by imprinted genes. *J Physiol* **547**, 35-44.

Reue, K. and Doolittle, M. H. (1996). Naturally occurring mutations in mice affecting lipid transport and metabolism. *J Lipid Res* **37**, 1387-405.

Robinson, W. P. and Lalande, M. (1995). Sex-specific meiotic recombination in the Prader--Willi/Angelman syndrome imprinted region. *Hum Mol Genet* **4**, 801-6.

Rodeheffer, M. S., Birsoy, K. and Friedman, J. M. (2008). Identification of white adipocyte progenitor cells in vivo. *Cell* **135**, 240-9.

Rogler, C. E., Yang, D., Rossetti, L., Donohoe, J., Alt, E., Chang, C. J., Rosenfeld, R., Neely, K. and Hintz, R. (1994). Altered body composition and increased frequency of diverse malignancies in insulin-like growth factor-II transgenic mice. *J Biol Chem* **269**, 13779-84.

Rommel, C., Bodine, S. C., Clarke, B. A., Rossman, R., Nunez, L., Stitt, T. N., Yancopoulos, G. D. and Glass, D. J. (2001). Mediation of IGF-1-induced skeletal myotube hypertrophy by PI(3)K/Akt/mTOR and PI(3)K/Akt/GSK3 pathways. *Nat Cell Biol* **3**, 1009-13.

Rosen, E. D., Walkey, C. J., Puigserver, P. and Spiegelman, B. M. (2000). Transcriptional regulation of adipogenesis. *Genes Dev* **14**, 1293-307.

Ross, D. A., Rao, P. K. and Kadesch, T. (2004). Dual roles for the Notch target gene Hes-1 in the differentiation of 3T3-L1 preadipocytes. *Mol Cell Biol* **24**, 3505-13.

Rossignol, S., Steunou, V., Chalas, C., Kerjean, A., Rigolet, M., Viegas-Pequignot, E., Jouannet, P., Le Bouc, Y. and Gicquel, C. (2006). The epigenetic imprinting defect of patients with Beckwith-Wiedemann syndrome born after assisted reproductive technology is not restricted to the 11p15 region. *J Med Genet* **43**, 902-7.

Rougier, N., Bourc'his, D., Gomes, D. M., Niveleau, A., Plachot, M., Paldi, A. and Viegas-Pequignot, E. (1998). Chromosome methylation patterns during mammalian preimplantation development. *Genes Dev* **12**, 2108-13.

Ruige, J. B., Dekker, J. M., Blum, W. F., Stehouwer, C. D., Nijpels, G., Mooy, J., Kostense, P. J., Bouter, L. M. and Heine, R. J. (1999). Leptin and variables of body adiposity, energy balance, and insulin resistance in a population-based study. The Hoorn Study. *Diabetes Care* **22**, 1097-104.

Ruiz-Hidalgo, M. J., Gubina, E., Tull, L., Baladron, V. and Laborda, J. (2002). dlk modulates mitogen-activated protein kinase signaling to allow or prevent differentiation. *Exp Cell Res* **274**, 178-88.

Sakajiri, S., O'Kelly, J., Yin, D., Miller, C. W., Hofmann, W. K., Oshimi, K., Shih, L. Y., Kim, K. H., Sul, H. S., Jensen, C. H. et al. (2005). Dlk1 in normal and abnormal hematopoiesis. *Leukemia* **19**, 1404-10.

Salas, M., John, R., Saxena, A., Barton, S., Frank, D., Fitzpatrick, G., Higgins, M. J. and Tycko, B. (2004). Placental growth retardation due to loss of imprinting of Phlda2. *Mech Dev* **121**, 1199-210.

Sanchez-Solana, B., Nueda, M. L., Ruvira, M. D., Ruiz-Hidalgo, M. J., Monsalve, E. M., Rivero, S., Garcia-Ramirez, J. J., Diaz-Guerra, M. J., Baladron, V. and Laborda, J. (2011). The EGF-like

proteins DLK1 and DLK2 function as inhibitory non-canonical ligands of NOTCH1 receptor that modulate each other's activities. *Biochim Biophys Acta* **1813**, 1153-64.

Sansing, R. C. and Chinnici, J. P. (1976). Optimal and discriminating birth weights in human populations. *Ann Hum Genet* **40**, 123-31.

Sanz, L. A., Chamberlain, S., Sabourin, J. C., Henckel, A., Magnuson, T., Hugnot, J. P., Feil, R. and Arnaud, P. (2008). A mono-allelic bivalent chromatin domain controls tissue-specific imprinting at Grb10. *EMBO J* **27**, 2523-32.

Sato, S., Yoshida, W., Soejima, H., Nakabayashi, K. and Hata, K. (2011). Methylation dynamics of IG-DMR and Gtl2-DMR during murine embryonic and placental development. *Genomics*.

Satran, L., Sharp, H. L., Schenken, J. R. and Krivit, W. (1969). Fatal neonatal heptic steatosis: a new familial disorder. *J Pediatr* **75**, 39-46.

Schmidt, J. V., Matteson, P. G., Jones, B. K., Guan, X. J. and Tilghman, S. M. (2000). The Dlk1 and Gtl2 genes are linked and reciprocally imprinted. *Genes Dev* **14**, 1997-2002.

Schuster-Gossler, K., Simon-Chazottes, D., Guenet, J. L., Zachgo, J. and Gossler, A. (1996). Gtl2lacZ, an insertional mutation on mouse chromosome 12 with parental origin-dependent phenotype. *Mamm Genome* **7**, 20-4.

Segal, K. R., Landt, M. and Klein, S. (1996). Relationship between insulin sensitivity and plasma leptin concentration in lean and obese men. *Diabetes* **45**, 988-91.

Sekita, Y., Wagatsuma, H., Nakamura, K., Ono, R., Kagami, M., Wakisaka, N., Hino, T., Suzuki-Migishima, R., Kohda, T., Ogura, A. et al. (2008). Role of retrotransposon-derived imprinted gene, Rtl1, in the feto-maternal interface of mouse placenta. *Nat Genet* **40**, 243-8.

Sell, C., Dumenil, G., Deveaud, C., Miura, M., Coppola, D., DeAngelis, T., Rubin, R., Efstratiadis, A. and Baserga, R. (1994). Effect of a null mutation of the insulin-like growth factor I receptor gene on growth and transformation of mouse embryo fibroblasts. *Mol Cell Biol* **14**, 3604-12.

Shemer, R., Birger, Y., Riggs, A. D. and Razin, A. (1997). Structure of the imprinted mouse Snrpn gene and establishment of its parental-specific methylation pattern. *Proc Natl Acad Sci U S A* **94**, 10267-72.

Shi, W., Lefebvre, L., Yu, Y., Otto, S., Krella, A., Orth, A. and Fundele, R. (2004). Loss-of-imprinting of Peg1 in mouse interspecies hybrids is correlated with altered growth. *Genesis* **39**, 65-72.

Shimomura, I., Hammer, R. E., Richardson, J. A., Ikemoto, S., Bashmakov, Y., Goldstein, J. L. and Brown, M. S. (1998). Insulin resistance and diabetes mellitus in transgenic mice expressing nuclear SREBP-1c in adipose tissue: model for congenital generalized lipodystrophy. *Genes Dev* **12**, 3182-94.

Shiura, H., Miyoshi, N., Konishi, A., Wakisaka-Saito, N., Suzuki, R., Muguruma, K., Kohda, T., Wakana, S., Yokoyama, M., Ishino, F. et al. (2005). Meg1/Grb10 overexpression causes postnatal growth retardation and insulin resistance via negative modulation of the IGF1R and IR cascades. *Biochem Biophys Res Commun* **329**, 909-16.

Shiura, H., Nakamura, K., Hikichi, T., Hino, T., Oda, K., Suzuki-Migishima, R., Kohda, T., Kaneko-ishino, T. and Ishino, F. (2009). Paternal deletion of Meg1/Grb10 DMR causes

maternalization of the Meg1/Grb10 cluster in mouse proximal Chromosome 11 leading to severe pre- and postnatal growth retardation. *Hum Mol Genet* **18**, 1424-38.

Sibley, C., Glazier, J. and D'Souza, S. (1997). Placental transporter activity and expression in relation to fetal growth. *Exp Physiol* **82**, 389-402.

Sibley, C. P., Coan, P. M., Ferguson-Smith, A. C., Dean, W., Hughes, J., Smith, P., Reik, W., Burton, G. J., Fowden, A. L. and Constancia, M. (2004). Placental-specific insulin-like growth factor 2 (Igf2) regulates the diffusional exchange characteristics of the mouse placenta. *Proc Natl Acad Sci U S A* **101**, 8204-8.

Simon, I., Tenzen, T., Reubinoff, B. E., Hillman, D., McCarrey, J. R. and Cedar, H. (1999). Asynchronous replication of imprinted genes is established in the gametes and maintained during development. *Nature* **401**, 929-32.

Smas, C. M., Chen, L., Zhao, L., Latasa, M. J. and Sul, H. S. (1999). Transcriptional repression of pref-1 by glucocorticoids promotes 3T3-L1 adipocyte differentiation. *J Biol Chem* **274**, 12632-41.

Smas, C. M., Green, D. and Sul, H. S. (1994). Structural characterization and alternate splicing of the gene encoding the preadipocyte EGF-like protein pref-1. *Biochemistry* **33**, 9257-65.

Smas, C. M., Kachinskas, D., Liu, C. M., Xie, X., Dircks, L. K. and Sul, H. S. (1998). Transcriptional control of the pref-1 gene in 3T3-L1 adipocyte differentiation. Sequence requirement for differentiation-dependent suppression. *J Biol Chem* **273**, 31751-8.

Smas, C. M. and Sul, H. S. (1993). Pref-1, a protein containing EGF-like repeats, inhibits adipocyte differentiation. *Cell* **73**, 725-34.

Smas, C. M. and Sul, H. S. (1997). Molecular mechanisms of adipocyte differentiation and inhibitory action of pref-1. *Crit Rev Eukaryot Gene Expr* **7**, 281-98.

Smith, F.M. (2004) An investigation of mouse Grb10, an imprinted gene that links foetal growth and insulin-regulated metabolism. *PhD Thesis, University of Bath*.

Smith, F. M., Garfield, A. S. and Ward, A. (2006). Regulation of growth and metabolism by imprinted genes. *Cytogenet Genome Res* **113**, 279-91.

Smith, F. M., Holt, L. J., Garfield, A. S., Charalambous, M., Koumanov, F., Perry, M., Bazzani, R., Sheardown, S. A., Hegarty, B. D., Lyons, R. J. et al. (2007). Mice with a disruption of the imprinted Grb10 gene exhibit altered body composition, glucose homeostasis, and insulin signaling during postnatal life. *Mol Cell Biol* **27**, 5871-86.

Smith, R. J., Dean, W., Konfortova, G. and Kelsey, G. (2003). Identification of novel imprinted genes in a genome-wide screen for maternal methylation. *Genome Res* **13**, 558-69.

Soga, M., Kishimoto, Y., kawaguchi, J., Nakai, Y., Kawamura, Y., Inagaki, S., Katoh, K., Oohara, T., Makino, S. and Oshima, I. (1999). The FLS mouse: a new inbred strain with spontaneous fatty liver. *Lab Anim Sci* **49**, 269-75.

Solter, D. (1994). Refusing the ovarian time bomb. *Trends Genet* **10**, 346; author reply 348-9.

Spencer, H. G., Clark, A. G. and Feldman, M. W. (1999). Genetic conflicts and the evolutionary origin of genomic imprinting. *Trends Ecol Evol* **14**, 197-201.

Spencer, J., Wang, Z. and Hoy, W. (2001). Low birth weight and reduced renal volume in Aboriginal children. *Am J Kidney Dis* **37**, 915-20.

Stadtfeld, M., Apostolou, E., Akutsu, H., Fukuda, A., Follett, P., Natesan, S., Kono, T., Shioda, T. and Hochedlinger, K. (2010). Aberrant silencing of imprinted genes on chromosome 12qF1 in mouse induced pluripotent stem cells. *Nature* **465**, 175-81.

Stanger, B. Z., Tanaka, A. J. and Melton, D. A. (2007). Organ size is limited by the number of embryonic progenitor cells in the pancreas but not the liver. *Nature* **445**, 886-91.

Stein, E., Cerretti, D. P. and Daniel, T. O. (1996). Ligand activation of ELK receptor tyrosine kinase promotes its association with Grb10 and Grb2 in vascular endothelial cells. *J Biol Chem* **271**, 23588-93.

Stein, E. G., Ghirlando, R. and Hubbard, S. R. (2003). Structural basis for dimerization of the Grb10 Src homology 2 domain. Implications for ligand specificity. *J Biol Chem* **278**, 13257-64.

Stein, E. G., Gustafson, T. A. and Hubbard, S. R. (2001). The BPS domain of Grb10 inhibits the catalytic activity of the insulin and IGF1 receptors. *FEBS Lett* **493**, 106-11.

Sul, H. S. (2009). Minireview: Pref-1: role in adipogenesis and mesenchymal cell fate. *Mol Endocrinol* **23**, 1717-25.

Surani, M. A., Barton, S. C. and Norris, M. L. (1984). Development of reconstituted mouse eggs suggests imprinting of the genome during gametogenesis. *Nature* **308**, 548-50.

Sutton, V. R. and Shaffer, L. G. (2000). Search for imprinted regions on chromosome 14: comparison of maternal and paternal UPD cases with cases of chromosome 14 deletion. *Am J Med Genet* **93**, 381-7.

Tada, T., Tada, M., Hilton, K., Barton, S. C., Sado, T., Takagi, N. and Surani, M. A. (1998). Epigenotype switching of imprintable loci in embryonic germ cells. *Dev Genes Evol* **207**, 551-61.

Takada, S., Paulsen, M., Tevendale, M., Tsai, C. E., Kelsey, G., Cattanach, B. M. and Ferguson-Smith, A. C. (2002). Epigenetic analysis of the Dlk1-Gtl2 imprinted domain on mouse chromosome 12: implications for imprinting control from comparison with Igf2-H19. *Hum Mol Genet* **11**, 77-86.

Takada, S., Tevendale, M., Baker, J., Georgiades, P., Campbell, E., Freeman, T., Johnson, M. H., Paulsen, M. and Ferguson-Smith, A. C. (2000). Delta-like and gtl2 are reciprocally expressed, differentially methylated linked imprinted genes on mouse chromosome 12. *Curr Biol* **10**, 1135-8.

Takahashi, M., Kamei, Y. and Ezaki, O. (2005). Mest/Peg1 imprinted gene enlarges adipocytes and is a marker of adipocyte size. *Am J Physiol Endocrinol Metab* **288**, E117-24.

Takahashi, N., Okamoto, A., Kobayashi, R., Shirai, M., Obata, Y., Ogawa, H., Sotomaru, Y. and Kono, T. (2009). Deletion of Gtl2, imprinted non-coding RNA, with its differentially methylated region induces lethal parent-origin-dependent defects in mice. *Hum Mol Genet* **18**, 1879-88.

Takeda, H., Caiment, F., Smit, M., Hiard, S., Tordoir, X., Cockett, N., Georges, M. and Charlier, C. (2006). The callipyge mutation enhances bidirectional long-range DLK1-GTL2 intergenic transcription in cis. *Proc Natl Acad Sci U S A* **103**, 8119-24.

Takeda, S., Bonnamy, J. P., Owen, M. J., Ducy, P. and Karsenty, G. (2001). Continuous expression of Cbfa1 in nonhypertrophic chondrocytes uncovers its ability to induce

hypertrophic chondrocyte differentiation and partially rescues Cbfa1-deficient mice. *Genes Dev* **15**, 467-81.

Tanimizu, N., Nishikawa, M., Saito, H., Tsujimura, T. and Miyajima, A. (2003). Isolation of hepatoblasts based on the expression of Dlk/Pref-1. *Journal of Cell Science* **116**, 1775-1786.

Taniura, H., Taniguchi, N., Hara, M. and Yoshikawa, K. (1998). Necdin, a postmitotic neuron-specific growth suppressor, interacts with viral transforming proteins and cellular transcription factor E2F1. *J Biol Chem* **273**, 720-8.

Temple, I. K. and Shield, J. P. (2002). Transient neonatal diabetes, a disorder of imprinting. *J Med Genet* **39**, 872-5.

Temple, I. K. and Shield, J. P. (2010). 6q24 transient neonatal diabetes. *Rev Endocr Metab Disord* **11**, 199-204.

Tevendale, M., Watkins, M., Rasberry, C., Cattanach, B. and Ferguson-Smith, A. C. (2006). Analysis of mouse conceptuses with uniparental duplication/deficiency for distal chromosome 12: comparison with chromosome 12 uniparental disomy and implications for genomic imprinting. *Cytogenet Genome Res* **113**, 215-22.

Thomas, J. H. (1995). Genomic imprinting proposed as a surveillance mechanism for chromosome loss. *Proc Natl Acad Sci U S A* **92**, 480-2.

Tornehave, D., Jansen, P., Teisner, B., Rasmussen, H. B., Chemnitz, J. and Moscoso, G. (1993). Fetal antigen 1 (FA1) in the human pancreas: cell type expression, topological and quantitative variations during development. *Anat Embryol (Berl)* **187**, 335-41.

Tsai, T. F., Jiang, Y. H., Bressler, J., Armstrong, D. and Beaudet, A. L. (1999). Paternal deletion from Snrpn to Ube3a in the mouse causes hypotonia, growth retardation and partial lethality and provides evidence for a gene contributing to Prader-Willi syndrome. *Hum Mol Genet* **8**, 1357-64.

Tseng, Y. H., Butte, A. J., Kokkotou, E., Yechoor, V. K., Taniguchi, C. M., Kriauciunas, K. M., Cypess, A. M., Niinobe, M., Yoshikawa, K., Patti, M. E. et al. (2005). Prediction of preadipocyte differentiation by gene expression reveals role of insulin receptor substrates and necdin. *Nat Cell Biol* **7**, 601-11.

Ueda, T., Abe, K., Miura, A., Yuzuriha, M., Zubair, M., Noguchi, M., Niwa, K., Kawase, Y., Kono, T., Matsuda, Y. et al. (2000). The paternal methylation imprint of the mouse H19 locus is acquired in the gonocyte stage during foetal testis development. *Genes Cells* **5**, 649-59.

Ulizzi, L., Gravina, M. F. and Terrenato, L. (1981). Natural selection associated with birth weight. II. Stabilizing and directional components. *Ann Hum Genet* **45**, 207-12.

Umlauf, D., Goto, Y., Cao, R., Cerqueira, F., Wagschal, A., Zhang, Y. and Feil, R. (2004). Imprinting along the Kcnq1 domain on mouse chromosome 7 involves repressive histone methylation and recruitment of Polycomb group complexes. *Nat Genet* **36**, 1296-300.

Urschel, S., Bassermann, F., Bai, R. Y., Munch, S., Peschel, C. and Duyster, J. (2005). Phosphorylation of grb10 regulates its interaction with 14-3-3. *J Biol Chem* **280**, 16987-93.

Varmuza, S. and Mann, M. (1994). Genomic imprinting--defusing the ovarian time bomb. *Trends Genet* **10**, 118-23.

Varrault, A., Gueydan, C., Delalbre, A., Bellmann, A., Houssami, S., Aknin, C., Severac, D., Chotard, L., Kahli, M., Le Digarcher, A. et al. (2006). Zac1 regulates an imprinted gene network critically involved in the control of embryonic growth. *Dev Cell* **11**, 711-22.

Vecchione, A., Marchese, A., Henry, P., Rotin, D. and Morrione, A. (2003). The Grb10/Nedd4 complex regulates ligand-induced ubiquitination and stability of the insulin-like growth factor I receptor. *Mol Cell Biol* **23**, 3363-72.

Victora, C. G., Adair, L., Fall, C., Hallal, P. C., Martorell, R., Richter, L. and Sachdev, H. S. (2008). Maternal and child undernutrition: consequences for adult health and human capital. *Lancet* **371**, 340-57.

Villena, J. A., Choi, C. S., Wang, Y., Kim, S., Hwang, Y. J., Kim, Y. B., Cline, G., Shulman, G. I. and Sul, H. S. (2008). Resistance to high-fat diet-induced obesity but exacerbated insulin resistance in mice overexpressing preadipocyte factor-1 (Pref-1): a new model of partial lipodystrophy. *Diabetes* **57**, 3258-66.

Vuocolo, T., Byrne, K., White, J., McWilliam, S., Reverter, A., Cockett, N. E. and Tellam, R. L. (2007). Identification of a gene network contributing to hypertrophy in callipyge skeletal muscle. *Physiol Genomics* **28**, 253-72.

Waddell, J. N., Zhang, P., Wen, Y., Gupta, S. K., Yevtodiyenko, A., Schmidt, J. V., Bidwell, C. A., Kumar, A. and Kuang, S. (2010). Dlk1 is necessary for proper skeletal muscle development and regeneration. *PLoS One* **5**, e15055.

Wagschal, A. and Feil, R. (2006). Genomic imprinting in the placenta. *Cytogenet Genome Res* **113**, 90-8.

Walter, J. and Paulsen, M. (2003). The potential role of gene duplications in the evolution of imprinting mechanisms. *Hum Mol Genet* **12 Spec No 2**, R215-20.

Wang, J., Dai, H., Yousaf, N., Moussaif, M., Deng, Y., Boufelliga, A., Swamy, O. R., Leone, M. E. and Riedel, H. (1999). Grb10, a positive, stimulatory signaling adapter in platelet-derived growth factor BB-, insulin-like growth factor I-, and insulin-mediated mitogenesis. *Mol Cell Biol* **19**, 6217-28.

Wang, L., Balas, B., Christ-Roberts, C. Y., Kim, R. Y., Ramos, F. J., Kikani, C. K., Li, C., Deng, C., Reyna, S., Musi, N. et al. (2007). Peripheral disruption of the Grb10 gene enhances insulin signaling and sensitivity in vivo. *Mol Cell Biol* **27**, 6497-505.

Wang, M. Y., Grayburn, P., Chen, S., Ravazzola, M., Orci, L. and Unger, R. H. (2008). Adipogenic capacity and the susceptibility to type 2 diabetes and metabolic syndrome. *Proc Natl Acad Sci U S A* **105**, 6139-44.

Wang, Y., Kim, K. A., Kim, J. H. and Sul, H. S. (2006). Pref-1, a preadipocyte secreted factor that inhibits adipogenesis. *J Nutr* **136**, 2953-6.

Wang, Y. and Sul, H. S. (2009). Pref-1 regulates mesenchymal cell commitment and differentiation through Sox9. *Cell Metab* **9**, 287-302.

Wang, Y., Zhao, L., Smas, C. and Sul, H. S. (2010). Pref-1 interacts with fibronectin to inhibit adipocyte differentiation. *Mol Cell Biol* **30**, 3480-92.

Ward, A. and Tosh, D., eds. (2008) Mouse Cell Culture: Methods and Protocols. Humana Press, pp. 19-27

Waterland, R. A. and Jirtle, R. L. (2004). Early nutrition, epigenetic changes at transposons and imprinted genes, and enhanced susceptibility to adult chronic diseases. *Nutrition* **20**, 63-8.

Weaver, J. R., Susiarjo, M. and Bartolomei, M. S. (2009). Imprinting and epigenetic changes in the early embryo. *Mamm Genome* **20**, 532-43.

Weinkove, D., Neufeld, T. P., Twardzik, T., Waterfield, M. D. and Leevers, S. J. (1999). Regulation of imaginal disc cell size, cell number and organ size by Drosophila class I(A) phosphoinositide 3-kinase and its adaptor. *Curr Biol* **9**, 1019-29.

Weisstein, A. E., Feldman, M. W. and Spencer, H. G. (2002). Evolutionary genetic models of the ovarian time bomb hypothesis for the evolution of genomic imprinting. *Genetics* **162**, 425-39.

Weksberg, R., Shuman, C. and Smith, A. C. (2005). Beckwith-Wiedemann syndrome. *Am J Med Genet C Semin Med Genet* **137C**, 12-23.

Weksberg, R., Teshima, I., Williams, B. R., Greenberg, C. R., Pueschel, S. M., Chernos, J. E., Fowlow, S. B., Hoyme, E., Anderson, I. J., Whiteman, D. A. et al. (1993). Molecular characterization of cytogenetic alterations associated with the Beckwith-Wiedemann syndrome (BWS) phenotype refines the localization and suggests the gene for BWS is imprinted. *Hum Mol Genet* **2**, 549-56.

Wermter, A. K., Scherag, A., Meyre, D., Reichwald, K., Durand, E., Nguyen, T. T., Koberwitz, K., Lichtner, P., Meitinger, T., Schafer, H. et al. (2008). Preferential reciprocal transfer of paternal/maternal DLK1 alleles to obese children: first evidence of polar overdominance in humans. *Eur J Hum Genet* **16**, 1126-34.

White, C. R. and Seymour, R. S. (2003). Mammalian basal metabolic rate is proportional to body mass2/3. *Proc Natl Acad Sci U S A* **100**, 4046-9.

White, J. D., Vuocolo, T., McDonagh, M., Grounds, M. D., Harper, G. S., Cockett, N. E. and Tellam, R. (2008). Analysis of the callipyge phenotype through skeletal muscle development; association of Dlk1 with muscle precursor cells. *Differentiation* **76**, 283-98.

Wick, K. R., Werner, E. D., Langlais, P., Ramos, F. J., Dong, L. Q., Shoelson, S. E. and Liu, F. (2003). Grb10 inhibits insulin-stimulated insulin receptor substrate (IRS)-phosphatidylinositol 3-kinase/Akt signaling pathway by disrupting the association of IRS-1/IRS-2 with the insulin receptor. *J Biol Chem* **278**, 8460-7.

Wilkins, J. F. and Haig, D. (2003). What good is genomic imprinting: the function of parent-specific gene expression. *Nat Rev Genet* **4**, 359-68.

Wilkinson, L. S., Davies, W. and Isles, A. R. (2007). Genomic imprinting effects on brain development and function. *Nat Rev Neurosci* **8**, 832-43.

Wolf, J. B. and Hager, R. (2006). A maternal-offspring coadaptation theory for the evolution of genomic imprinting. *PLoS Biol* **4**, e380.

Wolfrum, C., Shih, D. Q., Kuwajima, S., Norris, A. W., Kahn, C. R. and Stoffel, M. (2003). Role of Foxa-2 in adipocyte metabolism and differentiation. *J Clin Invest* **112**, 345-56.

Wutz, A., Theussl, H. C., Dausman, J., Jaenisch, R., Barlow, D. P. and Wagner, E. F. (2001). Non-imprinted Igf2r expression decreases growth and rescues the Tme mutation in mice. *Development* **128**, 1881-7.

Yamamoto, Y., Ishino, F., Kaneko-Ishino, T., Shiura, H., Uchio-Yamada, K., Matsuda, J., Suzuki, O. and Sato, K. (2008). Type 2 diabetes mellitus in a non-obese mouse model induced by Meg1/Grb10 overexpression. *Exp Anim* **57**, 385-95.

Yamamoto, Y., Sawa, R., Okamoto, N., Matsui, A., Yanagisawa, M. and Ikemoto, S. (1986). Deletion 14q(q24.3 to q32.1) syndrome: significance of peculiar facial appearance in its diagnosis, and deletion mapping of Pi(alpha 1-antitrypsin). *Hum Genet* **74**, 190-2.

Yamasaki-Ishizaki, Y., Kayashima, T., Mapendano, C. K., Soejima, H., Ohta, T., Masuzaki, H., Kinoshita, A., Urano, T., Yoshiura, K., Matsumoto, N. et al. (2007). Role of DNA methylation and histone H3 lysine 27 methylation in tissue-specific imprinting of mouse Grb10. *Mol Cell Biol* **27**, 732-42.

Yamazawa, K., Kagami, M., Nagai, T., Kondoh, T., Onigata, K., Maeyama, K., Hasegawa, T., Hasegawa, Y., Yamazaki, T., Mizuno, S. et al. (2008). Molecular and clinical findings and their correlations in Silver-Russell syndrome: implications for a positive role of IGF2 in growth determination and differential imprinting regulation of the IGF2-H19 domain in bodies and placentas. *J Mol Med* **86**, 1171-81.

Yanai, H., Nakamura, K., Hijioka, S., Kamei, A., Ikari, T., Ishikawa, Y., Shinozaki, E., Mizunuma, N., Hatake, K. and Miyajima, A. (2010). Dlk-1, a cell surface antigen on foetal hepatic stem/progenitor cells, is expressed in hepatocellular, colon, pancreas and breast carcinomas at a high frequency. *J Biochem* **148**, 85-92.

Yea, S. S. and Fruman, D. A. (2011). Cell signaling. New mTOR targets Grb attention. *Science* **332**, 1270-1.

Yevtodiyenko, A. and Schmidt, J. V. (2006). Dlk1 expression marks developing endothelium and sites of branching morphogenesis in the mouse embryo and placenta. *Developmental Dynamics* **235**, 1115-1123.

Yin, D., Xie, D., De Vos, S., Liu, G., Miller, C. W., Black, K. L. and Koeffler, H. P. (2004). Imprinting status of DLK1 gene in brain tumors and lymphomas. *Int J Oncol* **24**, 1011-5.

Yoshihashi, H., Maeyama, K., Kosaki, R., Ogata, T., Tsukahara, M., Goto, Y., Hata, J., Matsuo, N., Smith, R. J. and Kosaki, K. (2000). Imprinting of human GRB10 and its mutations in two patients with Russell-Silver syndrome. *Am J Hum Genet* **67**, 476-82.

Yu, O. H., Murawski, I. J., Myburgh, D. B. and Gupta, I. R. (2004). Overexpression of RET leads to vesicoureteric reflux in mice. *Am J Physiol Renal Physiol* **287**, F1123-30.

Yu, S., Castle, A., Chen, M., Lee, R., Takeda, K. and Weinstein, L. S. (2001). Increased insulin sensitivity in Gsalpha knockout mice. *J Biol Chem* **276**, 19994-8.

Yu, S., Gavrilova, O., Chen, H., Lee, R., Liu, J., Pacak, K., Parlow, A. F., Quon, M. J., Reitman, M. L. and Weinstein, L. S. (2000). Paternal versus maternal transmission of a stimulatory G-protein alpha subunit knockout produces opposite effects on energy metabolism. *J Clin Invest* **105**, 615-23.

Yu, S., Yu, D., Lee, E., Eckhaus, M., Lee, R., Corria, Z., Accili, D., Westphal, H. and Weinstein, L. S. (1998). Variable and tissue-specific hormone resistance in heterotrimeric Gs protein alpha-subunit (Gsalpha) knockout mice is due to tissue-specific imprinting of the gsalpha gene. *Proc Natl Acad Sci U S A* **95**, 8715-20.

Yu, Y., Yoon, S. O., Poulogiannis, G., Yang, Q., Ma, X. M., Villen, J., Kubica, N., Hoffman, G. R., Cantley, L. C., Gygi, S. P. et al. (2011). Phosphoproteomic analysis identifies Grb10 as an mTORC1 substrate that negatively regulates insulin signaling. *Science* **332**, 1322-6.

Zhang, H., Noohr, J., Jensen, C. H., Petersen, R. K., Bachmann, E., Teisner, B., Larsen, L. K., Mandrup, S. and Kristiansen, K. (2003). Insulin-like growth factor-1/insulin bypasses Pref-1/FA1-mediated inhibition of adipocyte differentiation. *J Biol Chem* **278**, 20906-14.

Zhang, H., Schulz, T. J., Espinoza, D. O., Huang, T. L., Emanuelli, B., Kristiansen, K. and Tseng, Y. H. (2010). Cross talk between insulin and bone morphogenetic protein signaling systems in brown adipogenesis. *Mol Cell Biol* **30**, 4224-33.

Zhang, Y., Proenca, R., Maffei, M., Barone, M., Leopold, L. and Friedman, J. M. (1994). Positional cloning of the mouse obese gene and its human homologue. *Nature* **372**, 425-32.

Zhou, Y., Cheunsuchon, P., Nakayama, Y., Lawlor, M. W., Zhong, Y., Rice, K. A., Zhang, L., Zhang, X., Gordon, F. E., Lidov, H. G. et al. (2010). Activation of paternally expressed genes and perinatal death caused by deletion of the Gtl2 gene. *Development* **137**, 2643-52.